24 April 2009 | $10

Science

Livestock Decoded

AAAS

cell sciences

signal transduction

Research products for the study of the important signal transduction pathways…

www.cellsciences.com

Abl SH3 domain, inactive
ABL1
ACV-R1
ADRBK1
ADRBK2
Akt1
Akt1, inactive
Akt2
Akt3
ALK/P80
AMPK-alpha1
ARK5
ASK1
ATF-2
Aurora A
Aurora B
Aurora C
AXL
BLK
BMX
BRAF
BRK
BRSK1
BTK
C-JUN
C-Src
CAMK1 delta
CAMK1 gamma
CAMK2 beta
CAMK2 delta
CAMK4
CDC42BPA/MRCKA
CDC42BPB/MRCKB
CDK1/CycB
CDK1/CycE
CDK2
CDK2/CycA
CDK2/CycE
CDK3/CycE
CDK4
CDK4/CycD1
CDK4/CycD3
CDK5
CDK5/p25NCK
CDK5/p35NCK
CDK6/CycD1
CDK7/CycH/MAT1
CDK8, inactive
CDK9/CycT
CHK2
CK1 alpha 1
CK1 delta
CK1 gamma 1
CK1 gamma 2
CK1 gamma 3
CK2 alpha 1
CK2 alpha 2
CK2 beta
CK2 holoenzyme
CKBB
CKMB
CKMBI type 1
CKMBI type 2
CKMM
CKMM Type 1
CKMM Type 3
CLK1
CREB-1
CSK
DAPK1
DAPK2
DAPK3
DCAMKL2
DDR2
DEK
DMPK
EGFR
eIF2 alpha
ELK-1
EphA1
EphA2
EphA3
EphA4
EphA5
EphA7
EphA8
EphB1
EphB2
EphB3
EphB4
ERBB2
ERBB4
Erk1
Erk2
FAK
FER
FGF-R1
FGF-R2
FGF-R3
FGF-R4
FGR
Flt-1
Flt3 Kinase
FRK
GCK
GRK5
GRK6
GSK3
GSK3 beta
Hck SH3 domain, inactive
Hck
HGK
HIPK1
HIPK3
I kappa B alpha
IGF1-R
IKK-beta
IKK-epsilon
INS-R
IRAK1
IRAK4
ITK
JAK2 JH1 JH2
JAK2
JAK3
JNK1
JNK2 alpha 1
JNK2 alpha 2
KDR/VEGFR2
KHS1/MAP4K5
KIT
LCK SH3 domain, inactive
LCK
LTK
LYN B
MAPK9
MAPK11/p38 beta
MAPK12/p38 gamma
MAPK14
MAPK14/p38
MAPKAPK2
MAPKAPK3
MAPKAPK5
MARK1
MARK2
MARK3
MARK4
MATK
MEK1
MEK2
MEK3
MET
MERTK
MINK1
MLK1
MLK2
MLK3
MST2
MST4
MUSK
MYLK
MYLK2
NCK2
NCOR2/SMRT
NEK2
NEK3
NEK6
NEK7
NEK11
NFAT
NLK
p110 alpha/p85 alpha
p38 alpha
p38 beta
p38 delta
p38 gamma
p70S6K
PAK1
PAK2
PAK4
PAK6
PAK7
PBK
PDGFR-alpha
PDGFR-beta
PDK1
PHKG1
PHKG2
PI3K p110d/p85a
PI3K p110g
PI3K beta p110ß/p85a
PI3K p110a/p85a
PI3K p110g
PIM1
PIM2
PKA holoenzyme type Ia
PKA holoenzyme type IIa
PKA regulatory subunit Ia
PKA regulatory subunit IIa
PKAc alpha
PKAc beta
PKAc gamma
PKAR-I alpha
PKC alpha
PKC beta 1
PKC beta II
PKC delta
PKC epsilon
PKC eta
PKC gamma
PKC iota/lambda
PKC mu
PKC nu
PKC theta
PKC zeta
PKD2
PKG1 beta
PLK1
PLK2
PLK3
PP2C alpha
PRK1
PTK2B
PYK2
Raf1
RET
RIPK2
ROCK1
ROCK2
RPS6KB1/p70S6K
RPS6KB2/p70S6Kbeta
RSK1
RSK2
RSK3
RSK4
S6K
SAK
SGK1
SGK2
SGK3
SNARK
SNK
Sphingosine Kinase 1
Sphingosine Kinase 2
Src
SRPK1
SRPK2
STAT1
STAT3
STK3
STK16/TSF1
STK17A (DRAK1)
STK22B/TSSK2
STK23/MSSK1
STK24/MST3
STK33
SYK
TBK1
TGFB-R1
Tie2
TRKA
TSF1
TSSK1
TSSK2
TTK
TYRO3
VEGF-R1
VEGF-R2/KDR
VEGF-R3
VRK1
WEE1
WNK2
WNK3
YES
ZAP70

CELL SCIENCES INC • 480 NEPONSET STREET, BUILDING 12A, CANTON, MA 02021 • INFO@CELLSCIENCES.COM

TOLL FREE: (888) 769-1246 • TEL: (781) 828-0610 • FAX: (781) 828-0542 • WEB WWW.CELLSCIENCES.COM

Download your free copy today.

ScienceCareers.org/booklets

From technology specialists to patent attorneys to policy advisers, learn more about the types of careers that scientists can pursue and the skills needed in order to succeed in nonresearch careers.

Science Careers
From the journal *Science* AAAS

Biacore systems

from inspiration ...to publication

Highest quality, information-rich interaction data from Biacore™ systems deepen your understanding of molecular mechanisms and interaction pathways and enable you to add function to structure.

Select the perfect solution for your application and draw conclusions with confidence – from the company that continues to set the standard for label-free protein interaction analysis.

For further information or register to have one of our scientific experts contact you, please visit **www.gelifesciences.com/biacore-science**

Biacore T100
unmatched performance

Biacore X100
ready to run research system

Biacore Flexchip
array-based comparative profiling

imagination at work

EDITORIAL

NEWS OF THE WEEK

NEWS FOCUS

LETTERS

BOOKS *ET AL.*

POLICY FORUM

EDUCATION FORUM

PERSPECTIVES

CONTENTS continued >>

page 454

page 468

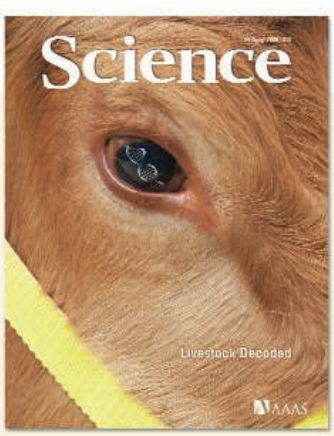

COVER

Animal domestication has been key to the development of human societies. The sequence of the bovine genome reveals new insights into the history and biology of cattle. See pages 522 and 528, and related research on horse and sheep genetics and domestication on pages 485 and 532.

Photo illustration: Yael Kats (images: Jupiterimages)

>> See also Policy Forum p. 468 and Perspective p. 478

DEPARTMENTS

Published by AAAS

Gene expression and function analysis sample and assay technologies by QIAGEN

Enjoy first-time success

Rely on QIAGEN's manual and automated workflow solutions for:

- **Sample collection and disruption**
- **RNA stabilization and purification**
- **Real-time PCR and RT-PCR and gene expression assays**
- **RNAi and gene silencing**
- **miRNA purification and assays**
- **Methylation analysis in epigenetics research**
- **Protein sample preparation and assays**

Making improvements in life possible — www.qiagen.com

GEPref030951WW

QIAGEN®

Sample & Assay Technologies

REVIEW

BREVIA

REPORTS

CONTENTS continued >>

page 472

page 488

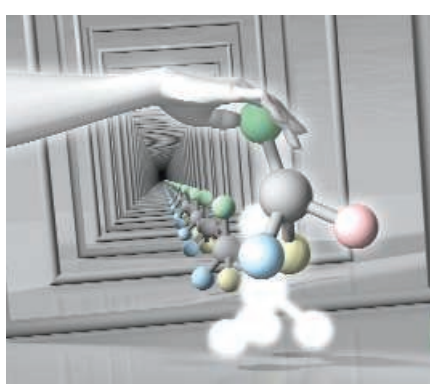

page 492

CREDITS (MIDDLE): SEUNG-MO LEE/MPI-HALLE; (BOTTOM) KENSO SOAI AND TSUNEOMI KAWASAKI

Published by AAAS

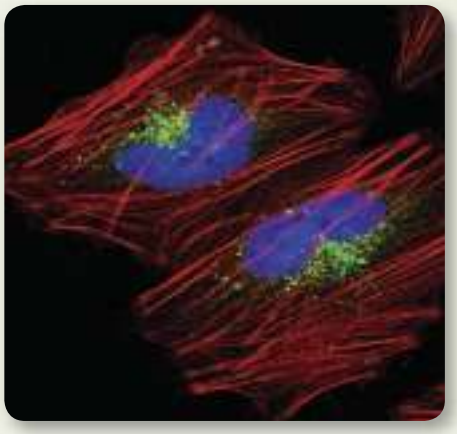

*Confocal immunofluorescent analysis of HeLa cells using **RagC Antibody #3360** (green). Actin filaments have been labeled with DY-554 phalloidin (red). Blue pseudocolor = DRAQ5™ (fluorescent DNA dye).*

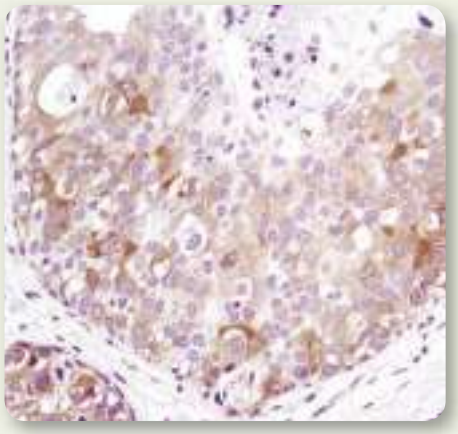

*Immunohistochemical analysis of paraffin-embedded human breast carcinoma using **Phospho-PRAS40 (Thr246) (C77D7) Rabbit mAb #2997.***

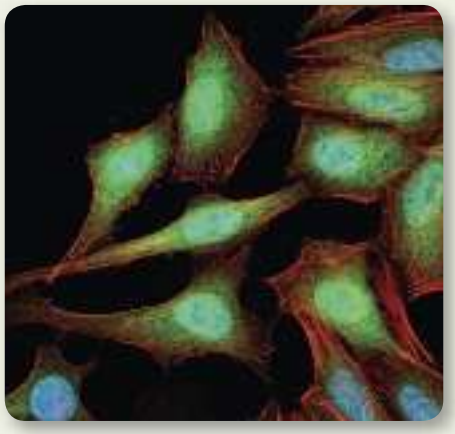

*Confocal immunofluorescent analysis of HeLa cells using **4E-BP1 (53H11) Rabbit mAb #9644** (green). Actin filaments have been labeled with Alexa Fluor® 555 phalloidin (red). Blue pseudocolor = DRAQ5™ (fluorescent DNA dye).*

Cutting-edge

mTOR Signaling Antibodies

...from Cell Signaling Technology®

Unparalleled product quality, validation and technical support.

:: Innovative products from Cell Signaling Technology offer unsurpassed sensitivity, specificity and performance.

:: Extensive in-house validation means that optimization is not left up to you, the user.

:: Technical support provided by the same scientists who produce and validate the antibodies — this translates into a thorough, fast and accurate response.

*Immunohistochemical analysis of paraffin-embedded human breast carcinoma using **Phospho-S6 Ribosomal Protein (Ser235/236) (D57.2.2E) Rabbit mAb #4858** in the presence of control peptide (left) or Phospho-S6 Ribosomal Protein (Ser235/236) Blocking Peptide #1220 (right).*

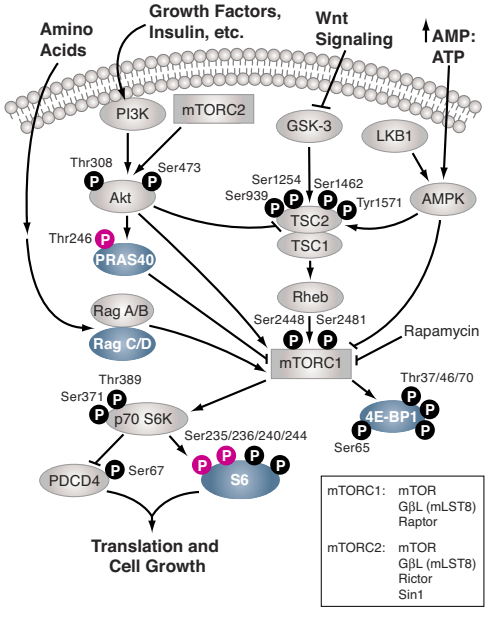

Antibodies against all of the targets in this pathway are available from Cell Signaling Technology.

for the most up-to-date product listing visit:

www.cellsignal.com

Cell Signaling TECHNOLOGY®

Orders (toll-free) 1-877-616-2355 | **Technical support** (toll-free) 1-877-678-8324 support@cellsignal.com | **Inquiries** info@cellsignal.com | **Environmental Commitment** eco.cellsignal.com

SCIENCEONLINE

SCIENCEXPRESS
www.sciencexpress.org

Phasic Firing in Dopaminergic Neurons Is Sufficient for Behavioral Conditioning
H.-C. Tsai et al.

High-frequency pulses in deep brain cells release dopamine and cause reward-related behavior in mice.
10.1126/science.1168878

Crystal Structure of the Nuclear Export Receptor CRM1 in Complex with Snurportin1 and RanGTP
T. Monecke et al.

The structure of an exportin complex shows how nuclear transport complexes differentially recognize cargo.
10.1126/science.1173388

Entropic Evidence for Linguistic Structure in the Indus Script
R. P. N. Rao et al.

Analysis of the pattern of symbols confirms the linguistic role of ancient signs.
10.1126/science.1170391

Magnetic Field Sensing Beyond the Standard Quantum Limit Using 10-Spin NOON States
J. A. Jones et al.

Quantum mechanical entanglement of nuclei in a single molecule results in an enhancement of the magnetic field sensitivity.
10.1126/science.1170730

Penultimate Deglacial Sea Level Timing from Uranium/Thorium Dating of Tahitian Corals
A. L. Thomas et al.

Sea levels rose during the penultimate deglaciation while Northern Hemisphere insolation was at a minimum.
10.1126/science.1168754

TECHNICALCOMMENTS

Comment on "Colossal Ionic Conductivity at Interfaces of Epitaxial ZrO_2:Y_2O_3/$SrTiO_3$ Heterostructures"
X. Guo

full text at www.sciencemag.org/cgi/content/full/324/5926/465a

Response to Comment on "Colossal Ionic Conductivity at Interfaces of Epitaxial ZrO_2:Y_2O_3/$SrTiO_3$ Heterostructures"
J. García-Barriocanal et al.

full text at www.sciencemag.org/cgi/content/full/324/5926/465b

SCIENCENOW
www.sciencenow.org
Highlights From Our Daily News Coverage

Neandertal Babies Didn't Do the Twist
Unlike in humans, Neandertal babies may not have rotated in the birth canal.

Closer Look at Einstein's Brain
A new anatomical study reveals unusual features in the physicist's parietal lobes.

The Mother of All Pileups
Crash of giant gas clouds suggests dark matter's hand.

SCIENCESIGNALING
www.sciencesignaling.org
The Signal Transduction Knowledge Environment

EDITORIAL GUIDE: Demystifying mTOR Signaling
N. R. Gough
The field of mTOR signaling is rapidly advancing.

PERSPECTIVE: The Pharmacology of mTOR Inhibition
D. A. Guertin and D. M. Sabatini
The quest for effective cancer therapies reveals insight into the regulation and function of the mammalian target of rapamycin.

PERSPECTIVE: Immune Regulation by Rapamycin: Moving Beyond T Cells
M. R. Janes and D. A. Fruman
Rapamycin regulates immune responses, in part, through its effects on macrophages and dendritic cells.

PERSPECTIVE: Akt Demoted in Glioblastoma
P. K. Vogt and J. R. Hart
PKCα is an essential component of a pathway linking EGFR signaling to mTOR and cell proliferation in glioblastoma.

PERSPECTIVE: New Insights into mTOR Signaling—mTORC2 and Beyond
D. R. Alessi et al.
mTORC2 promotes the phosphorylation of AGC kinase substrates at two distinct sites.

PODCAST
M. B. Yaffe and A. M. VanHook
Science Signaling's Chief Scientific Editor gives an overview of mTOR signaling.

SCIENCECAREERS
www.sciencecareers.org/career_magazine
Free Career Resources for Scientists

Special Feature: The Other Parts of Your Academic Job
J. Austin
Research gets more attention, but teaching and service are also important parts of an academic career.

Teach the Students You Have
S. Carpenter
To teach well, take a scholarly approach and make your expectations clear.

Professional Service
E. Pain
Institutional service may be an annoyance, but you still need to do your part.

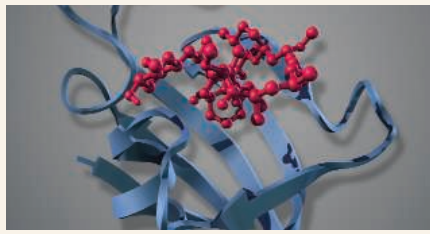

SCIENCESIGNALING
An mTOR inhibitor.

SCIENCECAREERS
Mastering the teaching and service career components.

SCIENCEPODCAST
www.sciencemag.org/multimedia/podcast
Free Weekly Show

Download the 24 April *Science* Podcast to hear about advances in livestock research, including the sequencing of the cattle genome and insights into the history of sheep domestication.

ORIGINSBLOG
blogs.sciencemag.org/origins
A History of Beginnings

SCIENCEINSIDER
blogs.sciencemag.org/scienceinsider
Science Policy News and Analysis

SCIENCE (ISSN 0036-8075) is published weekly on Friday, except the last week in December, by the American Association for the Advancement of Science, 1200 New York Avenue, NW, Washington, DC 20005. Periodicals Mail postage (publication No. 484460) paid at Washington, DC, and additional mailing offices. The title SCIENCE is a registered trademark of the AAAS. Domestic individual membership and subscription (51 issues): $146 ($74 allocated to subscription). Domestic institutional subscription (51 issues): $835; Foreign postage extra: Mexico, Caribbean (surface mail) $55; other countries (air assist delivery) $85. First class, airmail, student, and emeritus rates on request. Canadian rates with GST available upon request, GST #1254 88122. Publications Mail Agreement Number 1069624. **Printed in the U.S.A.**

Change of address: Allow 4 weeks, giving old and new addresses and 8-digit account number. **Postmaster:** Send change of address to AAAS, P.O. Box 96178, Washington, DC 20090–6178. **Single-copy sales:** $10.00 current issue, $15.00 back issue prepaid includes surface postage; bulk rates on request. **Authorization to photocopy** material for internal or personal use under circumstances not falling within the fair use provisions of the Copyright Act is granted by AAAS to libraries and other users registered with the Copyright Clearance Center (CCC) Transactional Reporting Service, provided that $20.00 per article is paid directly to CCC, 222 Rosewood Drive, Danvers, MA 01923. The identification code for *Science* is 0036-8075. *Science* is indexed in the *Reader's Guide to Periodical Literature* and in several specialized indexes.

AAAS
ADVANCING SCIENCE, SERVING SOCIETY

CREDITS: (*SCIENCE SIGNALING*) CHRIS BICKEL; (*SCIENCE CAREERS*) NATIONAL SCIENCE FOUNDATION

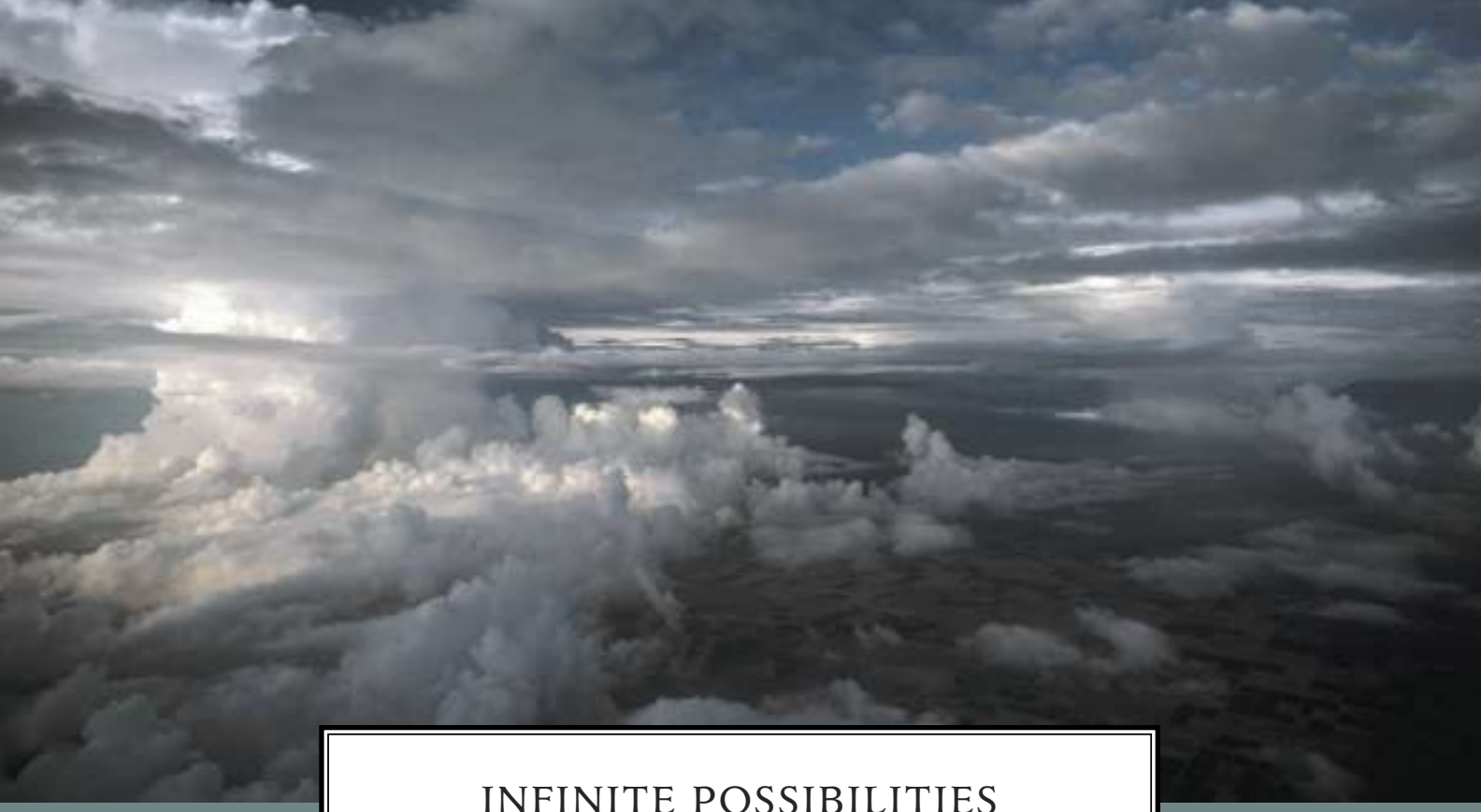

INFINITE POSSIBILITIES

Cellular Imaging & Analysis

NEB introduces SNAP-tag™ and CLIP-tag™ protein labeling systems. These innovative technologies provide simplicity and extraordinary versatility to the imaging of mammalian proteins *in vivo*, and to protein capture experiments *in vitro*. The creation of a single genetic construct generates a fusion protein which, when covalently attached to a variety of fluorophores, biotin, or beads provides a powerful tool for studying the role of proteins in living and fixed cells.

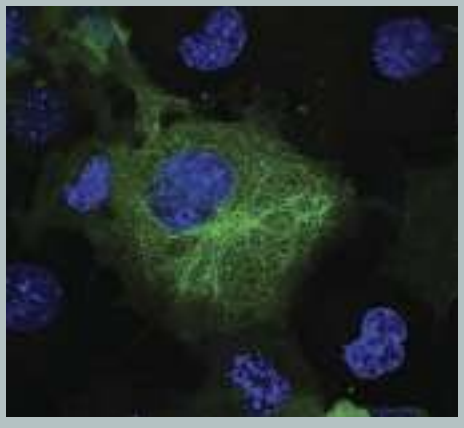

Live COS-7 cells transiently transfected with pSNAPm-Tubulinβ. Cells were labeled with SNAP-Cell TMR-Star (green pseudocolor) for 30 minutes and counterstained with Hoechst 33342 (blue) for nuclei.

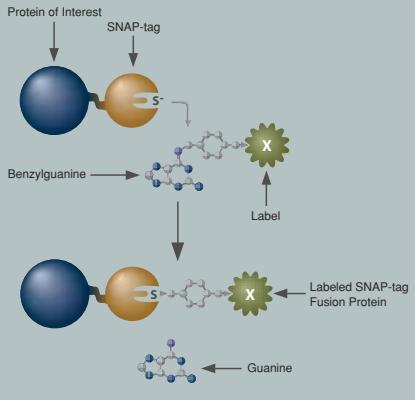

SNAP-tag Technology: *SNAP-tag (gold) fused to the protein of interest (blue) self labels releasing guanine.*

Advantages:

Versatile - Compatible systems enable dual labeling

Flexible - Multiple fluorophores allow for choice & flexibility

Innovative - A range of applications is possible with a single construct

NEW ENGLAND BioLabs® Inc.

<< Not Just Dinner on Legs

Several thousand years ago, human beings realized the virtues of domesticating wild animals as easy meat. Soon other possibilities became apparent, and as revealed in a series of papers in this issue, early pastoralists became selective about breeding for wool, leather, milk, and muscle power. In two papers, **Gibbs *et al.*** report on the bovine genome sequence (p. 522; see the cover, the Perspective by **Lewin**, and the Policy Forum by **Roberts**) and trace the diversity and genetic history of cattle (p. 528), while **Chessa *et al.*** (p. 532) survey the occurrence of endogenous retroviruses in sheep and map their distribution to historical waves of human selection and dispersal across Europe. Finally, **Ludwig *et al.*** (p. 485) note the origins of variation in the coat-color of horses and suggest that it is most likely to have been selected for by humans in need of good-looking transport.

Burn, Baby, Burn

Wildfires can have dramatic and devastating effects on landscapes and human structures and are important agents in environmental transformation. Their impacts on nonanthropocentric aspects of the environment, such as ecosystems, biodiversity, carbon reserves, and climate, are often overlooked. **Bowman *et al.*** (p. 481) review what is known and what is needed to develop a holistic understanding of the role of fire in the Earth system, particularly in view of the pervasive impact of fires and the likelihood that they will become increasingly difficult to control as climate changes.

Disappearing Stars

One way to identify and study the stars that have exploded as supernovae is to look for stars that are spatially coincident with the supernovae in pre-explosion images. The only way to be sure of their identifications is to wait for the light from the supernovae to fade and check that the stars have vanished from the sky. **Maund and Smartt** (p. 486, published online 19 March), using the Hubble Space Telescope and the Gemini telescope, have now shown that the red supergiant stars that have been found in pre-explosion images of SN 2003gd and SN 1993J are no longer seen in recent images of the supernovae sites. Their absence confirms that they were the supernovae's true progenitors.

Improving on Spider Silk?

In a conventional atomic layer deposition, alternating pulses of a reactive metal-based precursor and a reactant, such as water, are deposited onto a solid surface to create a coating that conforms closely to the original surface. **Lee *et al.*** (p. 488) apply this process to fibers of spider silk, which are soft and porous. In addition to forming a coating on the fibers, some of the metal ions penetrate the fibers and react with the protein structure. These doped fibers show significant increase in toughness as measured by the work required to deform them.

Boundary Issues of the Lithosphere

The depth of Earth's tectonic plates is defined by the lithosphere-aesthenosphere boundary (LAB), but its seismic signature is more subtle compared with other deeper boundaries within Earth (see the Perspective by **Romanowicz**). Under oceanic plates, the LAB is often defined by where temperatures are hot enough to cause some melting. This boundary has been hard to detect in older oceanic plates, but it is important for understanding how these plates thicken with age or distance from ocean ridges, and for assessing heat flow through the oceanic crust. **Kawakatsu *et al.*** (p. 499) use a detailed seismic array to detect a seismic velocity reduction beneath the Philippine Sea and Pacific plates. The data imply that 5%, or less, melt forms horizontal layers, and that oceanic plate thicknesses do indeed deepen with age. **Rychert and Shearer** (p. 495) used 15 years of seismic data to explore the global distribution of an anomaly imaged by conversion of pressure waves to shear waves (waves associated with a sharp velocity drop). The data reveal a broad signal at depths of 70 kilometers (km) beneath ocean islands to 95 km beneath Precambrian shields. It is not clear whether this boundary is the lithosphere-aesthenosphere boundary or a layer with a distinct horizontal fabric.

Methane from Wetlands

At the end of the cold climate interval called the Younger Dryas, approximately 11,600 years ago, global temperatures began their final ascent to the warmth of the Holocene, and the concentration of methane in the atmosphere increased rapidly and substantially. There has been much speculation about the cause of that increase, with most recent evidence pointing to wetlands as the source. The most direct proof of that explanation requires the measurement of the radiocarbon content of that methane. **Petrenko *et al.*** (p. 506; see the Perspective by **Nisbet and Chappellaz**) analyzed 1000 kilogram-sized samples of Greenland ice, which have sufficient methane to allow measurement of its ^{14}C content. They show that wetland sources indeed must have been responsible for the majority of the rise in atmospheric methane levels at the end of the Younger Dryas.

Hot Silent Quakes

Subduction zones tend to produce the largest and potentially most destructive earthquakes. Recent observations show that some deformation in several subduction zones seems to be occurring through small or "silent" quakes. The

Continued on page 437

CREDITS (TOP TO BOTTOM): ARPAT OZGUL; VASILII PETRENKO AND JEFFREY SEVERINGHAUS

www.roche-applied-science.com

FuGENE® HD Transfection Reagent

Measure the results of your *transfection*, not your *transfection reagent.*

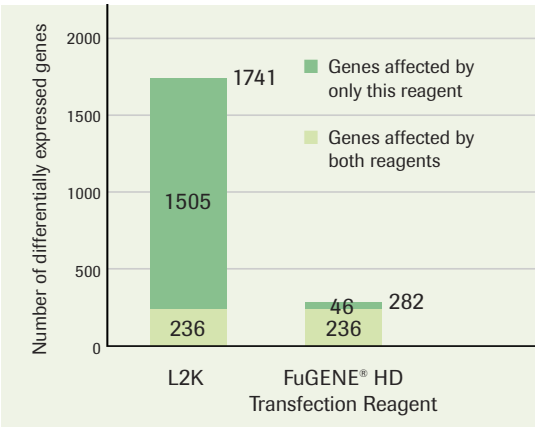

Figure 1. Minimize off-target effects by using FuGENE® HD Transfection Reagent. FuGENE® HD Transfection Reagent or a reagent from another supplier (L2K) was used to transfect MCF-7 cells (ATCC® HTB-22™). Subsequent microarray expression profiling experiments demonstrated that L2K significantly altered the expression levels of six times more genes than FuGENE® HD Transfection Reagent.

View the complete article online in *Biochemica* (2006) **4** at *www.roche-applied-science.com/publications/biochemica.htm*

Are you confident that the cellular effects you observe are the result of your transfected plasmid? Or are your results due to differential gene expression caused by the transfection reagent you use?

Rely on **FuGENE® HD Transfection Reagent** to avoid the high levels of nonspecific, off-target effects that can be generated with other transfection reagents (Figure 1).

- **Generate physiologically relevant data you can trust** with a unique non-liposomal formulation.
- **Achieve greater cell survival** when transfecting with this low-cytotoxicity reagent that is sterile filtered and free of animal-derived components.

Switch to FuGENE® HD Transfection Reagent to obtain meaningful results today!

For more information and a database of successfully transfected cell lines, or to purchase, please visit ***www.powerful-transfection.com***

Roche Diagnostics GmbH
Roche Applied Science
68298 Mannheim, Germany

Roche

Continued from page 435

origin of these silent quakes, and their effect on the seismic hazard, is uncertain. **Song *et al.*** (p. 502) use a specific seismic signal to map out thin regions with low seismic velocities on the subduction zone beneath southern Mexico. The regions seem to occur at depths below the seismogenic zone where temperatures are higher. These high temperatures and the silent quakes may reflect the release and episodic trapping of fluids from metamorphic reactions.

Resolving Isotopically Chiral Alcohols

Autocatalytic reactions, which are accelerated by their own product, can amplify small imbalances in the chiral distribution of starting materials. A particularly effective system is the alkylation of certain aldehydes by diisopropyl zinc, which becomes increasingly stereoselective as the chiral alkoxide product coordinates to unreacted zinc centers. **Kawasaki *et al.*** (p. 492, published online 26 March) show that the sense of enantioselection in this system can be influenced by a factor as subtle as chirality in an alcohol that arises only because two positions differ in having ^{12}C and ^{13}C atoms. Isotopically chiral ligands were carefully prepared by using methods that would avoid chiral contaminants, and each led to a distinct enantiomer with enantiomeric excesses exceeding 90%.

Early Birds and Night Owls

In humans, peaks and troughs in alertness and cognitive performance partly depend on the timing of daily activities. Using brain imaging from the extreme ends of the spectrum of individuals whose performance is better in the mornings to those who do best in the evenings, **Schmidt *et al.*** (p. 516) found that after more than 10 hours of wakefulness, morning types had less activity in brain areas linked to attention compared with evening types. Moreover, morning types felt sleepier and tended to perform slower on psychomotor vigilance tasks. It seems getting the balance of sleep at the right time is important for regulating the daily pattern of cognitive performance.

The Mystery of PolyP Polymerase

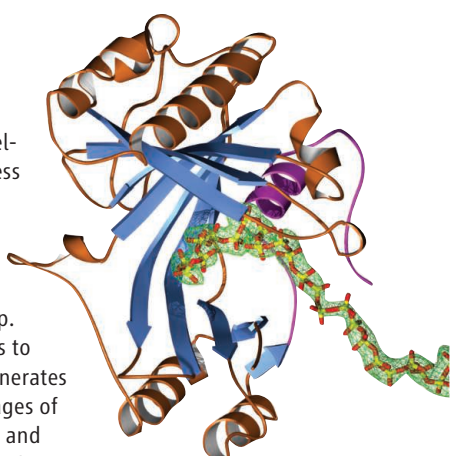

Inorganic polyphosphate (polyP) is found in all organisms. In bacteria it is involved in multiple cellular processes, but in eukaryotes its function is less clear and investigation is hampered because the identity of the polyP synthesizing enzyme has been elusive. Previous genetic screens suggested that a yeast vacuolar transporter chaperone may play a role in polyP metabolism. **Hothorn *et al.*** (p. 513) have used structural and biochemical studies to show that a domain in this chaperone complex generates polyP from ATP. Crystal structures from various stages of the reaction cycle supply clues for the mechanism and include a structure with a phosphate polymer bound in an enzyme tunnel. This polymerase has been found in a range of organisms where it appears to be important not only in deep-sea organisms contributing to global phosphate cycling, but also in symbiotic fungi exchanging phosphate with their hosts, through to phosphate storage in human protozoan parasites like *Leishmania*.

Model Progesterone Response

The hormone progesterone stimulates maturation of oocytes in the toad *Xenopus laevis* by binding to its receptor. Although receptor number and affinity for the hormone stay relatively constant, the dose of hormone required to stimulate meiotic maturation varies according to the environmental stimuli to which the animal is exposed, but little is known about how this is regulated. **Justman *et al.*** (p. 509; see the Perspective by **Skotheim**) combined experimental analysis and mathematical modeling to explore the role of glycogen synthase kinase–3β in desensitization, and a natural, sensitizing co-stimulus, the amino acid L-leucine. The results help to explain the layered complexity seen in signal transduction networks: If multiple stimuli act upon components of linked feedback loops, cells can tune their sensitivities dynamically to match their environment.

CREDIT: HOTHORN *ET AL.*

Trusted!

SIGMA® Life Science

Insist on Sigma's FLAG® System…
Original and Proven Performance

FLAG is the established system for recombinant protein expression, purification, and detection. Don't settle for inferior systems.

- **Proven**: Cited in more than 2,000 publications
- **Ultrasensitive**: Antibodies detect as little as 100 femtomoles of protein
- **Comprehensive**: Complete systems in multiple formats

View the full range of FLAG products at ***sigma.com/flagtag***

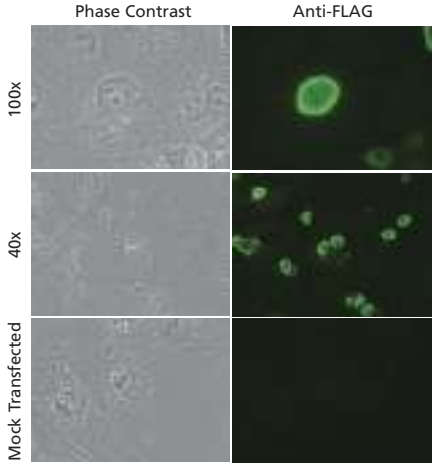

FLAG-p53 and mock transfected COS-7 cells were permeabilized, fixed, blocked, and incubated with anti-FLAG M2 antibody

Our Innovation, Your Research — Shaping the Future of Life Science

Ralph J. Cicerone is president of the U.S. National Academy of Sciences in Washington, DC.

How to Keep Science Moving

RECENT ENTHUSIASM FOR SCIENCE IN THE UNITED STATES IS CAUSE FOR CELEBRATION, BUT it's also food for thought: What can scientists do to build on this new excitement and support? If the U.S. Congress and administration are to continue to advance science research and education and to rely on science in policy-making, then scientists must do much more to show how science works and how scientific research contributes to the nation.

President Obama has made strong statements affirming the value of science and his commitment to it. He has appointed outstanding scientists to leadership positions. And by Executive Order, he has reversed the federal ban on human embryonic stem cell research and directed the Office of Science and Technology Policy to propose methods to ensure that science policies are not twisted for political or ideological purposes. Moreover, the federal stimulus package provides a great infusion of funds for research grants, major equipment, and facilities through the major science funding agencies. While testifying at a recent House Appropriations hearing, I witnessed much goodwill toward science, scientists, and science educators in the bipartisan support for items in the stimulus package. Members of Congress on both sides of the aisle also seemed motivated to improve science education at all levels.

However, Congress needs continual, vigorous contact with science and scientists. Its members support science but also must deal with many other demands for their attention: federal budget deficits; immediate social, physical infrastructure, and military needs; rising unemployment; and turmoil in the industrial and financial sectors. Scientists must do more to demonstrate the value of investing in science. Their first duty, of course, is to do good research while adhering to high ethical standards of openness and honesty. Yet to energize the public and its elected representatives, scientists must talk more with them, both through scientific societies and as individual scientists, person to person. As one example, providing Congress with postdoctoral fellows from scientific and engineering societies has proved to be very valuable for science, Congress, and the fellows involved, opening new career paths and generating critical support for policymakers from the scientific community.

Encounters at home are often more effective than those in Washington. Former Congressman John Porter, who did so much to double the budget of the U.S. National Institutes of Health, once told me that few of his congressional colleagues had much time for science, but that each and every one of them who had visited a science laboratory in his or her home district emerged as an enthusiast. Scientists should be recruiting deans, presidents, chancellors, alumni associations, and press officers to help them communicate with their local community and business leaders, as well as with members of Congress. They should create opportunities to invite the public into their laboratories, introduce them to their students, and give answers to questions such as: What do your results mean? What could they mean to the public? How does your research complement the work of others? How have you created good research experiences for students? Do you have any research connections with new or established businesses? These positive impacts of research are not always visible from a distance.

The reinvigorated research community must also engage the interests of new science students, so that U.S. science can maintain leadership in certain fields and be a strong, reliable partner in many critical international research efforts. That means becoming more deeply involved in improving science education at all levels, including working with precollege students and their teachers and exposing many more students to real science and scientists. Such interactions can raise the career aspirations of young people.

Only if scientists do their part will there be the broad and deep public support that is so essential for science to flourish and for the public to engage with science. Scientists have great stories to tell, and many important people want to hear them. So let's get going and tell them.

– Ralph J. Cicerone

10.1126/science.1174936

Published by AAAS

IMMUNOLOGY

Internal Indigestion

T cell–mediated responses to extracellular pathogens are initiated through a process called cross-presentation: Pathogens are internalized by dendritic cells via phagocytosis, partially degraded, and then presented on the cell surface by class I major histocompatibility molecules for recognition by cytotoxic T cells. Several immune cell types possess phagocytic capacity; in most cases, however, this leads to pathogen degradation. In contrast, dendritic cells that express CD8 are able to cross-present because of the low proteolytic activity and slightly alkaline pH of their phagosomes.

Savina *et al.* demonstrate that in contrast to non–cross-presenting dendritic cell subsets, $CD8^+$ dendritic cells assemble the NADPH oxidase complex (NOX_2) in their phagosomal membranes, which results in reactive oxygen species production and the maintenance of a high pH. Proper localization of a NOX_2 subunit to the phagosome was dependent on the small GTPase Rac2. In the absence of Rac2, NOX_2 did not assemble, high phagosomal pH was not maintained, and consequently, $CD8^+$ dendritic cells were not active in cross-presentation. These data provide a molecular rationale for why only particular subsets of phagocytes can trigger cytotoxic T cell responses to extracellular infections. — KLM

Immunity **30**, 10.1016/j.immuni.2009.01.013 (2009).

BIOCHEMISTRY

Matching Supply and Demand

In humans, a deficiency of the mitochondrial protein frataxin leads to Friedreich's ataxia, a progressive and fatal neurodegenerative disease. Frataxin has been implicated in heme metabolism and in the assembly of Fe-S clusters. In particular, it has been proposed to act as either an iron chaperone or an iron-storage protein.

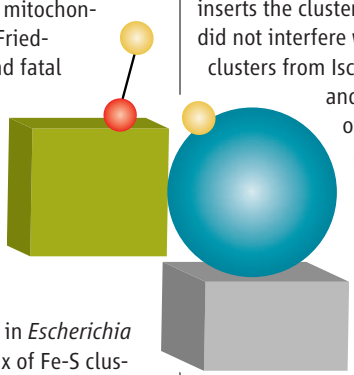

Adinolfi *et al.* propose that in *Escherichia coli*, frataxin fine-tunes the flux of Fe-S cluster synthesis. Using absorbance and CD spectroscopy, they showed that the bacterial frataxin ortholog CyaY (green in the above schematic) inhibits the formation of Fe-S clusters on the scaffold protein IscU (gray). Clusters are synthesized on IscU when iron (red) combines with sulfur (yellow) that has been extracted from cysteine by the disulfurase IscS (blue); IscU then inserts the clusters into the final acceptors. CyaY did not interfere with the transfer of assembled clusters from IscU to the acceptor ferredoxin and also did not affect the ability of IscS to convert cysteine to alanine. Fluorescence and NMR data revealed that CyaY did not compete with IscU for binding to IscS and that the IscS-binding surface of CyaY mapped to its iron-binding region. Mutants designed to disrupt the iron-binding capacity of CyaY reduced its inhibitory effect. The authors suggest that frataxins are iron sensors that interact with the IscS-IscU system at high iron concentrations and restrict the supply of clusters in the absence of needy acceptors. — VV

Nat. Struct. Mol. Biol. **16**, 390 (2009).

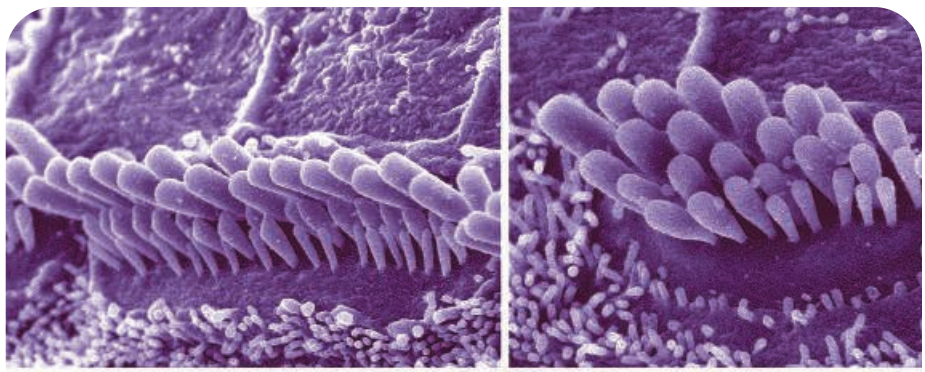

MOLECULAR BIOLOGY

RNA Silencing

Progressive hearing loss is a common disorder that appears to arise from a diverse range of genetic mechanisms, probably reflecting the anatomical and functional complexity of the human ear. Two studies of mice and humans with hearing loss have converged on a pathogenic mutation that is distinct from the 50 previously characterized mutations in that it affects a small regulatory RNA rather than a protein-coding gene.

In a genetic screen for hearing-impaired mice, Lewis *et al.* identified a mutation that, when present in heterozygous form, caused abnormalities of inner and outer hair cells [sensory receptors in the ear that are critical for hearing; wild-type (left) and heterozygous (right) inner cells are shown above] and progressive hearing loss beginning when the mice were 4 to 6 weeks old. The mutation resides within the functional "seed" region of a microRNA called miR-96 that is expressed in hair cells and that, like other microRNAs, is presumed to bind to and alter the expression of protein-coding messenger RNAs. Supporting the causal role of miR-96 in hearing loss, Mencia *et al.* found that two Spanish families with inherited progressive hearing loss harbored mutations in the seed region of the same microRNA and that these mutations impaired the processing of the RNA to its mature form. — PAK

Nat. Genet. 10.1038/ng.369; 10.1038/ng.355 (2009).

DEVELOPMENT

Endoderm Induction

There is great interest in generating pluripotent stem cells that might be used in regenerative therapies. However, before such cells can be applied effectively, methods that enable the directed differentiation of stem cells into a desired cell type, such as endoderm cells for the treatment of type I diabetes, are needed. The biological signaling factors activin A and Nodal are known inducers of endoderm, but Borowiak *et al.* have set out to find small, cell-permeant molecules that could channel embryonic stem cells into an endodermal lineage. Starting with a collection of 4000 compounds,

CREDITS (TOP TO BOTTOM): AGNIESZKA RZADZINSKA, *NAT. GENET.* 10.1038/NG.369; 10.1038/NG.355 (2009); ADAPTED FROM *NAT. STRUCT. MOL. BIOL.* **16**, 390 (2009)

they identified 27 primary hits—chemicals that promoted the expression of an endodermal marker—and further narrowed this list by negative selection and the examination of cell morphology to 2. These heptanoic acid derivatives (IDE1 and IDE2) directed the differentiation of roughly 70 to 80% of mouse and human embryonic stem cells into definitive endoderm. IDE1 and IDE2 come from a library of histone deacetylase inhibitors and appear to act through activation of the TGF-β signaling pathway. — BAP

Cell Stem Cell **4**, 348 (2009).

ASTRONOMY

Icy Remnants

Like Pluto, the dwarf planet Haumea is one of the largest known Kuiper Belt objects that lie beyond the orbit of Neptune. It is thought to be the remnant of an even larger body, which fragmented as a result of a collision, leaving behind Haumea itself, its two moons, Hi'iaka and Namaka, and a cluster of smaller icy debris whose surface properties and orbits have been shown to match those of Haumea. Now Fraser and Brown have taken near-infrared images of Haumea and its two satellites (illustrated at right) with the Hubble Space Telescope. The data showed that, like Haumea, Hi'iaka and Namaka are peculiar Kuiper Belt objects in that they are covered in pure water ice, reinforcing the idea that they are fragments of the collision that formed the triple system. Had Haumea gravitationally captured its two satellites, their surfaces would not be expected to match that of the dwarf planet, because Kuiper Belt objects have a wide range of surface compositions. — MJC

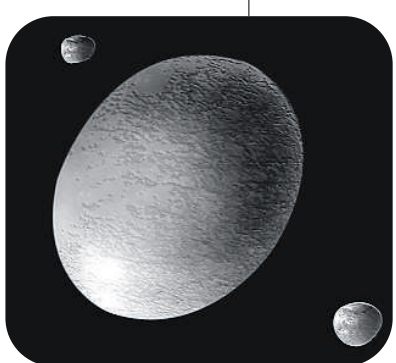

CREDIT: NASA

Astrophys. J. **695**, L1 (2009).

CLIMATE SCIENCE

Dust in the Wind

The ice core record of the past 800,000 years shows that glacial periods tend to be cold and dry, with above-average amounts of wind-blown dust in the air. In Antarctica, for example, where most of the dust trapped in the ice comes from southern South America, the closest terrestrial neighbor to the cold continent, dust was deposited during the last glacial period at a rate between 20 and 50 times higher than today. That general pattern makes intuitive sense, but what was the cause of the elevated dustiness? Sugden *et al.* show that dust peaks in Antarctic ice cores from the last glacial period occurred when rivers of glacial meltwater deposited sediment directly onto outwash plains in Patagonia, where the dust was easily mobilized by the stronger glacial winds, and that they were absent when the glaciers terminated directly into pro-glacial lakes. These observations may help explain why dust concentrations in Antarctic ice decreased before the main phase of warming occurred in Antarctica, when sea level began to rise and Southern Hemisphere sea-ice extent started to shrink. — HJS

Nat. Geosci. **2**, 281 (2009).

CHEMISTRY

When Ceria Met Titania

Mixed metal oxides, especially of redox-active metals, can play an important role in catalysis. Both titanium oxide, or titania (TiO_2), and cerium oxide (ceria, CeO_2) are widely applied individually, often in tandem with lower–oxidation-state transition metals such as platinum, palladium, and gold. It has been largely unclear, however, how these two high-valent metal oxides might behave chemically in tandem with one another. Park *et al*. sought to answer this question. Specifically, they used a combination of scanning tunneling microscopy (STM), photoemission spectroscopy, and density functional theory (DFT) calculations to examine the structures that form when ceria nanoparticles are grown on the TiO_2 (110) surface; growth was induced by deposition of cerium atoms onto the surface, followed by annealing in oxygen. The STM images revealed a structure for the adsorbed ceria nanoparticles that was rather distinct from that seen for adsorption on metal surfaces—dimers run diagonally to the rows and troughs of the titania surface—and photoemission revealed a reduced Ce^{3+} oxidation state. DFT calculations were consistent with the formation of Ce_2O_3 dimers. When gold was co-deposited along with the cerium, a highly active catalyst for the water-gas–shift and CO oxidation reactions resulted; much more effective than gold deposited on either metal oxide surface alone. — PDS

Proc. Natl. Acad. Sci. U.S.A. **106**, 4975 (2009).

www.sciencemag.org

Science

1200 New York Avenue, NW
Washington, DC 20005
Editorial: 202-326-6550, FAX 202-289-7562
News: 202-326-6581, FAX 202-371-9227
Bateman House, 82-88 Hills Road
Cambridge, UK CB2 1LQ
+44 (0) 1223 326500, FAX +44 (0) 1223 326501

Subscription Services For change of address, missing issues, new orders and renewals, and payment questions: 866-434-AAAS (2227) or 202-326-6417, FAX 202-842-1065. Mailing addresses: AAAS, P.O. Box 96178, Washington, DC 20090-6178 or AAAS Member Services, 1200 New York Avenue, NW, Washington, DC 20005

Institutional Site Licenses please call 202-326-6755 for any questions or information

Reprints: Author Inquiries 800-635-7181
Commercial Inquiries 803-359-4578

Permissions 202-326-7074, FAX 202-682-0816

Member Benefits AAAS/Barnes&Noble.com bookstore www.aaas.org/bn; AAAS Online Store www.apisource.com/aaas/ code MKB6; AAAS Travels: Betchart Expeditions 800-252-4910; Apple Store www.apple/eppstore/aaas; Bank of America MasterCard 1-800-833-6262 priority code FAA3YU; Cold Spring Harbor Laboratory Press Publications www.cshlpress.com/affiliates/aaas.htm; GEICO Auto Insurance www.geico.com/landingpage/go51.htm?logo=17624; Hertz 800-654-2200 CDP#343457; Office Depot https://bsd.officedepot.com/portalLogin.do; Seabury & Smith Life Insurance 800-424-9883; Subaru VIP Program 202-326-6417; VIP Moving Services www.vipmayflower.com/domestic/index.html; Other Benefits: AAAS Member Services 202-326-6417 or www.aaasmember.org.

science_editors@aaas.org	(for general editorial queries)
science_letters@aaas.org	(for queries about letters)
science_reviews@aaas.org	(for returning manuscript reviews)
science_bookrevs@aaas.org	(for book review queries)

Published by the American Association for the Advancement of Science (AAAS), *Science* serves its readers as a forum for the presentation and discussion of important issues related to the advancement of science, including the presentation of minority or conflicting points of view, rather than by publishing only material on which a consensus has been reached. Accordingly, all articles published in *Science*—including editorials, news and comment, and book reviews—are signed and reflect the individual views of the authors and not official points of view adopted by AAAS or the institutions with which the authors are affiliated.

AAAS was founded in 1848 and incorporated in 1874. Its mission is to advance science, engineering, and innovation throughout the world for the benefit of all people. The goals of the association are to: enhance communication among scientists, engineers, and the public; promote and defend the integrity of science and its use; strengthen support for the science and technology enterprise; provide a voice for science on societal issues; promote the responsible use of science in public policy; strengthen and diversify the science and technology workforce; foster education in science and technology for everyone; increase public engagement with science and technology; and advance international cooperation in science.

Information for Authors
See pages 807 and 808 of the 6 February 2009 issue or access www.sciencemag.org/about/authors

EDITOR-IN-CHIEF **Bruce Alberts**
EXECUTIVE EDITOR **Monica M. Bradford** NEWS EDITOR **Colin Norman**
MANAGING EDITOR, RESEARCH JOURNALS **Katrina L. Kelner**
DEPUTY EDITORS **R. Brooks Hanson, Barbara R. Jasny, Andrew M. Sugden**

Editorial **senior editor/perspectives** Lisa D. Chong; **senior editors** Gilbert J. Chin, Pamela J. Hines, Paula A. Kiberstis (Boston), Marc S. Lavine (Toronto), Beverly A. Purnell, L. Bryan Ray, Guy Riddihough, H. Jesse Smith, Phillip D. Szuromi (Tennessee), Valda Vinson; **associate editors** Kristen L. Mueller, Jake S. Yeston, Laura M. Zahn; **online editor** Stewart Wills; **associate online editors** Robert Frederick, Tara S. Marathe; **web content developer** Martyn Green; **book review editor** Sherman J. Suter; **associate letters editor** Jennifer Sills; **editorial manager** Cara Tate; **senior copy editors** Jeffrey E. Cook, Cynthia Howe, Harry Jach, Barbara P. Ordway, Trista Wagoner; **copy editors** Chris Filiatreau, Lauren Kmec; **editorial coordinators** Carolyn Kyle, Beverly Shields; **publications assistants** Ramatoulaye Diop, Carlos L. Durham, Joi S. Granger, Jeffrey Hearn, Lisa Johnson, Scott Miller, Jerry Richardson, Jennifer A. Seibert, Brian White, Anita Wynn; **editorial assistants** Emily Guise, Michael Hicks, Patricia M. Moore; **executive assistant** Sylvia S. Kihara; **administrative support** Maryrose Madrid

News **deputy news editors** Robert Coontz, Eliot Marshall, Jeffrey Mervis, Leslie Roberts; **contributing editors** Elizabeth Culotta, Polly Shulman; **news writers** Yudhijit Bhattacharjee, Adrian Cho, Jennifer Couzin, David Grimm, Constance Holden, Jocelyn Kaiser, Richard A. Kerr, Eli Kintisch, Andrew Lawler (New England), Greg Miller, Elizabeth Pennisi, Robert F. Service (Pacific NW), Erik Stokstad; **intern** Jackie D. Grom; **contributing correspondents** Dan Charles, Jon Cohen (San Diego, CA), Daniel Ferber, Ann Gibbons, Robert Koenig, Mitch Leslie, Charles C. Mann, Virginia Morell, Evelyn Strauss, Gary Taubes; **copy editors** Linda B. Felaco, Melvin Gatling, Melissa Raimondi; **administrative support** Scherraine Mack, Fannie Groom; **bureaus** New England: 207-549-7755, San Diego, CA: 760-942-3252, FAX 760-942-4979, Pacific Northwest: 503-963-1940

Production director James Landry; **senior manager** Wendy K. Shank; **assistant manager** Rebecca Doshi; **senior specialists** Steve Forrester, Chris Redwood; **specialist** Anthony Rosen; **Preflight director** David M. Tompkins; **manager** Marcus Spiegler; **specialist** Jason Hillman

Art director Yael Kats; **associate art director** Laura Creveling; **illustrators** Chris Bickel, Katharine Sutliff; **senior art associates** Holly Bishop, Preston Huey, Nayomi Kevitiyagala; **art associate** Jessica Newfield; **photo editor** Leslie Blizard

***Science* International**

Europe (science@science-int.co.uk) **editorial: international managing editor** Andrew M. Sugden; **senior editor/perspectives** Julia Fahrenkamp-Uppenbrink; **senior editors** Caroline Ash, Stella M. Hurtley, Ian S. Osborne, Peter Stern; **associate editor** Maria Cruz; **locum editor** Helen Pickersgill; **editorial support** Deborah Dennison, Rachel Roberts, Alice Whaley; **administrative support** John Cannell, Janet Clements; **news: europe news editor** John Travis; **deputy news editor** Daniel Clery; **contributing correspondents** Michael Balter (Paris), John Bohannon (Vienna), Martin Enserink (Amsterdam and Paris), Gretchen Vogel (Berlin); **intern** Claire Thomas

Asia Japan Office: Asca Corporation, Eiko Ishioka, Fusako Tamura, 1-8-13, Hirano-cho, Chuo-ku, Osaka-shi, Osaka, 541-0046 Japan; +81 (0) 6 6202 6272, FAX +81 (0) 6 6202 6271; asca@os.gulf.or.jp; **asia news editor** Richard Stone (Beijing: rstone@aaas.org); **contributing correspondents** Dennis Normile (Japan: +81 (0) 3 3391 0630, FAX +81 (0) 3 5936 3531; dnormile@gol.com); Hao Xin (China: +86 (0) 10 6307 4439 or 6307 3676, FAX +86 (0) 10 6307 4358; cindyhao@gmail.com); Pallava Bagla (South Asia: +91 (0) 11 2271 2896; pbagla@vsnl.com)

EXECUTIVE PUBLISHER **Alan I. Leshner**
PUBLISHER **Beth Rosner**

Fulfillment Systems and Operations (membership@aaas.org); **director** Waylon Butler; **senior systems analyst** Jonny Blaker; **customer service supervisor** Pat Butler; **specialists** Latoya Casteel, LaVonda Crawford, Vicki Linton, April Marshall; **data entry supervisor** Cynthia Johnson; **specialists** Eintou Bowden, Tarrika Hill, William Jones

Business Operations and Administration director Deborah Rivera-Wienhold; **assistant director, business operations** Randy Yi; **manager, business analysis** Michael LoBue; **manager, business operations** Jessica Tierney; **financial analysts** Priti Pamnani, Celeste Troxler; **rights and permissions: administrator** Emilie David; **associate** Elizabeth Sandler; **marketing director** Ian King; **marketing manager** Allison Pritchard; **marketing associates** Aimee Aponte, Alison Chandler, Mary Ellen Crowley, Julianne Wielga, Wendy Wise; **marketing executive** Jennifer Reeves; **marketing/member services executive** Linda Rusk; **director, site licensing** Tom Ryan; **director, corporate relations** Eileen Bernadette Moran; **publisher relations, eresources specialist** Kiki Forsythe; **senior publisher relations specialist** Catherine Holland; **publisher relations, east coast** Phillip Smith; **publisher relations, west coast** Philip Tsolakidis; **fulfillment supervisor** Iquo Edim; **fulfillment coordinator** Laura Clemens; **electronic media: manager** Lizabeth Harman; **project manager** Trista Snyder; **assistant manager** Lisa Stanford; **senior production specialists** Christopher Coleman, Walter Jones; **production specialists** Nichele Johnston, Kimberly Oster

Advertising director, worldwide ad sales Bill Moran

Product (science_advertising@aaas.org); **midwest/west coast/w. canada** Rick Bongiovanni: 330-405-7080, FAX 330-405-7081; **east coast/e. canada** Laurie Faraday: 508-747-9395, FAX 617-507-8189; **uk/europe/asia** Roger Goncalves: TEL/FAX +41 43 243 1358; **japan** Mashy Yoshikawa: +81 (0) 3 3235 5961, FAX +81 (0) 3 3235 5852; **senior traffic associate** Deiandra Simms

Commercial Editor Sean Sanders: 202-326-6430

Project Director, Outreach Brianna Blaser

Classified (advertise@sciencecareers.org); **u.s.: sales manager** Daryl Anderson: 202-326-6543; **inside sales representative** Tina Burks: 202-326-6577; **key account manager/midwest** Joribah Able; **east coast** Alexis Fleming: 202-326-6578; **west/south central** Nicholas Hintibidze: 202-326-6533; **sales coordinators** Rohan Edmonson, Shirley Young; **international: sales manager** Tracy Holmes: +44 (0) 1223 326525, FAX +44 (0) 1223 326532; **sales** Susanne Kharraz, Dan Pennington, Alex Palmer; **sales assistant** Louise Moore; **japan** Mashy Yoshikawa: +81 (0) 3 3235 5961, FAX +81 (0) 3 3235 5852; **advertising support manager** Karen Foote: 202-326-6740; **advertising production operations manager** Deborah Tompkins; **senior production specialist/graphic designer** Amy Hardcastle; **senior production specialist** Robert Buck; **senior traffic associate** Christine Hall; **publications assistant** Mary Lagnaoui

AAAS Board of Directors **retiring president, chair** James J. McCarthy; **president** Peter C. Agre; **president-elect** Alice Huang; **treasurer** David E. Shaw; **chief executive officer** Alan I. Leshner; **board** Alice Gast, Linda P. B. Katehi, Nancy Knowlton, Cherry A. Murray, Julia M. Phillips, Thomas D. Pollard, David S. Sabatini, Thomas A. Woolsey

AAAS
ADVANCING SCIENCE, SERVING SOCIETY

JULIUS AXELROD PRIZE

Supported by Eli Lilly Company Foundation

The Society for Neuroscience is pleased to announce the call for nominations for the Julius Axelrod Prize. The prize honors a scientist for his or her distinguished achievements in neuropharmacology or a related field and exemplary efforts in mentoring young scientists.

SOCIETY FOR NEUROSCIENCE

Deadline for receipt of nomination packages: FRIDAY, MAY 29, 2009.

For details please visit www.sfn.org/axelrod.

Working toward a better future?

So are we.

quality health selection delivery support

Diabetes. Heart disease. Cancer.

Every dollar spent on JAX® Mice & Services is an investment in our shared future. It supports our common research goals and helps to sustain the many valuable mouse models and resources available only from The Jackson Laboratory.

Ask for the J.

www.jax.org
1-800-422-6423

The Jackson Laboratory

Call for Papers

Science Signaling

Science Signaling, from the publisher of ***Science***, AAAS, features top-notch, peer-reviewed, original research. The journal publishes leading-edge findings in cellular regulation including:

- Molecular Biology
- Development
- Immunology
- Neuroscience
- Microbiology
- Pharmacology
- Biochemistry
- Cell Biology
- Bioinformatics
- Systems Biology
- Physiology and Medicine

Subscribing to ***Science Signaling*** ensures that you and your lab have the latest cell signal resources. To subscribe go to **http://pubs.aaas.org/pub7/pub7_setup.asp.**

Submit your research at: www.sciencesignaling.org/about/help/research.dtl

Science Signaling
AAAS
www.sciencesignaling.org

Scientific-Grade Spectroscopy for Life Sciences

QUANTUM EFFICIENCY TO 90% IN MINIMAL FOOTPRINT

The Ocean Optics QE65000 is a scientific-grade spectrometer that combines enhanced UV response and high sensitivity in a robust, low-noise instrument.

Its proprietary BRDF bench coating improves stray light performance and helps make the QE65000 more sensitive for demanding applications such as fluorescence, Raman, DNA sequencing and tissue analysis.

The QE65000 features a back-thinned FFT-CCD detector and TE-cooling, which enables integration times from 8 milliseconds to as long as 1,500 seconds.

The QE65000 can be configured with a choice of gratings, entrance aperture sizes, order-sorting filters and other optical bench accessories.

The QE65000 starts at under $12,000 and you can find more information at www.oceanoptics.com/products/qe65000.asp .

Ocean Optics www.oceanoptics.com | info@oceanoptics.com | +1 727-733-2447

Eppendorf Consumables – it's your sample

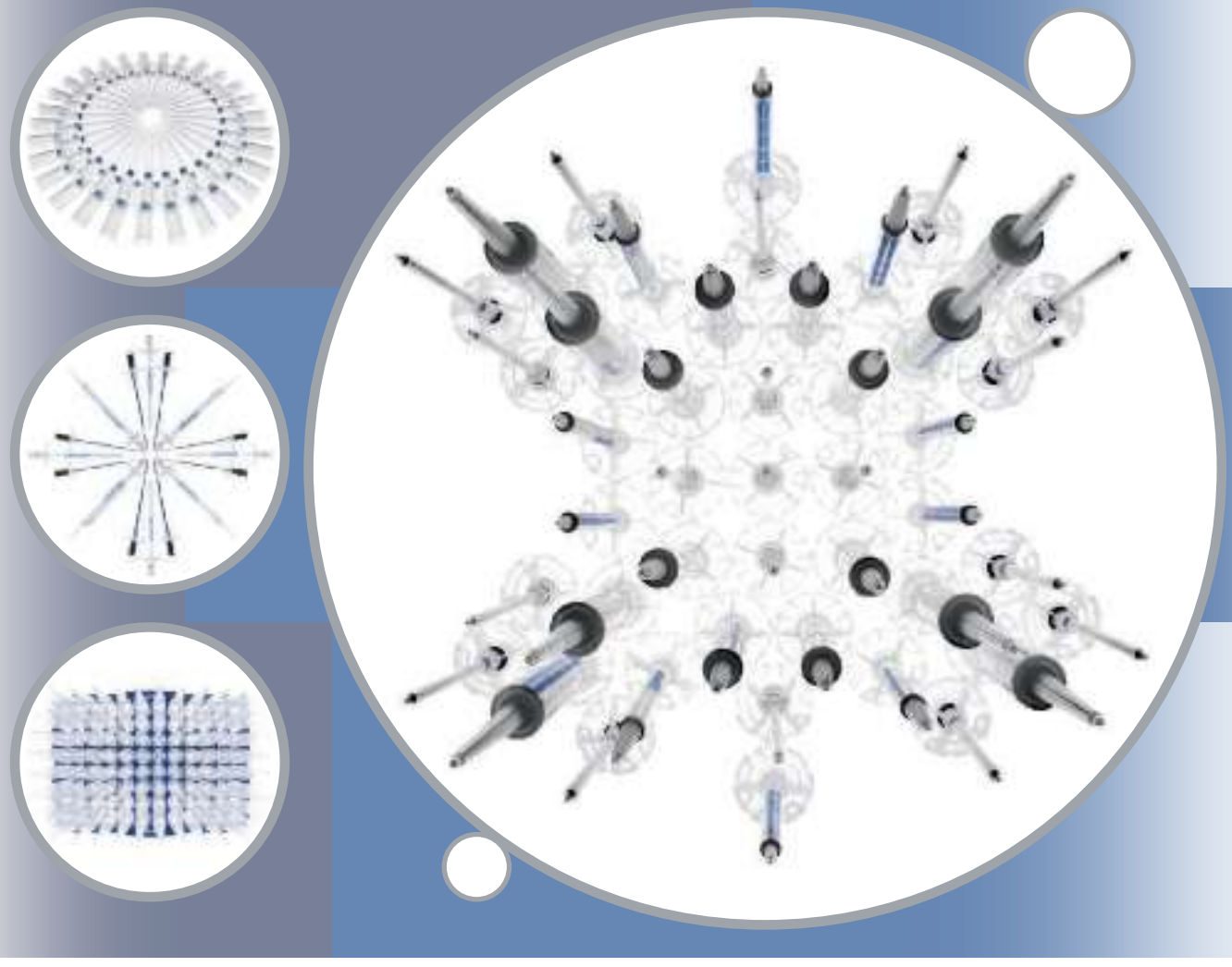

Make the best of it!

Top quality for your sample

Each of your valuable samples deserves the best treatment. See for yourself how the Eppendorf tips will save time and reduce costs.

With respect to material, fit, design and operating forces our tips set new standards. The close environment of each sample should be adapted to its specific quality and purity needs. This can involve a specific purity level or the absence of certain substances, but also stability, reliability, or geometry. The Eppendorf tips are designed to cover all of the specific needs of your samples!

Dispensing at its best! Eppendorf Combitips® plus

- Precise dispensing of liquids with high vapor pressure or higher viscosity
- Contamination-free dispensing due to positive-displacement principle
- Dispensing from 1 µl to 50 ml through 9 different sizes
- Automatic Combitip recognition with Multipette®* plus and Multipette* stream/Xstream®

Learn more about Eppendorf Combitips plus:
www.eppendorf.com/CBT

*Repeater in the U.S.

eppendorf

In touch with life

Your local distributor www.eppendorf.com/worldwide · **Application Support** E-Mail: support@eppendorf.com
Eppendorf AG · Hamburg · Germany · Tel: +49 40 538 01-0 · Eppendorf North America, Inc. · USA · Tel.: +1 800 645 3050

EDITED BY YUDHIJIT BHATTACHARJEE

ALL IN THE FAMILY

Charles II, the last king of the Spanish Habsburg dynasty, died without heirs in 1700 after a short, sickly life marked by deformity, impotence, and recurring bloody urine. A new genetic analysis suggests that royal inbreeding was to blame, as historians have long suspected.

Researchers led by Gonzalo Alvarez, a geneticist at the University of Santiago de Compostela in Spain, built a family tree of more than 3000 Habsburg relatives and calculated inbreeding coefficients for various family members. These coefficients give the probability that a person would have received identical copies of a gene from each parent—a chance that increases when the parents are blood relatives.

The inbreeding coefficient for the Habsburg kings increased 10-fold over five generations, from 0.025 in Philip I to 0.254 in Charles II. What that means, the authors reported 15 April in the online journal *PLoS One*, is that an extraordinary 25.4% of Charles II's genome could have consisted of pairs of identical genes—as many as in the child of a brother-sister union.

The authors suggest that Charles II's genome left him vulnerable to a host of rare recessive disorders, including a possible hormone deficiency and renal disease that would account for his unpleasant illnesses and death at age 38. But although inbreeding was "very likely" the culprit, says Rita Cantor, a geneticist at the University of California, Los Angeles, School of Medicine, only Charles's own DNA could pinpoint what made the king so sick.

CREDITS (TOP TO BOTTOM): WIKIPEDIA; NASA; U.S. LIBRARY OF CONGRESS/WIKIPEDIA; DEAN FALK/S. WITELSON *ET AL.*, *THE LANCET*, **353**, 19 JUNE 1999

A Croissant From the Sun

Every so often, powerful blobs of plasma and magnetic energy from the sun pummel Earth's magnetic field, playing havoc with satellites, GPS and cell phone signals, and electrical grids. Now, three-dimensional pictures of these so-called coronal mass ejections (CMEs)—40 of which have been observed by NASA's twin STEREO spacecraft since 2007—show that the ejections take on the shape of croissants as they billow through space. STEREO's measurements have also helped improve the accuracy of predicting a CME's intrusion into Earth's magnetosphere from within 12 hours to about three, says Michael Kaiser of NASA's Goddard Space Center in Greenbelt, Maryland.

The improved accuracy will help to better warn electrical companies and satellite operators when a strong CME event is on the way. Doug Biesecker of NOAA's Space Weather Prediction Center in Boulder, Colorado, says the new 3D imagery will also help researchers study the solar atmosphere and develop advanced CME models.

The Texture of Einstein's Genius

A new study of Albert Einstein's brain has identified unusual anatomical features that researchers say may be linked to the physicist's knack for conceptualizing physics problems and to his famed love of music.

When Einstein died in 1955 at Princeton Hospital in New Jersey, a local pathologist removed his brain, suspended it in preservative, and photographed and measured it. In a study published in 1999, a team led by Sandra Witelson of McMaster University in Hamilton, Canada, found that Einstein's parietal lobes—which are implicated in mathematical, visual, and spatial cognition—were 15% wider than normal parietal lobes.

Now Dean Falk, an anthropologist at Florida State University in Tallahassee, claims to have identified more than a dozen previously unrecognized features. They include a pronounced knoblike structure in the part of the motor cortex that controls the left hand; other studies have associated similar "knobs" with musical ability. (Einstein loved to play the violin and took lessons for many years as a child.) Falk says the parietal regions of both sides of Einstein's brain show a rare pattern of grooves and ridges that might be related to the great man's genius for conceptualizing problems. Einstein often reported that he thought in images and sensations rather than in words. Falk's findings are in press in *Frontiers in Evolutionary Neuroscience*.

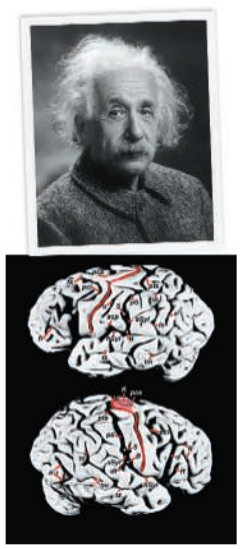

Frederick Lepore, a neurologist at Robert Wood Johnson University Hospital in New Brunswick, New Jersey, says that the features Falk identified are "unambiguously apparent" and that "Einstein's genius certainly exploited his ability to visualize physical problems, for example, what it would be like to ride on a beam of light."

An Editor With Punch

John Maddox, who captained *Nature* into the modern era with two transformative stints as editor, died on 12 April at the age of 83.

Maddox was born in Wales on 27 November 1925. After studying physics and chemistry, he taught theoretical physics at the University of Manchester in the United Kingdom. He went on to work as a science correspondent for *The Manchester Guardian* (now *The Guardian*) from 1955 to 1964.

Maddox brought his journalistic instincts with him when he joined *Nature* as its editor in 1966. He had manuscripts edited to make them more punchy and put in place a stringent peer-review system. *Nature* also became known for Maddox's animated and sometimes controversial editorials, and the journal grew to be a platform for opinionated and incisive science journalism. In 1973, he stepped down to start his own publishing company, resuming editorship of the journal in 1980. After his resignation in 1995, he was knighted for his services to science.

"He was most engaging, a real polymath," says Martin Rees, president of the Royal Society. "He exemplified [how] a generalist and a man of culture can contribute a great deal to the stimulus of the scientific community."

Published by AAAS

Are genomic studies off track?
448

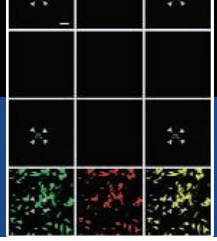

Behind a retracted paper
450

BIOMEDICAL POLICY

Draft Stem Cell Guidelines Please Many, Disappoint Some

They are not perfect, but they're a big improvement over what scientists have been living with since 2001. That's how most feel about the draft guidelines on human stem cell research released last week by the U.S. National Institutes of Health (NIH).

The proposed rules, to be finalized this summer, will expand the number of human embryonic stem (hES) cell lines available to researchers by eliminating the cutoff date for cell lines that qualify for federal funding. Acting NIH Director Raynard Kington predicted that "in a matter of months, we are likely to increase greatly the number of human embryonic stem cell lines eligible for federal funding." He said that NIH estimates up to 700 lines exist based on literature reviews and registries.

But some restrictions remain. The cell lines must be derived from surplus embryos donated by couples receiving fertility treatment. Stem cells lines derived through research cloning, or somatic cell nuclear transfer (SCNT), which many researchers are eager to try, will not be eligible.

Some researchers are also concerned about just how many of the existing hES cell lines will be eligible, given NIH's newly detailed requirements on informed consent. But most share the sentiments of stem cell researcher Sean Morrison of the University of Michigan Medical School in Ann Arbor, who says the proposed policy is "a huge advance" over the Bush policy and "a reasonable compromise based on where the science stands."

On 9 August 2001, then-President George W. Bush decreed that federal funding be restricted to research on stem cell lines derived before that date. To the delight of many scientists, President Barack Obama's 9 March executive order lifted those restrictions. But the order did not spell out the source of the embryos, leaving that to NIH to decide (*Science*, 20 March, p. 1552). Now researchers have the answer: The stem cells must be "derived from embryos created by in vitro fertilization (IVF) for reproductive purposes and were no longer needed for that purpose," NIH's draft states. The use of cells from "other sources, including [SCNT], parthenogenesis, and/or IVF embryos created for research purposes, is not allowed." It also notes that Congress has barred NIH from funding the derivation of stem cells from human embryos under the so-called Dickey-Wicker amendment.

Cells galore. Federally funded researchers will soon have access to hundreds more lines.

Kington explained to reporters last week that in drafting its guidelines, NIH heeded both legal restrictions and professional guidelines, including a 2005 report on stem cell research from the National Academies. "There's strong, broad support" for allowing research on surplus embryos from fertility clinics, he said, as shown by legislation that passed Congress twice (and was twice vetoed by Bush). "There's not similar broad support for using the other sources." Moreover, Kington pointed out, cell lines created solely for research either by IVF or SCNT don't yet exist as far as NIH is aware. NIH will review its policy as the science advances, he added. Funding continues to be allowed for research with induced pluripotent stem (iPS) cells—cultivated from adult cells—which many think will offer the same promise as cells from SCNT.

Many researchers would like to be able to work on hES cell lines derived in other ways—in particular, through SCNT. That technique might be used, for example, to make an embryo by inserting DNA from a skin cell of a patient with a disease into an enucleated egg. Researchers could then derive stem cells for studying that disease in test tube experiments.

Stanford University School of Medicine stem cell researcher Irving Weissman says the proposed ban on SCNT goes against the policy implied by Obama's earlier comments. "The NIH has not served its president well," Weissman said in a statement. He said there is no prohibition on SCNT in guidelines established by the International Society for Stem Cell Research (ISSCR) or by the National Academies.

It's unclear how many more lines will qualify under the new rules. A limiting factor could be the informed consent procedures. NIH hewed closely to those recommended by the National Academies and ISSCR. But Harvard University stem cell researcher George Daley points out that some of the 21 lines eligible for federal funding under the Bush policy would not qualify under the "exhaustive informed consent language" that was "not widely practiced before 2006." Therefore, there is some talk both at NIH and in Congress about the potential need to "grandfather" in some Bush-approved lines currently in use. (Grant applications already submitted to NIH will also need to pass muster.)

The draft policy includes a few other restrictions. NIH will not fund work that involves the possible introduction of pluripotent human cells (either iPS cells or ES cells) into the germ lines of any animals, a restriction recommended by the academies' report. Parthenotes, which are short-lived embryos created from an unfertilized egg, are also forbidden, as they qualify as human embryos under the Dickey-Wicker amendment.

The public has until 30 days after the policy is published this week in the *Federal Register* to submit comments, and NIH must issue final rules by 7 July. Some lawmakers have already weighed in. Representatives Michael Castle (R–DE) and Diana DeGette (D–CO), co-authors of the legislation that Bush vetoed, say they favor "more expansive guidelines"—a hint that an effort may be afoot to overthrow Dickey-Wicker. But Tom Harkin (D–IA), a Senate sponsor of the vetoed legislation, said he is "very pleased" with the NIH draft.

–CONSTANCE HOLDEN AND JOCELYN KAISER

CREDIT: JEFF MILLER/UNIVERSITY OF WISCONSIN, MADISON

Drought and the Maya
454

Neuroscience and compassion
458

ARCHAEOLOGY

Did Humans Learn From Hobbits?

Thousands of small, sharp-edged flakes of volcanic tuff and chert have been unearthed from the cave of the "hobbit," the roughly 1-meter-tall ancient human found on the island of Flores in Indonesia. The stone tools have puzzled researchers almost as much as the bones of the diminutive hobbits themselves. How could a hominid with a brain the size of a large pear craft tools? Now a detailed new analysis sheds light on the hobbit's technological capabilities and raises a new mystery: Why did the modern humans who arrived later on Flores make tools the same way hobbits did?

Archaeologist Mark Moore of the University of New England in Armidale, Australia, and his colleagues have been studying tools recovered from Liang Bua Cave on Flores since 2002. The most complete hobbit skeleton dates to about 17,000 years ago, but excavators claim other bones and tools date as far back as 95,000 years ago. All were excavated from below a layer of volcanic tuff dated to about 12,000 years ago. Above that layer, at 11,000 years and younger, researchers have found Holocene burials of *Homo sapiens*—modern humans—along with more tools.

Moore's team set out to analyze how the tools throughout the cave were made. The team reconstructed the sequence of blows struck thousands of years ago by analyzing the shapes of flakes, the position of scars left when flakes were struck off a stone, and other details. In a paper now in press at the *Journal of Human Evolution* and in a talk this week at a hobbit-themed meeting,* they report their analysis of 11,667 tools from five layers in the cave.

Moore found that hominids knapped stone in the same simple way throughout the 95,000 years represented in the cave layers they studied. Hominids first struck flakes off cores outside the cave. Then they brought large flakes into the cave to make smaller flakes, striking them directly with a hammerstone or using an anvil. They used a handful of simple knapping techniques in repeated patterns that changed little over time. For example, tools in both the upper and the lower layers of the cave averaged about nine blows per tool.

Tools in the younger, *H. sapiens* sediments tended to be made of higher quality raw materials; 60% in that layer were chert, compared with only 17% in the lower layers. And more of the Holocene tools were burned, apparently from being left near a fire. But they were constructed in the same way as those from lower layers.

To Moore, the "most parsimonious" explanation is that the hobbit, *H. floresiensis*, made the older tools, some found in layers with their bones. Later, *H. sapiens* arrived on the scene and made similar tools. Moore even suggests that there may have been contact between the species, with modern humans copying *H. floresiensis* toolmakers before they went extinct. "The striking thing to me is the degree of similarity in the various permutations [combinations of techniques]. I can see how different hominins might converge on the techniques themselves, but I find it more difficult to understand how those permutations could be so similar without more direct observation or interaction."

The analysis gets very high marks from other archaeologists. "They took a very close look at these materials, and I'd trust it," says Nicholas Toth of Indiana University, Bloomington. "A model study," pronounces archaeologist John Shea of Stony Brook University in New York state. Most important, the paper also "corrects an earlier impression that these are really sophisticated tools," adds Alison Brooks of George Washington University in Washington, D.C. Some early reports had implied that the Liang Bua tools were sophisticated like those of modern humans—a finding at odds with the hobbit's tiny brain. But many archaeologists think even small-brained hominids could make this kind of simple tool, which resembles much more ancient tools from Olduvai Gorge. In fact, Toth and Indiana colleague Kathy Schick have trained bonobos to make similar cutting-edge tools.

However, when it comes to humans imitating hobbits, many archaeologists aren't yet buying. Oldowan-type technology is so simple that modern humans could have converged on the toolmaking pattern because of environmental needs, Brooks and others said. More fundamentally, with a suite of similar tools throughout the cave layers, "*Homo sapiens* might have made the lot of them," says Shea. He points out that modern humans were moving through the Indonesian archipelago starting about 45,000 years ago and perhaps earlier. Toth agrees that when it comes to the identity of the toolmakers, "the jury is still out." Moore counters that some Liang Bua tools are about 100,000 years old—meaning they were made long before there's any sign of our species in the region. Having *H. sapiens* craft the older tools might be as surprising as humans copying hobbits.

–ELIZABETH CULOTTA

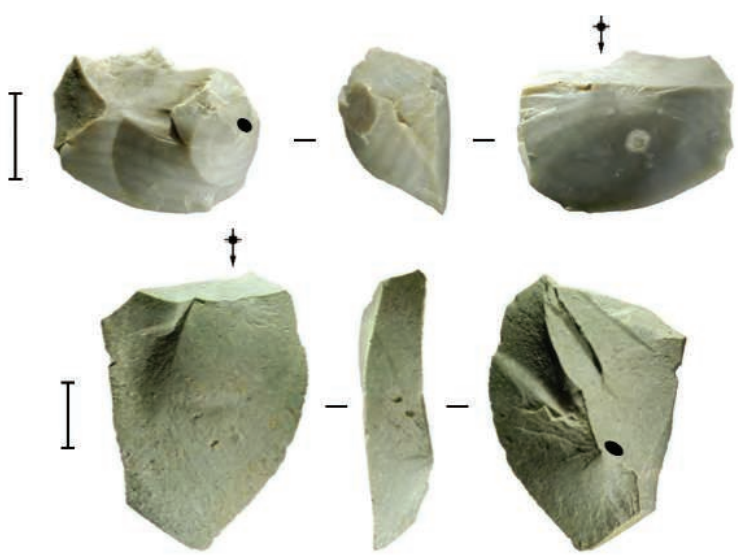

Copycat tools? A stone tool from younger *Homo sapiens* layers, seen in three views (*top*), resembles those from older hobbit layers.

*"Hobbits in the Haystack: *Homo floresiensis* and Human Evolution," Stony Brook University, New York, 21 April 2009.

Published by AAAS

BIOMEDICAL RESEARCH

Genome Scans: Impatient for the Payoff

A simmering debate in the genomics community about research strategy went public last week in commentaries published online by the *New England Journal of Medicine* (*NEJM*). A central disagreement concerns the likely value of chip-based genome scans to gauge inherited risks of developing common diseases. The discussion comes at a time when the U.S. National Human Genome Research Institute (NHGRI) is asking scientists to help set its course in a new 5-year road map.

In the most provocative of four *NEJM* articles, David B. Goldstein, director of the Center for Human Genome Variation at Duke University in Durham, North Carolina, says the first 100 or so genome-wide association studies (GWAS), which use gene chips to find associations between common gene variants and diseases, have identified important variants that appear to influence disease risk, but the impact of most of those variants is relatively low. He told *Science* that, once such association studies "have been run on the first few thousand patients for a given disease, there is only marginal return in pushing the sample sizes up further." Instead, he wants to shift more research to full sequencing of patients' genomes to find "rarer variants of larger effect" linked to disease.

Two views. David Goldstein (*top*) wants to move quickly to full-genome sequencing; David Altshuler sees more GWAS potential.

Other scientists, while agreeing with parts of Goldstein's commentary, argue that GWAS will be highly useful; they have already found more than 200 loci associated with certain diseases, even though most raise disease risks by relatively small amounts. They argue that improved chips may yet reveal a new cache of less common genetic variants that have a large effect on disease. Many also favor sequencing complete patient genomes, but only after the cost comes down.

The divergent perspectives about GWAS present "a classic example of the glass being half-full or half-empty," says Francis Collins, NHGRI's former director, who is writing a book on personalized medicine. "On the half-full side, researchers have now discovered a stunning number of genetic risk factors for common disease, after many years of frustration. While for the most part, those risk factors have only modest odds ratios, they are pointing us toward biological pathways that we desperately needed to understand." From the "half-empty" perspective, Collins says, "it is clear that most of the heritability for common disease has not yet been discovered—this is now generally referred to as 'the dark matter of the genome.' "

That dark matter is at the center of the current genomics debate. As part of a long-range planning effort, NHGRI is soliciting suggestions from scientists about the best ways to apply genomics to clinical problems and set the most productive course for genome sequencing. Teri Manolio, who directs NHGRI's Office of Population Genomics, says, "We plan to move in the direction that the science takes us," but strongly defends the results from the GWAS approach because it is identifying critical biological pathways involved in disease.

David Altshuler, who co-chairs the international consortium for the 1000 Genomes Project, which aims to sequence at low coverage the genomes of 1000 individuals, says that the massive new genome catalog he's helping to create will extend the reach of GWAS. The project will capture single-nucleotide polymorphisms (SNPs) that are rarer than those now available—including those present in 1% or more of the population—making it possible to probe genomes more completely (*Science*, 25 January 2008, p. 395). The consortium includes the Wellcome Trust Sanger Institute in the United Kingdom and the Beijing Genomics Institute in Shenzhen, China. Altshuler, with appointments at the Broad Institute in Cambridge, Massachusetts, and Massachusetts General Hospital in Boston, says the 1000 Genomes group aims to produce its first paper at the end of this year and a final publication by the end of 2010. While Collins hopes that the 1000 Genomes Project will help "uncover a whole new potential cache of less common variants of large effect," he cautions that those variants "will have to be tested in appropriate case-control studies, since there is no phenotypic information available on the 1000 Genomes DNA samples."

Judy H. Cho, genetics director of Yale University's Inflammatory Bowel Disease Center, who has helped identify some of the 35 or so genes now associated with Crohn's disease, says the GWAS approach "has been a victim of its own success. Four years ago, the concern was: Will we find *anything*? But now critics ask: Why didn't you find *everything*?"

Researchers contacted by *Science* agreed that far more work needs to be done before physicians can make good use of personal genomic assessments. Peter Kraft, a Harvard School of Public Health epidemiologist who co-authored with Harvard colleague David J. Hunter an *NEJM* commentary on the current limitations of genetic risk prediction, says, "If we go forward doing GWAS studies as we are now, testing for inherited susceptibility on the basis of common risk alleles may be more effective in 2 or 3 years."

Although it has become the focus of much public attention, predicting personal risk is not the point of GWAS, argues Joel N. Hirschhorn, a genomics researcher at the Broad Institute and Harvard University Medical School who wrote an *NEJM* commentary that offered a positive assessment of GWAS results. "The goal is not individual risk analysis but rather discovering the biological pathways underlying diseases," he says.

While he takes issue with Goldstein's overall assessment of GWAS, Collins agrees that "less common variants of larger effect … are going to account for a lot of the missing heritability, though copy-number variants will also likely play a role. To get those answers, we need to shift attention from SNP chips to actual sequencing." But despite recent advances in technologies, several scientists say, the full sequence strategy still looks expensive for now.

–ROBERT KOENIG

NEWSMAKER INTERVIEW

Brilliant Moves to Tackle Global Threats

Looming perils. Pandemics, climate change, and other challenges await Larry Brilliant in his new role.

Tackling big problems has been a lifetime pursuit for Larry Brilliant. A physician and epidemiologist, Brilliant played a key role in the World Health Organization's smallpox eradication program in the 1970s. More recently, he directed Google.org, the Internet company's philanthropic arm. In February, Brilliant stepped down from that role—amicably, he says—as Google narrowed its philanthropic focus to emphasize projects that tap into its strength in technology, such as Google Flu Trends, which maps flu activity based on online searches for flu-related terms. Brilliant stayed on as Google's Chief Philanthropy Evangelist but last week announced that he's leaving for a brand-new venture, a nonprofit foundation started by Jeffrey Skoll, the billionaire founding president of eBay.

Skoll has kicked in $100 million in seed money with a promise of more for the Skoll Urgent Threats Fund, which will tackle what he sees as five of the most urgent threats facing the planet: climate change, water scarcity, pandemics, nuclear proliferation, and conflict in the Middle East. As the organization's president, Brilliant's job is to make sure the money is well spent.

Brilliant spoke with *Science* on 16 April. His comments have been edited for brevity.

–GREG MILLER

Q: What's the idea here?

L.B.: The Earth has a number of urgent threats that are interwoven. If there were a single nuclear explosion in anger, all the work that we're doing on climate change, on trying to bridge the gap between rich and poor … would be set back generations. If any one of these urgent threats were to occur [or escalate], the work that we do would be so much more difficult. They have to be prevented or mitigated.

Q: How do you hope to accomplish that?

L.B.: We'll be trying to create the public will and confidence to tackle these seemingly impossible challenges. We'll be doing as much advocacy as grantmaking. Having the media savvy of Participant [Media, Skoll's production company, which has bankrolled socially conscious films such as *Fast Food Nation* and *An Inconvenient Truth*] was a huge draw for me. Jeff has learned how to stiffen the will of a community to fight the good fight.

Q: Will you be funding any research?

L.B.: Absolutely. I'm looking for research that changes people's minds. It's research that lets people know what you *can* do. In smallpox, when Bill Foege wrote his paper on selective epidemic control, we knew that by vaccinating 100 people—the right 100 instead of the wrong 100 million—you could extinguish the epidemic.

I'm very interested in digital surveillance technologies. In the area of drought, I'm very interested in ways to move water around. We've got plenty of water on the planet; we just don't have it where people live. Each of these different issues requires creative thinking and research to support breakthrough ideas that help change people's pessimism.

Q: What else?

L.B.: We need scientists for the next millennium. We don't have them. We don't have the half–genomic molecular biologist/half-epidemiologist and other dual-trained, cross-trained individuals or departments that are going to help us do the genomic epidemiology that will stop the next virus from jumping from an animal to a human and creating a pandemic. We are lacking scientific workforce for the 21st century because the problems of the 21st century have grown faster than the ability of training programs to keep up.

CREDITS (TOP TO BOTTOM): REUTERS/ROBERT GALBRAITH/LANDOV; MARCO ARCHETTI/HARVARD UNIVERSITY

ScienceNOW.org

From *Science*'s Online Daily News Site

Closer Look at Einstein's Brain. When a rare genius like Albert Einstein comes along, scientists naturally wonder if he had something special between his ears. The latest study of Einstein's brain, published in *Frontiers in Evolutionary Neuroscience*, concludes that certain parts of it were indeed very unusual and might explain how he was able to go where no physicist had gone before when he devised the theory of relativity and other groundbreaking insights. http://tiny.cc/F1MtB

Neandertal Babies Didn't Do the Twist. Giving birth is more difficult—and dangerous—for modern humans than for any other primate. Not only do human mothers have to push out babies with unusually big heads, but infants also have to rotate to fit their heads through the narrow birth canal. Now, a new virtual reconstruction of the pelvis of a Neandertal woman published in the *Proceedings of the National Academy of Sciences* suggests that Neandertal mothers also had a tough time giving birth to their big-headed infants—but the babies, at least, didn't have to rotate to get out. http://tiny.cc/Z5yEb

Red Leaves Say, "Bug Off!" Come autumn, leaves exchange their lush greens for deep reds, but why? Scientists have puzzled over this transformation for more than a century. Now a new study of aphids and apple trees in *Proceedings of the Royal Society B* reinforces the theory that the red hue wards off insects looking for a leafy snack or a place to nest. http://tiny.cc/dPeBA

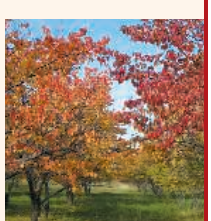

The Mother of All Pileups. In a faraway corner of the universe, a crash of cosmic proportions is under way, cramming more than 1000 galaxies into a space normally reserved for a handful. Astronomers studying the phenomenon report in *The Astrophysical Journal* that what they learn should improve their understanding about how the largest structures in the cosmos have evolved. http://tiny.cc/WqT5g

Read the full postings, comments, and more at **sciencenow.sciencemag.org**.

Published by AAAS

SCIENTIFIC MISCONDUCT

Science Retracts Discredited Paper; Bitter Patent Dispute Continues

In an unusual decision, *Science* this week retracted a 2005 report without the agreement of all the authors (see p. 463). The report, authored by a group at the Korea Advanced Institute of Science and Technology (KAIST) and at CGK Co., both in Daejeon, South Korea, describes a method, dubbed MAGIC, to identify drug targets by tracking protein movements in live cells (*Science*, 1 July 2005, p. 121). The retraction is based on an investigation by KAIST that concluded that although the technique might be valid, data in the paper were fabricated and "the extent of the fabrication is serious enough to damage the authenticity of the entire paper." The same group claimed in the journal *Nature Chemical Biology* in July 2006 that it had used MAGIC to identify an antiaging molecule; this report was retracted last July.

But in a twist, a legal battle is raging over the intellectual property at the heart of the discredited papers. "We strongly believe that there is value in the patent rights to the MAGIC technology," KAIST's Research Integrity Committee wrote in an e-mail responding to questions from a *Science* reporter. "Even though the data and results in the paper were fabricated, the idea of the methodology is original." And the senior author of both retracted papers staunchly defends the findings. "A number of strong evidences will be provided to prove that MAGIC technology and anti-aging compounds in two papers are real," chemical geneticist Tae Kook Kim, formerly at KAIST, wrote in an e-mail to a *Science* reporter. He added that he intends to take legal action "against several parties for my defamation and libel."

The convoluted saga began in July 2004 when Kim and several partners established CGK Co. to commercialize a technique for identifying drug targets. The method, MAGnetism-based Interaction Capture, works by coating a magnetized nanoparticle with a molecule of interest. The coated nanoparticle is then introduced into a cell in which a target protein has been tagged with a fluorescent label. Applying a magnetic field forces the nanoparticle to move. If the fluorescence moves in concert, that indicates that the molecule of interest has bound to the target protein. Kim and two members of his lab, Jaejoon Won and Yong-Weon Yi, are listed as inventors in a patent application, according to a translation of a Korean Intellectual Property Office document that CGK provided to a *Science* reporter.

After describing MAGIC in the *Science* paper, the group reported in *Nature Chemical Biology* how the technique had been used to identify a molecule, CGK733, that resets a cell's intrinsic aging clock by inhibiting a certain protein. Won was first author and Kim was corresponding author on both papers. In July 2006, the same month the report appeared in *Nature Chemical Biology*, CGK completed raising more than $2.5 million in venture capital, according to a statement CGK provided to a *Science* reporter on 10 March 2008.

But that statement also notes that CGK had trouble getting MAGIC to work. This led Yi—an author on both papers who by then had moved from KAIST to CGK to become the company's chief technology officer—to ask *Science* and *Nature Chemical Biology* to remove his name from the papers in December 2007, according to the CGK statement. On 11 February 2008, CGK informed KAIST of concerns about MAGIC. KAIST launched its own investigation on 12 February 2008.

On 28 February, the university informed both journals that although its investigation was continuing, the panel had come to a preliminary conclusion that "the two papers do not contain any scientific truth," according to an "editorial expression of concern" *Science* posted on its Web site on 3 March 2008 (*Science*, 14 March 2008, p. 1468). On 13 March, KAIST issued a press release in English summarizing the results of the preliminary investigation and alleging that Won, Yi, and Kim were involved in or aware of the misconduct. Unlike the press release, the final report later shared with *Science* does not assign responsibility for alleged misconduct.

In the e-mail to the *Science* reporter, Yi says he played a minor role in the project and even questioned Kim about his inclusion as an author "because I thought I hadn't contributed enough." Before the investigation, he claims, he hadn't suspected superiors would commit misconduct: "It was almost impossible for me to find out the truth" from them, he wrote.

In its July 2008 issue, *Nature Chemical Biology* published a letter signed by eight of the nine authors retracting the Won *et al.* paper. The letter states that the preliminary KAIST investigation "revealed several irregularities." One was that the "application of MAGIC technology for identifying ATM (a key protein) as the target of CGK733 was fabricated." It also says "our original notebooks and data are not available to substantiate the scientific claims of the paper." Kim did not sign the letter. An editor's note reads: "T.K. Kim supports the retraction of the paper but maintains that the irregularities are confined to Figure 2 of the paper—specifically, that the

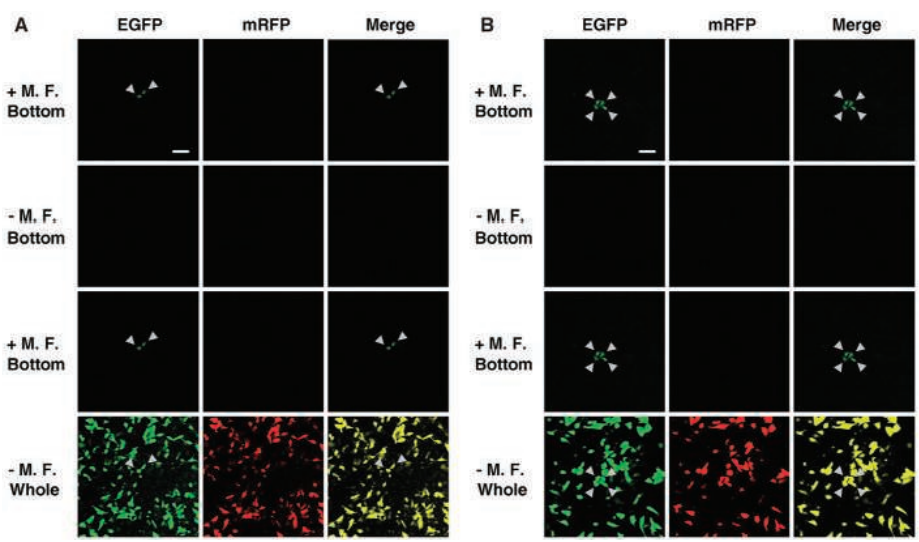

Seeing is not believing. An investigation by the Korea Advanced Institute of Science and Technology concluded that experiments to support these images were never conducted.

CREDIT: J. WON *ET AL.*, *SCIENCE* **309**, 121 (1 JULY 2005)

MAGIC screening was improperly performed and the chemical structure of CGK733 was misrepresented."

Retraction of the *Science* paper did not go as smoothly. *Science* requires that all authors agree to a retraction, says Monica Bradford, *Science*'s executive editor. But the journal could not reach one co-author, Neoncheol Jung, whose affiliation was listed as CGK. The whereabouts of Jung, who was CGK's founding CEO, remain unknown. Yeon-Soo Seo, a KAIST biochemist who served on the investigating committee, says his panel received one e-mail from Jung, who wrote that he was not involved in the case, he had nothing to do with the fabrication, and his name was included in the paper against his will. Lacking Jung's agreement and without full consent of authors and their institutions, Bradford says *Science* waited for KAIST to provide the investigating committee's final report, which had been completed in June 2008. But the report's release, she says, "got tied up with a legal dispute."

> *"The extent of the fabrication is serious enough to damage the authenticity of the entire paper."*
>
> —KAIST

The legal dispute is murky as well. CGK claims it reached an agreement in August 2004 with KAIST assigning intellectual property and commercial rights to the MAGIC technology to the company. But in March 2007, KAIST initiated legal action to reclaim those rights, according to statements from both CGK and KAIST. "KAIST hoped that through those legal proceedings they would have a chance to learn more from CGK," Bradford says she was told by a KAIST official. CGK, however, "was pushing for retraction," she says. CGK sent a copy of what it said is the KAIST investigating committee's final report, dated 22 May 2008, to *Science* editors, who had it translated. *Science* delayed taking action until it received an official version from KAIST, Bradford says.

Meantime, CGK devised an alternative to MAGIC, described by its researchers in the 10 December 2008 issue of the *Journal of the American Chemical Society*. CGK has applied for two patents, one of which has been granted, related to the technology, which, like MAGIC, relies on coated magnetic nanoparticles and fluorescent-tagged proteins. In an e-mail to a *Science* reporter, CGK charged that KAIST had delayed the retraction process to bolster its legal position; KAIST strongly denied this in an e-mail.

Although a Korean court on 9 December returned MAGIC patent rights to KAIST, the Korean Intellectual Property Office recommended on 19 January that the patent be rejected. The final decision is expected this summer; if it goes against KAIST, KAIST officials have said the company will appeal.

On 28 February 2009, KAIST forwarded to *Science* parts of the final report related to the *Science* paper. The authors could not provide notebooks or original data for any of the experiments described in the paper, according to a translation of the report prepared for *Science*. The KAIST report notes that Won and Tae Kook Kim admitted that experiments supporting Figure 2 in the *Science* paper, which purports to show magnetic manipulation of proteins tagged with fluorescent markers, were not carried out as reported. Based on the KAIST report, "The data, results, and conclusions in the Won *et al*. report are clearly not reliable," writes *Science* Editor-in-Chief Bruce Alberts.

Bradford says that when she informed senior author Tae Kook Kim that the paper would be retracted, he said he would agree if the wording was changed to indicate that only parts of the paper were not reliable. *Science* declined. "Our paper, as it stands, cannot be substantiated; it's got to go," Bradford says.

Repercussions for the Korean scientists have been severe. Last November, KAIST dismissed Tae Kook Kim; CGK is suing him for criminal fraud, says CGK's Dae-Joong Kim. Sometime after the papers were published but before problems arose, Won took an "associate specialist" position at the University of California, Los Angeles; he left that post in July 2008, according to a UCLA spokesperson who declined to describe the circumstances, citing privacy concerns. Won did not respond to an e-mail or to a voice mail message seeking comment.

Late last year, Yi sought to have criminal defamation charges brought against five members of KAIST's investigating committee, according to Yi's e-mail. Prosecutors declined to pursue criminal charges on 29 December, but Yi has appealed to a court.

The KAIST Research Integrity Committee says it "learned a lot from this incident" and is planning educational programs "to prevent research misconduct and to promote research ethics and integrity."

–DENNIS NORMILE

ScienceInsider

From the *Science* Policy Blog

An innovative approach to provide the best **malaria drugs** to the world's poor officially got under way last week in Oslo. Instead of providing money to governments to buy the medicines for their public health systems, the Affordable Medicines Facility for malaria (AMFm) (*Science*, 21 November 2008, p. 1174) will subsidize companies to sell the drugs on the private market at bargain prices. Most of the world's poorest rely on small pharmacies for their drugs, but to save money, they often pick cheap, ineffective drugs or counterfeits instead of state-of-the-art combination therapies. So far, AMFm has received $225 million to tackle the problem.

The U.S. Environmental Protection Agency has asked scientists how to revise the Clean Water Act to protect seas against **ocean acidification** from atmospheric carbon dioxide. Under the current rules, waters are designated as impaired if their pH deviates from naturally occurring levels by 0.2 units. But biologists say that some organisms are affected by smaller changes. A more complex approach would also take into account how organisms or ecosystems are affected differently by changing pH levels.

Last week's announcement that **William Brinkman**, former head of research at Bell Labs, would be nominated to run the $4.8 billion Office of Science at the Department of Energy suggests that Energy Secretary Steven Chu, another alum, hopes to tap the fabled lab's expertise at marrying basic and applied research.

Elsewhere … Bush science adviser **John Marburger** returned to Washington, D.C., to make science policy more scientific. The Union of Concerned Scientists released a report suggesting that **genetically engineered crops** have not outperformed more traditional varieties. **British spy service agency MI5 is looking** for a scientific adviser—the equivalent of James Bond's Q. Time to spell check your résumé.

For the full postings and more, go to **blogs.sciencemag.org/scienceinsider**.

Published by AAAS

A New Take on Doping in Iron-Based Superconductors

A year ago, physicists discovered a new family of high-temperature superconductors: materials that carry electricity without resistance at temperatures as yet inexplicably far above absolute zero. Immediately, researchers wondered whether the compounds, which contain planes of iron and arsenic atoms, work in the same way as the only other high-temperature superconductors, the copper-and-oxygen, or "cuprate," compounds that have defied explanation since their discovery in 1986 (*Science*, 16 May 2008, p. 870). New data suggest that a key step in making all the superconductors—"doping" them with impurities—plays a very different role in each of the two families.

In the cuprates, doping produces superconductivity by adjusting the number of electrons in the current-carrying copper-and-oxygen planes. But in the iron-and-arsenic compounds, doping appears to induce superconductivity by altering the material's crystal structure, report Helge Rosner and colleagues at the Max Planck Institute for Chemical Physics of Solids in Dresden. The result jibes with other evidence, says Dirk Johrendt, a chemist at Ludwig Maximilians University in Munich, who was not involved in the study. "One has to look to see if some sort of more subtle structural change is involved," he says.

In a cuprate such as strontium-doped lanthanum copper oxide, the lanthanum atoms lie between the copper-and-oxygen planes, in which the atoms form a pattern of squares. Without the strontium, the mobile electrons sit one to each copper atom and push against one another so hard that they get stuck in a giant traffic jam. The strontium atoms, which replace some of the lanthanum atoms, soak up enough electrons to break the impasse. The electrons then pair—in a way not yet fully understood—to flow without resistance.

Things seem to work similarly in an iron-based superconductor. For example, strontium iron arsenide is an ordinary metal. Replace enough of the strontium with potassium, however, and superconductivity appears at temperatures below 38 kelvin. But that's not necessarily because the number of electrons changes.

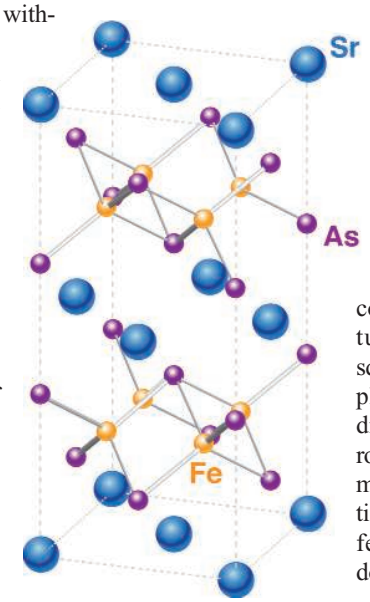

Either or. Replacing some of the strontium or iron makes strontium iron arsenide a superconductor.

To make that case, Rosner and colleagues left the strontium alone and instead replaced some of the iron with cobalt, an atom of almost the same size but with one more loosely bound electron. Such doping increased the density of mobile electrons but still induced superconductivity below 20 kelvin. The researchers also replaced some of the iron atoms with ruthenium atoms, which have as many loosely bound electrons but are bigger and put a larger strain on the crystal structure. Again, superconductivity emerged.

Those results suggest that changes in the material's crystal structure are the key. Physicists know that, at a temperature above the superconducting transition, an iron-and-arsenic superconductor undergoes a structural change in which the squares in the iron-and-arsenic planes squash slightly into a diamond shape. Neighboring rows of iron atoms also become magnetized in opposite directions in a pattern called "antiferromagnetism." The usual doping suppresses this transi-

Leverage: The Root of All Financial Turmoil

During the 1990s, physicists flocked to Wall Street and other financial hubs, eager to turn their analytical skills and phenomenological mindset to the problem of making a killing. Now that the world's stock markets are in retreat, they've turned to explaining why markets crash. According to one new analysis, leverage—the practice by hedge funds and other investors of borrowing money to buy investments—is the root of many nettlesome properties of financial markets that classical economics cannot explain, including a propensity to crash.

Given that in the buildup to the recent global economic meltdown hedge funds had been leveraging their deals by ratios of 30-to-1 (that is, borrowing $30 for every $1 of their own that they put in), it may seem obvious that massive leverage leads to trouble. But Stefan Thurner, an econophysicist and director of the complex systems research group at the Medical University of Vienna, Austria, and colleagues say their model shows that many of the distinctive statistical properties of financial markets emerge together as rates of leverage climb. "Leverage is the driver," Thurner says. "That wasn't obvious."

Financial markets behave in ways that, econophysicists say, classical economic theory cannot explain. Classical economics assumes that the fluctuations in stock prices conform to a so-called Gaussian distribution—a bell curve that gives little probability to large swings. In reality, the distribution has "fat tails" that make big changes more likely, and the shapes of those tails conform to a mathematical formula known as a power law. Classical economics assumes that the fluctuations are uncorrelated from one moment to the next, whereas big swings in prices tend to come together in the so-called clustering of volatility.

To try to explain those characteristics, over the past 5 years Thurner and colleagues have developed an "agent-based model" of a market. In such a computer model, virtual agents of various types interact according to certain rules, like robots playing a game. The researchers included hedge funds that could borrow to make their investments; banks to loan the money; "noise investors" who, like day traders, simply react to the market and have no other insight into the value of assets; and general investors who played the role of, for example, state pension funds.

The model contains more than a dozen adjustable parameters. However, Thurner and colleagues found that the maximum level of leverage exerts a curious, unifying effect. If they forbade leverage, the market behaved largely as classical economics would predict. But as they increased the maximum leverage,

SOURCE ILLUSTRATION: ALAN STONEBRAKER, ADAPTED FROM M. NORMAN, *PHYSICS* 1, 21 (2008)

SNAPSHOTS FROM THE MEETING >>

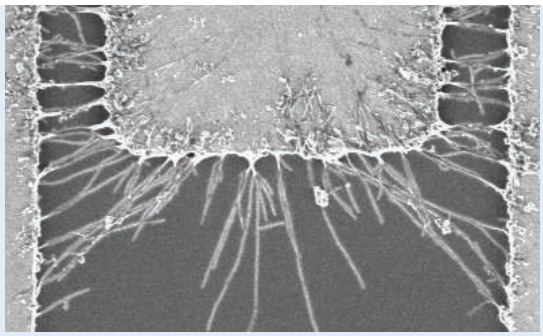

Dynamic duo. Carbon nanotubes are piped into place with microfluidic channels.

Piping in nanotubes. Carbon nanotubes could be made into minuscule electrical and mechanical devices on microchips—if researchers could put the things where they want them. Pushing tubes around with a tiny fingerlike probe is slow; depositing them in a solution is relatively imprecise. To do better, Sergei Loschek of the Chemnitz University of Technology in Germany and colleagues carve in a layer of polymer microfluidic channels to pipe the solution where they want it and rely on electric fields to pull the tubes into place. The polymer can be laid down and removed in minutes, Loschek says, making the method fast and precise.

A surprisingly squishy virus. Many viruses possess a hard shell of pure protein, but the influenza virus packs itself into a container with an inner layer of protein and an outer layer of fatty molecules called lipids. That shell is no harder than the lipid layer alone, as Iwan Schaap and colleagues at the British National Institute for Medical Research in London have shown by squeezing the viruses with a microscopic probe. The proteins in influenza's shell "are definitely not there to reinforce the virus," Schaap says. The question is, What purpose do they serve?

Back to school on university assignments. Four years ago, Germany scrapped its centralized system for assigning students to universities for competitive programs such as medicine. Now, students apply to individual universities. The best get accepted by all their choices whereas others get stuck on waiting lists—sometimes for half a year. But simulations by Christian Hirtreiter of the University of Regensburg and colleagues suggest that the old system placed as many students at their preferred schools. Moreover, they say, they can optimize the old system to cut by half the several percent of students whom it did not assign to one of their first-choice schools. **–A.C.**

tion and produces superconductivity. But so does the doping that leaves the electron density unchanged, suggesting that "you can get the same effect by making the structural change only," Rosner says.

The structural changes may be all that's relevant in the iron-and-arsenic compounds, Johrendt says. Rosner hesitates to go that far. In any case, such experiments underscore a difference between the iron-and-arsenic superconductors and the cuprates: Replace copper atoms in a cuprate's planes with anything else, and the material's superconductivity vanishes. **–A.C.**

the characteristics of real markets emerged together. "We can explain the fat tails, the right [power law], the clustering of volatility, all this," Thurner says. And when the leverage limit climbed to levels of 5-to-1 and beyond, the market became unstable and hedge funds went bust much more often.

"I thought it was rather brilliant," says Christoph Jan Hamer, an econophysicist with Solvency Fabrik in Köln, Germany. Hamer says he was impressed with a detail of the model: If leverage is high, then a tiny fluctuation created by the noise traders can trigger a much bigger swing. But Christian Hirtreiter of the University of Regensburg says, "I would think that leverage itself is not the problem. I would think it is a symptom of the problem."

Thurner, who managed a hedge fund that tanked, says that limiting leverage should help prevent crashes. He admits, however, that he would not have embraced that idea when the market was still going strong. **–A.C.**

Water Droplets Grow Faster Than Expected

Breathe on a pane of glass and droplets of water will condense on it. Physicists have analyzed that bit of everyday physics and have broken it down into three stages. First, tiny individual droplets form, or "nucleate." Then, the droplets grow. Finally, they bump into each other and merge. Assuming that moisture condenses out of the air at a constant rate, during the second phase, the volume of each individual droplet should increase linearly with time—that is, increasing by the same amount each second.

But is it so simple? Mordechai Sokuler of the Max Planck Institute for Polymer Research in Mainz, Germany, and colleagues have shown that, paradoxically, whereas droplets in a crowd do grow steadily with time, an isolated droplet grows faster as it gets bigger: Its volume increases in proportion to time raised to the 3/2 power.

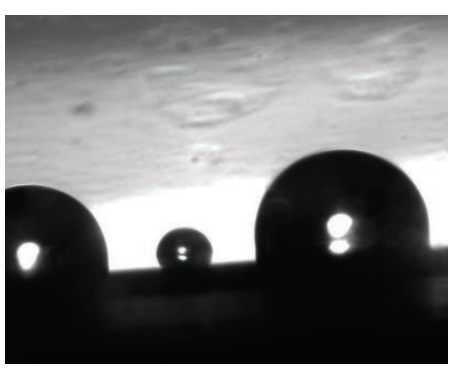

Peer pressure. An isolated droplet grows faster than one in a crowd, as the neighboring droplets affect the surrounding vapor distribution.

To prove it, Sokuler and colleagues performed one of the simpler of the thousands of experiments described at the meeting, growing drops in isolation or in groups on a small finger of glass in a chamber in which they could control the temperature and humidity. They then filmed the droplets condensing or evaporating. "I'm really glad that I got to do this project because it's so simple," Sokuler says. Nobody seems to have done the experiment before, he says.

At first blush, it seems contradictory that an isolated droplet would grow faster than one in a group, but the odd effect has an explanation, Sokuler reports. The growth rate depends on the amount of excess water vapor in the air. Above a single droplet, the vapor distribution conforms to the dome-shaped droplet, and the amount of vapor condensing into it at any moment increases with its radius. But when many droplets lie on a plane close together, each distorts the vapor distribution near its neighbors, effectively smoothing out the distribution across the plane. That makes all the droplets grow steadily in time, regardless of their size.

"His main argument was a change in geometry," says Thomas Thurn-Albrecht of Martin Luther University of Halle-Wittenberg. "This seems convincing to me." It's a simple effect, he says, "but sometimes to think of a simple experiment is an admirable thing." **–ADRIAN CHO**

CREDITS (TOP TO BOTTOM): SERGEI LOSCHEK/CHEMNITZ UNIVERSITY OF TECHNOLOGY; MORDECHAI SOKULER/MAX PLANCK INSTITUTE FOR POLYMER RESEARCH

Published by AAAS

A New Look at the Mayas' End

Climate researchers have fingered drought in the collapse of the great Maya civilization, but many archaeologists say it doesn't fit their data. Ultralocal paleoclimate indicators may spark a resolution

IN THE EARLY 8TH CENTURY C.E., THE MAYA city-state of Tikal eclipsed all rivals, becoming the most populous polity in the Americas. As many as 62,000 Maya nobles, artisans, and others squeezed into Tikal's crowded residential districts in what is now Guatemala; another 30,000 people, according to one estimate, toiled in verdant cornfields nearby. Tikal's divine kings ruled in splendor. They gleamed with jade jewels, commanded an army of artists and scribes, and presided over the construction of monumental causeways, temples, and pyramids.

During the century that followed, however, Tikal fell on hard times. Its building boom collapsed, its artists ceased to carve hieroglyphic inscriptions and paint murals, and its kings vanished. After 830 C.E., Tikal's population plummeted to just 15% to 20% of its peak. And Tikal was not alone. Elsewhere in the Maya world—a 324,000-square-kilometer area spanning southeastern Mexico and upper Central America (see map, p. 455)—dozens of other city-states crumbled between 695 and 1050 C.E. The big question is why?

Archaeologists have proposed many theories, from peasant revolts to plagues and volcanic eruptions. But starting in the 1980s, many researchers focused on the role of climate. The idea gained traction in the 1990s, and today paleoclimatic indicators from lakes in the Yucatán Peninsula and the ocean floor off Venezuela suggest that a series of devastating droughts struck the Maya lands beginning in 760 C.E. The evidence for these climatic catastrophes "is overwhelming now," says Richardson Gill, an independent archaeologist based in San Antonio, Texas. "How could 95% of the cities in the Maya lowland, which relied on surface water reservoirs that had to be replenished annually, survive a 9-year drought?"

Many other Maya archaeologists, however, say the megadrought theory just doesn't fit their findings. Some Maya centers fell before the proposed droughts began, whereas others flourished even during the parched times. Several cities in the humid lowlands failed before those in drier regions did. The wide variation in space and time of the collapse has left many climate scientists and archaeologists at loggerheads. "The idea that people were dying in the Maya plazas from thirst is all very overblown and oversensationalized," says archaeologist David Webster of Pennsylvania State University (PSU), University Park.

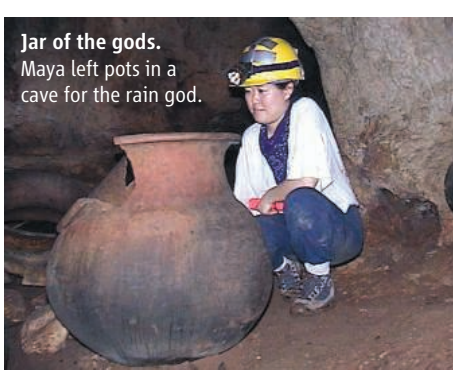

Jar of the gods. Maya left pots in a cave for the rain god.

New studies, several of which are being presented at the Society for American Archaeology (SAA) meetings in Atlanta, Georgia, this week, suggest productive ways out of this impasse. Researchers are using novel paleoclimatic indicators tied closely to specific archaeological sites to see just what ancient Mayans experienced; others are modeling the climatic impact of deforestation. These efforts show a new willingness among archaeologists to work hand-in-glove with the paleoclimatologists, says archaeologist Brian Fagan, a professor emeritus at the University of California, Santa Barbara (UCSB). "This is a form of multidisciplinary research that we never ever envisioned before," Fagan says. "It's very exciting."

The slow collapse

The Maya occupied one of the most environmentally varied territories in the world—a patchwork of coastal plains, scrub forest, tropical forest, and temperate highlands. Today, annual rainfall ranges from 500 millimeters in the north to 4000 mm in the central lowlands, but most rain falls from May to

CREDITS (TOP TO BOTTOM): JUPITERIMAGES; MICHAEL COE; H. MOYES

Published by AAAS

The power of water. Tikal's grand monuments depended on the favor of rain god Chac (*inset*).

December. To obtain water the rest of the year, the Maya settled along rivers and lakes and built reservoirs and canals to manage rainwater. By the Late Classic period, from 600 to 900 C.E., the Maya had founded more than 100 urban centers.

The collapse of the city-states began about 695 C.E., in the wet Petexbatún region of southern Guatemala, and proceeded sporadically over the next 350 years. Given the protracted timetable and the clues unearthed at individual sites, many archaeologists concluded by the early 1990s that the Classic Maya civilization was felled by a toxic cocktail of social and environmental factors, including war, overpopulation, soil erosion, and restive populations tired of the demands of self-aggrandizing rulers. It's a view many archaeologists still hold. "When you have something as complex as Classic Maya society, it's going to take a complex string of events to bring that to an end," says Andrew Scherer, an archaeologist at Baylor University in Waco, Texas.

But beginning in 1995, geologist David Hodell of the University of Cambridge in the United Kingdom and his team began pointing to the role of climate change. They analyzed gypsum—which accumulates as water evaporates in dry periods—in cores from a lake in northern Yucatán and showed that the period from 750 to 850 C.E. was the driest in a 7000-year-long period (*Science*, 18 May 2001, pp. 1293 and 1367). Other indicators supported this picture. A Swiss-led team studied titanium—which declines in river-borne sediments when water erosion decreases during parched periods—in a marine core from the Cariaco Basin off Venezuela. They found a dry period at 760 C.E. and then three severe multiyear droughts: 810, 860, and 910 C.E. (see graph, p. 456, and *Science*, 14 March 2003, p. 1731). Then in a 2007 paper in *Palaeogeography, Palaeoclimatology, Palaeoecology*, researchers analyzed a variety of data—oxygen isotopes for gauging rainfall, luminescence for studying the rate of water flow from a cave ceiling, and other indicators—from a stalagmite from the Macal Chasm cave in western Belize. They found four extreme dry periods centered at about 780, 910, 1074, and 1139 C.E.

Some archaeologists were convinced. But when others went looking for evidence of severe climate change at their sites, they could not find it. In the Petexbatún region, for example, a 7-year interdisciplinary project by Arthur Demarest of Vanderbilt University in Nashville, Tennessee, concluded that the inhabitants had a relatively stable diet of corn and meat throughout the collapse period. Skeletal remains displayed no increases in anemia or infectious disease, as might be expected in a starving populace. "If there's a drought, but it doesn't affect people's health, then what does it matter?" says Demarest. Instead, his team uncovered extensive evidence of a bitter, nearly century-long rivalry between the region's rulers over trade routes, which sparked intense warfare and the destruction of the site of Dos Pilas in 760 C.E.

One difficulty in correlating climatic and archaeological data at some sites is the relatively large error ranges of radiocarbon dates. Another may be regional variation:

Wet and dry. The Maya lived in a patchwork of environments, and some cities in wet areas collapsed before drier ones.

"Droughts can be quite localized," notes Jason Yaeger, an archaeologist at the University of Wisconsin, Madison. "So I'm a little skeptical about taking the Venezuela record and applying it directly to the Maya lowlands without local proxy records."

One way out is to devise paleoclimatic indicators that come directly from dated archaeological sites. That's just what zooarchaeologists Kitty Emery and Erin Kennedy Thornton of the University of Florida, Gainesville, set out to do, by using the animal bones that litter Maya deposits to track the proportions of wetland fauna over time. The researchers "have hit on something really exciting here that no one else has done before for the Maya. And that is to use the habitat information of the animals hunted, exploited, and eaten by the Maya as a proxy for climate change," says archaeologist Heather McKillop of Louisiana State University in Baton Rouge.

Emery and Thornton, who presented their unpublished study this week at SAA, compiled lists of animal bones from 22 dated Maya sites and selected 15,000 identified specimens from more than 65 species, including animals such as jaguars that sometimes hunt near water and storks and musk turtles that spend much of their lives in wetlands. Then the researchers gathered published habitat data on the proportion of time each animal spent in aquatic or wetland environments and verified this with ecologists. "We can say that a particular species will spend 20% its time in one habitat and 10% in another," says Emery.

She averaged the values of all species to get pictures of available habitat at given points in time and looked for changes in the proportion of wetland animals from 1800 B.C.E. to 1821 C.E. (Examining shifts in the proportion of wetland animals, rather than absolute numbers, should correct for varying hunting intensity and for animal responses to habitat change, she said.)

Although she cautions that larger samples are needed, the results so far fit well with the regional paleoclimate data: Swamp-loving species at 22 sites increased from 1% to 7% of specimens from 600 to 800 C.E., a period other proxies pointed to as relatively moist. But during the Maya collapse from 800 to 1000 C.E., swampland animals declined in all five watersheds from 7% to 2%, strongly suggesting that wetlands had shrunk markedly. However, when viewed from this ultralocal perspective, the dry periods look serious but not catastrophic, says Emery. Not one wetland species in the study disappeared completely between 800 and 1000 C.E. "I don't think there was anything that killed off enough fauna or enough landscape that it would have caused a collapse of human populations," she says.

Appeasing the rain gods

In bark-paper books, Maya scribes painted pictures of a rain god they called Chac. Artworks show Chac residing in a cave and cre-

SOURCE: AFTER SHARER AND TRAXLER, 2006

ating precipitation by pouring water from an overturned jar. Between 680 and 960 C.E., Maya in western Belize created a Chac-oriented drought cult, centered in caves, to appeal for rain, according to a study in the current issue of *Latin American Antiquity* by University of Arizona, Tucson, archaeologist Holley Moyes, Belize Institute of Archaeology president Jaime Awe, and their colleagues. At Chechem Ha Cave, the team mapped 300 meters of tunnels and excavated the central chamber. To illuminate the passages—which appear to have been used exclusively for ritual—the Maya carried wood torches that spewed charcoal, and Moyes's team plotted the specks on each excavated surface. The density pointed to the intensity of ritual use and to where ceremonies were performed. The charcoal provided 48 radiocarbon dates, showing that the Maya had visited the cave repeatedly from as early as 1300 B.C.E. to about 950 C.E. Over time, the Maya left behind 1901 ceramic shards or complete pots.

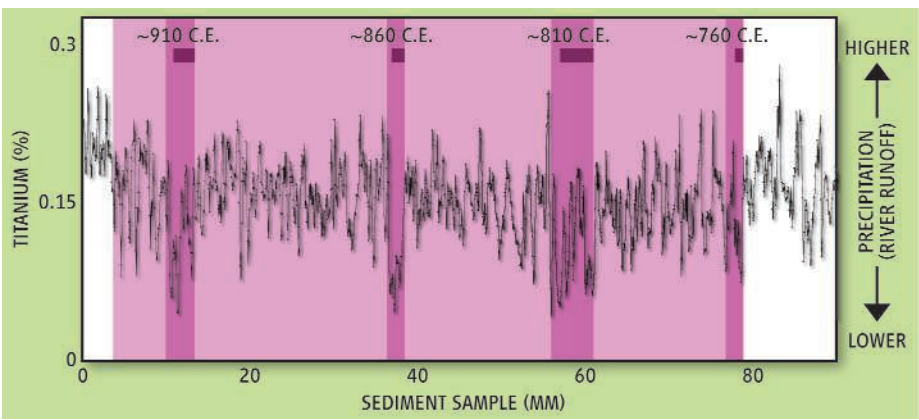

Sign of the times. The amount of titanium in sediment drops when rainfall and water erosion decline. These data from the Cariaco Basin spotlight four dry periods that may have affected the Maya lands.

The team discerned a major shift in ritual practices. Before 680 C.E., the Maya journeyed to the cave's central chamber to perform rites around a giant stalactite and pool, sometimes leaving broken pottery and twice leaving an intact jar and whole dish. After 680 C.E., however, ritualists deposited 51 whole jars and numerous other partially intact vessels, sometimes inverted, throughout the cave, including areas previously unvisited. "They left more ceramics between 680 and 960 C.E. than all the other periods put together," says Moyes. Many of the vessels were large, wide-mouthed jars likely used for water collection. "These jars are what rain deities use," says Moyes. "So this is the perfect gift for a rain deity."

The changing rituals occurred during a prolonged dry period in the region, from 700 to 1135 C.E., according to paleoclimate studies of luminescence, stable isotopes, and other data in a stalagmite from a cave only 15 kilometers away, done by geologist James Webster of the U.S. Environmental Protection Agency and colleagues. Moyes and Awe surveyed 53 caves in central and southern Belize and found a similar pattern of large, whole jars left on ledges during the proposed dry period—evidence, they suggest, of a previously unknown drought cult. "When things get really tough, I think the Maya elaborate on what they are willing to give these rain gods," Moyes says. "I think they are trying to give them nicer gifts."

Other researchers say that Moyes's work offers important insights. "This is a novel way to address the issue of drought," says Lisa Lucero, an archaeologist at the University of Illinois, Urbana-Champaign. "And the results support data from other sources, such as lake cores."

Clearing forests, drying climate

If drought helped drive the collapse of many Maya cities, the Maya themselves may be partly to blame: Their own practices, such as deforestation, may have changed climate and helped speed their downfall. That idea was popularized in environmental historian Jared Diamond's 2005 book *Collapse*.

The Maya cut trees to plant cornfields and use as fuel, both for cooking and for heating limestone to make lime for the plaster they lavished on their building projects. Evidence suggests that at least some city-states had extensively cleared forests at the time of the collapse. A 1988 pollen analysis indicated, for example, that the Maya at Copan cleared 23 square kilometers of pine forest by 800 C.E. And in a paper now in press in *Estudios de Cultura Maya*, archaeologists Isabel Villaseñor of University College London and James Aimers of the State University of New York, Geneseo, demonstrate that the Maya at Palenque and Calakmul substituted inferior clay for lime in their plasters just before the Classic collapse, suggesting most trees were gone.

At the SAA meeting, a team led by archaeologist Thomas Sever of the University of Alabama, Huntsville, reported the first results from a major computer simulation of climate and deforestation in the Maya lands. "There's always been the notional concept that deforestation leads to less rainfall," says Daniel Irwin, a research scientist at NASA in Huntsville, Alabama. "A lot of people have theorized about this impact going back in time to the Maya, but this, I believe, is the first time a research team has used climate models to demonstrate it."

Studies show that deforestation affects climate in several ways. A logged landscape absorbs more sunshine, and its new vegetation possesses shallow roots that reduce the amount of ground water returned to the atmosphere. It also offers less resistance to wind, so gusts can quickly replace humid air with dry air. To simulate deforestation, Sever and colleague Robert Oglesby, a paleoclimatologist at the University of Nebraska, Lincoln, used two climate models and ran two extreme scenarios—complete deforestation and an entirely treed landscape—to establish the boundaries of what might have happened.

Removing all trees across the Maya territory clearly changed climate for the worse. On average, says Sever, "there was a 3° to 5°[C] increase in temperature, and this led to a 20% to 30% reduction in rainfall." Each region was hit a little differently, however. "You get a varying amount of decreases in rainfall and increases in temperature," says team member Robert Griffin, a Ph.D. student at PSU, "so this adds a spatial pattern to it." Of course, not all Maya lands were deforested, and the study's next phase will examine how farm production affected the extent of deforestation and degree of drought.

Although Maya archaeologists clearly have their work cut out for them as they gather new kinds of data, some researchers think the picture is growing clearer. "Now that the data [are] coming in, we can really take the idea of climate change seriously," says UCSB's Fagan. "I don't think that anyone is saying that drought is the only cause, but it clearly is a significant factor."

–HEATHER PRINGLE

Heather Pringle is a contributing editor at *Archaeology* magazine.

CREDIT: ADAPTED FROM G. H. HAUG *ET AL.*, *SCIENCE* **299**, 1731 (2003)

From field to faculty. Kim (*right*) decided the time had come to swap reshaping health care in villages like this one in Bobete, Lesotho, for a chance to reshape academia at a leading university.

CREDIT: JUSTIN IDE/HARVARD UNIVERSITY NEWS OFFICE

NEWSMAKER INTERVIEW

Jim Kim on Why He Took the Top Job at Dartmouth

An Ivy League school has broken new ground by hiring an Asian global health specialist to build its future

Jim Yong Kim, 49, a global health leader whom Dartmouth College recently selected to be its next president, specializes in surprising juxtapositions. He is fluent in English, Korean, and Spanish. He was born in Seoul but grew up in Muscatine, Iowa. In high school, he was both valedictorian and quarterback. In 1987, Kim and fellow medical student Paul Farmer co-founded Partners in Health, now world-renowned for improving health care in Haiti and other poor countries. After completing his M.D., he earned a Ph.D. at Harvard University in medical anthropology and then launched a Partners in Health program to combat multidrug-resistant tuberculosis in Peru. The MacArthur Foundation awarded him a "genius" fellowship in 2003, and the next year he moved to Geneva, Switzerland, to run the HIV/AIDS program at the World Health Organization. Kim returned to Harvard in 2005 to direct the François-Xavier Bagnoud Center for Health and Human Rights and focus on health care delivery issues. He will take the helm at Dartmouth in July. Kim spoke with *Science* on 20 March; these comments are edited for clarity and brevity.

–JON COHEN

Q: Given your background, why do you want to head a university?

J.Y.K.: In every person's life you have to make a choice, and it's whether you continue to throw your own body at problems or step back and say my role is going to be leadership. I didn't think I was at that stage necessarily, but when Dartmouth asked whether I was interested in this job, those are thoughts that rushed into my mind. I've taken on some major problems in the last 25 years, drug-resistant tuberculosis and HIV, and those were fantastic experiences, but I felt very, very strongly that we needed to train the next generation of young people who would do this work.

Q: How did it happen?

J.Y.K.: A colleague at Harvard, Albert Mulley, was the chair of the selection committee. We sat down one day and talked about the science of health care delivery—he'd done such great work in the United States and was getting interested in global stuff. About a week later, he called me and said, "Hey, Jim, did you ever think about being a college president?" I said, "Sure, why not?" Here's why: One of my most important mentors, Howard Hiatt, former dean of the Harvard School of Public Health, said to me, "When people come to you and ask you to look at an academic job, even if you don't think that you'd take it, it's your duty as a citizen of the academic world to go look at it, think about it, and tell them what you would do if you were offered the job." I met with them four times. At each meeting I said, "I still don't understand why you guys would be interested in me, but if you were to offer me the job, here's what I'd do."

Q: And what's that?

J.Y.K.: One of the major crises in the world today is how we poorly execute around our most cherished social goals: health care, education, and social welfare. There's this overall ideology that once you have the pill, the surgical procedure, the content and the curriculum of a university course, the execution and delivery will take care of itself. Having the product is just the beginning. What I am most excited about in terms of going to Dartmouth is to really try and see if we can develop a science and an extraordinarily good practice in delivering around these goals. And it's about leadership, management, complex social organizations, engineering, and a lot of anthropology.

Q: Dartmouth emphasized that you're the first Asian to lead an elite Ivy League school. Does that have meaning to you?

J.Y.K.: It has a lot of meaning to my mother. And it seems to have a lot of meaning to the people in Korea. The Korean press has really responded to this with great energy. It's almost like I broke a barrier for Koreans.

Q: You're also the first global health specialist to lead an Ivy.

J.Y.K.: People who do global health now are not thought of as these fringe lunatics who wear boots and get malaria but [are thought of] as people who are relevant in the world today. We've kind of come of age if one of us can become president of an Ivy League institution.

Q: Your focus has always been on diseases of poverty. This is a major shift away from that, isn't it?

J.Y.K.: If I can train a whole bunch of people who are really committed to making the world better, and if as university president I continue to talk about social justice and health care in a way that makes sense to a broad population, I'm not sure my impact on global health is going to be diminished. I'm not going to Dartmouth to do global health; I'm going to Dartmouth to be president. But it turns out that the stuff I'm working on really fits with Dartmouth. It's a university that has a history of engaging with the rest of the world, and it's more committed to building the best possible undergraduate education than any institution I've ever seen.

Published by AAAS

CREDIT: HARISH TYAGI/EPA/CORBIS

NEUROSCIENCE

A Quest for Compassion

Guided by a passionate leader, a new research institute hopes to draw lessons from Buddhism to study altruism and make the world a better place

Back in 2000, James Doty was living the high life. He drove a Ferrari to work and was in the process of buying a private island in New Zealand, a villa in Tuscany, and a penthouse apartment in San Francisco. A neurosurgeon turned biotech investor, Doty had amassed more than $70 million, at least on paper. At 45, he was planning to retire, donate a large chunk of his fortune to charity, and divide his time between his three idyllic homes while doing medical volunteer work in developing countries.

Last month, Doty was standing behind a lectern at Stanford University in Palo Alto, California, explaining how he'd lost it all in the dot-com bust. "Within 6 weeks, I was $3 million in the hole," he said. He kissed the island, villa, and penthouse goodbye. But he decided, against the advice of friends and family, to follow through with stock donations that he'd promised before the crash to a handful of universities and health charities. (By holding on to the stock until the market recovered, the recipients ultimately received nearly $30 million.) Doty says that losing his material wealth made him more reflective. "Becoming completely detached from something you think you need is an interesting exercise," he said, his voice catching with emotion. "What you realize is … it doesn't define you as a person." His face flushed, he seemed unable to continue. Uncertainly at first, people began to clap.

It was an unusually personal speech for an academic conference, but it was also an unusual conference. The audience included psychologists, philosophers, economists, neuroscientists, and theologians who'd gathered for 2 days to inaugurate a new center at Stanford for the scientific study of compassion. Doty is the co-founder and director, and he provided $150,000 to get it started. The program has also received $1 million each from two Silicon Valley investors and $150,000 from the Dalai Lama, the most he has ever contributed to a research project.

The new Center for Compassion and Altruism Research and Education (CCARE) will study the biological roots of benevolent behavior and investigate whether mental exercises derived from the centuries-old tradition of Buddhist compassion meditation—but stripped of religious trappings—can foster compassion in nonbelievers. Doty says he is not a Buddhist and does not meditate, but he thinks such exercises could find many uses. Earlier this year, for example, he flew to Washington, D.C., to talk with military leaders about treating frontline medics and chaplains suffering from "compassion fatigue"—a form of traumatic stress brought on by caring for traumatized soldiers.

Doing good science in this area is tricky business, cautions CCARE co-founder William Mobley, a neurologist and soon-to-be head of the neurosciences department at the University of California, San Diego. On one hand, Mobley says, there's the risk of researchers' personal beliefs interfering with their objectivity. "Scientists are supposed to be professional skeptics, but there are people in the field … whose only interest is seeing God's face." And then there are experimental limitations, such as having to rely on first-person accounts of what's going through someone's mind during meditation. Even so, Mobley says, scientists who dismiss such work out of hand—and he has heard from plenty of them—are misguided. "Nothing is off-limits to science and critical thinking," he says. "We don't have great tools, but they're good enough to get started."

Defining compassion

One starting point for scientific inquiry is a clear definition of the object of study. Yet the recent CCARE meeting made clear that compassion is hard to pin down. If the participants had chosen, they might have drawn up a Venn diagram of overlapping terms—sympathy, empathy, and altruism, to name a few—preferred by scholars from different disciplines. Although most participants seemed receptive, the juxtaposition of science and faith wasn't to everyone's liking. "All of this quoting His Holiness left and right makes me a little queasy," grumbled one scientist.

Indeed, the meeting got off to a spiritual start with a haunting cello solo, *The Invocation for World Peace*, played by its composer, Michael Fitzpatrick, who has performed for the Dalai Lama. Thupten Jinpa, a former Buddhist monk who has been the principal English translator for the Dalai Lama since 1985, then described the long history of examining compassion in philosophy and religion and urged scientists to "approach the field with openness and perhaps humility." Central to the Buddhist concept of compassion, Jinpa explained, is the belief that the

Source material. A new center for the study of compassion and altruism aims to draw lessons from Buddhist teachings.

capacity to feel—and wish to relieve—the suffering of others is inborn. The ability to feel compassion for family and loved ones comes naturally, but people must deliberately cultivate compassion for wider "circles of concern," Jinpa said. "The highest form of compassion transcends all boundaries and embraces all sentient beings."

Psychologist Paul Ekman, a professor emeritus at the University of California, San Francisco, whose pioneering work on facial expressions and body language was the inspiration for the new TV series *Lie to Me*, spoke of the "amazing coincidence" between Charles Darwin's views on compassion and morality and those of Buddhism. Ekman noted that in *The Descent of Man*, Darwin wrote that one of humankind's noblest virtues "seems to arise incidentally from our sympathies becoming more tender and more widely diffused, until they are extended to all sentient beings." Ekman recounted reading the passage to the Dalai Lama (with whom he co-authored a book last year on emotion and compassion). When he was sure he had understood correctly, His Holiness declared: "I am a Darwinian," Ekman recalled.

Ekman also noted that Darwin's observation that the sight of suffering causes pain in those who observe it meshes well with the Buddhist notion that compassion involves feeling the suffering of others as unbearable. The idea also has a parallel in the research of cognitive neuroscientist Tania Singer of the University of Zurich in Switzerland, who reviewed her studies showing that brain areas involved in pain perception also respond when people observe another person wince from an electric shock (*Science*, 20 February 2004, p. 1121). Singer described newer evidence that one particular area, the anterior insula, has a key role in empathy. But, she added, such work points to a neural mechanism for just one facet of compassion, which, by most definitions, requires not just recognizing suffering in others but feeling compelled to do something about it.

The latter motivation appears to be innate, said Felix Warneken of the Max Planck Institute for Evolutionary Anthropology in Leipzig, Germany. He showed videos of experiments in which children as young as 18 months spontaneously came to his aid as he pretended to struggle with various tasks—reaching for a marker he'd dropped on the floor, for instance. Even chimpanzees sometimes give unsolicited help, Warneken and colleagues have found (*Science*, 3 March 2006, p. 1301), suggesting that spontaneous altruism is not uniquely human.

Philosopher Owen Flanagan of Duke University in Durham, North Carolina, prompted a lively discussion by asking whether compassion might be overrated. Contemporary moral philosophers and psychologists have suggested that morality comprises different modules (*Science*, 18 May 2007, p. 998), and Flanagan argued that putting too much emphasis on any single module, such as compassion, at the expense of others, such as a sense of fairness and justice, may not be in a society's best interest.

Translational meditation

Doty, whose life has cast him in the roles of both benefactor and beneficiary, is certain that more compassion would be a good thing. "I grew up in poverty and had a mother who was an invalid and a father who was an alcoholic," Doty said in a recent interview at his office at El Camino Hospital in Palo Alto, where he is again a practicing neurosurgeon. When he was 13, a local woman befriended him and taught him to meditate, which he says gave him the confidence and sense of control he needed to achieve his considerable professional and financial success. Having attained that mental fortitude, Doty says he stopped meditating in college.

Promoting humanity. James Doty's research goals spring from his life experience.

After hearing the Dalai Lama speak at Stanford in 2005 on a panel with several scientists organized by Mobley, Doty decided he wanted to foster more research in this area. After many discussions with other researchers, he and Mobley launched CCARE in January.

Several pilot studies funded by the project are getting under way, including a brain-imaging study with novice and expert meditators and a collaborative study between neuroscientists and economists that will be among the first to investigate the effects of charitable giving on its recipients—in this case undergraduate students who receive financial aid.

Stanford psychologist Jeanne Tsai recently completed a CCARE-funded study on a compassion-training protocol developed by Jinpa, who is currently a visiting scholar at the school. Undergraduate students without extensive experience with meditation or Buddhism took a weekly, 2-hour course in which they first learned meditation basics such as posture and breathing techniques. Next, over the course of 6 to 8 weeks, a trainer instructed them to picture a loved one as vividly as possible and concentrate on the sense of concern they feel for this person's well-being. In later sessions, they envisioned people they knew less well or even disliked and gradually expanded this concern to them.

Tsai randomly assigned 100 willing undergraduate students to receive the compassion training, training in mindfulness mediation, or classes in improvisational theater—to control for the possibility that simply learning a new skill or engaging in a new social activity is enough to elicit acts of kindness. (Volunteers were told they'd be participating in a study to evaluate several classes thought to improve physical and mental health.) Online questionnaires probed for changes in things such as empathic concern and the tendency to take another person's perspective. Participants also kept a daily diary of "positive and negative events," which the researchers are now combing for evidence of an uptick in compassionate acts. At the end of the experiment, participants read a letter written by a prisoner seeking correspondents and were given an opportunity to write back and/or donate money to a program aimed at stopping abuse inside prisons. Tsai says her group is now analyzing the data to see whether people who got compassion training wrote or donated more than those who didn't.

A similar study is getting under way to investigate whether compassion training for medical students might improve their bedside manner. If it works, it would illustrate Doty's greatest hope for CCARE: to take a centuries-old religious practice and extract from it a set of mental exercises with no religious overtones that can be scientifically proven to change the way people treat each other. It's a tall order, but without passion like Doty's, it wouldn't stand a chance.

–GREG MILLER

CREDIT: STANFORD OFFICE OF COMMUNICATION & PUBLIC AFFAIRS

Second sight. By studying old images, researchers like Ashley Pagnotta are stretching the time span of astronomical observation.

ASTRONOMY

Stars in Dusty Filing Cabinets

A campaign to digitize old sky photographs is squeezing new discoveries out of observations dating back to the mid–19th century

In 1962, astronomers discovered a shining dot in the sky that appeared to be moving at an astonishing 47,000 kilometers per second, or one-sixth the speed of light. The velocity indicated that the object—named 3C 273—was a few billion light-years away, yet it was so bright it could have been a nearby star.

To study the object further, researchers delved into a trove of the astronomical past: a collection of photographic plates at Harvard University dating as far back as the 1860s. They spotted 3C 273 on some 600 photographs taken with a variety of telescopes over 70 years, some of them days apart. The images showed fluctuations in the object's brightness on time scales as short as a week. Because the object could not be dimming or brightening faster than light could traverse it, the researchers inferred that in spite of being more luminous than a billion suns, the object had to be less than a light-week across—the size of the solar system. The finding helped characterize 3C 273 as a new type of object known as a quasar, one of the most powerful energy sources in the universe.

The discovery shows the value of historical sky observations, says Harvard astronomer Jonathan Grindlay, who is leading an initiative to scan the 500,000 plates in the university's collection and put them online. The project—called Digital Access to a Sky Century at Harvard (DASCH)—is part of a movement by a small but persistent group of astronomers to preserve, digitize, and study old astronomical photographs in hope of doing new science.

Proponents argue that old plates provide the only way modern astronomers can study astrophysical phenomena on time scales longer than a few decades. "Why would you want to wait another 100 years to learn how certain stars might be varying in brightness and position over long time periods when we have this resource right here in front of us?" asks Grindlay, referring to the Harvard collection.

> *"Each of these collections is like a time machine."*
>
> —GEOFFREY CLAYTON, LOUISIANA STATE UNIVERSITY

Preserving and scanning old plates, however, has been slow to win support from the broader astronomy community and funding agencies. Universities and observatories often discard plate collections when astronomers retire. Digitization projects in the United States and Europe—including DASCH—have proceeded in fits and starts on shoestring budgets.

"We live in a world where money is fixed—so the question is, what is the relative merit of the old data compared to new data?" says David Monet, an astronomer with the U.S. Naval Observatory's (USNO's) station in Flagstaff, Arizona, who until 2000 led the scanning of some 20,000 old plates for a searchable online sky catalog. Although he spent nearly 15 years on that project, Monet now thinks historical observations are of little value because of limitations on how accurately the brightness and position of objects can be determined on the images. "The thrill of going back 50 years" is one thing, he says, but "is the science case for doing so strong enough?"

Absolutely, say proponents, citing hundreds of newly identified variable stars in the tiny fraction of Harvard plates digitized to date. Meanwhile, the movement to digitize archives is getting a push from the Pisgah Astronomical Research Institute (PARI), a nonprofit in Rosman, North Carolina, which has started acquiring plate collections from institutions that no longer have room to house them. "Each of these collections is like a time machine. There's no substitute for having them," says Geoffrey Clayton, an astronomer at Louisiana State University (LSU) in Baton Rouge. "Even if you can't think of what can be done with them today, it's tremendously important that they be preserved."

Galaxies on glass

The Harvard collection occupies parts of three floors of an old brick building at Harvard College Observatory. The plates, slabs of thin glass coated with photosensitive emulsion, sit in crowded rows of green metal cabinets. Each rests in a yellowish brown envelope marked with handwritten details such as when the photograph was taken and with what instrument. The oldest is an image of the moon from 1849. Many show galaxies—a dot with a milky swirl around it, tiny yet somehow perfect. One plate shows the brilliant tail of comet Halley streaking across the sky in 1910.

The photographs were taken with some 20 telescopes operated by Harvard astronomers at the observatory, in other parts of the United States, and at remote observing

CREDIT: COURTESY OF ASHLEY PAGNOTTA

stations such as Arequipa Observatory on Monte Blanco, Peru. Around 1881, as more and more plates started coming in, the then-director of the observatory, Edward Pickering, realized that the work of documenting the positions and magnitudes of imaged objects had to be sped up. He put his Scottish maid, Williamina Fleming, on the job. She showed such talent that the observatory soon hired a legion of women, later known as the Harvard Computers, to catalog the observations.

Grindlay and his colleagues began digitizing the plates in 2008, using a souped-up commercial scanner and software specially written to translate the scanned images into crunchable data. The first step in the scanning process is cleaning each plate. "There's 100 years of Cambridge grime on them. If we didn't clean them, there would be 10,000 more stars per plate," says Alison Doane, curator of the collection. Doane and her assistant then transfer the plates to the scanning room where Edward Los, a retired software engineer, loads two at a time onto the machine. The plates move on a cushion of air, like a puck on an air-hockey table, for precise alignment. After 90 seconds, an image of each plate appears on a nearby computer screen.

Old and new. Curator Alison Doane preps plates before they are loaded onto a scanner customized for Harvard's digitization project.

CREDIT: Y. BHATTACHARJEE/*SCIENCE*

Digital haystacks

Usually, as in the search for 3C 273, researchers turn to archival plates in search of specific objects that have grabbed their attention. Bradley Schaefer, an LSU astronomer, is typical. In recent years, he has searched the Harvard archives and the collection of 300,000 plates at the 84-year-old Sonneberg Observatory in Germany for past records of recurrent novae. Recurrent novae (RNe) are white dwarfs that erupt in brilliance every few years or decades as they capture material from an orbiting companion star.

Schaefer says he studied thousands of images of sky regions where sightings of any of the 10 known galactic RNes had been reported. The tedious task paid handsome dividends, Schaefer reported at the American Astronomical Society meeting in Long Beach, California, in January. He and colleagues, including his student Ashley Pagnotta, discovered six previously unknown eruptions, established the orbital periods for all RNes except one, and predicted when they would erupt next. Schaefer says the most significant result was detecting long-term changes in the orbital periods of two RNes, evidence that both white dwarfs were gaining mass between successive eruptions. He concludes that these two RNes will "soon enough collapse" as Type 1a supernovae—white dwarfs that burn with an extraordinarily high but fixed amount of incandescence because they've reached a critical mass from the matter acquired from the companion. He says the finding supports the idea that Type 1as are born from RNes.

Grindlay says digitizing old plates can allow researchers to find interesting phenomena instead of being limited to searching for specific objects. "Once you've identified your needle in the haystack, then you can figure out what's going on with it," he says. His doctoral student, Sumin Tang, has been trying out the approach using an algorithm to search for variable stars on the 1500 or so plates that have been scanned so far at Harvard. Among three long-term variable stars she has found is one that appears to have dimmed significantly over the past 90 years. "One hypothesis is that the star is throwing off a dust shell to make itself obscured. Maybe we are seeing the star in an interesting stage in its evolution," says Tang, who is following up with targeted spectroscopic measurements.

Old data, new science

So far, the $4 million needed to scan the whole Harvard collection hasn't materialized. However, Grindlay is optimistic about persuading university administrators to make the funds available, not least because digitizing the plates would allow Harvard to reclaim the room the collection currently occupies. "You'll never find a more inexpensive way to clear out that much office space in Cambridge," he points out. The project has until now been supported by $600,000 from the National Science Foundation, used primarily to build the scanner and develop software to handle and analyze images.

Digitization efforts are under way at other places as well. More than a third of the 300,000 plates at the Sonneberg Observatory have been scanned in the past 5 years. The scanned images are sitting on compact discs, says astronomer Peter Kroll, who formerly worked at the observatory and now heads a software company—4pi Systeme GmbH—that has run the institution since late 2003. The company, which has bankrolled the project with profits from its other ventures, hopes to put the image database on the Web in the coming months, Kroll says.

The Royal Observatory of Belgium (ROB) in Ukkel, which like Harvard has developed a special scanner for old photographic plates, is digitizing a collection of some 3000 images of the moons of Jupiter and Saturn. The observations, made by Dan Pascu of USNO in Washington, D.C., will help "recalculate the orbital parameters" of the moons and study how the orbits of certain moons like Io "have changed over time," says Jean-Pierre de Cuyper, an astronomer at ROB, which is collaborating with USNO and the Paris Observatory.

For every collection being scanned, many others are gathering dust, says Michael Castelaz of PARI. In the past 5 years, the nonprofit has "rescued" half a dozen collections from institutions that could no longer house them. One example: some 10,000 plates from the Warner and Swasey Observatory at Case Western Reserve University in Cleveland, Ohio, which were sitting in shrink-wrapped cabinets in "the back of a large university storage room behind old office and classroom furniture," Castelaz says.

Castelaz says it will take a lot of time and tedium to put the images online. But to him and other proponents of archival astronomy, the effort is entirely worthwhile. As they see it, the future of astronomy would be poorer without revisiting its past.

–YUDHIJIT BHATTACHARJEE

Published by AAAS

SIGMA Life Science

Imagine a tool that gives **you the power**

to navigate a comprehensive universe

of continually curated **biological data**

and **interactive** genetic networks,

all with a **single, simple click.**

Your Favorite Gene SEARCH
Powered By INGENUITY

It's the all-new YFG. And it's free.

Think forward, work smarter with Your Favorite Gene powered by Ingenuity. > *sigma.com/yfg*

LETTERS

edited by Jennifer Sills

Retraction

SCIENCE HAS RECEIVED THE RESULTS OF THE KAIST RESEARCH INTEGRITY COMMITTEE INVESTIGATION of the Report published in *Science* by J. Won *et al*. (*1*). According to an English translation commissioned by *Science*, the committee found that the original data underlying the experiments reported in *Science* are not available and that many of the results in the paper were fabricated. Therefore, the data, results, and conclusions in the Won *et al*. Report are clearly not reliable, and *Science* is hereby retracting the paper.

BRUCE ALBERTS

Reference

1. J. Won *et al*., *Science* **309**, 121 (2005).

Opportunity in the Wake of Natural "Disasters"

THE MEDIA AND GENERAL PUBLIC OFTEN PERceive major natural disturbances as catastrophies that destroy the environment. However, this view is derived from the perspective of human population and infrastructure. From an ecosystem perspective, natural disturbances are often required to maintain ecosystem function (for example, some plant germination occurs by way of fire, and sediments and nutrients are redistributed by floods). The inappropriate impression of total destruction can give rise to inappropriate environmental responses, such as widespread and intensive salvage logging.

Unfortunately, in many cases, excellent opportunities for scientific and management learning from large natural disturbances are limited or lost because of the absence of readily available funding to implement a rapid research response. In the United States, the National Science Foundation has a small program called Special Grants for Ecological Research for immediate research response following major natural disturbances. This program does not provide for long-term support for research on ecosystem responses and post-disturbance management, and, to our knowledge, there are no parallels in other countries.

More funding for scientific and management learning after major natural disturbances is crucial given that (i) evidence suggests the prevalence of large natural disturbances will increase, and (ii) we need to better understand how to respond to such disturbances, especially to ensure that post-disturbance management activities do not make recovering ecosystems even more risk-prone to subsequent disturbances (*1*).

CREDIT: JUPITERIMAGES

After the flood. Although major events such as floods can be catastrophic for humans, ecosystems can benefit from them. More research funding can lead to a better understanding of these overlooked effects.

DAVID B. LINDENMAYER,[1]* GENE E. LIKENS,[2] JERRY F. FRANKLIN,[3] RACHEL MUNTZ[1]

[1]Fenner School of Environment and Society, The Australian National University, Canberra, ACT 0200, Australia. [2]Cary Institute of Ecosystem Studies, Millbrook, NY 12545, USA. [3]College of Forest Resources, University of Washington, Seattle, WA 98195, USA.

*To whom correspondence should be addressed. E-mail: david.lindenmayer@anu.edu.au

Reference

1. J. R. Thompson, T. A. Spies, L. M. Ganio, *Proc. Natl. Acad. Sci. U.S.A.* **104**, 10743 (2007).

The Hard Problem

IN THE LETTER "NEUROSCIENCE AND THE soul" (27 February, p. 1168), M. J. Farah and N. Murphy state that eventually neuroscience and the material system it describes may be able to explain all facets of being human. This idea strikes me as a somewhat naïve and simple faith in scientific progress rather than an accurate assessment of current thinking on this issue. Some years ago, the philosopher David Chalmers referred to the problem of consciousness (how physical processes in the brain give rise to subjective experience) as the "hard problem" (*1*). We are no closer to knowing or understanding how this happens today, so the problem remains hard and should be acknowledged as hard. In the absence of such understanding, personal opinions and beliefs about this question should not be presented as genuine knowledge.

EDWARD J. NEAFSEY

Department of Cell Biology, Neurobiology and Anatomy, Loyola University, Chicago Stritch School of Medicine, Maywood, IL 60153, USA. E-mail: eneafse@lumc.edu

Reference

1. D. Chalmers, *J. Consciousness Stud*. **2**, 200 (1995).

The Way Forward in the World of Robotics

N. SHARKEY EXAGGERATED THE DANGERS OF robotics use in his Perspective on "The ethical frontiers of robotics" (19 December 2008, p. 1800). Although the number of child-minding robots has increased in some countries, such technology should perhaps be regarded as a special case of ubiquitous medical computing, smart homes, and telemedicine; these are sources of ethical challenges, to be sure, but they do not warrant preying on emotions by

Published by AAAS

invoking threats of child neglect and abuse (*1*, *2*). Intuitively, we also suspect that nannybots are not good for the psychological development of children left in their care, but until empirical research demonstrates this, we must suspend judgment; such research might, in fact, find no harm at all. Similarly, we are as horrified and angry as Sharkey is when noncombatants are harmed by military robots, but whether such devices generally increase or reduce the number of civilian casualties is also an empirical question.

The job of applied ethics is not limited to warning about worst-case scenarios. Rather, it must include the identification and analysis of challenges raised by new technologies and the identification of suitable precautions, constraints, and trade-offs required to protect safety, privacy, and liberty.

Sharkey has made a start as regards robotics, but much more needs to be done. The agencies that fund these technologies should ensure that adequate resources are devoted to the analysis of concomitant ethical, legal, and social issues.

KENNETH W. GOODMAN[1]* AND NORMAN G. EINSPRUCH[2]

[1]Ethics Programs, University of Miami, Miami, FL 33101, USA. [2]Department of Electrical and Computer Engineering, University of Miami, Coral Gables, FL 33124, USA.

*To whom correspondence should be addressed. E-mail: kgoodman@miami.edu

References

1. K. W. Goodman, in *Ethics, Computing, and Medicine: Informatics and the Transformation of Health Care,* K. W. Goodman, Ed. (Cambridge Univ. Press, Cambridge, 1998), pp. 1–31.
2. K. W. Goodman, in *The Handbook of Information and Computer Ethics*, K. E. Himma, H. T. Tavani, Eds. (Wiley, Hoboken, NJ, 2008), pp. 293–309.

Response

I THANK GOODMAN AND EINSPRUCH FOR their thoughtful comments on my paper. I agree that the job of applied ethics should not be limited to worst-case scenarios, but I feel that the issues I raised about robotics in care and in the military need to be dealt with urgently before we sleepwalk into a world of neglect and indiscriminate killing.

I disagree with Goodman and Einspruch's suggestion that we should wait for the empirical evidence before placing ethical constraints on the use of autonomous weapons. There is an ongoing and accelerating proliferation of military robots in research, development, and application. What evidence there is about the development of smart bombs and weapons technology since World War II indicates an increase rather than a decrease in the numbers of civilian casualties (*1*). I value empirical methods, but not when it comes to betting on the lives of innocent civilians. Moreover, I am doubtful as to the impact of empirical findings about noncombatant deaths. Until these weapons can be shown to discriminate between civilians and combatants, I believe that they belong in the same class as mines and sensor-fuzed weapons that have been banned by many countries.

In addition, I do not regard child-minding robots "as a special case of ubiquitous medical computing, smart homes, and telemedicine." It is the mobility and exploitation of the children's anthropomorphic projection to create bonding, trust, and attachment that makes robots different from other smart sensing systems. Again, I think that waiting for empirical research to demonstrate psychological harm to children is dangerous. Suspending judgment about possible harm when many empirical studies show the lasting effects of neglect is not a good option.

Goodman and Einspruch and I agree that considerably more ethical appraisal is required before and at the time of developing new technologies rather than waiting to see the outcomes. History has taught us that once a technological genie is out of the bottle, we can't get it back in again.

NOEL SHARKEY

Department of Computer Science, University of Sheffield, Sheffield, S1 4DP, UK. E-mail: noel@dcs.shef.ac.uk

Reference

1. S. Peterson, "Smarter bombs still hit civilians," *The Christian Science Monitor*, 22 October 2002 (www.csmonitor.com/2002/1022/p01s01-wosc.html).

Culling Whales: Ethically and Ecologically Wrong

WE APPRECIATED THE POLICY FORUM "SHOULD whales be culled to increase fishery yield?" (L. R. Gerber *et al*., 13 February, p. 880), which showed that a removal of whale biomass would prove largely ineffective in rebuilding fish stocks, and hope that the work will have the desired impact on international discussions. However, it is important not to miss an opportunity to state that culling whales would be ecologically wrong and ethically unsound regardless of its likely consequences on fish stock biomass.

The complex and often fragile interactions among organisms, and between them and the natural environment, make it unreasonable to reduce ecology to a sum of cause-and-effect phenomena. Recent studies have shown the dramatic consequences of biodiversity loss in the oceans and its ripple effects on trophic webs (*1*–*3*). Such dramatic changes have occurred as a by-product of unsustainable fisheries management; fiddling with the system by actively removing cetacean populations would result in unfathomable damages.

Even if cetaceans were significantly hampering the rebuilding of fish stocks and their removal were inconsequential for the system, would anyone have the right to "intervene" and cull? From a purely ethical standpoint, the answer is no. It would be farcical to let an entire order of already endangered mammals take the blame for our gross mismanagement of the planet's living resources.

DAVID BALATA* AND STEFANO MARIANI

School of Biology and Environmental Science, University College Dublin, Dublin, Ireland.

*To whom correspondence should be addressed. E-mail: david.balata@ucd.ie

References

1. J. B. C. Jackson, *Proc. Natl. Acad. Sci. U.S.A.* **105**, 11458 (2008).
2. R. A. Myers *et al*., *Science* **315**, 1846 (2007).
3. B. Worm *et al*., *Science* **314**, 787 (2006).

Linguistics More Robust Than Genetics

IN THEIR RESEARCH ARTICLE "LANGUAGE phylogenies reveal expansion pulses and pauses in Pacific settlement," 23 January, p. 479), R. D. Gray *et al*. analyzed a very large lexical data set on 400 Austronesian languages to shed light on Polynesian origins. The study raises the classic issue of how closely patterns of genetic and linguistic evolution correspond, and which better reflects ancient population histories (the Research Article rejects some genetic-based reconstructions of Austronesian history).

Other recent studies in the Pacific have shown the robustness of linguistic phylogenetic reconstructions in comparison to genetic ones, when adequate linguistic data sets are available (*1*, *2*). Any congruence between linguistics and genetics is disrupted when populations speaking unrelated languages are in close contact. In such cases, genetic distinctions between groups rapidly become blurred, because genetic exchange

Letters to the Editor

Letters (~300 words) discuss material published in *Science* in the previous 3 months or issues of general interest. They can be submitted through the Web (www.submit2science.org) or by regular mail (1200 New York Ave., NW, Washington, DC 20005, USA). Letters are not acknowledged upon receipt, nor are authors generally consulted before publication. Whether published in full or in part, letters are subject to editing for clarity and space.

is generally more prevalent and pervasive than is language borrowing or adoption. Languages are more integrated sets of features than are gene pools. Language change does not occur in a social vacuum, and sociolinguistic pressures to maintain distinctions between groups can evidently have a strong inhibitory effect against linguistic convergence. This underlines the comparative power of historical linguistics for reconstructions of population histories, especially in contact situations.

JONATHAN FRIEDLAENDER,[1]* KEITH HUNLEY,[2] MICHAEL DUNN,[3,4] ANGELA TERRILL,[3] EVA LINDSTRÖM,[5] GER REESINK,[3] FRANÇOISE FRIEDLAENDER[1]

[1]23 Hunting Ridge Road, Sharon, CT 06069, USA. [2]Department of Anthropology, University of New Mexico, Albuquerque, NM 87131, USA. [3]Centre for Language Studies, Radboud University, 6525 HT Nijmegen, Netherlands. [4]Language and Cognition Group, PB 310, NL-6500 AH Nijmegen, Netherlands. [5]Department of Linguistics, Stockholm University, 106 91 Stockholm, Sweden.

*To whom correspondence should be addressed. E-mail: jfriedla@temple.edu

References

1. K. Hunley *et al*., *PLoS Genet*. **4**, e1000239 (2008).
2. J. S. Friedlaender *et al*., *PLoS Genet*. **4**, e19 (2008).

TECHNICAL COMMENT ABSTRACTS

Comment on "Colossal Ionic Conductivity at Interfaces of Epitaxial ZrO_2:Y_2O_3/$SrTiO_3$ Heterostructures"

Xin Guo

García-Barriocanal *et al*. (Reports, 1 August 2008, p. 676) reported colossal conductivity enhancements in yttria-stabilized zirconia (YSZ)/strontium titanate (STO) epitaxial heterostructures and claimed that the conductivity was ionic. I argue that the claimed ionic conductivity lacks experimental support and that the observed conductivity enhancement is most probably due to the p-type conductivity of STO.

Full text at www.sciencemag.org/cgi/content/full/324/5926/465a

Response to Comment on "Colossal Ionic Conductivity at Interfaces of Epitaxial ZrO_2:Y_2O_3/$SrTiO_3$ Heterostructures"

J. García-Barriocanal, A. Rivera-Calzada, M. Varela, Z. Sefrioui, E. Iborra, C. Leon, S. J. Pennycook, J. Santamaría

Guo suggests that the reported ionic conductivity of ZrO_2:Y_2O_3/$SrTiO_3$ heterostructures might be due to the electronic conductivity from the $SrTiO_3$. We point out shortcomings in his reasoning and underscore that our results show that any electronic contribution to the conductance is at least three orders of magnitude lower than the ionic contribution determined by ac methods.

Full text at www.sciencemag.org/cgi/content/full/324/5926/465b

CORRECTIONS AND CLARIFICATIONS

News of the Week: "India allows government scientists to own companies" by P. Bagla (6 March, p. 1278). The caption for the photograph was incorrect. It should have read, "More freedom. Kapil Sibal, Indian science minister, holds an Indian-made hand-held computer. The change in regulation will help government inventors go commercial."

Reports: "Mutations in the *FUS/TLS* gene on chromosome 16 cause familial amyotrophic lateral sclerosis" by T. J. Kwiatkowski Jr. *et al*. (27 February, p. 1205). The fifth author should have been listed as Charles R. Vanderburg. His affiliation also was incorrect; it should be Harvard NeuroDiscovery Center, Harvard University, Boston, MA 02115, USA.

Reviews: "Network analysis in the social sciences" by S. P. Borgatti *et al*. (13 February, p. 892). On page 892, the final sentence in the legend for Fig. 1 was missing. The sentence should read: "Dashed lines represent mutual repulsion."

Reports: "Coherence factors in a high-T_c cuprate probed by quasi-particle scattering off vortices" by T. Hanaguri *et al*. (13 February, p. 923). The present address for K. Ohishi should read: "Advanced Meson Science Laboratory, RIKEN, Nishina Center for Accelerator-Based Science, Wako 351-0198, Japan."

BIOETHICS

Early Steps Toward Animal Rights

Charles G. Gross

For the Love of Animals
The Rise of the Animal Protection Movement
by Kathryn Shevelow
Henry Holt, New York, 2008. 365 pp. $27.50, C$30.50. ISBN 9780805080902.

The abuse of animals has a long history, as do religious and philosophical justifications for such practices. Ancient Greek scientists dissected live mammals with no compunction. After all, unlike humans, other mammals did not possess the highest form of pneuma, rational or psychic pneuma. [However, the great Roman physician-researcher Galen did prefer to work on pigs rather than monkeys, to avoid the "unpleasant expression" (*1*) on the monkeys' faces when they were tied down and cut into.] Saint Augustine thought there was no "community of right" between humans and animals and therefore no restriction on using or killing them. Later Saint Thomas Aquinas set the Christian line: "By the divine providence [animals] are intended for man's use. … Hence it is not wrong for man to make use of them, either by killing or in any other way whatever." Aquinas did note, in a continuing tradition, that being cruel to animals might be bad as it could lead to being cruel to people. Descartes, the uber-rationalist pillar of the Enlightenment (and a physiologist as well), taught that humans and all other animals were machines. Nevertheless, he held that only humans had a rational soul, making them alone capable of feeling pain. In doing so, he deviated from almost every commentator from Aristotle on—including the church fathers, who realized that animals could suffer. The screams of a tortured animal, Descartes believed, were just squeaks of a machine.

Kathryn Shevelow's *For the Love of Animals* offers a fascinating account of the development of the animal protection movement in Great Britain in the 18th and early 19th centuries. There were plenty of animals to be protected—and not merely working animals. Bear baiting, dog fights, bull runs, cockfights, public executions of "criminal" animals, and a great variety of other entertainments involving the maiming and usually death of animals were popular entertainments across classes. These activities seem to have been endemic and gave us such terms as cockpit (where cocks fought), hangdog (the expression on the face of a dog executed for a crime like filching a piece of meat), dogfight, top dog, and underdog. Such occasions were considered valuable to developing British virility, as in The Beggar's Opera when Polly Peachum advised the beginning pickpocket Filch, "You must go to Hockley in the Hole and Marybone, child, to learn valour." Those were sites of bearbaiting, a euphemism for dogs tearing apart a chained bear or being killed in the attempt.

The book's hero is Colonel Richard "Humanity Dick" Martin, M.P., a fiery Irish aristocrat, scarred from multiple duels. He played a major role in the "world's first animal protection law," Parliament's "Ill-Treatment of Cattle Act" of 1822. In 1835, a year after he died, the act was extended to bulls, dogs, and even cats. Previously, starting in 1800, proposed laws against bull baiting or for the protection of other animals had been repeatedly defeated. The arguments against such laws were manifold but boiled down to three principal objections: If one stopped bull and bear baiting, next might be upper-class blood sports like fox hunting (not outlawed until 2005). The working classes should not be deprived of their traditional British entertainments. And Parliament had no right to interfere with personal life.

Banned in 1835. Bull baiting (print, 1820).

CREDIT: HULTON-DEUTSCH COLLECTION/CORBIS

The strengths of *For the Love of Animals* are the many well-told anecdotes. These illuminate the horrors of lower-class blood sports, the growth of the practice of keeping pets, performing animals, fake and real monsters, animal "crimes," and the colorful personalities of those supporting or opposing animal protection laws.

Alas, the book does not deal adequately or at all with a number of important developments in the history of animal rights through this period. One is the influence of Jeremy Bentham's utilitarianism. He wrote in 1789, "The day *may* come when the rest of the animal creation may acquire those rights which never could have been withheld from them but by the hand of tyranny.… The question is not Can they *reason*? nor Can they *talk*? but, Can they *suffer*?" (*2*). Another is the startling difference between the British (who Shevelow makes out to be particularly bloodthirsty) and the French. Francois Magendie and Claude Bernard, the French founders of modern experimental physiology, routinely carried out vivisection on awake animals and were French heroes. By contrast, English biologists such as Marshall Hall and Charles Bell inveighed against such practices. Indeed, a famous portrait of Bernard vivisecting a rabbit became an antivivisection poster in England. A third important but omitted subject is the widespread interest in evolution—from the writings of Jean-Baptiste Lamarck, Robert Chambers, Erasmus Darwin, and others—that clearly implied the continuity of human and other animals.

Lastly, it was disappointing that Shevelow ends her account before discussing the great struggle over animal experimentation in the 1870s. That decade, the formidable Frances Power Cobbe headed a coalition of feminists, abolitionists, vegetarians, and anti-immunizers against the medical and scientific establishment, including Thomas Huxley and Charles Darwin. The extended battle involved Queen Victoria and Disraeli, the arrest of the physiologist David Ferrier, and real street agitation. It led to the compromises that became the bases of laws regulating animal experimentation in the United Kingdom and, eventually, the rest of the world. All these developments have been treated in detail in works by Richard French (*3*) and Nicolaas Rupke (*4*), neither of which, curiously, is cited in the book.

Shevelow (a specialist in 18th-century British literature at the University of Cali-

The reviewer is at the Department of Psychology and the Neuroscience Institute, Princeton University, Princeton, NJ 08544, USA. E-mail: cggross@princeton.edu

Published by AAAS

fornia, San Diego) makes her position clear at the end of the book. There she solicits contributions to, among other groups, People for the Ethical Treatment of Animals, some of whose leadership and members have been involved in advocating and carrying out actions against animal experimentation. Although sometimes sentimental and even treacly, *For the Love of Animals* provides an interesting if rather anecdotal prehistory of the animal rights movement in Britain.

References

1. Galen, *On Anatomical Procedures: The Later Books*, W. L. H. Duckworth, Transl. (Cambridge Univ. Press, Cambridge, 1962).
2. J. Bentham, *An Introduction to the Principles of Morals and Legislation*, J. H. Burns, L. L. A. Hart, Eds. (Oxford Univ. Press, Oxford, 1996).
3. R. D. French, *Antivivisection and Medical Science in Victorian Society* (Princeton Univ. Press, Princeton, NJ, 1975).
4. N. A. Rupke, Ed., *Vivisection in Historical Perspective* (Croom-Helm, London, 1987).

10.1126/science.1173236

MULTICELLULAR ORGANIZATION

Hows and Whys of Coming Together

Rex L. Chisholm

The cellular slime molds occupy an interesting place in biology. Sometimes viewed by model-organism purists as a stepsister in the family of model systems, their intriguing place in evolution, their interesting life-style, and (to some extent) their gee whiz curiosity factor put *Dictyostelium* into nearly every basic biology textbook. In *The Social Amoebae*, John Tyler Bonner, the current patriarch of the slime mold community, provides a personal, insightful, and sometimes whimsical overview of the biology of these fascinating organisms. Bonner (an emeritus professor of biology at Princeton University) sets out to give a broad picture of the state of knowledge and to highlight key outstanding questions where study of the social amoebae might offer important new insights. He succeeds admirably at these goals.

The book consists of eight short chapters focused on topics that include evolution, ecology, behavior, morphogenesis, and differentiation. In each chapter, Bonner lays out his view of what is known about *Dictyostelium*, placing it in the context of broader biological questions of biology, and points to interesting aspects that still need to be explored.

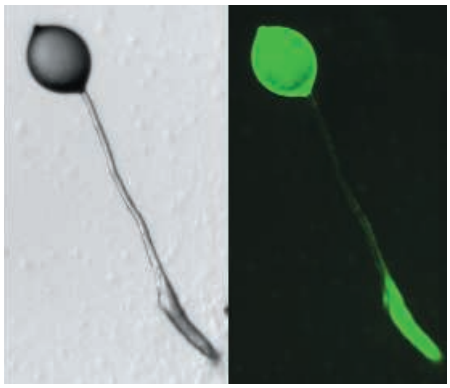

Marked for study. A *Dictyostelium discoideum* fruiting body whose spores have been tagged with green fluorescent protein in (left, transmitted light; right, fluorescent microscopy).

When considering evolution, the author focuses on why these organisms might have come to be "social." A crucial feature of the social amoebae life cycle is the transition from single amoebae to a multicellular "tissue" composed of hundreds of thousands of individual cells. It is widely believed the main value of this interesting example of biological cooperation is to maximize the spread of the organism. Typically, this cooperation is driven by starvation—a key biological indicator of hard times. Most of the social amoebae use the power of cooperation to produce structures that elevate the spores from the surfaces on which the cells had been growing, with the spores sitting atop (or along) a stalk of some sort. Bonner discusses the idea that this maximizes the possibility of insects picking up spores and carrying them much greater distances than might happen by more passive modes of distribution, such as being blown by the wind. He wonders whether the social nature of the slime molds arose after the appearance of insects that could serve to maximize the dispersion of spores. One interesting observation Bonner notes is that the evolutionarily more recent species tend to have larger fruiting bodies than the more ancient species—a potential point of support for ongoing selection for maximizing spore dispersion.

The social amoebae provide a nearly unique experimental opportunity to explore biological "altruism." A typical feature of their life cycle is the sacrifice of some cells to become stalk cells that ultimately die and play only a supporting role for the spores that have the opportunity to live on. Bonner explores how this behavior is influenced by genetic relatedness. It is interesting and important that mixtures of species will sort themselves out—limiting the benefit of loss of self to genetically related individuals. One fascinating story highlights mutants that cheat death by preferentially becoming spores when mixed with normal cells, but which produce normal fruiting bodies and stalks when in pure populations composed only of cheaters. This behavior raises a number of compelling questions for biologists to ponder—exactly Bonner's goal for telling the story.

Although it is amazing that individual cells sacrifice their individuality for the good of the species, equally astonishing are the complex behaviors the tissues they form can exhibit. In his chapter on behaviors of the amoebae and cell masses, Bonner highlights the phototactic and thermotactic capabilities of the multicellular pseudoplasmodium or slug stage. There is still much to be learned about how these tissues coordinate activities of thousands of cells to produce a slug that can crawl directionally in response to its environment. Unlike the typical metazoan, social amoebae populations grow to maximize their numbers of individual amoebae, whereas most multicellular organisms grow in the context of tissue formation. Bonner suggests slime molds offer many lessons about how to make a tissue. He describes what happens when a slug is cut in half—it forms two new slugs that ultimately produce two smaller but normally proportioned fruiting bodies—or when one slug happens to crawl across another—they are as likely to swap posterior halves as not. Bonner correctly notes that we have a lot to learn from these "simple" organisms.

The Social Amoebae
The Biology of Cellular Slime Molds
by John Tyler Bonner
Princeton University Press, Princeton, NJ, 2009.
156 pp. $19.95, £11.95.
ISBN 9780691139395.

The Social Amoebae is certainly a must-read for anyone working with these organisms. It should also reward any biologist interested in social behavior, ecology, and evolution. An easy Sunday afternoon read, the book will keep the biologist engaged and provide the nonbiologist many interesting phenomena to ponder. In an era when research is driven by technological developments and sophisticated instrumentation, Bonner celebrates the power of keen observation, simple but insightful experiments, and the importance of keeping in mind the big picture. These are worthwhile reminders for all who love science.

10.1126/science.1172838

The reviewer is at the Feinberg School of Medicine, Northwestern University, 303 East Superior Street, Chicago, IL 60611, USA. E-mail: r-chisholm@northwestern.edu

CREDIT: PETRA FEY AND REX CHISHOLM/NORTHWESTERN UNIVERSITY

Published by AAAS

RESEARCH PRIORITIES

Farm Animal Research in Crisis

Inadequate funding threatens vital agricultural and biomedical research with farm animals.

R. M. Roberts,[1] G. W. Smith,[2] F. W. Bazer,[3] J. Cibelli,[2] G. E. Seidel Jr.,[4] D. E. Bauman,[5] L. P. Reynolds,[6] J. J. Ireland[2]*

The annual economic value of livestock and poultry sales in the United States currently exceeds $132 billion (*1*), yet only about 0.04% ($32.15 million) (*2*) of the $88 billion Department of Agriculture (USDA) budget in fiscal year 2007 (*3*) was allocated to its competitive grants program for research that directly involves agriculturally important domestic animals. By contrast, the Department of Health and Human Services (DHHS) apportioned 4.1% ($29.5 billion) of its $716 billion budget in fiscal year 2008 to the National Institutes of Health (NIH) of which ~80% supported extramural research (*4*). Whether this direct comparison between USDA and DHHS is appropriate may be debatable; still, it clearly illustrates the huge disparity in total budget available for research grants focused on animal agriculture, about 1/918th that for human health. The private sector does invest in agricultural research and development, but, understandably, such funds are highly focused on commercial interests and not on basic research of the kind we discuss.

The Hatch Act of 1887 provided the USDA with the first mandate to sponsor extramural research in the United States. It funds federal laboratories and provides annual support to state agricultural colleges through a formula based on each state's share of rural and farm populations. In general, "formula funds" support little fundamental research, but instead are focused on applied, mission-orientated programs, teaching, and extension of information to the public in the nation's land-grant colleges. Although this formula for distributing funds may be outmoded, the program has been largely responsible for the strength of U.S. agricultural research.

As time has passed, however, Hatch funds and other research formula funds, even with the help of matching dollars from states, have declined markedly in constant dollars and have been insufficient to maintain research farms and other infrastructure—let alone the research programs—necessary for colleges of agriculture to remain viable (*5*). Instead, faculty researchers have been obliged to seek alternative sources of funds to support their programs, including "earmarks" from influential lawmakers.

Unfortunately, the U.S. Congress failed to authorize USDA to conduct a well-funded, comprehensive, peer-reviewed, competitive grants program for agriculture after World War II. Indeed, in its first report in 1972 (*6*), the National Research Council (NRC) warned ominously that "grossly inadequate support has been given to the basic sciences that underpin agriculture." Subsequent reports echoed this same theme (*7*, *8*). Nonetheless, the forerunner of the present-day competitive USDA grants program grew out of the NRC report and has funded many notable advances in agricultural practices for increased food safety, reproductive efficiencies, and diets to meet specific animal production systems. Since 1990, this program has been called the National Research Initiative or NRI, and it currently supports studies in domestic species, from applied to very basic mechanistic and molecular studies. In October 2009, a new granting body, The National Institute for Food and Agriculture will be established to replace the USDA CSREES (Cooperative State, Research, and Education Service).

Furthermore, as of 1 October 2008, the NRI was replaced by a new competitive grants program for agriculture, the Agriculture and Food Research Initiative (AFRI), which has a greater level of congressionally authorized funding in the farm bill (e.g., $700 million per year for AFRI versus $500 million per year for the NRI). However, an appropriation exceeding $150 million is only a fairly recent event (*9*), and the total AFRI budget in the 2009 appropriation only amounted to $201.5 million (*10*). Moreover, in contrast to NIH, AFRI received no funding from the recently enacted economic stimulus package. Thus, it remains to be seen whether the change in title and mandate of the agency will improve future prospects for research on farm animals and whether the congressionally authorized $700 million per year in funding for AFRI will be appropriated.

Dismal funding for basic mechanistic and molecular research in farm animals has paralleled other trends within colleges of agriculture and departments of animal sciences. In the last two decades, there has been a 44% decrease in research support from federal and state agencies (*5*). Faculty positions in animal science departments at some of the larger land-grant institutions have fallen by more than 50% over the last 30 years. That this decline is systemic is supported by NSF's Survey of Earned Doctorates, which indicates that awarded doctorate degrees in the animal sciences declined 30% from 1985

FARM ANIMALS AS BIOMEDICAL MODELS

Obesity	Ovarian cancer
Diabetes	Nutrition
Aging	Immunology
Cardiovascular disorders	Genomics
Infectious disease	Therapeutics
Neurobiology	Ophthamology
Epigenetics & environment	Reproduction

Research areas that could potentially be advanced by using farm animals as biomedical models. For appropriate farm animal models for specific diseases and references, see www.adsbm.msu.edu.

[1]Division of Animal Sciences, University of Missouri–Columbia, Columbia, MO 65211, USA. [2]Department of Animal Science, Michigan State University, East Lansing, MI 48824, USA. [3]Department of Animal Science, Texas A&M University, College Station, TX 77843–2471, USA. [4]Department of Biomedical Sciences, Colorado State University, Fort Collins, CO 80523–1683, USA. [5]Department of Animal Science, Cornell University, Ithaca, NY 14853, USA. [6]Department of Animal Sciences, North Dakota State University, Fargo, ND 58105, USA.

*Author for correspondence. E-mail: Ireland@msu.edu

to 2004 (*11, 12*). In addition, enrollment in Master's and Ph.D. programs declined 9 and 16%, respectively, between 2004 and 2006 alone (*12*). Equally troubling is the rapid disappearance of breeds and genetic lines of domestic species, especially evident for poultry (*13*); these are irreplaceable genetic resources.

Are farm animals really necessary to advance biomedical research? Seventeen Nobel Prize winners have used farm animals such as cattle, pigs, sheep, goats, horses, and chickens as research models (*14*), yet their value is generally underappreciated. Recently, application of the tools of genetic manipulation and extending genome sequencing efforts in farm animal species [e.g., the published sequence for the bovine (*15*) and for the chicken (*16*) genomes and ongoing sequencing efforts in swine (http://piggenome.org/index.php)] have provided new opportunities. The data will generate insights not only into gene function, but also into genetic and environmental influences on animal production and human disease.

There are numerous examples of compelling domestic species models relevant to diverse areas of biomedical research, including comparative physiology and genomics, cloning, artificial insemination, "biopharming" to produce high-value pharmaceuticals in milk, osteoporosis, diabetes-induced accelerated atherosclerosis, asthma, sepsis, alcoholism, and melanoma (see figure). Because of their size and relatively long generation interval, domestic species such as sheep are widely used to unravel the mechanisms whereby the environment (e.g., diet, temperature, and toxicants) may "program" the developing embryo and fetus, resulting in adult onset of disease (*17*, *18*). Mice with a disrupted *CFTR* gene are helpful in studying some aspects of cystic fibrosis, but they fail to develop the hallmark pancreatic, lung, and intestinal obstructions that occur in humans. The *CFTR* knockout pig model, derived by somatic cell nuclear transfer using *CFTR*-null fibroblasts, better mimics human pathology than do mouse models (*19*). The baby pig is the model of choice for research on human infant nutrition, and swine also develop chronic diseases (atherosclerosis, gastric ulcers, and obesity) observed in humans (*20*). Further, size does matter when it comes to animal models. Surgery, blood sampling, tissue recovery, serial biopsies, instrumentation, whole-organ manipulations, cloning, and many other biomedical applications (*21*) are more easily achieved in animals larger than a mouse.

As pointed out in recent commentaries (*5*, *22*), the number of scientists trained to work with large animal models is decreasing along with numbers of research centers. There is also an idiosyncratic, but long-standing, "cultural" segregation between colleges of agriculture and colleges of human medicine, veterinary medicine, and the basic life sciences disciplines, even when all are located on the same campus. This situation has diminished collaboration and often has failed to challenge traditional animal science thinking. At many institutions, the isolation of animal science programs has, we believe, contributed to poor recruitment of top-notch researchers with an appreciation of newer and emerging technologies.

There also are perceived concerns, raised during recent USDA- and NIH-sponsored workshops (www.adsbm.msu.edu), that proposed uses of agricultural species as models for biomedical research are not received well by NIH study sections and require more extensive justification than research proposed using rodent models. An analysis of funded NIH grants from 2002 to 2006 that made use of animals revealed that ~98% employed rodents, primarily mice, whereas the already small number of funded grants that used farm animals declined by 30% (*5*). The mouse is now overwhelmingly the comparative animal model of choice in such studies because its small size and relatively low cost of maintenance trump the numerous attributes of the cows, sheep, pigs, and other farm animals as valuable biomedical models. But, the economic value of farm animals often offsets much of the associated expenses for their use in research. The mouse, however, reproduces rapidly, has a fully sequenced genome that can be readily manipulated by either adding or knocking out selected genes, and is available as a myriad of inbred and mutant strains. Despite the attractiveness of the mouse, a range of animal models is required to understand how genomes have evolved to drive processes such as reproduction and memory and to extrapolate this genetic information to humans (*23*).

Although a cost-benefit analysis of research specifically on animal agriculture has never been performed, annual returns on federal investment for all agricultural research is reported to be 49 to 62% (*24*). There certainly must also be improved use of existing public funds for the public good. For example, federal agencies should develop joint strategies and adjust portfolios to encourage funding focused on large animal models when appropriate, including establishment of research centers comparable to the NIH-funded National Swine Research Center on the University of Missouri campus. The NIH could develop a funded program committed to advancement of promising alternative animal models, including farm animals. The NIH Center for Scientific Review should ensure that applications that plan to use domestic animal models receive informed input by including individuals with the necessary expertise on review panel rosters. Within colleges of agriculture and veterinary medicine, there should be incentives to recruit nontraditional faculty who are prepared to interact with the broader life sciences community and to pursue funding aggressively from NIH. In particular, administrators must not back away from defending the use of farm animals for both agricultural and biomedical research. The "protected island fortress" of agriculture, usually located on the "other side of campus," is an anachronism that is no longer viable as state and federal support for research with large animal models declines.

References and Notes

1. The 2007 Census of Agriculture, "Economics," www.agcensus.usda.gov/Publications/2007/Online_Highlights/Fact_Sheets/economics.pdf.
2. NRI Competitive Grants Program, www.csrees.usda.gov/funding/nri/pdfs/2007_ann_report.pdf.
3. *USDA FY2007 Budget Summary and Annual Performance Plan*, www.obpa.usda.gov/budsum/fy08budsum.pdf
4. U.S. DHHS, *Budget in Brief*, www.hhs.gov/budget/09budget/2009BudgetInBrief.pdf.
5. J. J. Ireland *et al.*, *J. Anim. Sci.* **86**, 2797 (2008).
6. NRC, *Report of the Committee on Research Advisory to the U.S. Department of Agriculture* (National Academy Press, Washington, DC, 1972).
7. NRC, *Investing in Research: A Proposal to Strengthen the Agricultural, Food and Environment System* (National Academy Press, Washington, DC, 1989).
8. NRC, *National Research Initiative: A Vital Competitive Grants Program in Food, Fiber, and Natural-Resources Research* (National Academies Press, Washington, DC, 2000).
9. M. A. Mirando *et al.*, *Biol. Reprod.* **74**, 459 (2006).
10. *Appropriations Request, National Institute of Food and Agriculture, AFRI;* www.nasulgc-bac.com/documents/FY2010/KB/AFRI.pdf.
11. USDA Research, Education, and Economics Information System, Reports (2007); www.reeis.usda.gov/portal/page?_pageid=193,1&_dad=portal&_schema=PORTAL).
12. Food and Agricultural Education Information System, "Animal Science Graduate Enrollment" (2007); http://faeis.ahnrit.vt.edu/newsletter/december_07/newsletter.html.
13. J. E. Fulton, M. E. Delany, *Science* **300**, 1667 (2003).
14. Foundation for Biomedical Research, *Nobel Prizes*; www.fbresearch.org/Education/NobelPrizes/tabid/427/Default.aspx.
15. The Bovine Genome Sequencing and Analysis Consortium, *Science* **324**, 522 (2009).
16. International Chicken Genome Sequencing Consortium, *Nature* **432**, 695 (2004).
17. A. J. King *et al.*, *Am. J. Physiol. Endocrinol. Metab.* **292**, E1837 (2007).
18. V. Padmanabhan, *Rev. Endocrin. Metab. Disord.* **8**, 67 (2007).
19. C. S. Rogers *et al.*, *Science* **321**, 1837 (2008).
20. D. L. Brooks, P. C. Tillman, S. M. Niemi, in *Laboratory Animal Medicine*, J. G. Fox, B. J. Cohen, F. M. Lowe, Eds. (Academic Press, New York, 2006), pp. 273–295.
21. L. P. Reynolds *et al.*, *J. Nutr.* **139**, 427 (2009).
22. L. P. Reynolds *et al.*, *J. Anim. Sci.* **86**, 2445 (2008).
23. R. Gibbs *et al.*, *Bovine Genomic Sequencing Initiative: Cattle-izing the Human Genome* (NHGRI), NIH, Bethesda, MD, 2004); www.genome.gov/ 12512284.
24. W. E. Huffman, R. E. Evenson, *Am. J. Agr. Econ.* **88**, 783 (2006).

25. We thank numerous colleagues, including R. Prather, K. Wells, M. Mirando, D. Hamernik, and L. De Paolo.

10.1126/science.1168521

PROFESSIONAL DEVELOPMENT

Summer Institute to Improve University Science Teaching

The goal of the National Academies Summer Institute is to change teaching practices in introductory, undergraduate biology courses.

Christine Pfund,[1,2*] Sarah Miller,[1] Kerry Brenner,[3] Peter Bruns,[4] Amy Chang,[5] Diane Ebert-May,[6] Adam P. Fagen,[3] Jim Gentile,[7] Sandra Gossens,[1] Ishrat M. Khan,[8] Jay B. Labov,[3] Christine Maidl Pribbenow,[1,9] Millard Susman,[10] Lillian Tong,[10] Robin Wright,[11] Robert T. Yuan,[12] William B. Wood,[13] Jo Handelsman[1†]

Introductory science courses at large universities in the United States serve as the portals that connect undergraduates to frontiers in research and scientific ways of thinking (*1*–*3*). According to the National Research Council report, *BIO2010* (*4*), however, teaching practices have not changed in correspondence with advances in scientific research. Consequently, the gateway through which most students pass is antiquated and misrepresents the interdisciplinary, collaborative, evidence-based culture of science. To provide faculty with the knowledge and skills they need to improve undergraduate teaching, *BIO2010* recommended an annual summer institute for biology faculty devoted to teaching and learning. Here, we report the design of such an institute and its impact on participants' teaching practices, challenges faced when they returned to their institutions, and how they disseminated institute practices.

Dissemination activity	Respondents (%) who engaged in activity
Mentored a colleague in teaching	89
Presented a seminar or workshop about teaching	72
Submitted a manuscript about teaching	25

SI alumni as agents of change. Two years after the SI, most SI alumni report leading educational reform efforts at their home campuses (n = 75).

The Summer Institute

The Howard Hughes Medical Institute, the National Academies, and the University of Wisconsin–Madison partnered to create and implement the National Academies Summer Institute on Undergraduate Education in Biology (SI) (*5*, *6*) (http://academiessummerinstitute.org). Offered annually since 2004, the SI has as its goal helping biology faculty learn the skills necessary to transform high-enrollment undergraduate courses into more effective, learner-centered environments, by using practices proven to be effective. During the week-long institute (*7*), SI participants learn about "scientific teaching" (*8*–*10*); they develop teaching materials that define students' learning goals, include classroom activities that address these goals, and assess student learning. Participants also explore the challenges and benefits of diversity in teaching methods and in the students they teach. They also are expected to practice and disseminate the new activities they developed upon returning to their home campuses. Starting in 2007, SI participants were provided additional training and resources to conduct workshops about scientific teaching for other faculty at their institutions.

Admission to the SI is by competitive application. Priority is given to universities that send teams of two to three instructors, ideally including both junior and senior faculty, who teach large introductory biology courses. Applicants must demonstrate financial support from their campus for travel to the SI and for implementation of new teaching practices when they return to their campuses. Since 2004, five cohorts from 64 U.S. institutions in 36 states have participated in the SI. These include public and private institutions, of which 69% are research-extensive (offering a wide range of baccalaureate programs, and committed to graduate education through the doctorate). The 107 male and 102 female participants include 39% tenured faculty, 33% untenured faculty, and 27% instructional staff (*7*). Collectively, these SI alumni teach an estimated student population of over 90,000 undergraduates annually.

Reported Changes in Teaching Practices

On leaving the SI, participants reported by survey significant learning gains in areas of scientific teaching ($P < 0.001$) (*7*). Most SI alumni (87%, n = 135) reported increased confidence in their ability to implement these strategies after the SI and expressed their intentions to do so. To determine whether these attitudes persisted and the intentions were realized, we again surveyed SI alumni 1 and 2 years after the SI. Over the 2-year period following the SI, alumni reported sustained learning gains and confidence, and 98% indicated that they were still experimenting to improve their teaching (*7*). When asked to describe evidence that their teaching had changed over the past 2 years, 96% of the survey respondents provided examples that ranged from identifying specific activities that are now different in their

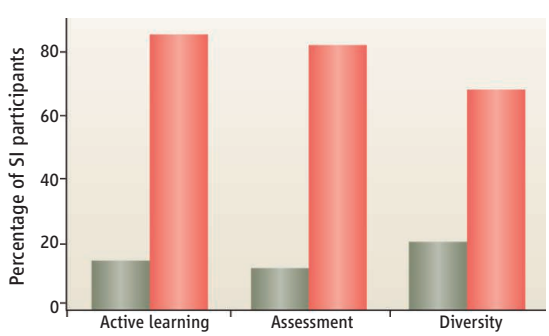

The effect of SI on reported teaching practices. SI alumni (n = 68) used scientific teaching approaches more frequently two years after the SI (red) than before the SI (blue).

[1]Wisconsin Program for Scientific Teaching, Department of Bacteriology, University of Wisconsin–Madison. [2]Delta Program in Research, Teaching, and Learning, University of Wisconsin–Madison. [3]National Research Council of the National Academies. [4]Howard Hughes Medical Institute. [5]American Society for Microbiology. [6]Department of Plant Biology, Michigan State University. [7]Research Corporation for Science Advancement. [8]Department of Chemistry, Clark Atlanta University. [9]Wisconsin Center for Education Research, University of Wisconsin–Madison. [10]Center for Biology Education, University of Wisconsin–Madison. [11]Department of Genetics, Cell Biology, and Development, University of Minnesota. [12]Department of Cell Biology and Molecular Genetics, University of Maryland, College Park. [13]Department of Molecular, Cellular, and Developmental Biology, University of Colorado at Boulder.

*Complete author affiliations are available in the supporting online material.

†To whom correspondence should be addressed. E-mail: joh@bact.wisc.edu

classrooms—using case studies, clickers (audience-response systems), or cooperative groups—to describing general attributes about their teaching and student learning generally. These perspectives included demonstrations of improved learning by their students, and attempts to research, measure, and document the effects of their changed practices.

The frequency with which SI alumni reported using learner-centered classroom activities (active learning), measuring student learning and teaching effectiveness (assessment), and employing diversity-aware teaching strategies (diversity) increased substantially in the two years after their participation in the SI; more than 68% of participants reported using these methods in at least half of their class sessions (see chart, p. 470, right). SI alumni also reported using techniques to engage students such as problem–based and cooperative learning multiple times each semester (*7*).

SI alumni reported using multifaceted assessments of student learning and teaching effectiveness, and teaching methods that provide immediate feedback about learning, including listening to groups of students discuss problems, inviting student responses (often using clickers), and scoring rubrics (*7*). One alumnus summarized his changes in teaching practice as follows: "I look over the material I presented … [before the SI] and realize how much I have changed the emphasis to student learning…. My syllabus lists learning objectives for each class period, and those learning objectives are reflected in multiple forms of formative assessment and in the exams students take." SI alumni also reported gains in broadening their definition of diversity to include diversity of student learning styles and the application of diverse teaching methods (*7*).

Challenges: Anticipated and Actual

Upon leaving the SI, participants were asked what challenges they anticipated facing as they implemented new instructional materials and teaching approaches at their home campuses. Many participants predicted that gaining cooperation of colleagues in their departments would be most difficult.

One year later, the group of alumni were asked to rate what actually proved to be the major challenges. They found that time pressures, balancing responsibilities, and lack of recognition for their teaching efforts were most challenging (see chart, below). However, some alumni commented that the SI enabled them to negotiate change. For example: "The stature of attending the SI has helped me gain respect of colleagues in the department to foster their consideration of such methods…." This recognition may be aided by naming each participant as a National Academies Education Fellow in the Life Sciences.

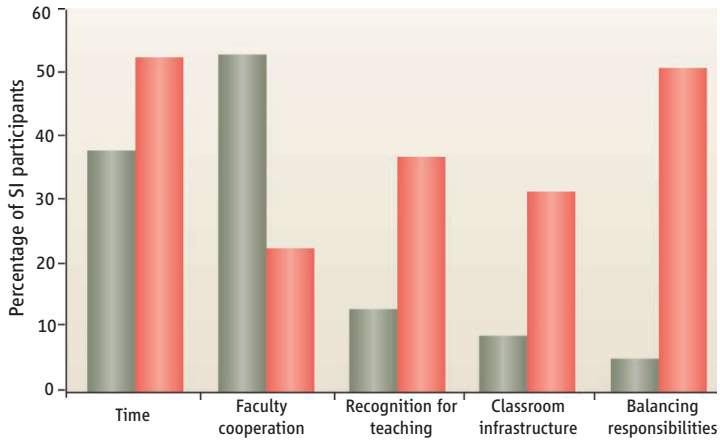

Implementation challenges. Challenges predicted by participants at the end of SI (blue, $n = 67$); reported challenges 1 year after SI (red, $n = 101$).

Other barriers, such as funding limitations, also did not turn out to be as significant as predicted. One participant stated: "Before this workshop, I thought lack of resources (funds!) would be a problem. Now I know that lack of funds for various gadgets is just an excuse on my part. No funds are required for: forming student groups, pre-testing, post-testing, etc."

Dissemination

SI alumni are asked to become agents of change and to promote improvements in undergraduate biology education at their home institutions and nationally. They have taken this charge seriously (see table, p. 470); most have talked informally about the SI to colleagues in their departments (98%); others have led events, including formal seminars, workshops, and institutes; 25% reported writing manuscripts about their teaching efforts [e.g. (*11*–*17*)]. Many alumni (74%) reported that colleagues in their department were positively affected by their team's experience in the SI. In addition, 44% of the respondents reported mentoring a colleague in teaching within 6 months of the SI; and 2 years after the SI, this number increased to 89%.

Conclusions

The SI changes the university experience for the faculty participants and the students they teach. SI alumni disseminate the principles of scientific teaching, thereby acting as a coherent force for advancement in science education and improvement in student learning. The participants chose to attend the SI; consequently, they may be predisposed to consider change in teaching practices and, therefore, are not representative of undergraduate science educators. However, independent of their starting points on the continuum, the SI participants reported substantial change in their teaching practices and efforts to disseminate information both formally and informally. Some have also published effects on student learning. Further research is needed to triangulate these results with independent assessment of classroom teaching practices and their effects on student learning. Such studies are under way, as are those that examine the impact of SI participants on their departments and broader teaching communities.

References and Notes

1. E. Seymour, N. M. Hewitt, *Talking About Leaving: Why Undergraduates Leave the Sciences* (Westview Press, Boulder, CO, 1997).
2. J. B. Labov, *Cell Biol. Educ.* **3**, 212 (2004).
3. R. L. DeHaan, *J. Sci. Educ. Technol.* **14**, 253 (2005).
4. National Research Council, *BIO2010: Transforming Undergraduate Education for Future Research Biologists* (National Academies Press, Washington, DC, 2003).
5. W. B. Wood, J. Handelsman, *Cell Biol. Educ.* **3**, 215 (2004).
6. J. B. Labov, *Cell Biol. Educ.* **2**, 202 (2003).
7. Materials and methods are available as supporting online materials.
8. J. Handelsman *et al.*, *Science* **304**, 521 (2004).
9. J. Handelsman, S. Miller, C. Pfund, *Scientific Teaching* (W. H. Freeman, New York, 2007).
10. D. Ebert-May, J. Hodder, *Pathways to Scientific Teaching* (Sinauer Associates, Sunderland, MA, 2008).
11. J. K. Knight, W. B. Wood, *Cell Biol. Educ.* **4**, 298 (2005).
12. C. Dirks, M. Cunningham, *CBE Life Sci. Educ.* **5**, 218 (2006).
13. N. Armstrong, S.-M. Chang, M. Brickman, *CBE Life Sci. Educ.* **6**, 163 (2007).
14. S. Freeman *et al.*, *CBE Life Sci. Educ.* **6**, 132 (2007).
15. A. Crowe, C. Dirks, M. P. Wenderoth, *CBE Life Sci. Educ.* **7**, 368 (2008).
16. M. K. Smith, W. B. Wood, J. Knight, *CBE Life Sci. Educ.* **7**, 422 (2008).
17. N. Aguilar-Roca, A. Williams, R. Warrior, D. K. O'Dowd, *Int. J. Scholarship Teach. Learn.* **3**, 1 (2009).
18. Supported by the HHMI Professors Program, The National Academies, the Research Corporation for Science Advancement, NSF, and the University of Wisconsin–Madison Provost's Office. Several of the authors (A.C., K.B., J.G., I.M.K., M.S., R.W., W.B.W., J.H., J.B.L., A.P.F., and R.T.Y.) have served on the SI Advisory Board.

Supporting Online Material
www.sciencemag.org/cgi/content/full/324/5926/470/DC1

10.1126/science.1170015

PLANT SCIENCE

Exploring Terra Incognita

A tree new to science dominates the vegetation over an area of at least 8000 km^2 in an African war zone.

David J. Mabberley

During visits in May 2006 and February 2007 to Ogaden (or the Somali National Regional State of Ethiopia, as it is formally called), the botanist Mats Thulin and his team encountered a tree previously unknown to science on limestone hills southeast of the town Kebri Dehar. The researchers soon found that it dominates the vegetation over large areas in southeastern Ogaden, covering an area of at least 8000 km^2 (see the figure, panel A). For comparison, the Greek island of Crete has an area of 8379 km^2. Hundreds of the trees were inspected on the ground, and tens or probably hundreds of thousands were seen with binoculars; the total number must be in the millions. The tree, a species of *Senegalia* (Leguminosae), is about 6 m tall, with a canopy 8 to 10 m in diameter. It flowers when leafless during the dry season (see the figure, panel C). Thulin has recently formally described it as *Acacia fumosa* (*1*). It differs from its relatives by having, among other things, a gray, smooth bark and pink flowers (see the figure, panels B and C).

About 10,000 new species across all groups of organisms are described each year (*2*). Some 2350 of these are flowering plants (*3*). From Africa alone, around 300 new species of flowering plants are described each year; in the past two decades, one of the African countries with the most newly described species has been Somalia. The high figure for that country, which has a long border with Ogaden, reflects the activities of the Flora of Somalia project, which was completed in 2006 (*4*). During the course of this project alone, 400 new species of flowering plants were discovered and described (*4*).

The vast majority of the new species of flowering plants described from Somalia and elsewhere in recent years are either confined to small areas, where they may be locally common, or are rare plants with scattered distributions. For example, *Cyclamen somalense*, discovered in 1986 (*5*), is known only from ~1 km^2 in northern Somalia. In the case of some species of large rain-forest trees recently described from Cameroon (*6, 7*), only a few individuals are known. As a rule, the most conspicuous or dominating elements of any flora in the world have long been known.

Royal Botanic Gardens, Kew, Richmond TW9 3AE, UK. E-mail: d.mabberley@kew.org

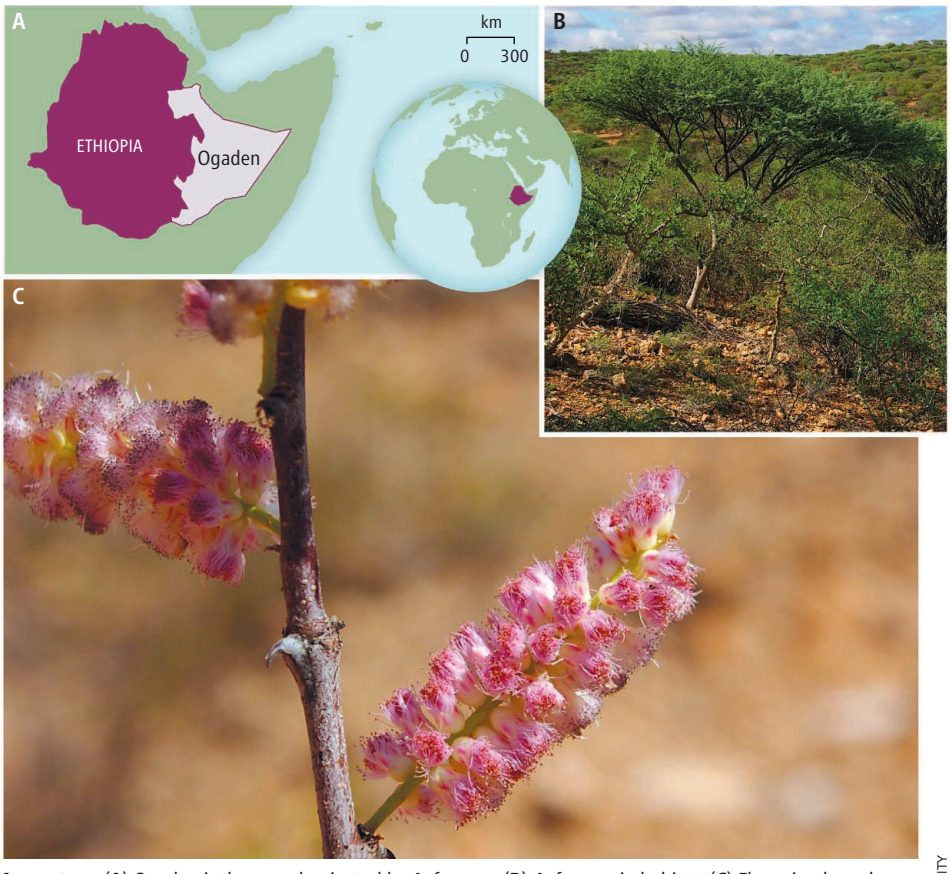

A new tree. (**A**) Ogaden is the area dominated by *A. fumosa*. (**B**) *A. fumosa* in habitat. (**C**) Flowering branch.

There are unusual cases, such as *Commiphora chiovendana* (*8*), a common shrub or small tree in Somalia known from an area of more than 200,000 km^2 (almost the size of Great Britain). However, this plant had been known since 1924, but was incorrectly identified with another species. This is not the case for *A. fumosa*. It was of course known to the few local inhabitants, who do not, however, seem to have a specific vernacular name for it; nor was it said to have any particular uses.

How can a conspicuous tree like this, which covers practically every hill-slope over an area as large as Crete, be unknown to science? The probable explanation is the inaccessibility of the area (it can be seen from a drivable track only in a few places) and the general unrest that has plagued the region throughout its history. As a result, the area has been very little visited by botanists or other scientists.

One may ask what else can be found in a terra incognita like this. There are certainly more new species of plant to be discovered in Ogaden (*9*) and in other parts of the world, but the existence of another unknown tree dominating the vegetation over such a large area is highly unlikely.

References

1. M. Thulin, *Nord. J. Bot.* **25**, 272 (2008).
2. A. E. Magurran, *Curr. Biol.* **15**, R115 (2005).
3. G. T. Prance, H. Beentje, J. Dransfield, R. Johns, *Ann. Miss. Bot. Gard.* **87**, 67 (2000).
4. M. Thulin, Ed., *Flora of Somalia* (Royal Botanic Gardens, Kew, UK, 2006), vol. 3.
5. M. Thulin, A. M. Warfa, *Plant Syst. Evol.* **166**, 249 (1989).
6. X. M. van der Burgt, D. M. Newbery, *Kew. Bull.* **61**, 79 (2006).
7. X. M. van der Burgt, M. B. Eyakwe, D. M. Newbery, *Adansonia*, sér. **3**, 29, 59 (2007).
8. M. Thulin, *Nord. J. Bot.* **20**, 395 (2001).
9. M. Thulin, D. Goyder, S. Liede-Schumann, *Kew Bull.* **63**, 617 (2009).

10.1126/science.1173323

PHOTO CREDITS: (PANEL B) M. THULIN/UPPSALA UNIVERSITY; (PANEL C) ANDERS LARSSON/UPPSALA UNIVERSITY

PHYSICS

Where Is My Quantum Computer?

With applications in quantum cryptography, rudimentary quantum computers already exist.

P. Hemmer[1] and J. Wrachtrup[2]

The title question is echoed by electrical engineers and consumers alike. It has now been 15 years since quantum computing came to the forefront of popular science with its promise of superpowered computers for the future, so it is natural to be wondering when the first commercial products will appear on the market.

Actually, the answer may seem somewhat surprising: The quantum computer is already here. Demonstration versions are available from several companies (*1*, *2*), and high-performance versions have been (*3*) and are currently being (*4*) constructed. Although these devices are referred to as quantum cryptography or quantum key distribution systems (*5*), they operate on similar principles as does a quantum computer. Individual quantum bits (qubits) in the form of photons are sent out one at a time in one of four polarizations that redundantly encode 0s and 1s. When a qubit is received, an attempt is made to perform a single qubit operation, called the Hadamard transformation (see the figure); this operation is one of the most elemental quantum computing operations, from which more complex codes can be constructed. Whenever this operation succeeds, the data are discarded; what is left behind is a random one-time code that can be used as an unbreakable cipher.

This seems a long way from what we would consider to be a superpowered quantum computer capable of doing sophisticated calculations using quantum entanglement, but consider the next generation of quantum secure communication systems, currently under development, that are based on the theoretical concept of quantum teleportation (*6*). Here, the information itself is never even transmitted but appears at the receiver as a result of the peculiar properties of quantum mechanics. What could be more secure than that? A quantum teleporter additionally requires two qubit operations to be performed to create entangled states. Measurements determine what kind of entangled state dominates, and this is much like reading out the answer from a quantum computation. Photons were teleported long ago, but it is generally accepted that qubits in material systems are needed to store entanglement long enough to ensure its presence before attempting teleportation. This was recently shown using atomic vapors as a qubit storage medium. Long-distance matter qubit teleportation has also been accomplished with individual trapped ions (*7*), opening the door to error-correction protocols needed to make teleportation practical.

Single-qubit and two-qubit gates like those used in teleportation are sufficient to construct even the most complex quantum computer (*8*). A quantum teleporter will be the first to incorporate all the key elements of a general purpose quantum computer.

Also under development are quantum repeaters that are needed to make secure quantum communication work over long distances, such as over Internet optical fibers (*9*). These repeaters perform even more complex quantum computation operations such as entanglement purification, and it is expected that nontrivial quantum computers will be needed at the repeater nodes to accomplish these tasks. For example, the purification protocol (*10*) that can be implemented on a few-qubit quantum computer for a diamond-based system (*11*) holds the promise to do these operations in a scalable microchip system. Some key components have already been demonstrated at room temperature (*12*).

So quantum computers are now a reality and will continue to be developed. However, the long-term emphasis will shift from factoring large numbers to break classical codes, to applications that emphasize the unbreakable nature of quantum codes.

What will be the first consumer product? Every time we search the Internet, information is collected about us and our personal habits, whether we like it or not. A quantum computer could prevent this from happening. For example, a recently proposed quantum algorithm uses the highly fragile nature of quantum entanglement to let us know whether the search engine we queried peeked at our search terms or not (*13*). The implementation of this is not unlike the quantum key distribution

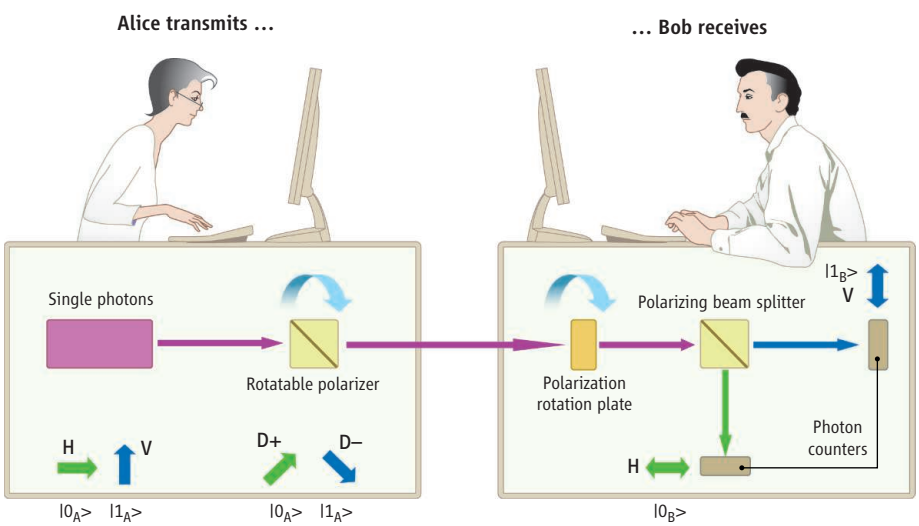

Quantum key distribution. The transmitter, Alice, sends single photons with linear polarization oriented in one of four possible directions, chosen at random. Orthogonal polarization directions encode logical 0s and 1s. For example, a photon in the horizontal-vertical (HV) basis H can represent logical 0 and V a logical 1. In the diagonal (DI) basis D+ can represent logical 0 and D– a logical 1. If the receiver, Bob, selects the same basis as Alice, then he can determine with 100% accuracy whether a 0 or 1 was transmitted. If the bases are different then there is a 50% chance of getting the wrong answer. Discarding this data leaves behind a random shared code that can give absolute security when used as a one-time cypher. However, if we look more closely at the polarizing beam splitter Bob uses to distinguish polarization states, we find that it can actually create well-defined mixed polarization states. For example, if Alice transmits the D+ state and Bob receives in the HV basis, there is equal amplitude in H and V states. In essence, the input state $D+ = |0_A\rangle$ is converted to the output state $H + V = |0_B\rangle + |1_B\rangle$. Similarly the input state $D- = |1_A\rangle$ is converted to $H - V = |0_B\rangle - |1_B\rangle$. But this is exactly the action of a single qubit Hadamard gate.

[1]Electrical and Computer Engineering, Texas A&M University, College Station, TX 77843, USA. [2]Institute of Physics, University of Stuttgart, 70550 Stuttgart, Germany. E-mail: prhemmer@ece.tamu.edu; wrachtrup@physik.unistuttgart.de

Published by AAAS

systems that allow us to detect the presence of an eavesdropper by an unexplained increase in error rate. There may well be a valuable consumer product in a few years.

Other possible applications include implementing quantum games (*14*). Again, security is the key consideration. If you are playing a big-stakes game—such as sealed-bid auctions, digital rights management, or looking for alternatives to taxation for public goods allocation—you want to be sure that the other gamers, or even the system administrator, are not cheating. You may also want to ensure that your move is anonymous, so that it is more difficult for other players to guess your strategy. Quantum computers may offer a way to provide these functions, and, additionally, the inherent randomness of some quantum measurements may be able to enhance fairness.

Whether or not we eventually have quantum security chips in our laptops, the spin-offs from quantum computing research are likely to be at least as exciting. Consider, for example, that single-spin qubits in diamond might be used as ultrasensitive magnetometers operating as nanoscale probes in living cells (*15*). Other applications include quantum imaging for superresolution and lensless ghost imaging (*16*), as well as ultraprecise atomic clocks (*17*) that can measure general relativistic effects in the universe or at least give us a more accurate global positioning system. Quantum computers are here and are likely to become an important part of our everyday lives in the not-so-distant future.

References

1. MagiQ, www.magiqtech.com.
2. ID Quantique, www.idquantique.com/company/overview.htm.
3. C. Elliott, *New J. Phys.* **4**, 46 (2002).
4. R. Ursin *et al.*, *Proceedings of the 2008 Microgravity Sciences and Process Symposium*, Glasgow, Scotland, 29 September to 3 October 2008.
5. C. H. Bennett, G. Brassard, *Proceedings of the IEEE International Conference on Computers, Systems, and Signal Processing*, Bangalore, India, 9 to 12 December 1984, p. 175.
6. C. H. Bennett *et al.*, *Phys. Rev. Lett.* **70**, 1895 (1993).
7. S. Olmschenk *et al.*, *Science* **323**, 486 (2009).
8. S. Lloyd, *Phys. Lett. A* **167**, 255 (1992).
9. Z.-S. Yuan *et al.*, *Nature* **454**, 1098 (2008).
10. L. Childress, J. M. Taylor, A. S. Sørensen, M. D. Lukin, *Phys. Rev. A* **72**, 052330 (2005).
11. J. Wrachtrup, F. Jelezko, *J. Phys. Condens. Matt.* **18**, S807 (2006).
12. M. V. G. Dutt *et al.*, *Science* **316**, 1312 (2007).
13. V. Giovannetti, S. Lloyd, L. Maccone, arXiv:0708.2992v2 [quant-ph] (2007).
14. H. Guo, J. Zhang, G. J. Koehler, *Decis. Support Syst.* **46**, 318 (2008).
15. G. Balasubramanian *et al.*, *Nature* **455**, 648 (2008).
16. R. Meyers, K. S. Deacon, Y. Shih, *Phys. Rev. A* **77**, 041801R (2008).
17. A. Andre, A. S. Sorensen, M. D. Lukin, arXiv:quant-ph/0401130 (2006).

10.1126/science.1170912

GEOPHYSICS

The Thickness of Tectonic Plates

Seismic studies continue to refine the elusive boundary that defines the depth at which the lithosphere ends.

Barbara Romanowicz

A fundamental premise of plate tectonics on Earth is that rigid lithospheric plates, formed at mid-ocean ridges, float above a more deformable substratum, the asthenosphere (*1*). The precise nature of the asthenosphere is still debated. Mechanical models predict a well-defined, sharp lithosphere-asthenosphere boundary (LAB), but evidence for such a boundary from conventional seismic measurements is ambiguous. On pages 499 and 495 of this issue, Kawakatsu *et al*. (*2*) and Rychert and Shearer (*3*) present analyses of more sophisticated seismic studies that help refine the LAB and hence the thickness of the lithosphere and tectonic plates, although challenges still remain in picking out this boundary versus other structures within the lithosphere.

Observations of seismic surface waves reveal a well-developed zone where seismic wave velocities are low under the ocean basins, at depths of about 80 to 200 km. This low-velocity zone (LVZ), which also causes strong losses of seismic energy, likely corresponds to the low-viscosity asthenosphere. The thickness of the overlying high-velocity lithospheric "lid" increases with age, which would be expected as the plates cool after formation. The lithosphere is thickest under the oldest, most stable part of continents, the cratons, and here the asthenosphere is poorly developed. Recent estimates that combine seismic tomography, heat flow, and geochemical data from kimberlites (rocks that originate from the mantle) constrain the lithospheric thickness to about 200 to 250 km under the cratons (*4*–*6*).

Other major boundaries in the earth, such as the core-mantle boundary, are more readily observed by seismic body waves that travel through the planet and encounter compositional discontinuities or phase changes. In contrast, detection of the LAB has been elusive, and it has been difficult to determine whether the seismic properties of the LVZ arise from partial melting of rocks (*7*), from increased water content (*8*, *9*), or simply from the competing effects of increasing temperature and pressure with depth (*10*).

One approach that has been successful for detecting and characterizing fainter mantle discontinuities is that of "receiver functions" (*11*), in which conversions of elastic energy from compressional to shear (Ps) or from shear to compressional (Sp) waves are identified on broadband seismic records. This approach constrains the depth, sign, and amplitude of velocity jumps across discontinuities. Receiver function studies have identified drops in velocity at candidate LABs at depths of about 70 to 80 km under ocean islands (*12*) and from 80 to 110 km under relatively young parts of continents (*13*).

Ocean islands, however, generally sit on "anomalous" mantle, such as regions of hotspot plumes. The observation of the LAB under the more representative ocean basins has been hampered by the lack of seismic stations on the ocean floor. The high-quality observations of both Ps and Sp conversions at LAB depths made by Kawakatsu *et al*. were enabled by the long-term operation of several low-noise seismic borehole observatories on the ocean floor in the western Pacific Ocean (*14*). The sharpness of the LAB boundary rules out a purely thermal origin or one arising only from increased water content. The authors convincingly argue that partially melted rock must be present. This melting process is enhanced by the presence of increased amounts of water at this depth, as was predicted experimentally (*15*).

The LAB has also been difficult to detect at the expected depths under the cratonic parts of continents (*16*). Numerous other discontinuities, with either positive or negative jumps in seismic velocity, have been observed at shallower depths and are often referred to as the Hales discontinuity (*17*). Rychert and Shearer present the results of a global study of Ps receiver functions in vari-

Berkeley Seismological Laboratory and Department of Earth and Planetary Science, University of California at Berkeley, Berkeley, CA 94720, USA. E-mail: barbara@seismo.berkeley.edu

ous tectonic settings, such as ocean islands, tectonic or stable parts of continents, in which they consistently detect a sharp negative gradient that may correspond to the LAB at a depth that varies surprisingly little between oceanic islands (70 ± 4 km) and Precambrian shields and platforms that make up continental cratons (95 ± 4 km). The large velocity drop of shear waves of 6 to 9% indicates that this effect is not caused by changes in temperature or composition alone.

The study of Rychert and Shearer raises several intriguing questions. Is the nature of the discontinuity found by them worldwide and the same everywhere, and is it the same as that found by Kawakatsu *et al.* in the ocean basins? How is the ~95-km discontinuity found under shields and platforms related to the LAB? Why is the expected LAB at depths of about 200 km so hard to detect?

One approach for resolving the different seismic signatures is to make comparisons with the results of high-resolution studies of the continental lithosphere from dense, long-range seismic profiles (LRSPs). These studies consistently find a negative compressional velocity jump at a depth of about 100 km (the so-called "8 degree discontinuity") (*18*). At greater depths, the waves are strongly scattered, which suggests that fine layers are present that alternate between high and low velocities. Such a structure could form if heterogeneous inclusions (which could be fluid inclusions) were present (*18*). These features are likely related to the discontinuity found by Rychert and Shearer as well as to the Hales discontinuity.

The LRSP studies also see features below the 8 degree discontinuity. In shield regions, the LVZ is narrow (10 to 20 km); below it, seismic velocities are faster down to depths of about 200 km. In the younger tectonic parts of continents, the LVZ extends to greater depths. A localized zone of somewhat depressed shear-wave velocities in the cratonic lithosphere is also consistent with some recent tomographic shear-wave velocity models (see the figure). These results suggest that the continental discontinuity seen at about 100 km is not the LAB but more likely the remnant signature of the formation of cratons in archean times (*19*).

Although negative velocity jumps at depths of around 100 km under cratons have been attributed to the LAB (*20*), such conclusions are incompatible with surface wave and teleseismic travel-time data, which tightly constrain the average seismic velocities in the upper mantle. Rather, there seem to be two distinct features: a negative discontinuity with little topography (from 60 to 70 km in tectonic regions to about 100 km under cratons) that is not a mechanical boundary, and a LAB that is not as sharp but has much greater topography, ranging in depth from 60 to 80 km in ocean basins to 200 to 250 km under cratons. Under shields and platforms, the LAB may not be detectable as a discontinuity, because it may extend over a larger depth range and may not involve partial melt but, rather, a change in anisotropy related to the strong shear experienced at the base of the plates. This difference could explain why receiver function studies fail to detect it consistently. Such a scenario is compatible with some LRSP results (*21*), as well as the observation of a change in the direction of fast axis of azimuthal anisotropy in the velocity of shear waves around the expected depth of the LAB, both in ocean basins (*22*) and under cratons (*23*). Under the oceans and under the younger parts of continents, the zones of partial melt and strong seismic anisotropy, because of shear at the base of the lithospheric plates, would overlap, in agreement with Kawakatsu *et al.*'s finding of partial melt zones that are horizontally elongated.

Finally, in the Rychert and Shearer study, only Ps conversions were considered, but in continental settings where the crust is thick, strong multiple reflections from the crust can mask the signal from possible discontinuities at depths around 200 km. The Sp conversion approach does not have this drawback (*24*). As the Transportable Array component of Earthscope is moved across the Rocky Mountain front and into the North American shield (*25*), the combination of surface wave, Ps and Sp receiver function, and other scattered wave field approaches should shed more light on the fine structure of continental roots and their formation, as will similar efforts worldwide. Likewise, further confirmation of the partial melt at the oceanic LAB detected by Kawakatsu *et al.* will require sustained efforts in the installation of broadband ocean floor observatories in oceanic basins.

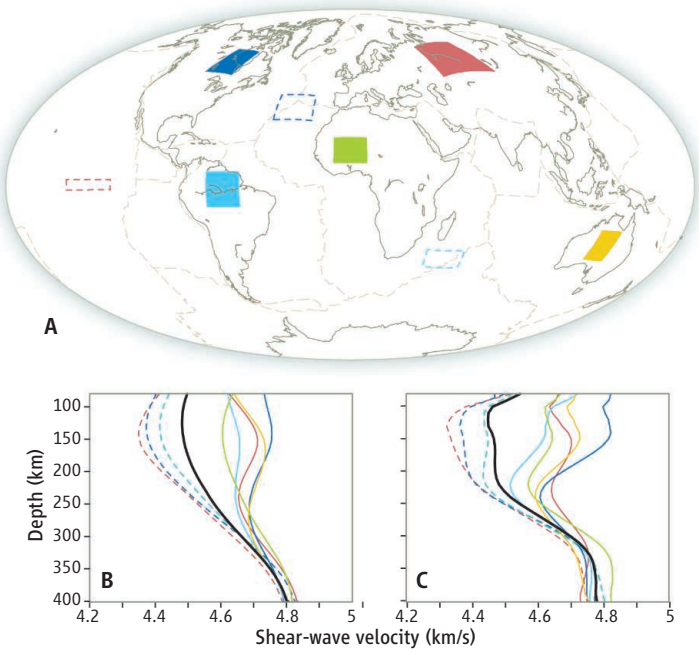

Shear-wave slowdown. How seismic shear-wave velocity changes with depth in the upper mantle differs for oceanic and continental regions. Results from two recent global tomographic models illustrate the difficulty in identifying a signature of the lithosphere-asthenosphere boundary. (**A**) The regions sampled in the profiles are indicated by different colors for continental cratons (solid) and ocean floor (broken lines). Black lines indicate global averages. The global data sets are not identical, but in both cases, they include long-period seismic waveforms sensitive to shear velocity in the upper mantle. The models differ in the initial one-dimensional model used in the linearized inversion. In (**B**), it is designed to fit the global data on average while keeping variations with depth smooth (*26*). In (**C**), it is a mineralogically meaningful (pyrolite) model with more detailed depth variations (*27*). In both models, velocities are greater under cratons than under oceans down to 200 km depth, and velocity decreases with depth, with a minimum centered at 100 to 150 km under the oceans (similar to results of Kawakatsu *et al.*) and 200 to 250 km in the cratons. In the higher-resolution model (C), a stronger, more localized negative gradient at the base of the cratonic lithosphere is present. A "dip" in velocity occurs at depths around 100 km for both continents and oceans (as seen also by Rychert and Shearer).

References and Notes

1. D. L. Anderson, *Rev. Geophys.* **33**, 125 (1995).
2. H. Kawakatsu *et al.*, *Science* **324**, 499 (2009).
3. C. A. Rychert, P. M. Shearer, *Science* **324**, 495 (2009).
4. C. Jaupart *et al.*, *J. Geophys. Res.* **103**, 15269 (1998).
5. Y. Gung, M. Panning, B. Romanowicz, *Nature* **422**, 707 (2003).
6. R. Rudnick, W. McDonough, R. O'Connell, *Chem. Geol.* **145**, 395 (1998).
7. D. L. Anderson, C. Sammis, *Phys. Earth Planet. Inter.* **3**, 41 (1970).
8. G. Hirth, D. L. Kohlstedt, *Earth Planet. Sci. Lett.* **144**, 93 (1996).
9. S.-I. Karato, H. Jung, *Earth Planet. Sci. Lett.* **157**, 193 (1998).

10. U. H. Faul, I. Jackson, *Earth Planet. Sci. Lett.* **234**, 119 (2005).
11. L. P. Vinnik, *Phys. Earth Planet. Inter.* **15**, 39 (1977).
12. X. Li *et al.*, *Nature* **427**, 827 (2004).
13. C. A. Rychert, S. Rondenay, K. M. Fischer, *J. Geophys. Res.* **112**, B08314 (2007).
14. M. Shinohara *et al.*, *Phys. Earth Planet. Inter.* **170**, 95 (2008).
15. K. Mierdel, H. Keppler, J. R. Smyth, F. Langenhorst, *Science* **315**, 364 (2007).
16. P. Kumar, X. Yuan, R. Kind, J. Ni, *J. Geophys. Res.* **111**, B06308 (2006).
17. A. L. Hales, *Earth Planet. Sci. Lett.* **7**, 44 (1969).
18. H. Thybo, E. Perchuc, *Science* **275**, 1626 (1997).
19. J. P. Mercier *et al.*, *J. Geophys. Res.* **113**, B04308 (2008).
20. P. Kumar *et al.*, *Nature* **449**, 894 (2007).
21. T. Ryberg *et al.*, *Bull. Seism. Soc. Am.* **86**, 857 (1996)
22. D. B. Smith, M. H. Ritzwoller, N. M. Shapiro, *J. Geophys. Res.* **109**, B11309 (2004).
23. F. Marone, B. Romanowicz, *Nature* **447**, 198 (2007).
24. V. Farra, L. Vinnik, *Geophys. J. Int.* **141**, 699 (2000).
25. www.iris.edu/USArray
26. B. Kustowski, G. Ekström, A. M. Dziewonski, *J. Geophys. Res.* **113**, B06306 (2008).
27. F. Cammarano, B. Romanowicz, *Proc. Natl. Acad. Sci. U.S.A.* **104**, 9139 (2007).
28. Supported by the Earthscope program of NSF.

10.1126/science.1172879

CELL SIGNALING

To Divide or Not to Divide

The analysis of signaling circuits governed by threshold-sensitive switches may reveal why a particular network architecture is selected to control a biological process.

Jan M. Skotheim

The irreversible decision a cell makes when choosing its fate is based on diverse sources of information. How a cell integrates multiple signals into an all-or-none decision is the fascinating subject of a new study by Justman *et al*. (*1*) on the maturation of amphibian oocytes in response to the hormone progesterone. On page 509 of this issue, the authors show that interacting feedback loops within the network of cellular signaling pathways modulate sensitivity to progesterone in response to external cues. Depending on the generality of the solution, this work may have broad implications for cellular transitions contingent on multiple signals.

In the frog *Xenoupus laevis*, an oocyte arrests cell division (meiosis) and remains quiescent until progesterone triggers its maturation into a fertilizable egg. The hormone rapidly activates signaling pathways that induce the oocyte to resume meiosis. This switchlike response in maturation is based on a positive feedback loop that is activated by the input progesterone signal (*2*). For an intermediate progesterone input, there is great cell-to-cell variability in the response: Some oocytes proceed through meiosis, whereas others do not respond. Commitment is determined by engagement of the core positive feedback loop (see the figure). Beyond the initiation of positive feedback, removing the activating progesterone signal has no effect, a characteristic of bistable dynamical systems. That is, the system (oocyte) can exist in either of two stable states and transition from one (immature) to the other (mature).

Positive-feedback motifs are found in many genetic and biochemical circuits that control transitions in cellular states. However, positive feedback does not imply bistability. In addition to feedback, bistable systems require nonlinear elements to produce a dramatic threshold response (such as the transition from an immature to mature oocyte). Thus, an input signal (such as progresterone) that exceeds a critical value will rapidly ramp up output, whereas subthreshold signals produce little, if any, response. In the context of oocyte maturation, the mitogen-activated protein kinase (MAPK) signaling cascade is a component of the positive feedback loop that exhibits a nonlinear input-output relationship and is likely to be central to the bistable system response (*3*).

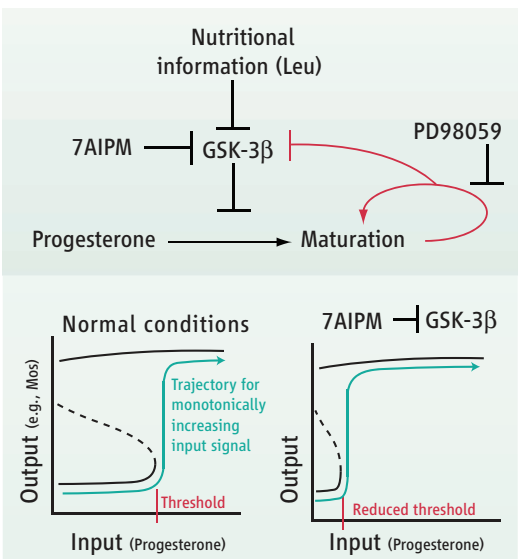

Looped organization. (**Top**) GSK-3β forms part of a double-negative feedback loop that modulates the progesterone threshold required to induce positive feedback–driven meiotic maturation in *Xenopus* oocytes. (**Bottom**) The solid lines indicate the steady-state output for a constant input signal. Two solid lines for the same input indicate hysteresis, i.e., that the eventual steady-state output reflects the time-dependent history of the input.

Although the feedback-driven nature of the dynamical system producing a threshold response to progesterone had been characterized, it remained unclear whether this response might be modulated to produce a robust output in different environments. Justman *et al.* show that two physiological signals—hormone and nutrient—are integrated into the feedback circuit responsible for oocyte maturation. They also identify a previously uncharacterized, additional double-negative feedback loop that shifts the progesterone threshold in response to environmental conditions.

The molecular link that connects the double-negative loop and raises the progesterone threshold is glycogen synthase kinase–3β (GSK-3β). Treatment of oocytes with a specific GSK-3β inhibitor [7-azaindolyl-pyrazinyl-maleimide (7AIPM)] reduced the progesterone threshold. Similarly, addition of leucine, sufficient to stimulate the target of rapamycin pathway that responds to nutrients (*4*), also reduced the threshold. Adding both leucine and 7AIPM produced an effect similar to that of 7AIPM acting alone, implying that nutritional information may be transmitted through GSK-3β.

However, GSK-3β may modulate the progesterone threshold through a variety of molecular architectures. For example, the progesterone signal might directly inactivate GSK-3β. To identify the correct regulatory network, Justman *et al.* used PD98059, which inhibits MAPK kinase (MEK), a central component of the positive feedback loop. Adding PD98059 before progesterone stimulation resulted in incomplete GSK-3β inactivation, thereby revealing a substantial effect of feedback on GSK-3β inhibition. Similarly, chemical induction of the feedback loop in the absence of progesterone completely inactivated GSK-3β. Although this work clearly displays the under-

Department of Biology, Stanford University, Stanford, CA 94305, USA. E-mail: skotheim@stanford.edu

lying double-negative feedback architecture, further research is required to uncover where the negative regulation of GSK-3β branches off from the core positive feedback loop. This information could then be used to assay the specific effect on the progesterone threshold of negative feedback on GSK-3β.

The system's double-negative feedback loop for threshold modulation is reminiscent of the *Start* transition in budding yeast, where multiple signals are integrated to produce an all-or-none decision to progress through the mitotic cell cycle. Beyond *Start*, a point within the G_1 phase of the cell division cycle, a cell remains committed to DNA replication and subsequent division in spite of severe environmental changes. Briefly, the molecular regulatory system underlying Start includes a cyclin-Cdk protein complex (Cln3-Cdc28) that initiates a transcriptional positive feedback loop of two more G_1 cyclins (Cln1 and Cln2), which ensure cell cycle progression (*5*). In the presence of yeast mating factor, a MAPK signaling pathway activates Far1, which inhibits G_1 cyclin activity (*6*, *7*). The inhibition of Far1 by G_1 cyclins (*8*, *9*) implies that pheromone-modulated G_1 control shares the same double-negative and positive feedback architecture as progesterone-induced *Xenopus* oocyte maturation. The similar regulatory architecture of these two well-studied systems suggests their widespread application.

As noted in the modeling efforts of Justman *et al*., different network architectures can produce the same dynamical response. Furthermore, identical networks can produce radically different dynamics depending on their parameters. The lack of a 1:1 correspondence between network architecture and phenotype (i.e., dynamics) indicates that the primacy given to network architecture over topology (e.g., bistability and phenotype) is misplaced. Furthermore, there is no a priori reason, from a dynamical systems point of view, to expect double-negative feedback rather than another network architecture to modulate a threshold. It is therefore likely that only the detailed investigation of a series of natural threshold-producing circuits may yield the reasons, perhaps of an evolutionary origin, for the selection of one network architecture over another.

References

1. Q. A. Justman, Z. Serber, J. E. Ferrell Jr., H. El-Samad, K. M. Shokat, *Science* **324**, 509 (2009).
2. W. Xiong, J. E. Ferrell Jr., *Nature* **426**, 460 (2003).
3. J. E. Ferrell Jr., E. M. Machleder, *Science* **280** 895 (1998).
4. C. J. Lynch *et al.*, *J. Cell Biochem*. 77, 234 (2000).
5. J. M. Skotheim *et al.*, *Nature* **454**, 291 (2008).
6. M. Peter, I. Herskowitz, *Science* **265**, 1228 (1994).
7. A. Gartner *et al.*, *Mol. Cell. Biol*. **18**, 3681 (1998).
8. J. D. McKinney *et al.*, *Genes Dev*. **7**, 833 (1993).
9. S. Henchoz *et al.*, *Genes Dev*. **11**, 3046 (1997).

10.1126/science.1173769

ATMOSPHERIC SCIENCE

Shifting Gear, Quickly

Methane bursts during a past warming transition may provide a guide to future Arctic climate change.

E. G. Nisbet[1] and J. Chappellaz[2]

Earth's climate can change gear very quickly, either sharply warming or fiercely cooling (*1*). Past shifts of this kind were massive, and some took place within a few years (*2*). About 11,600 years ago, at the end of the Younger Dryas cold period, the planet warmed very suddenly, with strong increases in atmospheric greenhouse gases, especially methane. On page 506 of this issue, Petrenko *et al.* use radiocarbon (^{14}C) data to identify the sources of the additional methane (*3*).

^{14}C is essentially absent in old geological methane sources but is present in biological methane. Thus, any fossil input—for example, from methane hydrates—should be detectable in methane extracted from bubbles in ice. However, the measurement effort required is heroic: 1000 kg of ice are needed to obtain a few hundred thousand ^{14}C atoms per sample of time studied. Petrenko *et al.* mined the ice like a geological seam at Pakitsoq on the West Greenland ice margin (see the figure), where the time horizon outcrops. Making sense of the measurements is difficult, however, as very large corrections must be applied, especially for the effect of cosmic rays. Because of these and other corrections, the absolute $^{14}CH_4$ concentrations are meaningless. However, the relative changes in a time sequence of measurements do carry meaning, varying as sources shifted during the warming event.

Although the new ^{14}C results do not elucidate the nature of the initial trigger that ended the Younger Dryas, they suggest that much of the new methane sustaining the warming came from wetlands, at least in the earlier part of the warming event. Less direct approaches to this problem—such as measuring the interpolar gradient (*4*), the hydrogen isotope ratio (expressed as δD) (*5*), and the carbon isotope ratio (expressed as $\delta^{13}C$) (*6*) in the ice core methane record—also point to changes in wetland emissions. Boreal wetlands would have been essentially shut down during glacial episodes

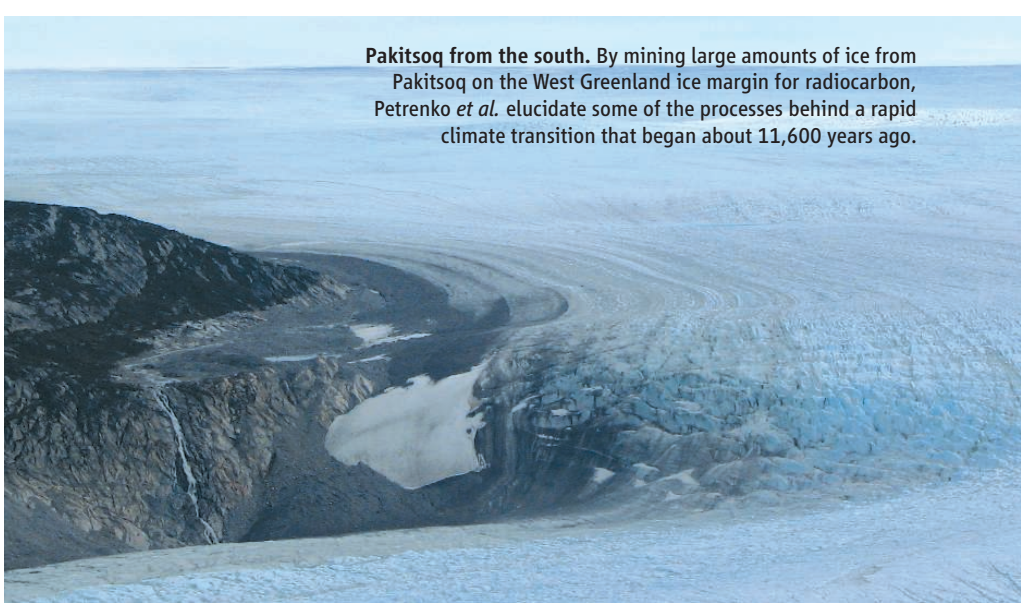

Pakitsoq from the south. By mining large amounts of ice from Pakitsoq on the West Greenland ice margin for radiocarbon, Petrenko *et al.* elucidate some of the processes behind a rapid climate transition that began about 11,600 years ago.

CREDIT: V. V. PETRENKO/UNIVERSITY OF COLORADO

[1]Department of Earth Sciences, Royal Holloway, University of London, Egham TW20 0EX, UK. [2]Laboratoire de Glaciologie et Géophysique de l'Environnement, CNRS, University of Grenoble, BP 96, 38402 St. Martin d'Hères, France. E-mail: e.nisbet@es.rhul.ac.uk; chappellaz@lgge.obs.ujf-grenoble.fr

but could have switched on quickly in ice-free areas. In contrast, biomass burning sources were stable, showing little change between cool and warm times (*7*). As a warming event is sustained, decomposing northern methane hydrates (clathrates) may inject fossil methane into the air, with wetland, thawing permafrost, and clathrate emissions reinforcing each other in a feedback loop (*8*). Petrenko *et al*.'s data leave such a scenario unconstrained but imply that wetlands were the main driver.

A possible explanation for the sudden end of the Younger Dryas is that, at a time of high Arctic insolation, an initial outburst of methane—perhaps from a geological source such as methane clathrates—triggered global warming, initiating both strong wetland emission in the tropics and north (*8*), and further hydrate responses as the thermal shock penetrated the permafrost (*9*, *10*), freeing methane from decomposing clathrate hydrates and releasing gas pools trapped beneath them. The clathrate gun hypothesis (*11*) postulates the dominant role of hydrate decomposition, as opposed to wetland emission, as the principal driver of change. Organic matter in thawing permafrost can also generate large emissions of methane (*12*). Detailed comparison in Greenland ice cores between the methane record and warming, as shown in nitrogen and argon isotopic signals (*13*, *14*), suggests that warmer air reached Greenland before the main rise in methane, thus challenging the clathrate gun scenario (*11*).

δD results (*5*) have been used to argue against the hypothesis that an outburst of methane from clathrate hydrates drove the change. However, although marine hydrates supplied by gas from deep geological sources are enriched in deuterium relative to terrestrial methane sources, shallow hydrate and decaying permafrost sources can be depleted. Moreover, the interpretation of the D/H signature during the decades of most sharply rising atmospheric methane is complex, because the global methane budget is not in equilibrium.

The jury thus remains out on the initial trigger, but it is clear that a very rapid wetland response plays a major role in driving the main methane increase. In addition, the end of the Younger Dryas is accompanied by a large increase of another greenhouse gas: N_2O (*15*), produced, for example, in soils and marine upwelling areas.

There are clear analogies with the modern Arctic, especially because global warming is expected to be strongest in the Arctic. Within the next few decades, reduced summer ice cover, earlier springs, and later freeze-up may cause radical change in Arctic wetland and permafrost regions. There was a sudden decrease in ice cover in summer 2007 (*16*). Very warm summer weather, possibly driven by global warming, has occurred recently in the Arctic. This may trigger new wetland sources (*17*, *18*) as well as fossil and thermokarst methane emissions (*12*, *19*).

Could the Arctic be preparing to shift gear again? If a shift on the scale and rapidity of past changes were to happen tomorrow— including intensified methane emissions from wetlands, decaying permafrost, and hydrate breakdown on Arctic continental margins and slopes—then the consequences for humanity could be very severe. Far from the Arctic, crops could fail and nations crumble. It is thus essential to decipher what took place in the past.

The hard labors of Petrenko *et al*. in mining tons of ice show the way, as there is plenty more ice to extract on outcropping blue ice fields at both poles. There is now a strong case for horizontal ice mining at the right depths in polar ice caps, far from surface cosmic ray in situ production. Large-sample ice collection from vanishing tropical ice caps is also urgently needed to assess the past history of other factors influencing methane, such as biomass burning. Humanity is triggering great changes; it would be wise to document and understand the past before we face the future.

References

1. J. Chappellaz *et al*., *Nature* **366**, 443 (1993).
2. J. P. Steffensen *et al*., *Science* **321**, 680 (2008); published online 19 June 2008 (10.1126/science.1157707).
3. V. V. Petrenko *et al*., *Science* **324**, 506 (2009).
4. J. Chappellaz *et al*., *J. Geophys. Res*. **102**, 15987 (1997).
5. T. Sowers, *Science* **311**, 838 (2006).
6. H. Schaefer *et al*., *Science* **313**, 1109 (2006).
7. H. Fischer *et al*., *Nature* **452**, 864 (2008).
8. E. G. Nisbet, *J. Geophys. Res*. **97**, 12859 (1992).
9. E. G. Nisbet, *Can. J. Earth Sci.* **26**, 1603 (1989).
10. E. G. Nisbet, *Can. J. Earth Sci.* **27**, 148 (1990).
11. J. P. Kennett, K. G. Cannariato, I. L. Hendy, R. J. Behl, *Science* **288**, 128 (2000).
12. K. M. Walter, M. E. Edwards, G. Grosse, S. A. Zimov, F. S. Chapin III, *Science* **318**, 633 (2007).
13. J. Severinghaus *et al*., *Nature* **391**, 141 (1998).
14. E. J. Brook *et al*., *Global Biogeochem. Cycles* **14**, 559 (2000).
15. J. Flückiger *et al*., *Science* **285**, 227 (1999).
16. R. W. Lindsay *et al*., *J. Clim.* **22**, 165 (2009).
17. M. Rigby *et al*., *Geophys. Res. Lett.* **35**, L22805 (2008).
18. E. J. Dlugokencky *et al*., *Eos* **89** (fall meet. suppl.), A12A-05 (2008).
19. N. Shakhova *et al*., *Eos* **89** (fall meet. suppl.), U23D-0081 (2008).

10.1126/science.1172001

GENETICS

It's a Bull's Market

Harris A. Lewin

Research on domesticated livestock heralds new advances in evolutionary biology, animal breeding, and animal models for human diseases.

From Darwin to Dolly, domesticated livestock have guided our understanding of evolution and biology. Moreover, for the past 10,000 years, livestock have provided sustenance to humans with their hides, hair, meat, milk, strength, speed, and companionship. Now, livestock are poised to give us even more, thanks to new insights from genomics and molecular phylogenetics. Five articles in this issue deal with the biogeography of domestication (*1*, *2*), the development of modern breeds (*1*, *3*), the genes responsible for agriculturally important traits (*3*, *4*), and the potential use of livestock species as models for human diseases (*5*).

The publication by the Bovine Genome Sequencing and Analysis Consortium describing the sequence, annotation, and comparative analysis of the cattle genome marks a major milestone in animal genetics (*3*). The Cetartiodactyl order of mammals, to which cattle and all other ruminants belong, is phylogenetically distant from the primates, and thus contains invaluable information for understanding human genome evolution. Cattle have numerous adaptive traits that underlie their unique biology, including a four-chambered stomach for digesting fiber, as well as specialized immune, endocrine, and reproductive system functions and architectures. Comparison of the cattle genome to that of other mammals was thus expected to yield exciting new information on how mammalian genomes evolve, mechanisms of gene regulation, genetic control of complex traits, and host-microbe interactions. The cows have not disappointed us.

At the gene level, there are tantalizing clues to explain the "essence of bovinity." Seventy-one genes show evidence of positive selection. Several immune function–related genes are expanded in copy number, such as the β-defensin and interferon genes, and rearrangements occur in key genes involved

Institute for Genomic Biology and Department of Animal Sciences, University of Illinois at Urbana-Champaign, Urbana, IL 61801, USA. E-mail: h-lewin@uiuc.edu

in lactation. The bacteria-busting lysozyme genes used by white blood cells have been expanded in copy number and adapted to a similar function in the ruminant abomasum, the glandular stomach (similar to the human stomach) where microbes that digest cellulose and ferment complex sugars in the rumen are broken down. (The rumen is also an excellent source of cellulytic bacteria that may be important for biofuels production.) As with rodents and dogs, cattle have about 1000 genes not found in the human genome, and 1217 genes occur only in eutherian (placental) mammals. These intriguing genes complement the large number of variants in promoter sequences and transcription factors that are thought to contribute to differences in mammalian development and physiology.

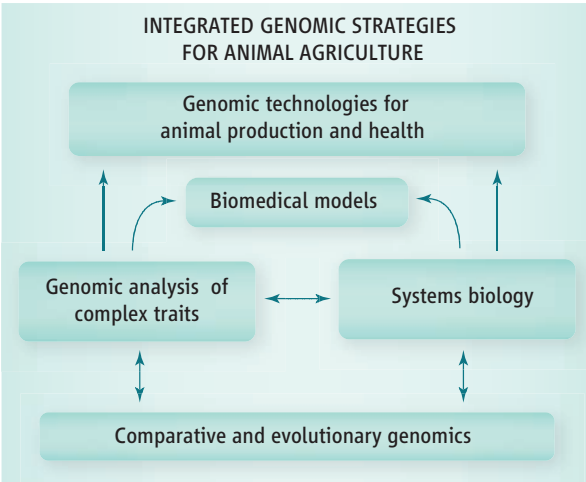

Research roadmap. An integrated approach to animal studies will support advances in sustainable agriculture and animal and human health.

The high quality of the cattle genome assembly enabled a detailed multispecies comparison of chromosome organization that produced novel insights into mammalian chromosome evolution. A major finding was that higher densities of segmental duplications, retroposons, and retrovirus long terminal repeats are present in chromosome regions that were rearranged during the last 80 million years, leading to the *Bos taurus* karyotype. Thus, specific kinds of repetitive elements and segmental duplications appear to directly promote the chromosome rearrangements associated with speciation in multiple mammalian lineages. With additional mapped and sequenced genomes on the horizon, it will be possible to explore further the relationship between chromosome rearrangements and adaptive evolution of mammals (*6*).

In his1868 opus *The Variation of Animals and Plants Under Domestication*, Charles Darwin wrote: "I have often speculated on the probable causes through which each separate district in Great Britain came to possess in former times its own peculiar breed of cattle…." What Darwin was trying to distinguish were the roles of common ancestry, natural selection, and artificial (human-assisted) selection in the extraordinary diversity of cattle phenotypes. The Bovine HapMap Consortium describe (*4*) the genetic structure of modern taurine and indicine (humped) breeds and the factors that may have shaped the breeds' genetic diversity, thus addressing Darwin's muse. High levels of genetic diversity were found in all cattle breeds, even higher than those found in human and dog populations (*7*, *8*). The greatest diversity was found in indicine Brahman cattle, with one SNP (single-nucleotide polymorphism, a DNA sequence variation) every 285 base pairs of DNA. That's more than twice the number for the taurine Holstein and Angus breeds, thus indicating that more individuals were involved in forming indicine cattle before domestication. Following domestication, the genetic evidence suggests that cattle breeds went through mild bottlenecks, possibly due to a limited number of founder individuals or selection for production traits. Furthermore, several regions of the genome were differentiated in breeds used for milk and meat production, and many of these regions contain genes responsible for quantitative variation in milk production and meat-quality traits. This reveals a fascinating linkage between traditional animal breeding and genomic architecture and suggests that genetic diversity should be carefully monitored as genomic selection for quantitative traits (*9*) takes its place as a routine technology for animal genetic improvement.

Genome analyses, coupled with molecular phylogenetic techniques, have also revealed new historical insights into the domestication of other livestock species, such as sheep and horses. It is now clear that sheep were domesticated in Southwest Asia and then spread to Europe in two distinct waves. Most modern-day sheep breeds appear to be a result of this second migration (*1*). Horse domestication has proved difficult to pin down, but Ludwig *et al.* (*2*), using six coat-color genes, provide strong support for an earlier conclusion (*10*) that links horse domestication to the Botai culture, which flourished in Kazakhstan in the fourth millennium B.C.E.. Wild predomesticated horses found in Siberia and Eastern and Central Europe were homozygous for all six coat-color genes, which likely made these ancient animals "bay" colored. However, coat-color variants rapidly increased during and after the Bronze Age, which coincides with the timing of domestication proposed by Outram *et al*. (*10*), suggesting a human hand in their spread. Apparently, a horse of a different color was a thing to be cherished by our ancestors.

The barnyard door is now open. We can expect that any animal with medically or agriculturally useful traits will be sequenced and resequenced. Similar to the primate-human comparisons geneticists are making to understand the origins of human intelligence, comparative genomic studies of cattle, pigs, sheep, and goats, may help us to better understand the genetics of wool production, lactation, growth, metabolism, and environmental adaptation. This will further accelerate the development of new technologies for sustainable animal agriculture (see the figure). Moreover, as outlined by Roberts *et al.* (*5*), cattle and other livestock have played important roles in advancing biomedical research, leading to new technologies including assisted reproduction and organ transplants. With the genome sequence of cattle in hand, and that of other livestock species soon to follow, we can for the first time select animal models of human diseases on the basis of trait homology as well as gene structure, chromosome organization, and transcription factor binding sites. This will help increase the reliability of animal models, because common genomic architecture may more accurately predict the regulation of disease-related genes. The anticipated rapid advances in comparative and functional genomics will make genome-enabled livestock models an increasingly valuable resource for biomedical research. In a bull's market, everyone wins.

References and Notes

1. B. Chessa *et al., Science* **324**, 532 (2009).
2. A. Ludwig *et al., Science* **324**, 485 (2009).
3. The Bovine Genome Sequencing and Analysis Consortium, C. G. Elsik, R. L. Tellam, K. C. Worley, *Science* **324**, 522 (2009).
4. The Bovine HapMap Consortium, *Science* **324**, 528 (2009).
5. R. M. Roberts *et al., Science* **324**, 468 (2009).
6. D. M. Larkin *et al., Genome Res.* 10.1101/gr.086546.108 (2009).
7. E. A. Ostrander, R. K. Wayne, *Genome Res.* **15**, 1706 (2005).
8. G. Marth *et al. Proc. Natl. Acad. Sci. U.S.A.* **100**, 376 (2003).
9. B. J. Hayes *et al., J. Dairy Sci.* **92**, 433 (2009).
10. A. K. Outram *et al., Science* **323**, 1332 (2009).
11. I thank G. E. Robinson and R. Oliveira for their helpful suggestions.

10.1126/science.1173880

GRADUATE EDUCATION

Dramatic Rise in Minority Science Ph.D.'s Detailed in New Report

The number of science and engineering Ph.D. recipients has increased dramatically among underrepresented minorities under a program started a decade ago by the National Science Foundation (NSF), according to a new report released by AAAS.

At 66 of the 79 U.S. universities participating in the Alliances for Graduate Education and the Professoriate (AGEP) program, the annual number of science, technology, engineering, and mathematics (STEM) doctoral degrees awarded to minority students increased by 33.9% from 2001 to 2008. The gains were even more remarkable among the natural sciences and engineering fields, where Ph.D.'s for minorities increased by 50%.

Participants in the AGEP program say its success can be traced to a comprehensive rethinking of the minority graduate experience—from targeted recruiting efforts to employment placement.

The success of the program has been widespread, with schools as diverse as the University of Utah, Howard University, and the University of Florida each surpassing 25 doctoral degrees to underrepresented minorities in 2007–2008.

"We have had low numbers that have been lagging," said Shirley Malcom, head of Education and Human Resources at AAAS. "So, finally, here's some good news about a set of institutions that have set out to increase the participation of minorities within the sciences, and they've done it."

Shirley Malcom

The AGEP program "is making important contributions to the nation's science and engineering workforce," said James H. Wyche, director of the Division of Human Resource Development at NSF.

Since AGEP's inception in 1998, AAAS has received consecutive NSF grants to track the progress of the program and has worked with AGEP universities to help them assess their own performance and identify where improvements can be made. [AAAS's most recent report on the program is available at http://nsfagep.org/publications.php.]

"What's different about this program is that it is about changing the strategies and the processes that institutions are using to recruit and support underrepresented minorities," said Yolanda George, deputy director of AAAS Education and Human Resources.

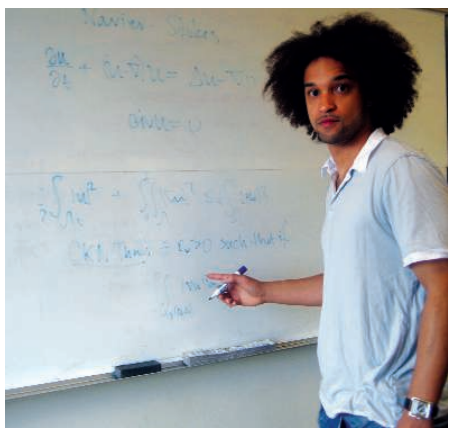

Berkeley's Edge. Mathematics Ph.D. candidate Ryan Hynd was recruited by the school's AGEP program.

Some of the changes have been relatively straightforward, such as initiating personal contact with potential students, said Patricia Campbell, president of Campbell-Kibler Associates, who worked with George to analyze the data for the new report. "If you want someone to consider your institution, ask them. That's something that hasn't been in a number of admissions policies and programs."

The University of California, Berkeley, was the top producer of Ph.D.'s in the AGEP program, graduating 57 students in 2007–2008. Berkeley recruits underrepresented minorities at conferences and institutions such as historically black colleges, said Colette Patt, director of the school's science diversity programs, but AGEP resources "made sure all of those opportunities were covered, that we weren't sporadic, that we went every place and every year."

The school's AGEP program, called Berkeley Edge, offers professional development lunches and a yearly retreat where students can learn skills like networking at a conference, setting up a lab, and hunting down a suitable postdoctoral position. One of the program's major activities, said Patt, is an annual pre-admission conference that has helped the school recruit "from places that are not our typical feeder schools."

Ryan Hynd, a Ph.D. candidate in the school's mathematics department, attended the conference before deciding on Berkeley and now talks with potential new graduate students at the venue. Hynd selected Berkeley based on its stellar academic reputation, but he also appreciates how the Edge has "fostered a sense of community" among the school's minority Ph.D. students.

Patty Garcia, a Ph.D. candidate in Berkeley's molecular and cell biology department, used an AGEP-supported study group to prepare for her doctoral qualifying exams last year. And she singles out the program as "our biggest supporter" when she helped start a chapter of SACNAS, a national society for Latinos and Native Americans in science.

AGEP's participants say that much of the program's strength comes from its dedicated faculty. "Lots of credit needs to be given to the scientists who take time from their actual research to work on the AGEP pieces," said Campbell. "That they're not only willing to do it, but do it year after year—it's just phenomenal."

—Molly McElroy and Becky Ham

SCIENCE AND SOCIETY

Expert: Bioethics Council Should Expand Mission

Advances in neuroscience and synthetic life research are outpacing a discussion of the research's ethical implications, making them prime candidates for the agenda of the next national bioethics commission, according to AAAS expert Mark S. Frankel.

At a 12 March meeting of the U.S. President's Council on Bioethics, Frankel said the ethics of doing research in virtual online communities such as Second Life, and in recruiting subjects for personalized medicine, are also emerging topics for a national debate.

Established by U.S. President George W. Bush in 2001, the council's work has included reports on stem cell research, human cloning, and genetic screening. While these topics remain relevant, said Frankel, a new commission should expand its purview when President Barack Obama renews its charter in September, as he is expected to do.

The new council should seek more public input, said Frankel, director of the AAAS Scientific Freedom, Responsibility and Law Program. He suggested that the council redesign its makeup so that at least 25% of its members represent public groups, and that members "get out of Washington periodically" to learn more about how these ethical issues are perceived outside of government.

—Becky Ham

MIDDLE LINE PHOTO CREDIT: RYAN HYND

Published by AAAS

Fire in the Earth System

David M. J. S. Bowman,[1*] Jennifer K. Balch,[2,3,4*†] Paulo Artaxo,[5] William J. Bond,[6] Jean M. Carlson,[7] Mark A. Cochrane,[8] Carla M. D'Antonio,[9] Ruth S. DeFries,[10] John C. Doyle,[11] Sandy P. Harrison,[12] Fay H. Johnston,[13] Jon E. Keeley,[14,15] Meg A. Krawchuk,[16] Christian A. Kull,[17] J. Brad Marston,[18] Max A. Moritz,[16] I. Colin Prentice,[19] Christopher I. Roos,[20] Andrew C. Scott,[21] Thomas W. Swetnam,[22] Guido R. van der Werf,[23] Stephen J. Pyne[24]

Fire is a worldwide phenomenon that appears in the geological record soon after the appearance of terrestrial plants. Fire influences global ecosystem patterns and processes, including vegetation distribution and structure, the carbon cycle, and climate. Although humans and fire have always coexisted, our capacity to manage fire remains imperfect and may become more difficult in the future as climate change alters fire regimes. This risk is difficult to assess, however, because fires are still poorly represented in global models. Here, we discuss some of the most important issues involved in developing a better understanding of the role of fire in the Earth system.

Over the past decade, a surge in the incidence of large, uncontrolled fires has occurred on all vegetated continents, irrespective of national fire-fighting capacity or management tactics (*1*–*5*). These episodic fires have high economic costs. The fires in Southeast Asia's tropical forests related to the 1997–1998 El Niño–Southern Oscillation (ENSO) event, for example, resulted in economic costs near $U.S. 8.8 to 9.3 billion, of which a conservative estimate of $U.S. 1 billion was from adverse health effects of smoke haze (*6*). During the same period, more than 20 million ha burned in Latin America, causing an estimated $U.S. 10 to 15 billion in damages (*4*). The ubiquity of such large fires calls into question our capacity for fire control and highlights our limited understanding of fire's causes, effects, and feedbacks.

There is growing awareness of the deleterious effects of such uncontrolled fires on biodiversity, human health, and the economy (*2*). However, there remains a serious lack of knowledge about fire's fundamental role in Earth system processes, as well as an insufficient appreciation of fire's interaction with anthropogenic global environmental change. For example, though the Intergovernmental Panel on Climate Change (IPCC) report concluded that global climate change will increase the risk of extreme fire events (*7*), its assessment did not quantify potential fire-climate feedbacks. In order to achieve a better understanding of fire, it must be understood as an integral Earth system process that links and influences regional and global biogeochemical cycles, human activity, and vegetation patterns. Failure to develop a coordinated and holistic fire science will slow efforts to adapt to changing fire regimes and manage fire.

Fire in Earth History

Fossil charcoal indicates that wildfires began soon after the appearance of terrestrial plants in the Silurian [420 million years ago (Ma)] (*8*). Combustion occurs when atmospheric O_2 concentrations are above 13%, and variation in O_2 levels correlates with fire activity throughout Earth history (*8*) (Fig. 1). Many Permian coals contain large quantities (70%) of charcoal during a period when atmospheric oxygen was thought to have exceeded 30%, making even moist vegetation flammable (*8*). Counterintuitively, the burial of decay-resistant charcoal and organic matter following postfire erosion may have increased oxygen levels and caused long-term reduction of atmospheric carbon dioxide levels (*9*). Fire also influences the geological cycling of other elements, such as phosphorus, by volatization and leaching (*10*).

Fire's occurrence throughout the history of terrestrial life invites conjecture that fire must have had pronounced evolutionary effects on biotas. However, the evolution of adaptations to fire remains a difficult topic to explore because traits that increase the rate of occurrence of fire, or of recovery following burning, are not unambiguously the result of natural selection by fire regimes (*11*) (table S1). Nonetheless, flammable vegetation types leave distinct signatures in the fossil record, chronicling changes in their abundance and geographic range. For example, tropical grasses produce large quantities of fine, aerated fuels that become highly flammable during dry periods, and their C_4 photosynthetic pathway produces organic matter characteristically depleted in ^{13}C. Stable isotope analyses of carbon in sediments have shown that tropical savanna biomes simultaneously spread in Asia, Africa, and the Americas, approximately 7 to 8 Ma, coinciding with a substantial spike in charcoal in marine sediments (*12*). It has even been suggested that fire led to the expansion of savannas due to climate feedbacks that created hotter, drier conditions that favored savannas (*13*).

Humans and Fire

The spread of highly flammable savannas, where hominids originated, likely contributed to their eventual mastery of fire (*14*). The hominid fossil record suggests that cooked food may have appeared as early as 1.9 Ma (*15*), although reliable evidence for controlled fire use does not appear in the archaeological record until after 400,000 years ago, with evidence of regular use much later (*16*). The routine domestic use of fire began around 50,000 to 100,000 years ago (*17*), which may have influenced the evolution of human tolerance to air pollution (*18*), and hunter-gatherers used fire to reduce fuels and manage wildlife and plants beginning tens of thousands of years ago (*19*).

In recent history, the ongoing transition from subsistence to industrial economies is typified by the conversion of forests into agricultural or pastoral landscapes through the use of fire. For example, fire-resistant tropical rainforests are rapidly being cleared with fire in agricultural frontiers (*20*) (Fig. 2). Conversely, in the developed world, suburban sprawl into rural and natural landscapes, where people and their dwellings are juxtaposed with flammable vegetation types, is accompanied by substantial fire-suppression efforts (*21*). Worldwide, fire is used to minimize fuel hazard, maintain habitat quality, and stimulate forest and pasture regeneration. Despite human use of fire to achieve economic and ecological benefits (*22*), fire remains an unreliable tool, often evading control, particularly during extreme drought events (*3*, *23*). This imperfect mastery of fire manage-

[1]The University of Tasmania, Hobart, TAS 7001, Australia. [2]National Center for Ecological Analysis and Synthesis, Santa Barbara, CA 93101, USA. [3]Yale University, School of Forestry and Environmental Studies, New Haven, CT 06511, USA. [4]Woods Hole Research Center, Woods Hole, MA 02543, USA. [5]Universidade de São Paulo, Instituto de Física, CEP 05508-900, São Paulo, Brazil. [6]University of Cape Town, Department of Botany, Cape Town, South Africa. [7]University of California, Department of Physics, Santa Barbara, CA 93106, USA. [8]South Dakota State University, Geographic Information Science Center of Excellence, Brookings, SD 57007, USA. [9]University of California, Environmental Studies Program and Department of Ecology, Evolution & Marine Biology, Santa Barbara, CA 93106, USA. [10]Columbia University, Ecology, Evolution and Environmental Biology, New York, NY 10027, USA. [11]California Institute of Technology, Department of Control and Dynamical Systems, Pasadena, CA 91125, USA. [12]School of Geographical Sciences, University of Bristol, Bristol BS8 1SS, UK. [13]University of Tasmania, Menzies Research Institute, Hobart, TAS 7001, Australia. [14]U.S. Geological Survey, Western Ecological Research Center, Sequoia-Kings Canyon Field Station, Three Rivers, CA 93271, USA. [15]University of California, Department of Ecology and Evolutionary Biology, Los Angeles, CA 90095, USA. [16]University of California, Ecosystem Sciences Division, Department of Environmental Science, Policy, and Management, Berkeley, CA 94720, USA. [17]Monash University, School of Geography and Environmental Science, Melbourne, VIC 3800, Australia. [18]Brown University, Department of Physics, Providence, RI 02912, USA. [19]QUEST, Department of Earth Sciences, University of Bristol, Bristol BS8 1RJ, UK. [20]Ohio State University, Department of Anthropology, Columbus, OH 43210, USA. [21]Royal Holloway University of London, Department of Earth Sciences, Egham, Surrey TW20 0EX, UK. [22]The University of Arizona, Laboratory of Tree-Ring Research, Tucson, AZ 85721, USA. [23]VU University, Faculty of Earth and Life Sciences, Department of Hydrology and Geo-environmental Sciences, 1081 HV, Amsterdam, Netherlands. [24]Arizona State University, School of Life Sciences, Tempe, AZ 85287, USA.

*These authors contributed equally to this work.
†To whom correspondence should be addressed. E-mail: balch@nceas.ucsb.edu

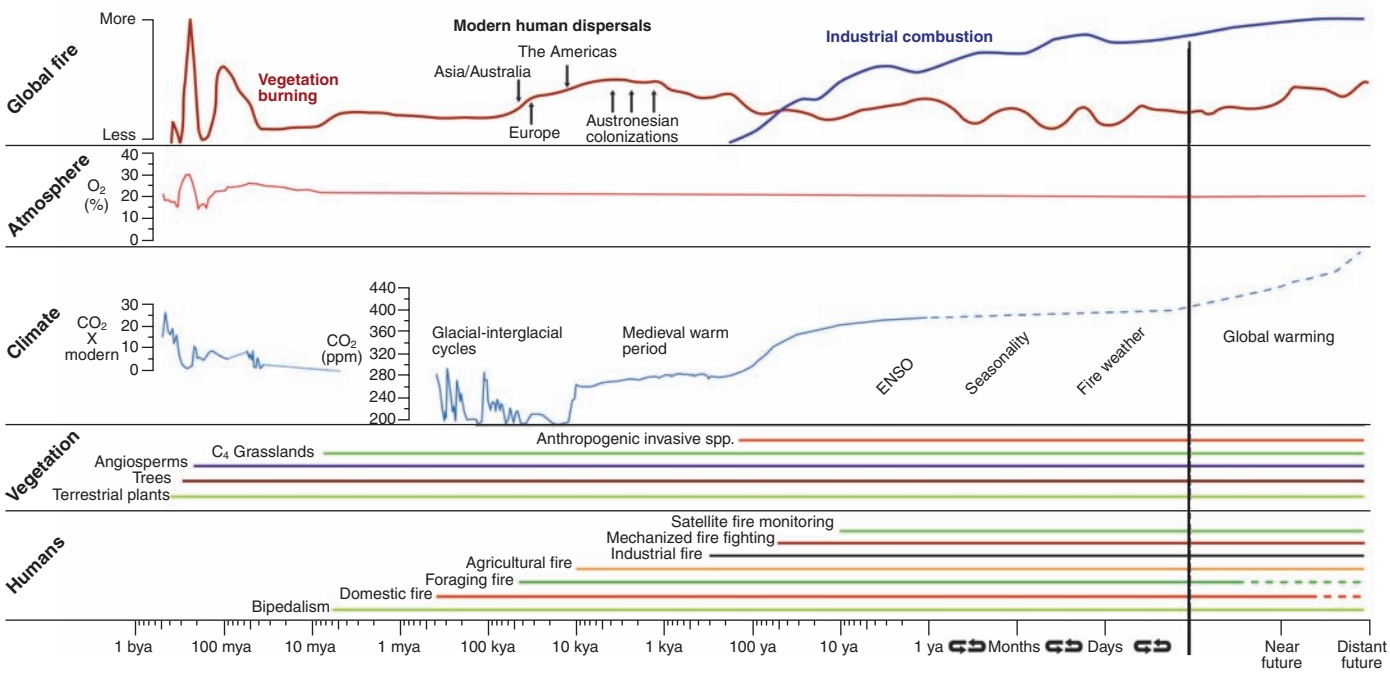

Fig. 1. Qualitative schematic of global fire activity through time, based on pre-Quaternary distribution of charcoal, Quaternary and Holocene charcoal records, and modern satellite observations, in relation to the percentage of atmospheric O_2 content, parts per million (ppm) of CO_2, appearance of certain vegetation types, and the presence of the genus *Homo*. (See supporting online text for data sources used.) Dotted lines indicate periods of uncertainty.

ment raises the unsettled issue of whether humans or climate are more important in determining fire patterns.

Distribution and Diversity of Fire

Earth is an intrinsically flammable planet owing to its cover of carbon-rich vegetation, seasonally dry climates, atmospheric oxygen, and widespread lightning and volcano ignitions. Yet, despite the human species' long-held appreciation of this flammability, the global scope of fire has been revealed only recently by satellite observations available beginning in the 1980s (*24*) (Fig. 2). This record shows a strong association between high fire activity and areas of intermediate primary production, particularly in tropical savannas (*25*). However, the satellite record does not adequately capture fire activity in ecosystems that have long (>100-year) fire intervals, nor in cases in which fire behavior is highly variable. Satellite products that provide those data on area burned, fire intensity, and completeness of combustion are still being developed (*26*).

Fires burn with different intensities and frequencies, resulting in a wide variety of ecological effects. To capture this diversity, ecologists define the "fire regime" on the basis of a range of variables including fuel type (ground, surface, and crown), temporal nature (rate of spread, seasonality, and frequency), spatial pattern (size and patchiness), and consequences (impacts on vegetation and soils) (*27*). The association of plant species having distinct reproductive and survival strategies with different fire regimes suggests that fire is a potent biological filter (table S1) influencing biomass production, vegetation distribution, and thus the risk of fire. Indeed, a notable feature of fire's distribution is the broad correlation between vegetation formations and fire regimes (*28*). Furthermore, fire can sometimes explain the presence of alternate ecosystem states within the same climatic zone (*28*).

Vegetation transitions can occur when fire regimes are altered substantially beyond historical norms, owing to changes in ignition sources or fuel mass, and variations in structure caused by fire protection, grazing, or the spread of invasive plants. For example, nonflammable tropical rainforests, evergreen woodlands, and arid shrublands can abruptly convert to highly flammable plant communities with increasing anthropogenic ignitions and fine fuels from invasive grasses (*29*). Fire protection, by contrast, promotes dense regrowth and closed woodlands. In the southwestern United States, this has led to an associated switch from surface to crown fires (*30*). Human landscape management is implicated in these fire regime transitions, yet underlying climate patterns also alter fire behavior.

Climate and Human Drivers of Fire

Analyses of historical meteorological data and national fire records show the primacy of climate in driving large regional fires, e.g., via antecedent wet periods that create substantial herbaceous fuels or drought and warming that extend conducive fire weather (*1*). Additionally, dendrochronological and observational analyses show tight coupling between high fire activity and interannual- and decadal-scale climate oscillations (*31*, *32*). For example, fire occurrence increases during the La Niña phase of the ENSO in the southern United States and Patagonia, Argentina (*25*, *33*), whereas a marked increase in fire activity occurs in tropical rainforests during El Niño phases (*34*). Sedimentary charcoal records also show a strong link between climate and fire activity, with reduced fire in cold intervals and increased fire in warm intervals, regardless of whether humans were present (*35*). However, charcoal records do show a reduction in fire after ~1870 C.E. in most regions, apparently in response to agricultural intensification and introduced animal grazing (*36*).

Abrupt changes in fire activity during island colonization offer insight into human influence on fire, beyond background climate conditions. For example, the colonization of the southern island of New Zealand by the Maori about 700 to 800 years ago was characterized by widespread destruction of forests by burning, causing the loss of half of the island's temperate rainforests (*37*). Likewise, it has been argued that fire usage during the late Pleistocene colonization of Australia triggered a series of megafaunal extinctions and vegetation changes (*38*).

Fire, Carbon, and Climate

Humans and climate both play a role in determining fire patterns and, in turn, fire influences the climate system via the release of carbon. Fires accelerate the natural cycle of primary production and respiration. In a world without fire, more carbon would be stored in woody vegetation (*39*). If climate and fire regimes equilibrate, then fire-induced atmospheric CO_2 emissions are balanced by uptake from surviving vegetation or via regeneration. The individual contribu-

tions of landscape fires, biomass combustion for domestic and industrial uses, and fossil-fuel combustion to total carbon emissions remain difficult to separate. Currently, all sources of fire (landscape and biomass) cause CO_2 emissions equal to 50% of those stemming from fossil-fuel combustion (2 to 4 Pg C year^{-1} versus 7.2 Pg C year^{-1}) (*7*, *40*, *41*). Of the fire-related emissions, we estimate that burning related to deforestation, a net CO_2 source, contributes about 0.65 Pg C year^{-1} (supporting online material). In contrast, the regrowth of vegetation and the production of black carbon (which is a by-product of burning, with a long residence time in soils) are sinks of atmospheric CO_2 and may be expanded with targeted management (*42*).

Between 1997 and 2001, biomass burning accounted for about two-thirds of the variability in the CO_2 growth rate (*34*, *43*). During the 1997-1998 ENSO-related drought event, Indonesian peat fires contributed an estimated 0.8 to 2.6 Pg C (*3*), while Amazon forest fires committed 0.024 to 0.165 Pg C to the atmosphere from just understory fires (*23*). These deforestation-related fires contribute substantially to the global burden of greenhouse gases, and the associated global warming that they will cause is projected to increase extreme fire weather (*1*), leading to further spikes of carbon emissions (*44*).

Fire also influences climate by releasing atmospheric aerosols and changing surface albedo. An appreciable fraction of biomass-burning emissions consists of black carbon aerosols that have strong solar radiation absorption properties, and may have the strongest effect on global warming after CO_2 (*45*). Regionally, smoke plumes inhibit convection, and black carbon warms the troposphere, thereby reducing vertical convection and limiting rain-cloud formation and precipitation (*46*). Locally, fire heats the surface by reducing albedo. However, albedo may increase over longer time periods owing to larger exposure of snow following boreal fires, or replacement of dark forests with brighter pastures and croplands following deforestation. Indeed, aerosol and surface albedo effects could even cancel each other [e.g., (*47*)].

Fire influences most radiative forcing components and has a substantial positive feedback on the climate system. We estimate that global CO_2 emissions from deforestation fires alone contribute up to ~19% of the total increased radia-

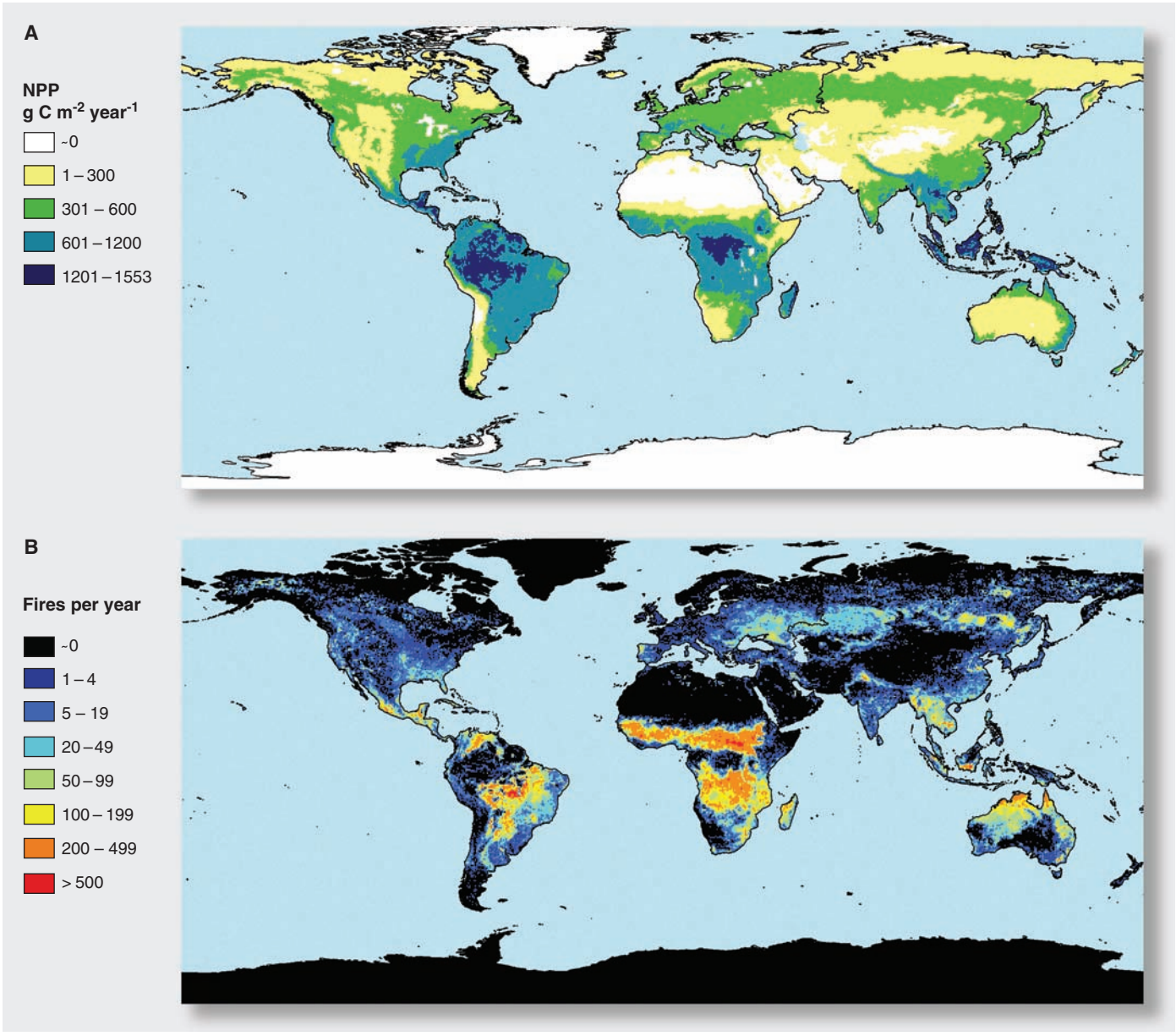

Fig. 2. Current pyrogeography on Earth, illustrated by (**A**) net primary productivity (NPP, g C m^{-2} year^{-1}) (*40*) from 2001 to 2006, by 1° grid cells; and (**B**) annual average number of fires observed by satellite (*49*).

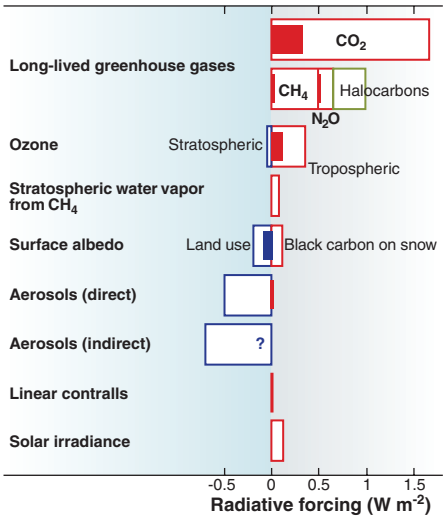

Fig. 3. Estimated contribution of fire associated with deforestation to changes in radiative forcing compared to 1750 C.E. (*7*), assuming a steady state for other fire emissions. The shaded inner bar (blue indicates cooling; red, warming) is the estimated fire contribution to the total radiative forcing of individual agents identified by the IPCC (unshaded, outlined bar) (*7*). Several assumptions had to be made to estimate these contributions, and more interdisciplinary research is needed to reduce uncertainties, especially for ozone, albedo, and the complicated effect of aerosols.

tive forcing since preindustrial times, following IPCC definitions (*7*) (Fig. 3 and supporting online text). The positive and negative fire-related contributions of the other radiative forcing components are assumed to cancel each other. Excluding deforestation fires, we also assume that fire-related emissions over the long term are at a steady state because of the natural successional cycle. Improved estimates of the climate forcing of fire must address fire's complex web of interactions with other radiative forcing components and must resolve how fire activity and land-cover change have varied through the industrial period.

Fire Feedbacks

At the flame front, fire instantaneously links the atmosphere, biosphere, and hydrosphere via the release of heat, gases (notably water vapor), and matter. The composition of these products is influenced by fuel type, moisture content, and combustion type (smoldering versus flaming), which in turn is influenced by temperature and available oxygen. At the landscape scale, fire responds predictably to variation in fuel types, vegetation structure, topographic features, and weather conditions. At regional and global scales, the interaction of fire with vegetation types and human land use results in characteristic fire regimes. Climate conditions are a fundamental driver of fire spread, and fire-induced emissions influence future climate scenarios and fire weather.

Simulations using physiologically based global vegetation models suggest that forests would at least double in extent in the absence of fire, particularly in the flammable savanna biome (*39*). The difference between simulated and observed vegetation distribution highlights the importance of including fire in terrestrial ecosystem modeling. Indeed, some global carbon and dynamic global vegetation models explicitly include fires (*34*, *48*).

Conclusions

Progress in understanding fire on Earth has been hampered by cultural aversions to accepting fire as a fundamental global feature and disciplinary parochialism (*19*, *22*). An Earth system perspective is essential to understanding how fire has developed throughout Earth history, and teasing apart the direct and indirect interactions between humans and fire. Understanding global trends in fire activity demands greater development of fire regime mapping, as well as global modeling approaches that are more sophisticated than the current generation. Such an integrated perspective is necessary and timely, given that a diversity of fragmented research programs have identified the pervasive influences of fire on the Earth system. Indeed, future IPCC assessments of anthropogenic global climate forcing should include specific analyses of the role of fire.

References and Notes

1. A. L. Westerling, H. G. Hidalgo, D. R. Cayan, T. W. Swetnam, *Science* **313**, 940 (2006).
2. D. J. Lohman, D. Bickford, N. S. Sodhi, *Science* **316**, 376 (2007).
3. S. E. Page *et al.*, *Nature* **420**, 61 (2002).
4. UNEP, *Spreading Like Wildfire—Tropical Forest Fires in Latin America and the Caribbean: Prevention, Assessment and Early Warning* [United Nations Environment Programme (produced by M.A. Cochrane), Panama, 2002].
5. G. G. Forsyth, B. W. van Wilgen, *Koedoe Afr. Protected Area Conserv. Sci.* **50**, 3 (2008).
6. J. Schweithelm, D. Glover, T. Jessup, in *Indonesia's Fire and Haze: The Cost of Catastrophe,* D. Glover, T. Jessup, Eds. (International Development Research Centre and the Institute of Southeast Asian Studies, Ottawa and Singapore, 1999, reprinted 2006).
7. IPCC, *Climate Change 2007: The Physical Science Basis*, Contribution of Working Group I to the Fourth Assessment Report of the IPCC (Cambridge Univ. Press, Cambridge, 2007).
8. A. C. Scott, I. J. Glasspool, *Proc. Natl. Acad. Sci. U.S.A.* **103**, 10861 (2006).
9. R. A. Berner, D. J. Beerling, R. Dudley, J. M. Robinson, R. A. Wildman, *Annu. Rev. Earth Planet. Sci.* **31**, 105 (2003).
10. T. M. Lenton, *Glob. Change Biol.* **7**, 613 (2001).
11. D. W. Schwilk, B. Kerr, *Oikos* **99**, 431 (2002).
12. J. E. Keeley, P. W. Rundel, *Ecol. Lett.* **8**, 683 (2005).
13. D. J. Beerling, C. P. Osborne, *Glob. Change Biol.* **12**, 2023 (2006).
14. L. Ségalen, J. A. Lee-Thorp, T. Cerling, *J. Hum. Evol.* **53**, 549 (2007).
15. R. W. Wrangham, J. H. Jones, G. Laden, D. Pilbeam, N. Conklin-Brittain, *Curr. Anthropol.* **40**, 567 (1999).
16. P. Karkanas *et al.*, *J. Hum. Evol.* **53**, 197 (2007).
17. O. Bar-Yosef, *Annu. Rev. Anthropol.* **31**, 363 (2002).
18. S. M. Platek, G. G. Gallup, B. D. Fryer, *Med. Hypotheses* **58**, 1 (2002).
19. S. J. Pyne, *Fire: A Brief History* (Univ. of Washington Press, Seattle, 2001).
20. F. Mouillot, C. B. Field, *Glob. Change Biol.* **11**, 398 (2005).
21. D. Theobald, W. Romme, *Landsc. Urban Plan.* **83**, 340 (2007).
22. S. J. Pyne, *Int. J. Wildland Fire* **16**, 271 (2007).
23. A. Alencar, D. C. Nepstad, M. C. V. Diaz, *Earth Interact.* **10**, 1 (2006).
24. O. Arino, J.-M. Rosaz, P. Goloub, *Earth Obs. Q.* **64**, 1 (1999).
25. G. R. van der Werf, J. T. Randerson, L. Giglio, N. Gobron, A. J. Dolman, *Global Biogeochem. Cycles* **22**, GB3028 (2008).
26. K. Tansey *et al.*, *Geophys. Res. Lett.* **35**, L01401 (2008).
27. W. J. Bond, J. E. Keeley, *Trends Ecol. Evol.* **20**, 387 (2005).
28. D. M. J. S. Bowman, *Australian Rainforests: Islands of Green in a Land of Fire* (Cambridge Univ. Press, Cambridge, 2000).
29. C. M. D'Antonio, P. M. Vitousek, *Annu. Rev. Ecol. Syst.* **23**, 63 (1992).
30. C. D. Allen *et al.*, *Ecol. Appl.* **12**, 1418 (2002).
31. T. Kitzberger, P. M. Brown, E. K. Heyerdahl, T. W. Swetnam, T. T. Veblen, *Proc. Natl. Acad. Sci. U.S.A.* **104**, 543 (2007).
32. T. W. Swetnam, *Science* **262**, 885 (1993).
33. T. Kitzberger, T. W. Swetnam, T. T. Veblen, *Glob. Ecol. Biogeogr.* **10**, 315 (2001).
34. G. R. van der Werf *et al.*, *Science* **303**, 73 (2004).
35. M. J. Power *et al.*, *Clim. Dyn.* **30**, 887 (2008).
36. J. Marlon *et al.*, *Nat. Geosci.* **1**, 697 (2008).
37. M. S. McGlone, J. M. Wilmshurst, *J. Quat. Sci.* **14**, 239 (1999).
38. G. H. Miller *et al.*, *Science* **309**, 287 (2005).
39. W. J. Bond, F. I. Woodward, G. F. Midgley, *New Phytol.* **165**, 525 (2005).
40. G. R. van der Werf *et al.*, *Atmos. Chem. Phys.* **6**, 3423 (2006).
41. M. O. Andreae, P. Merlet, *Global Biogeochem. Cycles* **15**, 955 (2001).
42. J. Lehmann *et al.*, *Nat. Geosci.* **1**, 832 (2008).
43. R. L. Langenfelds *et al.*, *Global Biogeochem. Cycles* **16**, 1048 (2002).
44. J. B. Marston, M. Oppenheimer, R. M. Fujita, S. R. Gaffin, *Nature* **349**, 573 (1991).
45. V. Ramanathan, G. Carmichael, *Nat. Geosci.* **1**, 221 (2008).
46. M. O. Andreae *et al.*, *Science* **303**, 1337 (2004).
47. J. T. Randerson *et al.*, *Science* **314**, 1130 (2006).
48. V. K. Arora, G. J. Boer, *J. Geophys. Res. Biogeosci.* **110**, G02008 (2005).
49. L. Giglio, I. Csiszar, C. O. Justice, *J. Geophys. Res. Biogeosci.* **111**, G02016 (2006).

50. We thank L. Curran, M. Einhorn, D. Gross, S. Hampton, D. Nepstad, and R. Whittaker for encouraging this synthesis, and G. Williamson for assistance with Fig. 2. This work was conducted as part of the Pyrogeography and Climate Change Working Group supported by the Kavli Institute for Theoretical Physics (KITP) and the National Center for Ecological Analysis and Synthesis (NCEAS), funded by NSF grants PHY05-51164 and DEB-0553768, respectively; the University of California, Santa Barbara; and the State of California. Additional support was provided by NCEAS (to J.K.B., the Postdoctoral Associate in the Group); CNPq/MCT Instituto do Milênio Program (to P.A.); and the U.S. Geological Survey (to J.E.K.). Contributions: D.M.J.S.B. conceived of the original idea; J.K.B. and D.M.J.S.B. co-organized the KITP/NCEAS workshop and assumed editorial responsibility; all authors participated in the workshop and/or contributed to manuscript writing; G.R.W., P.A., and I.C.P. developed the radiative forcing figure; C.A.K., C.I.R., and A.C.S. designed the timeline diagram.

Supporting Online Material

www.sciencemag.org/cgi/content/full/324/5926/481/DC1
SOM Text
Table S1
References

10.1126/science.1163886

Coat Color Variation at the Beginning of Horse Domestication

Arne Ludwig,[1]*† Melanie Pruvost,[1,2]* Monika Reissmann,[3]* Norbert Benecke,[2] Gudrun A. Brockmann,[3] Pedro Castaños,[4] Michael Cieslak,[1] Sebastian Lippold,[5] Laura Llorente,[6] Anna-Sapfo Malaspinas,[7] Montgomery Slatkin,[7] Michael Hofreiter[5]*†

The transformation of wild animals into domestic ones was a key prerequisite for modern human societies (*1*). A variety of species have been domesticated, but no species has had such an impact on warfare, transportation, and communication capability as the horse. Despite its importance for human history, the time and place of horse domestication have remained enigmatic for a long time (*2*, *3*). Recently, evidence was found for horse domestication having occurred in Kazakhstan about 5500 years before the present (yr B.P.) (*4*). Genetic studies have shown that coat color variation arose rapidly during domestication, resulting from human selection (*5*). To further investigate the dynamics and place of horse domestication, we investigated DNA sequence polymorphisms responsible for coat color variation in fossil horses.

We successfully typed eight mutations in six genes (*6*) responsible for coat color variation for 89 [out of 152 tested; tables S1 to S5 (*6*)] ancient samples. To assess coat color variation of predomestic horses, we analyzed the bones of wild horses from the Late Pleistocene and Early Holocene found in Siberia, East and Central Europe, and the Iberian Peninsula. We found no variation in the Siberian and European Pleistocene horses, suggesting that these horses were bay or bay-dun in color. There is evidence that the wild type is dun, but, because the nondun mutation has not yet been identified, we cannot distinguish between dun and nondun horses. In contrast, Iberian Early Holocene horses carried both the nonblack allele *A* (25%) and the black allele *a* (75%) at the *ASIP* gene, resulting in four black and four bay horses. An analysis of 21 Neolithic and Copper Age samples, dating to the millennia before archaeological evidence for domestication exists, produced similar allelic patterns. These periods are characterized by an absence of horse bones in the archaeological record for some regions, which prevents the inclusion of Siberian horses from 8000 to 5000 yr B.P. (table S6). East European horses dating to 7000 to 6000 yr B.P. revealed a mixed population (76% bay and 24% black). All these horses are regarded as wild because they clearly predate the earliest evidence for horse husbandry in this region. Because black horses are found neither in Siberia nor in East and Central Europe during the Late Pleistocene, their occurrence in the Early Holocene is probably the result of postglacial immigration or of selection caused by increased forest cover, as recently shown for wolves (*7*). Human selection is less likely because we observed no other coloration. A binomial test furthermore shows that, given the sample size of our predomestic horses, the chance that we missed any color allele with a frequency larger than 4% is $P \leq 0.05$ (*6*) (table S7).

In contrast, a rapid and substantial increase in the number of coat colorations is found in both Siberia and East Europe beginning in the fifth millennium B.P. (Fig. 1 and figs. S1 and S2). Although the earliest chestnut allele (*MC1R* gene) was identified in a Romanian sample from the late seventh millennium B.P., chestnut horses were first observed in Siberia (fifth millenium B.P.). Their prevalence increased rapidly, reaching 28% during the Bronze Age.

Mutations responsible for coat color dilutions or spottings seem to appear later. Cream (buckskin) and (black) silver dilutions (2800 to 2600 yr B.P.) were first observed in Siberia. Sabino is the first spotting phenotype, appearing during the fifth millennium B.P. in Siberia, and present in Armenia and Moldavia during the middle Bronze Age. The Tobiano spotting was first found in a single Eastern European sample (3500 to 3000 yr B.P.) and later also in Asia. Unlike in samples from Siberia and Eastern Europe, we observed no color change in Spanish samples until medieval times.

Although we cannot statistically reject neutrality for four out of six loci tested, the selection coefficient for *ASIP* and *MC1R* was found to be significantly different from zero (*6*, *8*); (table S8, and fig. S3). Our results are therefore best explained by selective breeding, which supports domestication as the cause for the observed changes in coloration. Given the rapid change, we conclude that horse domestication started in the Eurasian steppe region around at least 5000 yr B.P.

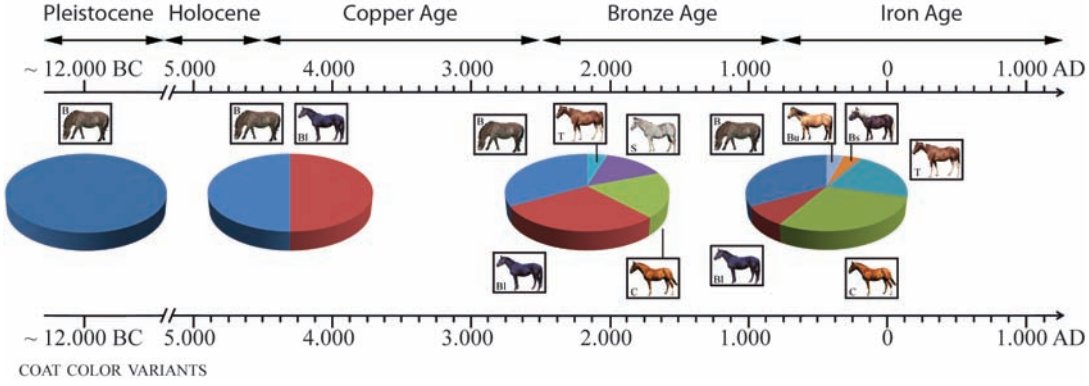

Fig. 1. Timeline showing the rapid increase in coat color variation in horses around the Bronze Age. The size of the pie charts corresponds to the frequency of the respective phenotype. B indicates bay color; Bl, black; C, chestnut; T, tobiano; S, sabino; Bu, buckskin; and Bs, black silver. Sample sizes from left to right are 16, 18, 26, and 29 specimens.

References and Notes

1. J. Diamond, *Nature* **418**, 700 (2002).
2. T. Jansen *et al.*, *Proc. Natl. Acad. Sci. U.S.A.* **99**, 10905 (2002).
3. C. Vila *et al.*, *Science* **291**, 474 (2001).
4. A. K. Outram *et al.*, *Science* **323**, 1332 (2009).
5. M. Fang *et al.*, *PLoS Genet.* **5**, e1000341 (2009).
6. Materials and methods are available as supporting material on *Science* Online.
7. T. M. Anderson *et al.*, *Science* **323**, 1339 (2009).
8. J. P. Bollback, T. L. York, R. Nielsen, *Genetics* **179**, 497 (2008).

9. We thank D. Lieckfeldt, S. Aksu, M. Meixner, and N. Hensel for technical assistance; K. Finstermeier and D. Blum for help with the figure design; and numerous scientists, horse breeders, and curators, especially A. Morales, who provided material for DNA analyses. This work was funded by the Deutsche Forschungsgemeinschaft (A.L., M.P., M.C., and N.B.), the Max Planck Gesellschaft (S.L. and M.H.), and the Janggen Pöhn Foundation (A.-S.M.). A.-S.M. thanks J. Jensen and O. Malaspinas for very helpful discussions.

Supporting Online Material

www.sciencemag.org/cgi/content/full/324/5926/485/DC1
Materials and Methods
Figs. S1 to S3
Tables S1 to S8
References

25 February 2009; accepted 1 April 2009
10.1126/science.1172750

[1]Leibniz Institute for Zoo and Wildlife Research, 10252 Berlin, Germany. [2]German Archaeological Institute, Im Dol 4-6, 14165 Berlin, Germany. [3]Institute for Animal Sciences, Humboldt University Berlin, 10115 Berlin, Germany. [4]Sociedad de Ciencias Aranzadi, San Sebastián, Spain. [5]Max Planck Institute for Evolutionary Anthropology, Deutscher Platz 6, 04103 Leipzig, Germany. [6]Laboratory of Archaeozoology, Universidad Autonoma Madrid, 28049 Madrid, Spain. [7]Department of Integrative Biology, University of California, Berkeley, CA 94720, USA.

*These authors contributed equally to this work.
†To whom correspondence should be addressed. E-mail: ludwig@izw-berlin.de (A.L.); hofreiter@eva.mpg.de (M.H.)

The Disappearance of the Progenitors of Supernovae 1993J and 2003gd

Justyn R. Maund[1,2]* and Stephen J. Smartt[3]

Using images from the Hubble Space Telescope and the Gemini Telescope, we confirmed the disappearance of the progenitors of two type II supernovae (SNe) and evaluated the presence of other stars associated with them. We found that the progenitor of SN 2003gd, an M-supergiant star, is no longer observed at the SN location and determined its intrinsic brightness using image subtraction techniques. The progenitor of SN 1993J, a K-supergiant star, is also no longer present, but its B-supergiant binary companion is still observed. The disappearance of the progenitors confirms that these two supernovae were produced by red supergiants.

Analysis of archival pre-explosion images has helped to identify the progenitors of type II supernovae (SNe), which are thought to result from the explosion of red supergiant stars. In most cases, the progenitors have only been confirmed to be spatially coincident with the SNe, leaving some uncertainty over their correct identification. So far, only one star has been shown to have disappeared after it exploded—the star that exploded as SN 1987A in the Local Group of galaxies (*1*). Seven other stars have been discovered to be spatially coincident with bright, nearby type II SNe (*2*), but none of them have been shown to have disappeared [although recent evidence has suggested the possible disappearance of the progenitor of SN 2005gl (*3*)]. Here, we examine postexplosion images of the sites of two type II SNe to confirm their progenitors' identities.

SN 2003gd was discovered in the galaxy M74 and classified as a type II-plateau SN (*4*). The plateau in its light curve and the strong hydrogen P Cygni profiles in its spectrum indicated that it arose from a red supergiant star with a massive hydrogen envelope (*5*). Analysis of pre-explosion images from the Hubble Space Telescope (HST) and Gemini Telescope archives revealed a red supergiant star, with $V = 25.8$, $I = 23.3$ and an initial mass of 8^{+4}_{-2} solar masses ($M_\odot$), at the position where the SN occurred (Fig. 1) (*6*, *7*). Five years after the explosion, it is time to verify that this star has disappeared, hoping that the SN remnant has faded to a luminosity below that of its progenitor (as achieved for SN 1987A).

We reimaged the site of SN 2003gd on 6 and 10 September 2008 using the multiobject spectrograph on the Gemini Telescope [GMOS, (*8*)] with the Sloan g', r', and i' filters, under excellent seeing conditions (see Table 1). Using differential astrometry, we matched previous observations of SN 2003gd, acquired with the HST Advanced Camera for Surveys High Resolution Channel (ACS HRC) (*6*), with our GMOS frames to locate the SN position to within 0.031" (Fig. 1). At this position, a single point source is not detected in the i' image, but the SN is still detected significantly at $m_{g'}(AB) = 25.00 \pm 0.04$ and $m_{r'}(AB) = 24.65 \pm 0.05$ [see supporting online material (SOM)]. We compared our i' image with a pre-explosion i' image taken with the GMOS instrument on 14 August 2001, in which the progenitor candidate was detected. After aligning the two images, we scaled the flux levels and the point spread function (PSF) of the postexplosion i'-band image to match those of the pre-explosion image, using the ISIS image subtraction package (*9*, *10*). We then subtracted the scaled post-explosion image from the pre-explosion frame, such that only photometrically variable objects remained (see the SOM for details of the procedure). A point source residual, consistent with a single-star PSF, is present in the pre-explosion image to within 0.023″ of the transformed SN position (Fig. 1) (see SOM). Smartt *et al.* (*6*) found a large offset between the transformed SN position and the object on the pre-explosion frame (0.137 ± 0.071"), leading them to suggest that the object was a blend of the progenitor (Star A) and a nearby star (Star C) (Fig. 1). We find no such offset with our differential astrometric solution, such that the object on the pre-explosion frame is completely consistent with a single star located at the position of Star A. All other single nonvariable stellar objects were cleanly subtracted from the pre-explosion image, with only minor residuals remaining for obviously extended features such as resolved clusters. Hence, the point source visible in the subtracted frame is the i'-band flux from the progenitor, which has now disappeared. There clearly is a faint, extended background feature in the post-explosion image, but this is inconsistent with a single PSF. By conducting forced photometry at the SN position and by adding artificial stars to our postexplosion i' image and attempting to recover them using the ISIS package, we conserv-

[1]Dark Cosmology Centre, Niels Bohr Institute, University of Copenhagen, Juliane Maries Vej 30, 2100 Copenhagen Ø, Denmark. [2]Department of Astronomy and Astrophysics, University of California, Santa Cruz, CA 95064, USA. [3]Astrophysics Research Centre, School of Mathematics and Physics, Queen's University Belfast, Belfast BT7 1NN, UK.

*To whom correspondence should be addressed. E-mail: justyn@dark-cosmology.dk

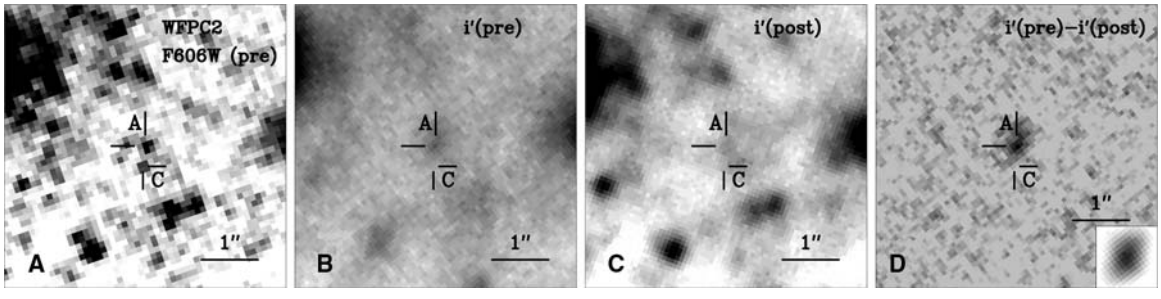

Fig. 1. Pre- and post-explosion images of the site of SN 2003gd taken with the HST WFPC2 and Gemini GMOS instruments (see Table 1 for details). (**A**) Pre-explosion WFPC2 F606W image, with the previously identified progenitor object marked as Star A and a nearby star labeled Star C. (**B**) Pre-explosion Gemini GMOS i' band image, with spatial resolution 0.57'', in which the progenitor is detected. (**C**) Postexplosion Gemini GMOS i' band image where a single point source is not detected at the transformed position of SN 2003gd, with a limit on any remaining SN flux of $m_{i'}(AB) > 26.3$. The image has a spatial resolution of 0.36'', and no point source is detected at the position of Star C, which suggests a negligible contribution in the i'-band from that star. (**D**) Pre-explosion image with the flux/PSF-scaled postexplosion image subtracted. The residual object at the position of SN 2003gd is the progenitor, with any contaminating flux from nearby stars subtracted. The object at the SN location, marked as Star A, is consistent with single-star PSF ($\chi^2 = 0.9$) and has a Johnson I magnitude of 23.14 ± 0.08 [$m_{i'}(AB) = 24.25 \pm 0.04$]. In the bottom right corner, a model single-star PSF is shown. It was determined by ISIS and is consistent with the source detected in this subtraction image.

atively estimate that the upper brightness limit for a single point source is $m_{i'}(AB) > 26.3$ at the SN location. This corresponds to a magnitude difference between the pre- and postexplosion i' images of $\Delta m_{i'} > 2$. The absence of an obvious point source in the postexplosion image, which is within 2 magnitudes of the detected progenitor, further confirms that the star has disappeared.

We transformed the pre-explosion i' band photometry to the Johnson system by bootstrapping the photometry with Wide-Field Camera images from the Isaac Newton Telescope and the M74 standard star sequence used for monitoring both SN 2003gd and SN 2002ap (*11*). These data imply that the progenitor star had a final Johnson I band magnitude of 23.14 ± 0.08, tightening earlier constraints (*6*). This is 0.2 magnitudes brighter than previously reported, due to our determination that Star C contributed negligible i' flux.

Using the HSTphot package (*12*), we analyzed pre-explosion HST Wide-Field Planetary Camera 2 WFPC2 images taken with the F606W filter, which is close to the V-band filter. We used the I-band magnitude determined above to solve the color-transformation equations that convert the F606W instrumental magnitude to the Johnson system and found that the progenitor has a Johnson V magnitude of 25.72 ± 0.09. Correcting for a reddening of $E(B - V) = 0.14 \pm 0.06$, which was determined from photometry of SN 2003gd (*5*), implies an intrinsic color of $(V - I)_0 = 2.41 \pm 0.14$. This is consistent with the progenitor being an M0 to M2 red supergiant star (*13*) but disfavors warmer K-supergiant stars. Applying the appropriate bolometric correction for this range of allowed red supergiants, and correcting for a distance of 9.3 ± 1.8 Mpc to M74 (*5*), yields a luminosity of $\log (L/L_\odot) = 4.29 \pm 0.2$, with an effective temperature of $\log T_{\rm eff} = 3.54 \pm 0.02$. Comparison with the end points of stellar evolution models shows that this luminosity and temperature region of the Hertzprung-Russell diagram constrains the progenitor to have had initial mass of $7^{+6}_{-1}\ M_\odot$ (*2*).

At the epoch of 6 September 2008 (~2000 days after explosion), the SN is still visible in the wavelength range corresponding to the F622W and Sloan r' filters (see table S7). This is due to the presence of considerable $H\alpha$ emission in the band-passes of these filters, typical of type II SNe at late times (*5*, *14*). The fact that the SN is bright in the late-time F622W observations precludes the use of image subtraction techniques to determine the true progenitor brightness in the pre-explosion WFPC2 F606W image. We need to wait longer until the $H\alpha$ flux fades well below the magnitude of the progenitor star detected in the F606W filter.

One could argue that the star identified as the progenitor was a neighboring star that is now obscured by dust formation in the foreground SN remnant. However, the internal extinction in the SN 2003gd remnant, due to newly formed dust, was estimated to be $A_R < 1.48$ (*15*) or $A_{i'} < 1.22$ (*16*) at 678 days. Using this as the maximum value of the extinction across the SN remnant at the epoch of our GMOS images (assuming no further dust formation), this amount of extinction is insufficient to cause $\Delta m_{i'}$ measured by us. This implies that the object we have identified as the progenitor is not simply obscured by dust in the intervening SN remnant and has actually disappeared.

The progenitor of the hydrogen-bearing (type IIb) SN 1993J was identified as a K-supergiant star, with excess flux at ultraviolet (UV) wavelengths, possibly because of a binary companion or nearby stars (*17*). The model for this binary system was of a 15 $M_\odot$ progenitor star, with a binary companion of slightly lower mass (*18*–*20*). Because the progenitor star evolved faster, it underwent mass transfer onto the binary companion, which removed a substantial amount of its hydrogen envelope, causing a shift to the bluer K spectral type [rather than the canonical M spectral type (*2*)]. The binary companion grew to 22 $M_\odot$ and became the source of the excess UV flux. A later study, using high-resolution HST images, found that some of the UV excess could be explained by nearby previously unresolved stars but that a UV excess still remained unaccounted for (*21*). The binary progenitor scenario was confirmed when spectral features of a massive blue supergiant were detected in late-time spectroscopy (*22*).

The site of SN 1993J was imaged several times over the 2 to 13 years after explosion with the HST WFPC2 ACS HRC and Wide-Field Channels (WFC) (see SOM for full list of dates). By the epoch of the 2004 observation, the red portion of the SN spectral energy distribution (SED) had faded below the level of the SED of

Table 1. Pre- and postexplosion observations of the site of SN 2003gd (*, pixel scale).

Telescope/ instrument	Date	Program	Filter	Exposure time (s)	Seeing ('')
Gemini GMOS	14 August 2001	GN-2001B-SV-102	i'	480	0.57
HST/WFPC2	25/28 August 2002	GO-9676	F606W	2100	0.1*
HST/ACS/HRC	01 August 2003	GO-9733	F814W	1350	0.025*
Gemini GMOS	10 September 2008	GN-2008B-Q-67	g'	4050	0.53
Gemini GMOS	06 September 2008	GN-2008B-Q-67	r'	1590	0.42
Gemini GMOS	06 September 2008	GN-2008B-Q-67	i'	3180	0.36

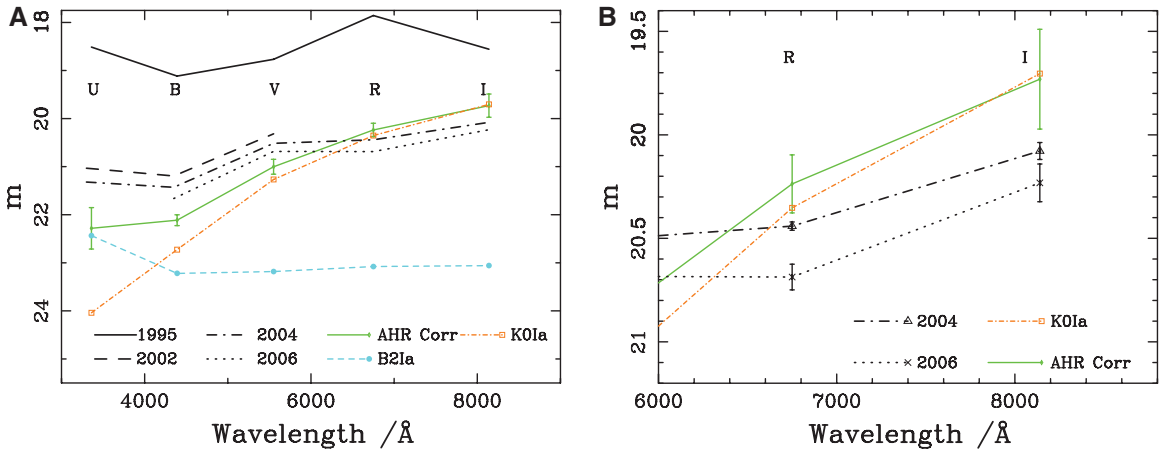

Fig. 2. The SED of the progenitor binary system of SN 1993J. The SED (AHR Corr) (*17*) has been corrected for the excess flux contribution from four nearby stars, unresolved in the low-resolution ground-based pre-explosion imaging, for comparison with photometry of high-resolution HST imaging in which the SN is resolved. (**A**) Overlaid SN 1993J SEDs, measured with HST WFPC2, ACS/HRC, and ACS/WFC, at 31 January 1995, 28 May 2002, 15 July 2004, and 1 and 3 November 2006. The B- and K- supergiant components are the result of a χ^2 fit to the excess corrected pre-explosion photometry (*22*, *26*). (**B**) A zoom in on the R_C and I_C photometric points. Errors on the 2004 and 2006 photometry are calculated from PSF photometry of SN 1993J.

the binary progenitor system (Fig. 2) (see SOM), ruling out the continued presence of the K-supergiant star and, hence, confirming it as the progenitor of SN 1993J. At the current rate of decay of the SN SED, the U- and B-band fluxes will have reached the level of the proposed B-supergiant component by 2012, at which stage it will be possible to directly measure the properties of the remaining companion star.

These results provide observational proof that red supergiant stars are the progenitors of type II SNe, through the disappearance of the previously identified candidate stars of two SNe. Our best estimate for the mass of the progenitor of the type IIP SN 2003gd is 7 $M_\odot$ which is at the lower end of the mass range considered theoretically possible to produce core-collapse events. Although the uncertainties (7^{+6}_{-1} $M_\odot$) would comfortably allow a large mass for this object, it is interesting that five progenitors of type IIP SNe are found with best estimates at 9 $M_\odot$ or below (*2*). This limit is predicted by stellar and SN evolution models (*23*) and is consistent with the upper initial mass limit observed for white dwarfs (*24*). The confirmation of the disappearance of the K-type progenitor star of SN 1993J is further evidence that the binary model previously suggested is valid. It demonstrates the importance of binary interactions for the production of hydrogen-poor SNe (*25*).

References and Notes

1. R. Gilmozzi *et al*., *Nature* **328**, 318 (1987).
2. S. J. Smartt, J. J. Eldridge, R. M. Crockett, J. R. Maund, *ArXiv*, astro-ph/0809.0403 (2008).
3. A. Gal-Yam, D. Leonard, *Nature* 10.1038/nature07934 (2009).
4. R. Evans, R. H. McNaught, *IAU Circ.* **8150**, 2 (2003).
5. M. A. Hendry *et al*., *Mon. Not. R. Astron. Soc.* **359**, 906 (2005).
6. S. J. Smartt *et al*., *Science* **303**, 499 (2004).
7. S. D. Van Dyk, W. Li, A. V. Filippenko, *Publ. Astron. Soc. Pac.* **115**, 1289 (2003).
8. I. M. Hook *et al*., *Publ. Astron. Soc. Pac.* **116**, 425 (2004).
9. C. Alard, R. H. Lupton, *Astrophys. J.* **503**, 325 (1998).
10. C. Alard, *Astron. Astrophys. Suppl. Ser.* **144**, 363 (2000).
11. A. Henden, *GRB Coord. Network* **1242**, 1 (2002).
12. A. E. Dolphin, *Publ. Astron. Soc. Pac.* **112**, 1383 (2000).
13. J. H. Elias, J. A. Frogel, R. M. Humphreys, *Astrophys. J. Supp. Ser.* **57**, 91 (1985).
14. A. Pastorello *et al*., *ArXiv*, astro-ph/0901.2075 (2009).
15. B. E. K. Sugerman *et al*., *Science* **313**, 196 (2006).
16. J. A. Cardelli, G. C. Clayton, J. S. Mathis, *Astrophys. J.* **345**, 245 (1989).
17. G. Aldering, R. M. Humphreys, M. Richmond, *Astron. J.* **107**, 662 (1994).
18. K. Nomoto *et al*., *Nature* **364**, 507 (1993).
19. P. Podsiadlowski, J. J. L. Hsu, P. C. Joss, R. R. Ross, *Nature* **364**, 509 (1993).
20. S. E. Woosley, R. G. Eastman, T. A. Weaver, P. A. Pinto, *Astrophys. J.* **429**, 300 (1994).
21. S. D. Van Dyk *et al*., *Publ. Astron. Soc. Pac.* **114**, 1322 (2002).
22. J. R. Maund, S. J. Smartt, R. P. Kudritzki, P. Podsiadlowski, G. F. Gilmore, *Nature* **427**, 129 (2004).
23. J. J. Eldridge, C. A. Tout, *Mon. Not. R. Astron. Soc.* **353**, 87 (2004).
24. K. A. Williams, M. Bolte, D. Koester, *ArXiv*, astro-ph/0811.1577 (2008).
25. P. Podsiadlowski *et al*., *Astrophys. J.* **612**, 1044 (2004).
26. J. R. Maund, thesis, Institute of Astronomy, Cambridge (2005), www.dark-cosmology.dk/~justyn/research
27. J.R.M. is a Sophie and Tycho Brahe Fellow.

Supporting Online Material

www.sciencemag.org/cgi/content/full/1170198/DC1
SOM Text
Figs. S1 to S4
Tables S1 to S9
References

23 December 2008; accepted 11 March 2009
Published online 19 March 2009;
10.1126/science.1170198
Include this information when citing this paper.

Greatly Increased Toughness of Infiltrated Spider Silk

Seung-Mo Lee,[1]* Eckhard Pippel,[1] Ulrich Gösele,[1] Christian Dresbach,[2] Yong Qin,[1] C. Vinod Chandran,[3] Thomas Bräuniger,[3] Gerd Hause,[4] Mato Knez[1]*

In nature, tiny amounts of inorganic impurities, such as metals, are incorporated in the protein structures of some biomaterials and lead to unusual mechanical properties of those materials. A desire to produce these biomimicking new materials has stimulated materials scientists, and diverse approaches have been attempted. In contrast, research to improve the mechanical properties of biomaterials themselves by direct metal incorporation into inner protein structures has rarely been tried because of the difficulty of developing a method that can infiltrate metals into biomaterials, resulting in a metal-incorporated protein matrix. We demonstrated that metals can be intentionally infiltrated into inner protein structures of biomaterials through multiple pulsed vapor-phase infiltration performed with equipment conventionally used for atomic layer deposition (ALD). We infiltrated zinc (Zn), titanium (Ti), or aluminum (Al), combined with water from corresponding ALD precursors, into spider dragline silks and observed greatly improved toughness of the resulting silks. The presence of the infiltrated metals such as Al or Ti was verified by energy-dispersive x-ray (EDX) and nuclear magnetic resonance spectra measured inside the treated silks. This result of enhanced toughness of spider silk could potentially serve as a model for a more general approach to enhance the strength and toughness of other biomaterials.

In the field of biomaterials research, Bryan and Gibbs suggested that metals such as Cu and Zn, which are incorporated in an inner protein matrix, might play a role in mechanical hardening of the jaws of the marine polychaete worm *Nereis* (*1*, *2*). Many groups have investigated the correlation between the presence of some metal elements, such as Zn, Mn, Ca, or Cu, accumulated in the cuticles of insects or other organisms (in body parts such as mandibles, stingers, claws, and ovipositors) and their enhanced mechanical properties (particularly stiffness and hardness) (*3*–*15*). We demonstrated that inorganic impurities such as Zn, Ti, and Al can be inserted into biomaterials by the multiple pulsed vapor-phase infiltration (MPI) process (Fig. 1), performed with equipment conventionally used for atomic layer deposition (ALD).

For testing, we selected spider dragline silk from major ampullate silk glands, which outperforms almost any human-made fiber in its combination of tensile strength (σ) and extensibility (ε) (its so-called extreme toughness, $\int \sigma d\varepsilon$) (*16*, *17*). A number of scientists have claimed a strong relation between Zn accumulated in insect cuticles, such as the mandibles of the leaf-cutter ant (*3*, *6*), locust (*9*), and marine polychaete worm *Nereis* (*10*), and the enhanced hardness and stiffness of these biomaterials. Broomell *et al*. showed that a metal ion (Zn^{2+}) plays a critical role in the mechanical properties of *Nereis* jaws, by nanoindentation measurements performed before and after Zn chelation (*12*). Therefore, we initially alternately exposed the dragline silk to the vapor of diethylzinc (DEZ) [$Zn(C_2H_5)_2$] and water (H_2O) (table S1) (*18*) in an ALD reactor and observed a considerable increase of both σ_{max} (the maximum stress) and E_{ini} (the initial Young's modulus) as compared to those of the untreated native (N) dragline spider silk (SS) (SS/N), which had mechanical properties close to those reported in the literature for the *Araneus* spider's dragline silk [σ_{max} (SS/N) $\approx$ 1.1 GPa and E_{ini} (SS/N) $\approx$ 10 GPa)] (*19*) (fig. S2 and table S2). We subsequently observed that dragline silks exposed to $Al(CH_3)_3$ [trimethylaluminum (TMA)]/H_2O or $Ti(OCH(CH_3)_2)_4$ [titanium(IV) isopropoxide (TIP)]/H_2O pulse pairs showed considerably larger improvements in toughness than silks exposed to the DEZ/H_2O pair.

An ALD process conventionally leads to thin deposited layers of metal oxide on a fiber (Fig. 1). Therefore, the question arises whether the increased σ_{max} could be considered a result of

[1]Max Planck Institute of Microstructure Physics, Weinberg 2, D-06120 Halle, Germany. [2]Fraunhofer Institute for Mechanics of Materials, Walter-Hülse-Straße 1, D-06120 Halle, Germany. [3]Institute of Physics–Nuclear Magnetic Resonance Group, Martin-Luther-University Halle-Wittenberg, Friedemann-Bach-Platz 6, D-06108 Halle, Germany. [4]Microscopy Unit Biocenter, Martin-Luther-University Halle-Wittenberg, Weinbergweg 22, D-06120 Halle, Germany.

*To whom correspondence should be addressed. E-mail: smlee@mpi-halle.de (S.-M.L.); mknez@mpi-halle.de (M.K.)

these deposited layers. SS/Al_2O_3 (dragline silk + Al_2O_3 by a TMA/H_2O pulse pair) and SS/TiO_2 (dragline silk + TiO_2 by a TIP/H_2O pulse pair) fibers were prepared. When those fibers were compared to native dragline silk, σ_{max} and ε_{max} were increased (Fig. 2, A and B). Taking into account that thin Al_2O_3 or TiO_2 films generally fail by brittle fracture (fracture strain ε_f on the order of 10^{-3}) (*20*), it seems that because of the outer Al_2O_3 or TiO_2 coating of the silk, E_{ini} in the range of $0 < \varepsilon < 0.002$ increased from E_{ini}(SS/N) ≈ 9.7 GPa to E_{ini}(SS/Al_2O_3) = 53 to 68 GPa or E_{ini} (SS/TiO_2) = 53 to 66 GPa (table S2). However, the increase of the maximum tensile stress and strain was independent of the contribution of the Al_2O_3 or TiO_2 coating. From these results, it was concluded that both σ_{max} and ε_{max} of the native spider dragline silk can be generally increased by MPI, and the contribution of the outer metal oxide layer coating on the fiber to the improvement of its mechanical properties is of minor importance.

The question still remains whether separate individual pulses [water pulse (WP) exposure without a TMA pulse (TP) exposure and vice versa] would also affect the silk properties. We prepared samples with 100 pulses of individual precursor vapors (SS/TP/100 and SS/WP/100, table S1 and fig. S3) under the same processing conditions as the MPI samples (SS/Al_2O_3/100). The overall σ_{max} and E_{ini} of both SS/TP/100 and SS/WP/100 were somewhat decreased and, in contrast, ε increased only slightly (Fig. 2C). However, the overall toughness was much smaller than that of SS/Al_2O_3/100. Pulses of only one reactant (TMA or H_2O) were not effective for the enhancement of the mechanical properties of the silk. Additionally, the exposure times appear to play an

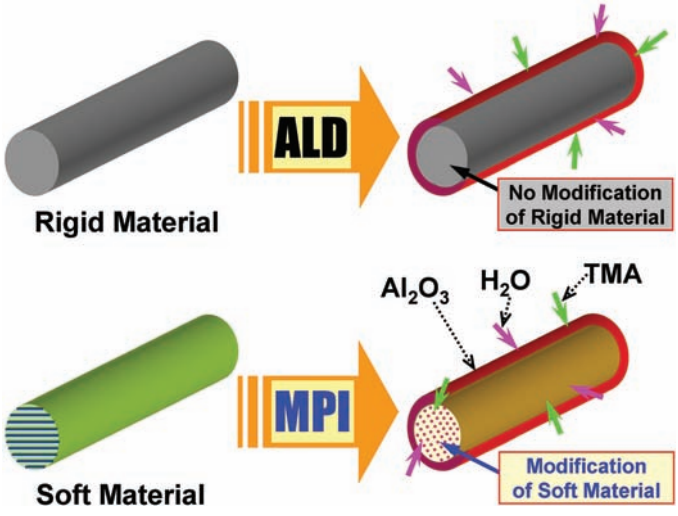

Fig. 1. Schematic of the difference between conventional ALD (thin-film deposition, top) and MPI (thin-film deposition plus chemical modification by metal infiltration, bottom). Conventionally, by multiple pulses of ALD precursors such as TMA (green arrows) and water (H_2O, pink arrows), thin films [such as alumina (Al_2O_3), illustrated by the red shell] are deposited on rigid materials (such as metals) without chemical modification of the bulk. In contrast, in the case of soft materials such as biomaterials or polymers, MPI provides a chemical modification of the bulk in addition to the thin-film deposition.

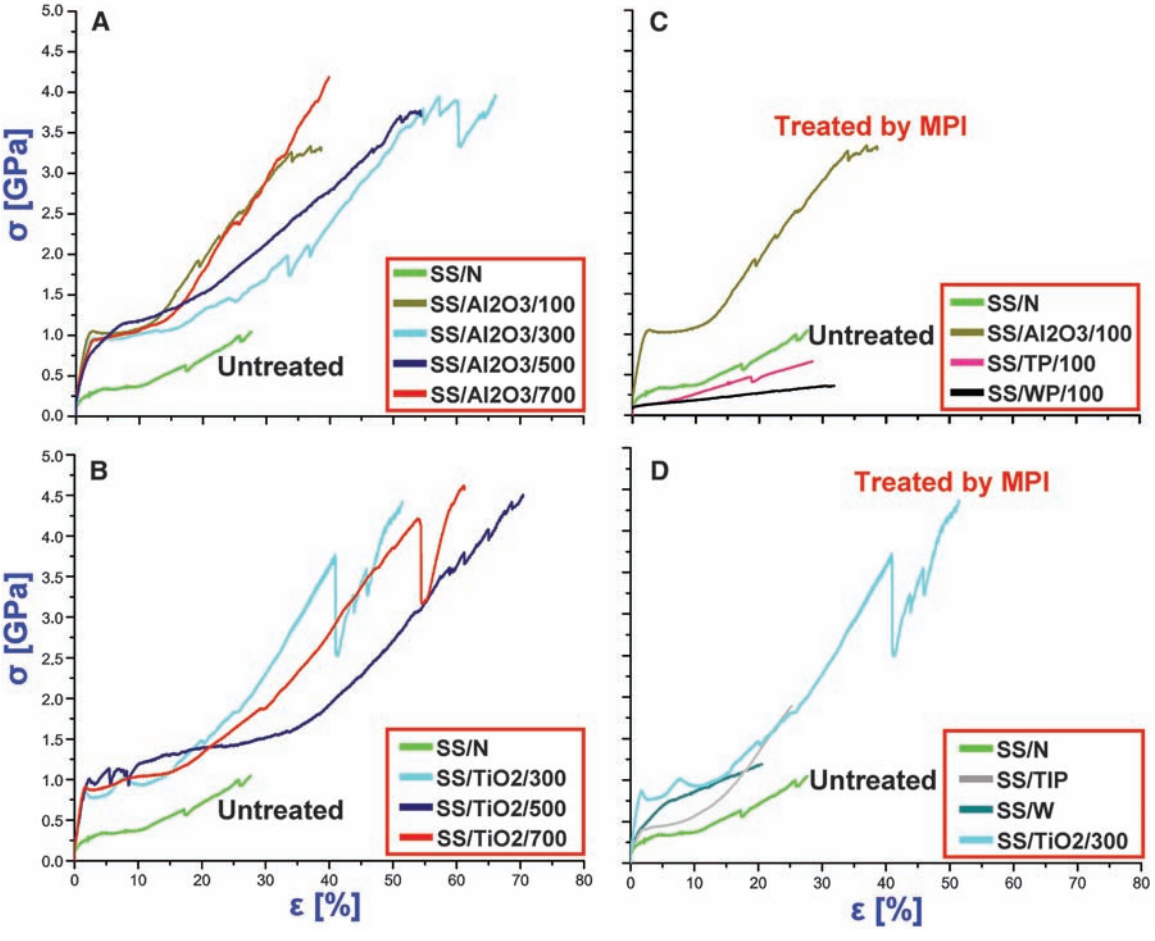

Fig. 2. Tensile test curves of silk fiber samples treated by TMA/H_2O and TIP/H_2O pulse exposure pairs and comparison to untreated samples and samples treated with various different processes. (**A**) and (**B**) Stress (σ) and strain (ε) curves of silk fibers treated with TMA/H_2O and TIP/H_2O pulse pairs in various numbers of cycles ranging from 100 to 700. (**C**) σ-ε curves of silk fibers treated by individual vapor pulses (SS/TP/100, TMA without water; SS/WP/100, water without TMA; sample denotation and information can be found in table S1 and see fig. S3) together with a comparative (σ-ε) curve of SS/Al_2O_3/100. (**D**) σ-ε curves of silks dipped into either a TIP (SS/TIP) or H_2O (SS/W) solution for 10 hours, followed by drying at room temperature, and SS/TiO_2/300 as a comparative σ-ε curve. In all graphs, the green line indicates the σ-ε curve of the native spider silk without any treatment (details are given in table S1).

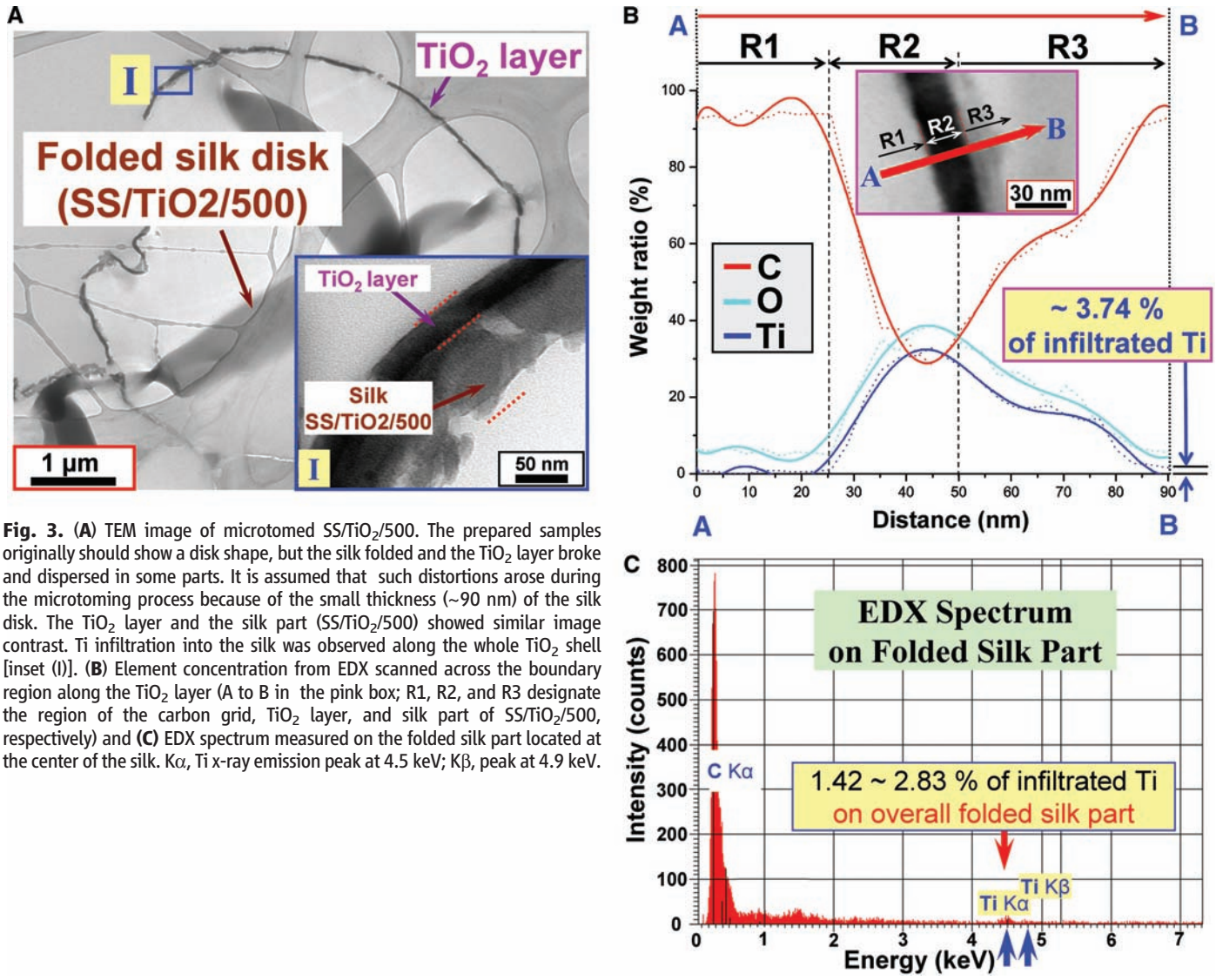

Fig. 3. (**A**) TEM image of microtomed SS/TiO_2/500. The prepared samples originally should show a disk shape, but the silk folded and the TiO_2 layer broke and dispersed in some parts. It is assumed that such distortions arose during the microtoming process because of the small thickness (~90 nm) of the silk disk. The TiO_2 layer and the silk part (SS/TiO_2/500) showed similar image contrast. Ti infiltration into the silk was observed along the whole TiO_2 shell [inset (I)]. (**B**) Element concentration from EDX scanned across the boundary region along the TiO_2 layer (A to B in the pink box; R1, R2, and R3 designate the region of the carbon grid, TiO_2 layer, and silk part of SS/TiO_2/500, respectively) and (**C**) EDX spectrum measured on the folded silk part located at the center of the silk. Kα, Ti x-ray emission peak at 4.5 keV; Kβ, peak at 4.9 keV.

important role. For the current results, we used a chamber-type ALD setup with exposure times for individual pulses of up to 40 s (see also table S1). Control experiments with a flow-type ALD process, which only allows for an exposure time of less than 1 s, did not yield considerable enhancement of the mechanical properties, clearly indicating a more complex process than simple coating of the structure as would be expected in a regular ALD process (*21*).

We also investigated whether simple dipping of silks into the highly reactive liquid ALD precursor would enhance the mechanical properties. We prepared various samples that were separately dipped into the individual precursor solutions (SS/TIP, dipped into TIP; and SS/W, dipped into water; table S1) under ambient conditions (at a temperature of 15°C and at atmospheric pressure) for 10 hours, followed by drying under the same conditions (*22*). E_{ini} and σ_{max} increased and ε_{max} decreased slightly as compared to SS/N (Fig. 2D). However, like the samples produced by the individual pulses of only one reactant under ALD conditions, the overall mechanical properties of those samples (SS/TIP and SS/W) were not comparable to those of SS/TiO_2/300.

The increased toughness of the above-mentioned silks appears to be caused by an infiltration of inorganic impurities such as Al or Ti, which presumably react with proteins after a preconditioning by the water penetrating into the fiber (*23*, *24*), a process probably similar to the hardness- and stiffness-increasing effects on *Nereis* jaws produced by a small amount of artificial Zn incorporation into the jaw (*12*). As shown in transmission electron microscopy (TEM) images of SS/TiO_2/500 (Fig. 3A, inset I, and B), along the TiO_2 shell, a region of ~100 nm in depth shows a high image contrast. Considering the relative weight ratio of carbon (C), oxygen (O), and Ti, a large amount of Ti was infiltrated in this shell region. In the center part of the silks (folded region), energy-dispersive x-ray (EDX) analysis detected weak but clear Ti signals (1.42 to 2.83% by relative weight ratio). Because the resolution limit of the system amounts to about 0.5 to 1.0%, the spectrum under those limits has not been quantified. But qualitatively, the small amount of Ti shown as the Ti-K peak is well above the background. In addition, indirect but similar evidence for the infiltrated Al ions into silk, which interact with the silk proteins, was observed by magic angle spinning nuclear magnetic resonance (NMR) measurements of SS/Al_2O_3/300 [supporting online material (SOM) text 1].

Spider silk is generally regarded as a semicrystalline biopolymer containing two major parts: β-sheet crystalline parts consisting of hydrophobic polyalanine sequences and amorphous parts composed of amino acid residues, linked via hydrogen bonds (*19*). The exact infiltration mechanism and intermolecular bonding states between proteins and metals has not been determined. However, considering the severe attack of water occurring at the hydrogen bonds that interconnect the proteins (*25*), a global weakening of the hydrogen bonds in proteins with increasing water vapor temperature (*26*) can be assumed. In addition, the strong reactivity to chemical bonds (*23*) and deep penetrat-

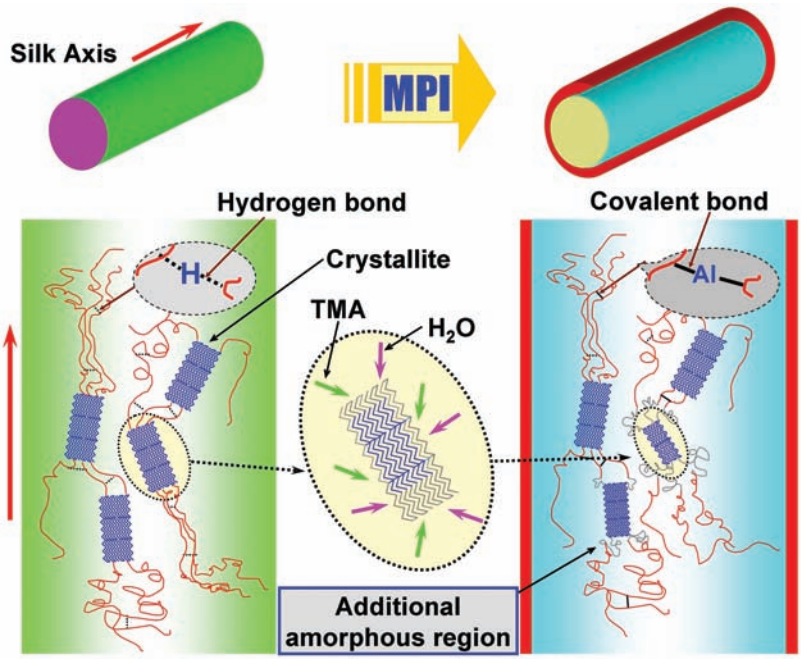

Fig. 4. Schematic description of proposed molecular changes in the silk produced by MPI. The detailed explanation can be found in the text and in fig. S6.

ing capability of metal-containing ALD precursors (such as TMA, TIP, and DEZ) into soft materials such as polymers (*24*) and the metal ions' preferential binding features to the proteins (*27*, *28*) could lead to stable metal-protein compounds by chelating ions (*29*, *30*) such as Al^{3+} (*31*), Ti^{4+} (*32*), or Zn^{2+} (*33*) to form metal-protein complexes. During long exposure times to water vapor (5 to 40 s) (*34*), the inner hydrogen bonds of the silk protein are likely to weaken or break in some regions upon water vapor attack at 70°C. Subsequently after long-term exposure to the metal precursor vapor, Al^{3+}, Ti^{4+}, or Zn^{2+} is likely to infiltrate the protein and bind to the broken bonding sites, thereby resulting in the formation of metal-coordinated or even covalent bonds. As a minor additional effect, methane (TMA/H_2O) or isopropanol (TIP/H_2O) as reaction byproducts may have additional effects to weaken or break the remaining hydrogen bonds. Consequently, the recoverable hydrogen bonds may be changed to permanent covalently bonded or coordinated Al-, Ti-, or Zn-protein complexes (Fig. 4 and fig S6). Therefore, unlike native silks, which are highly sensitive to environmental conditions such as humidity and temperature (mainly caused by the hydrogen bond breaking and recovery feature between water and amide groups in the protein chains) (*19*), the metal-infiltrated silks, which presumably may have covalent or coordinated bonds, are hardly affected by these conditions (*35*).

By wide-angle x-ray scattering (WAXS) measurements of SS/Al_2O_3/300 and SS/TiO_2/500, an inner-protein matrix structure change, caused by metal incorporation, was observed. More specifically, the size of silk protein β-sheet crystallites decreased after the MPI treatment (SOM text 2, figs. S4 and S5, and table S3). The strength of the silk is strongly dependent on the sizes of the polyalanine crystals, which are either small and perfect or large and imperfect (*36*), as proposed by Termonia (*37*) and experimentally validated by Du *et al*. (*38*). The extensibility of the silk is determined by the orientation and amount of amorphous chains, as proposed by Termonia (*37*) and elucidated by Lefèvre *et al*. (*39*). From these WAXS results (a decrease in the size of the protein crystallites), it could be easily conjectured that parts of protein crystals (probably large imperfect crystallites) are likely to be converted into protein chains by hydrogen bond breaking and metal substitution caused by MPI, thus resulting in additional amorphous regions. From the theoretical model by Termonia and supportive experimental results by Du *et al*. (*38*) and Lefèvre *et al*. (*39*), it is likely that additional amorphous regions and size-reduced protein crystallites, induced by metal infiltration, function as factors to enhance ε_{max} and σ_{max} of MPI-treated silks (Fig. 4 and fig. S7). On the other hand, we observed that the individual TMA or H_2O pulses produced no major enhancement of the mechanical properties of the silk composites (Fig. 2C). It appears that even though the individual pulsed vapor molecules contribute to the severe hydrogen bond breaking on the overall silk, because of the strong recovery behavior of the hydrogen bonds, some are reestablished. The resulting silks show an analogous curve profile to those of slightly contracted silk fibers, caused by local hydrogen bond breaking (*40*). We also observed that direct dipping of the silk into the pure liquid TIP precursors at ambient conditions had only a slight enhancement effect on the mechanical properties (increased σ_{max} of SS/TIP in Fig. 2D), similar to the hardness enhancement of the polychaete worm's jaws caused by Zn incorporation through incubation in $ZnCl_2$ solution at 25°C (*12*). Unlike TIP, which has low polarity (*41*), water causes a large shrinkage of silks by the destruction of hydrogen bonds in silk proteins (mainly amorphous regions), due to the high polarity (*42*) when the silks are immersed in water. We speculate that subsequent drying of the contracted silk fibers under axially restrained conditions, due to fixing the silk fibers on a paper clip (see table S1 for the details of sample preparation), leads to better alignment of the protein amorphous chains (*43*), resulting in decreased strain and slightly increased stress (*44*) (see result for SS/W in Fig. 2D).

We showed a large enhancement of the mechanical properties of spider silks via the MPI process and realized the prediction of Porter and Vollrath (*45*) that mineral-infused silk would show much greater toughness than native silk. This effect is not limited to spider silks but could also be shown to work for other biomaterials, such as collagen membranes from avian eggs (fig. S8).

References and Notes

1. G. W. Bryan, P. E. Gibbs, *J. Mar. Biol. Assoc. U.K.* **59**, 969 (1979).
2. P. E. Gibbs, G. W. Bryan, *J. Mar. Biol. Assoc. U.K.* **60**, 205 (1980).
3. J. E. Hillerton, J. F. V. Vincent, *J. Exp. Biol.* **101**, 333 (1982).
4. J. E. Hillerton, B. Robertson, J. F. V. Vincent, *J. Stored Prod. Res.* **20**, 133 (1984).
5. R. Schofield, H. Lefevre, *J. Exp. Biol.* **144**, 577 (1989).
6. A. J. Edwards, J. D. Fawke, J. G. McClements, S. A. Smith, P. Wyeth, *Cell Biol. Int.* **17**, 697 (1993).
7. D. L. J. Quicke, P. Wyeth, J. D. Fawke, H. H. Basibuyuk, J. F. V. Vincent, *Zool. J. Linn. Soc.* **124**, 387 (1998).
8. H. C. Lichtenegger, T. Schoberl, M. H. Bartl, J. H. Waite, G. D. Stucky, *Science* **298**, 389 (2002).
9. R. M. S. Schofield, M. H. Nesson, K. A. Richardson, *Naturwissenschaften* **89**, 579 (2002).
10. H. C. Lichtenegger *et al*., *Proc. Natl. Acad. Sci. U.S.A.* **100**, 9144 (2003).
11. T. D. Morgan, P. Baker, K. J. Kramer, H. H. Basibuyuk, D. L. J. Quicke, *J. Stored Prod. Res.* **39**, 65 (2003).
12. C. C. Broomell, M. A. Mattoni, F. W. Zok, J. H. Waite, *J. Exp. Biol.* **209**, 3219 (2006).
13. M. G. Pontin, D. N. Moses, J. H. Waite, F. W. Zok, *Proc. Natl. Acad. Sci. U.S.A.* **104**, 13559 (2007).
14. B. W. Cribb *et al*., *Naturwissenschaften* **95**, 17 (2008).
15. C. C. Broomell, F. W. Zok, J. H. Waite, *Acta Biomater.* **4**, 2045 (2008).
16. F. Vollrath, D. P. Knight, *Nature* **410**, 541 (2001).
17. A. Lazaris *et al*., *Science* **295**, 472 (2002).
18. Materials and methods are available as supporting material on *Science* Online.
19. J. M. Gosline, P. A. Guerette, C. S. Ortlepp, K. N. Savage, *J. Exp. Biol.* **202**, 3295 (1999).
20. J. C. Grosskreutz, *J. Electrochem. Soc.* **116**, 1232 (1969).
21. In this experiment, we tried both a chamber-type ALD setup with variable precursor exposure times (the Savannah 100, Cambridge Nanotech) and a flow-type ALD setup (the SUNALE R75, Picosun, Finland) with negligible exposure times.
22. We dipped the silk in solutions for 10 hours and compared the results with SS/TiO_2/300, the processing time of which also lasts ~10 hours. Because of the extreme volatility and hazard of the pure TMA or DEZ solution even in a glovebox, we were not able to perform the analogous experiment by dipping into TMA or DEZ.
23. C.-Y. Chang, F.-Y. Tsai, S.-J. Jhuo, M.-J. Chen, *Org. Electron.* **9**, 667 (2008).

24. C. A. Wilson, R. K. Grubbs, S. M. George, *Chem. Mater.* **17**, 5625 (2005).
25. A. Fernández, L. R. Scott, *Phys. Rev. Lett.* **91**, 018102 (2003).
26. F. Cordier, S. Grzesiek, *J. Mol. Biol.* **317**, 739 (2002).
27. F. R. N. Gurd, P. E. Wilcox, *Adv. Protein Chem.* **11**, 311 (1956).
28. F. H. Arnold, B. L. Haymore, *Science* **252**, 1796 (1991).
29. J. T. Kellis, R. J. Todd, F. H. Arnold, *Nat. Biotechnol.* **9**, 994 (1991).
30. K. H. Gustavson, *Nature* **182**, 1125 (1958).
31. K. S. J. Rao, G. V. Rao, *Mol. Cell. Biochem.* **137**, 61 (1994).
32. H. Sun, H. Li, R. A. Weir, P. J. Sadler, *Angew. Chem. Int. Ed.* **37**, 1577 (1998).
33. T. Handel, W. F. DeGrado, *J. Am. Chem. Soc.* **112**, 6710 (1990).
34. Generally, in our ALD process, ZnO deposition has shown relatively poor self-limiting features. At longer exposure times, the process shows parasitic chemical vapor deposition (high film thickness with relatively poor uniformity). Therefore, in case of ZnO, an exposure of only 5 s was applied.
35. It has been observed that in the case of the metal-infiltrated silks, the contraction ratio produced by humidity up to 100% or temperature up to 70°C is in an almost negligible range (<3%).
36. A. H. Simmons, C. A. Michal, L. W. Jelinski, *Science* **271**, 84 (1996).
37. Y. Termonia, *Macromolecules* **27**, 7378 (1994).
38. N. Du *et al.*, *Biophys. J.* **91**, 4528 (2006).
39. T. Lefèvre, M-.E. Rousseau, M. Pézolet. *Biophys. J.* **92**, 2885 (2007).
40. Y. Liu, Z. Shao, F. Vollrath, *Nat. Mater.* **4**, 901 (2005).
41. A. L. Let, D. E. Mainwaring, C. Rix, P. Murugaraj, *J. Non-Cryst. Solids* **354**, 1801 (2008).
42. Z. Shao, R. J. Young, F. Vollrath, *Int. J. Biol. Macromol.* **24**, 295 (1999).
43. R. E. Fornes, R. W. Work, N. Morosoff, *J. Polym. Sci. Polym. Phys. Ed.* **21**, 1163 (1983).
44. G. V. Guinea, M. Elices, J. Pérez-Rigueiro, G. R. Plaza, *J. Exp. Biol.* **208**, 25 (2005).
45. D. Porter, F. Vollrath, *Adv. Mater.* **21**, 487 (2009).

46. We thank W. Lee from the Korea Research Institute of Standards and Science in Daejeon, Korea; H. Han from the Department of Material Science and Engineering, Pohang University of Science and Technology in Pohang, Korea; and G.-M. Kim from the Department of Physics, Martin-Luther-University Halle-Wittenberg in Merseburg, Germany, for their helpful discussions on physical and chemical interpretations of mechanical properties, WAXS, NMR spectra, Raman spectra, energy-filtered TEM (EFTEM), and time-of-flight secondary ion mass spectroscopy (TOF-SIMS) data. We also thank J. Woltersdorf, M. Becker, and J. Liu from the Max Planck Institute of Microstructure Physics in Halle, Germany, for EFTEM and Raman measurements. We appreciate TOF-SIMS measurement by M. Krause and help and support in arranging the mechanical properties measurements and TOF-SIMS measurement by M. Petzold from the Fraunhofer Institute for Mechanics of Materials in Halle, Germany. This work has received financial support from the Bundesministerium für Bildung und Forschung (grant FKZ 03X5507) and Deutsche Forschungsgemeinschaft (grants BR 3370/3-1 and Mi 390/17-1).

Supporting Online Material

www.sciencemag.org/cgi/content/full/324/5926/488/DC1
Materials and Methods
SOM Text
Figs. S1 to S11
Tables S1 to S4
References

6 November 2008; accepted 11 March 2009
10.1126/science.1168162

Asymmetric Autocatalysis Triggered by Carbon Isotope ($^{13}C/^{12}C$) Chirality

Tsuneomi Kawasaki, Yukari Matsumura, Takashi Tsutsumi, Kenta Suzuki, Masateru Ito, Kenso Soai*

Many apparently achiral organic molecules on Earth may be chiral because of random substitution of the 1.11% naturally abundant ^{13}C for ^{12}C in an enantiotopic moiety within the structure. However, chirality from this source is experimentally difficult to discern because of the very small difference between ^{13}C and ^{12}C. We have demonstrated that this small difference can be amplified to an easily seen experimental outcome using asymmetric autocatalysis. In the reaction between pyrimidine-5-carbaldehyde and diisopropylzinc, addition of chiral molecules in large enantiomeric excess that are, however, chiral only by virtue of isotope substitution causes a slight enantiomeric excess in the zinc alkoxide of the produced pyrimidyl alkanol. Asymmetric autocatalysis then leads to pyrimidyl alcohol with a large enantiomeric excess. The sense of enantiomeric excess of the product alcohol varies consistently with the sense of the excess enantiomer of the carbon isotopically chiral compound.

The limits of knowledge in recognizing and understanding chirality are continually pushed back by innovative methods (*1*–*4*). Although the theory of a tetrahedral asymmetric carbon atom with four differing substituents has been understood since the 19th-century work of van't Hoff and LeBel (*5*–*9*), molecules for which this characteristic arises solely from carbon isotopic substitution are rare (*10*). It is not known whether a reactive difference between enantiomers can arise solely from a difference in carbon isotopic substitution. Such an observation has been experimentally inaccessible. Considering that the natural abundance of ^{13}C is ~1.11% on Earth, many organic molecules may be chiral arising from carbon isotope differences in enantiotopic groups, although the enantiomeric excess arising from this source may be minute (Fig. 1).

There are reports on enantioselective reactions (*11*, *12*) or on a kinetic resolution (*13*) induced by hydrogen isotope (H/D) replacement, and the use of hydrogen isotopes to explore enzymatic mechanisms is well known (*14*). In a polymer, isotope chirality (H/D) has been shown to cooperatively control macromolecular helical handedness (*15*). However, the effect of carbon isotope substitution is expected to be far smaller. Thus, enantioselective reactions induced by molecules that are chiral solely by virtue of carbon isotope substitution present a challenging problem. To the best of our knowledge, there have been no reports in which carbon isotopically substituted chiral compound induces enantioenrichment in an asymmetric reaction.

Here, we show that asymmetric autocatalysis with amplification of enantioenrichment (*16*, *17*) can be successfully applied to the discrimination between enantiomers that differ solely in substitution of carbon isotopes. Asymmetric autocatalysis has enormous power to recognize molecular chirality (*18*–*22*). In the reaction between pyrimidine-5-carbaldehyde **4** and diisopropylzinc (*i*-Pr_2Zn), the zinc alkoxides of the isotopically substituted chiral alcohols **1** to **3** cause a slight enantiomeric excess (ee) in the zinc alkoxide of pyrimidyl alkanol **5**. After autocatalytic amplification of this enantiomeric excess, alkanol **5** accumulates an enhanced ee with a sense that varies consistently with that of the abundant enantiomer of the isotopically substituted chiral compound **1, 2,** or **3** (Fig. 2).

The isotopically chiral compounds **1** to **3** were synthesized as shown in Fig. 3 (*23*). First, methyl-^{13}C-methylphenyl methanol **1** was prepared. To restrict chiral effects to the influence of the carbon isotopic chirality, both enantiomers of **1** were prepared from the same chiral ligand (–)-**8** as shown in Fig. 3, route I. The enantiomers could be synthesized by direct asymmetric dimethylzinc addition to acetophenone using sulfonamide (–)-**8** (*24*) as a chiral ligand. (*R*)-Alcohol **1** was synthesized using ^{13}C-labeled acetophenone **6** as the substrate. On the other hand, (*S*)-**1** was

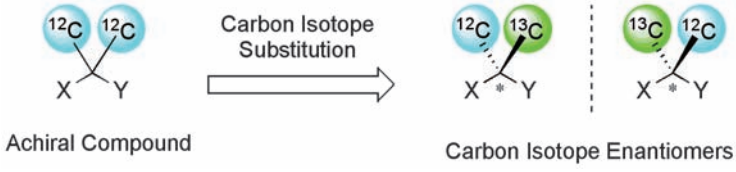

Fig. 1. Generation of chirality by carbon isotope substitution.

Department of Applied Chemistry, Tokyo University of Science, Kagurazaka, Shinjuku-ku, Tokyo 162-8601, Japan.

*To whom correspondence should be addressed. E-mail: soai@rs.kagu.tus.ac.jp

prepared from the ^{13}C-labeled dimethylzinc and unlabeled acetophenone **7** using the same chiral ligand (–)-**8**. In route II, asymmetric centers of *tert*-alcohol **1** were introduced by asymmetric epoxidation (*25*) to the ^{13}C-labeled allyl alcohol **9**, followed by reduction of the tosylate and the epoxide, which afforded the enantiomers of the desired tertiary alcohol **1**.

Next, (*S*)- and (*R*)-1-methyl-^{13}*C*-oxy-3-methoxy-2-propanol **2** were synthesized from (*R*)- and (*S*)-glycidyl methyl ether **11** using ^{13}C-labeled sodium methoxide. The stereoinversion reaction (*26*) of (*S*)-**2** and alcoholysis also afforded the opposite (*R*)-**2**. Thus, both enantiomers **2** could be prepared from (*R*)-**11** as the chiral substrate.

Finally, phenyl-1,2,3,4,5,6-$^{13}C_6$-phenylmethanol **3** was synthesized by a diphenyl(1-methylpyrrolidin-2-yl)methanol (DPMPM)–catalyzed asymmetric aryl transfer reaction (*27*, *28*) to the ^{13}C-substituted benzaldehyde **12** to afford **13** with a chiral stereogenic center. Reductive removal of the bromide substituent gave the isotopically substituted enantiomers of diphenylmethanol **3**. The reduction of the aryl bromide via the corresponding highly polar boronic acid facilitated separation of unreacted compounds in each step. The enantiomeric excess of the synthesized alcohols **1** and **2** could be determined from proton nuclear magnetic resonance (^{1}H-NMR) spectra of their diastereomeric esters of α-methoxy-α-trifluoromethylphenylacetic acid (MTPA). Because the chemical shift differences for the pair of normal and ^{13}C-labeled groups can be observed, the integration of these peaks shows the diastereomeric excess of these MTPA esters, that is, the enantiomeric excess of the synthesized carbon isotopic chiral alcohols.

We found that the isotopic chirality in alcohols **1** to **3** was successfully discriminated by asymmetric autocatalysis. The results of asymmetric autocatalysis triggered by the carbon isotopically chiral alcohols are shown in Table 1. First of all, we investigated methyl-^{13}*C*-methylphenyl methanol **1**, which is a chiral tertiary alcohol formed by the substitution of the ^{13}C-methyl group. In series A1, asymmetric autocatalysis was performed in the presence of (*R*)-**1** with 89% ee; the synthesis of the isotopically substituted alcohol proceeded via route I, including an asymmetric dimethylzinc addition using the same chiral ligand (–)-**8**, and production of (*S*)-**5** with 92% ee was observed (entry 1). In turn, when (*S*)-**1** was used as the chiral trigger, (*R*)-**5** with 96% ee was obtained in 95% yield (entry 2). These relationships of absolute configurations between **1** and the resulting **5** are highly reproducible (entries 3 to 8). Additional eight experiments of autocatalytic reaction performed using (*R*)-**1** (table S1, entries 1 to 4) and (*S*)-**1** (entries 5 to 8), have also strongly supported the stereochemical correlations between (*R*)- and (*S*)-alcohol **1** and pyrimidyl alkanol (*S*)- and (*R*)-**5** (*23*). These results using carbon isotopic chiral *tert*-alcohol **1**, whose enantiomers were synthesized from the same chiral source, clearly indicate that the direction of asymmetric induction is strongly correlated to the carbon isotopic chirality in compound **1**.

Using the single enantiomer (–)-**8** in synthesizing both (*R*)- and (*S*)-alcohols **1** excluded the possibility that residual contamination from **8** could have induced the enantiomeric excess of the product alkanol **5.** If trace amounts of **8** in the added sample of alcohol **1** were responsible for the asymmetric induction, we would expect compound **5** to exhibit the same absolute configura-

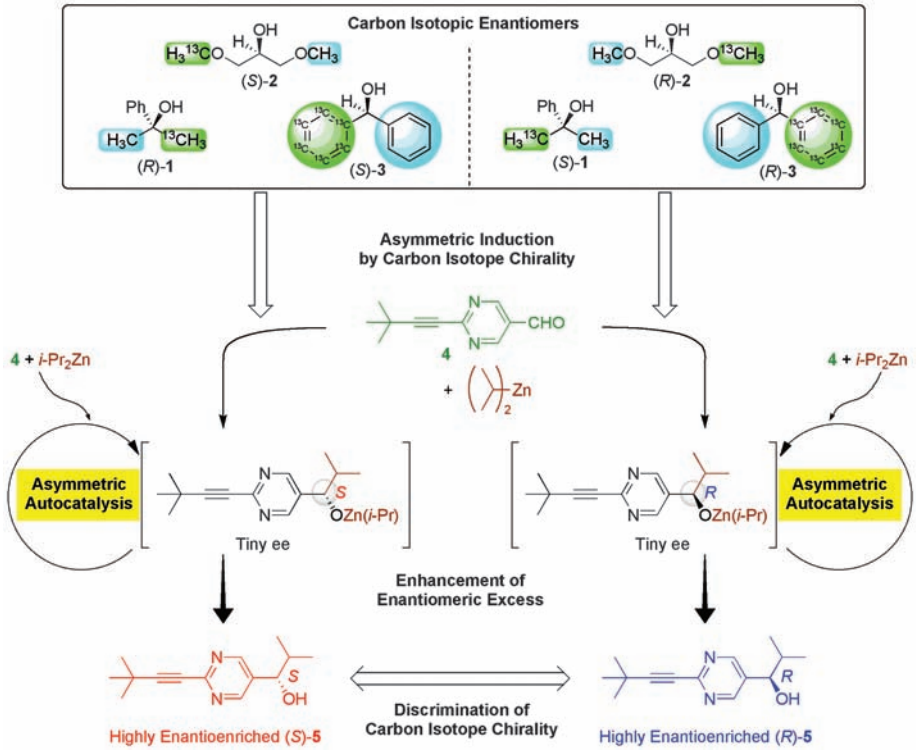

Fig. 2. Discrimination of carbon isotopic chirality by asymmetric autocatalysis.

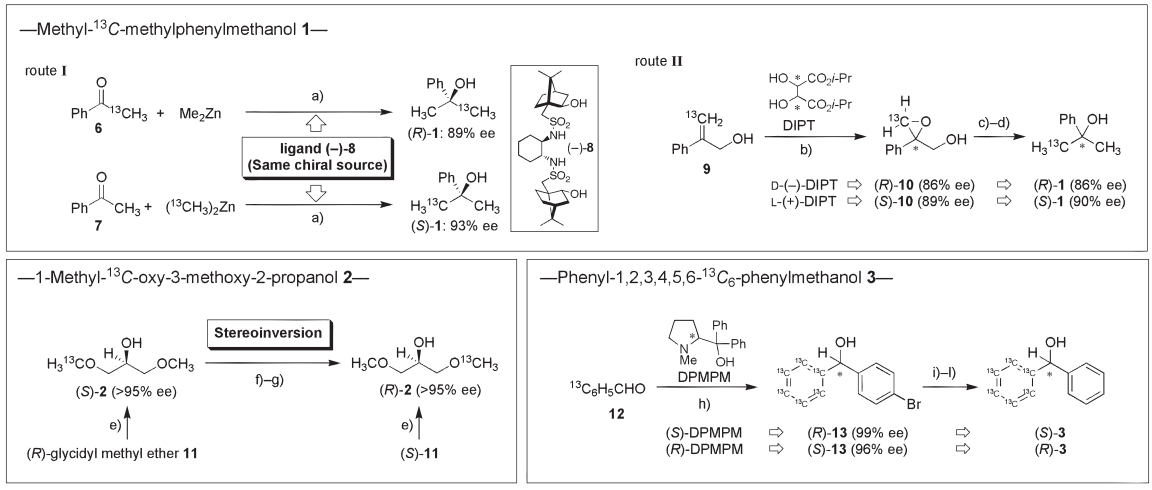

Fig. 3. Synthetic routes to carbon isotope-modified chiral compounds. a) Ti(O*i*-Pr)$_4$, ligand (–)-**8**, toluene or ether; b) diisopropyl tartrate (DIPT), Ti(O*i*-Pr)$_4$, *t*-BuOOH, CH_2Cl_2; c) *p*-toluenesulfonic anhydride, 4-(dimethylamino)pyridine, pyridine; d) $LiAlH_4$, ether; e) Na, $^{13}CH_3OH$; f) Ph_3P, diisopropyl azodicarboxylate, (*p*-NO_2)$C_6H_4CO_2H$, tetrahydrofuran (THF); g) K_2CO_3, MeOH; h) diphenyl(1-methylpyrrolidin-2-yl)methanol (DPMPM), (*p*-Br)$C_6H_4B(OH)_2$, diethylzinc, toluene then recrystallization; i) chlorotrimethylsilane, Et_3N, THF; j) *n*-BuLi, $B(OEt)_3$, THF; k) diethylzinc, toluene then H_2O; l) tetra-*n*-butylammonium fluoride, THF.

tion regardless of the choice of (*R*)- or (*S*)-**1** as a potential trigger. Instead, as confirmed in Table 1, entries 1 to 8, and table S1, entries 1 to 8, (*R*)- and (*S*)-alkanols **5** were obtained reproducibly from adding isotopically chiral (*S*)- and (*R*)-alcohols **1**, respectively, ruling out any role of trace **8**.

In series A2 of Table 1, the enantiomers of *tert*-alcohols **1** were synthesized via route II. In this series, the induction sense was the same as observed in series A1, with high reproducibility: Chiral alcohol (*R*)-**1** acts as an initiator of (*S*)-alkanol **5** formation (entries 9, 11, 13, and 15), and (*S*)-**1** leads to (*R*)-**5** (entries 10, 12, 14, and 16, respectively). When other samples of (*R*)- and (*S*)-*tert*-alcohol **1**, which were prepared in different vessels, were used as chiral inducers, the same stereochemical outcomes were obtained. To establish reproducibility, we carried out an additional 16 asymmetric autocatalysis experiments, using isotopically chiral (*R*)- and (*S*)-**1** each 8 times (table S1, entries 9 to 16 and 17 to 24). The results show consistent stereochemical correlations without any exception (*23*).

To check for chiral influences other than that arising from the isotopically chiral compound, we conducted the autocatalytic reaction induced by the achiral alcohol **1**, which was synthesized by route II using unlabeled **9**. Previously, we have reported spontaneous absolute asymmetric synthesis in the autocatalytic pyrimidine-5-carbaldehyde/diisopropylzinc system (*29*, *30*). That is, under achiral conditions, enantioenriched (*S*)- or (*R*)-alkanol **5** could be obtained by the reaction of aldehyde **4** and *i*-Pr_2Zn in combination with asymmetric autocatalysis. The stochastic behavior of the formation of (*S*)- and (*R*)-alkanol **5** was observed during 84 trials (*30*). Thus, we considered that if there is no chiral factor, which can induce the chirality in asymmetric autocatalysis, the formation of both (*S*)- and (*R*)-alkanol should be observed. On the other hand, if there were some chiral factors in the reaction, predominant formation of (*S*)- or (*R*)-pyrimidyl alkanol **5** correlated to the chiral factor should be observed. When the autocatalysis was performed in the presence of unlabeled achiral compound **1** prepared using D-(–)–diisopropyl tartrate (DIPT) in the epoxidation step, enantioenriched (*S*)- and (*R*)-alkanol **5** were obtained in three and five instances from eight attempts, respectively. In addition, achiral compound **1,** prepared by using tartrate with the opposite absolute configuration as a chiral ligand, initiated the formation of enantiomers of **5** with equal frequency, that is, four occurrences of *S* and four of *R*. Detailed experimental results of asymmetric autocatalysis in the presence of nonlabeled achiral alcohol **1** are given in table S2 and supporting text (*23*). Considering the 24 reproducible asymmetric induction results obtained using isotopically chiral **1** (Table 1, entries 9 to 16, and table S1, entries 9 to 24), these observations of both enantiomers of **5** during 16 trials with achiral **1** confirm the absence of any chiral contaminants in the synthesized sample of **1** that can influence the asymmetric autocatalysis.

In series B of Table 1, *sec*-alcohol **2** was used to trigger asymmetric autocatalysis. In the presence of (*S*)-alcohol **2**, enantioselective *i*-Pr_2Zn addition to pyrimidine-5-carbaldehyde **4** led to (*S*)-pyrimidyl alkanol **5** with 97% ee (entry 17). On the other hand, the opposite enantiomer (*R*)-**2** induced the production of (*R*)-**5** with 93% ee (entry 18). When we repeated the experiments, (*S*)- and (*R*)-*sec*-alcohol **2** induced the formation of (*S*)- and (*R*)-alkanol **5** with the same sense of stereochemistry, respectively (entries 19 to 21). To exclude any chiral influence other than that of carbon isotopic chirality, the (*R*)-alcohol **2** used as the chiral initiator in entries 22 to 24 was prepared from the opposite enantiomer (*S*)-**2** by the stereoinversion reaction; the same stereochemical correlation as before was observed in formation of enantioenriched (*R*)-**5**. The reproducibility was further established by an additional 14 asymmetric autocatalysis experiments

Table 1. Chiral discrimination of the carbon isotopically chiral alcohols using asymmetric autocatalysis.

Entry	$^{13}C/^{12}C$ chiral alcohol (ee)	Pyrimidyl alkanol 5		
		Isolated yield	ee	Configuration
Series A1*†‡				
1	(*R*)-**1** (89% ee)	94	92	*S*
2	(*S*)-**1** (93% ee)	95	96	*R*
3	(*R*)-**1** (89% ee)	80	88	*S*
4	(*S*)-**1** (93% ee)	94	96	*R*
5	(*R*)-**1** (89% ee)	96	88	*S*
6	(*S*)-**1** (93% ee)	97	94	*R*
7	(*R*)-**1** (89% ee)	[not determined]	93§	*S*
8	(*S*)-**1** (93% ee)	92	93	*R*
Series A2†‡‖				
9	(*R*)-**1** (86% ee)	94	94	*S*
10	(*S*)-**1** (86% ee)	87	95	*R*
11	(*R*)-**1** (86% ee)	93	94	*S*
12	(*S*)-**1** (90% ee)	98	93	*R*
13	(*R*)-**1** (86% ee)	85	92	*S*
14	(*S*)-**1** (84% ee)	93	88	*R*
15	(*R*)-**1** (86% ee)	88	89	*S*
16	(*S*)-**1** (90% ee)	93	90	*R*
Series B‡¶				
17	(*S*)-**2** (>95% ee)	92	97	*S*
18	(*R*)-**2** (>95% ee)	86	93	*R*
19	(*S*)-**2** (>95% ee)	89	92	*S*
20	(*R*)-**2** (>95% ee)	89	76	*R*
21	(*S*)-**2** (>95% ee)	90	83	*S*
22#	(*R*)-**2** (>95% ee)	90	95	*R*
23#	(*R*)-**2** (>95% ee)	92	89	*R*
24#	(*R*)-**2** (>95% ee)	78	89	*R*
Series C‡**				
25	(*S*)-**3** (99% ee)	96	95	*S*
26	(*R*)-**3** (96% ee)	96	92	*R*
27	(*S*)-**3** (99% ee)	73	94	*S*
28	(*R*)-**3** (96% ee)	80	92	*R*
29	(*S*)-**3** (99% ee)	84	94	*S*
30	(*R*)-**3** (96% ee)	87	92	*R*
31	(*S*)-**3** (99% ee)	85	70	*S*
32	(*R*)-**3** (96% ee)	80	76	*R*

*Carbon isotopically chiral initiator **1** was synthesized via route I in Fig. 3. †The molar ratio of **1**:**4**:*i*-Pr_2Zn = 0.05:1.05:2.15. Aldehyde **4** and *i*-Pr_2Zn were added in three separate portions. ‡Forty-six additional runs were carried out in this way, further confirming the invariance of the relationship between the handedness of alcohol **1**–**3** and that of product **5**, but with a variation in the absolute value of the product ee. In series A1 (8 further runs) with alcohol **1** of 89% ee (*R*) or 93% ee (*S*), the range of product ee was 79 to 94%; for series A2 (16 further runs) with alcohol **1** varying in ee between 84 and 90%, the range of product ee was between 32 and 95%; for series B (14 further runs) with alcohol **2** (*R*) or (*S*) of >95% ee, the range of product ee was between 63 and 88%, and for series C (8 further runs) with alcohol **3** of 99% ee (*S*) or 96% ee (*R*), the range of ee of the product **5** was between 63 and 88%. See table S1 for the full data. §The enantioenrichment of product alkanol **5** amplifies according to the addition of aldehyde **4** and *i*-Pr_2Zn: For example, in this entry the step-by-step measured ee values of alkanol **5** during three consecutive reactions were 5% ee (after the initial dropwise addition of **4** and *i*-Pr_2Zn), 32% ee (after the second addition), and then 93% ee (after the third addition). ‖Carbon isotopically chiral alcohol **1** was synthesized via route II in Fig. 3. ¶The molar ratio of **2**:**4**:*i*-Pr_2Zn = 0.04:1.8:3.74. Aldehyde **4** and *i*-Pr_2Zn were added in four separate portions. The ee values of **2** were determined from ^{1}H-NMR of its MTPA-ester. #(*R*)-Alcohol **2** used as chiral initiator was synthesized by a stereoinversion reaction from (*S*)-**2**. **The molar ratio of **3**:**4**:*i*-Pr_2Zn = 0.025:0.75:1.525. Aldehyde **4** and *i*-Pr_2Zn were added in four separate portions. The ee of **3** was assigned based on the measured ee of **13**.

using isotopically chiral (*S*)- and (*R*)-**2** eight and six times, respectively (table S1, entries 25 to 32 and 33 to 38). The results show the same stereochemical correlations without any exception (*23*).

Finally, in series C of Table 1, (*S*)- and (*R*)-phenyl-1,2,3,4,5,6-$^{13}C_6$-phenylmethanol **3** were used as chiral initiators of asymmetric autocatalysis. When (*S*)-**3** was used as the chiral trigger, enantioselective addition of *i*-Pr_2Zn to pyrimidine-5-carbaldehyde **4** afforded (*S*)-pyrimidyl alkanol **5** with 95% ee in 96% yield (entry 25). In contrast, the reaction in the presence of (*R*)-**3** gave (*R*)-alkanol **5** with 92% ee (entry 26). These correlations between the ^{13}C isotope chirality and the configuration of the produced alkanol **5** also showed strong reproducibility, with (*S*)- and (*R*)-**3** inducing the production of (*S*)- and (*R*)-**5**, respectively (Table 1, entries 27 to 32, and table S1, entries 39 to 46) (*23*).

In these enantioselective reactions, the initial formation of the zinc alkoxide of the isotopically chiral alcohol tips the enantiomeric balance of the initial *i*-Pr_2Zn addition to aldehyde **4**; thus, a small enantiomeric excess of the zinc alkoxide of **5** is induced. After this step, the subsequent autocatalytic amplification of the small enantiomeric excess causes the zinc alkoxide of **5** to accumulate at enhanced ee, with an absolute configuration tied to that of the ^{13}C-labeled chiral alcohol (**1**, **2**, or **3**) used to trigger the process. Thus, the extremely small chiral effect generated by the substitution of the carbon isotope must be responsible, not for the amplification of the enantiomeric excess in the asymmetric autocatalysis, but for the enantioselection observed, that is, for the enantiomer produced in excess in the formation of the initial zinc alkoxide intermediate and therefore in the final production of **5**.

Only minute energy differences can be associated with the isotopically substituted enantiomer of **1**, **2**, or **3** in causing the tiny enantiomeric excess of the alkoxide that triggers the asymmetric autocatalysis arising from the dialkylzinc addition to **4** (Fig. 2). It has been recognized that such minute energy differences are not interpretable with the tools available to structural theory (*15*, *31*). In the initial reaction stage, the minute energy differences have a tiny effect, which is then cooperatively amplified to the final large enantiomeric excess. It is therefore impossible to disclose a structural reason for the difference in frequency of these initial enantiotopic face selectivities. The "cooperation–amplification" effect, which has been discussed regarding the structural effect of hydrogen deuterium chiral substitution in a helical polymer (*15*), finds reactive analogy in this autocatalytic system. The product handedness is entirely predictable, but the absolute value of the ee varies from run to run. This observation indicates a stochastic influence in the initiation phase biased by the chiral additive. The locally induced enantiomeric excess of zinc alkoxide is then amplified by the normal asymmetric autocatalytic process (*32*).

The neglected carbon isotopic chirality of many organic compounds on Earth—a characteristic that has largely eluded discrimination using contemporary methods—can thus be discriminated by asymmetric autocatalysis, which is a highly sensitive reaction for recognizing and amplifying the extremely small chiral influence between ^{12}C and ^{13}C. The method described above may expand the scope of research on carbon isotope chirality in organic molecules in nature (*33*). Natural enantiomeric excesses in this class of carbon isotopically chiral compounds may be very low, however. The possible role in asymmetric autocatalytic reactions of such compounds with low ee remains to be clarified.

References and Notes

1. K. Nakanishi, N. Berova, R. W. Woody, *Circular Dichroism: Principles and Applications* (Wiley, New York, 2000).
2. J. Haesler, I. Schindelholz, E. Riguet, C. G. Bochet, W. Hug, *Nature* **446**, 526 (2007).
3. L. A. Nafie, T. B. Freedman, *Enantiomer* **3**, 283 (1998).
4. L. D. Barron, *Nature* **238**, 17 (1972).
5. K. Mislow, *Top. Stereochem.* **22**, 1 (1999).
6. M. Tsukamoto, H. B. Kagan, *Adv. Synth. Catal.* **344**, 453 (2002).
7. I. Weissbuch, L. Addadi, M. Lahav, L. Leiserowitz, *Science* **253**, 637 (1991).
8. A. Eschenmoser, *Science* **284**, 2118 (1999).
9. J. R. Cronin, S. Pizzarello, *Science* **275**, 951 (1997).
10. M. A. Evans, J. P. Morken, *J. Am. Chem. Soc.* **124**, 9020 (2002).
11. H. Pracejus, *Tetrahedron Lett.* **7**, 3809 (1966).
12. I. Sato, D. Omiya, T. Saito, K. Soai, *J. Am. Chem. Soc.* **122**, 11739 (2000).
13. A. Horeau, A. Nouaille, K. Mislow, *J. Am. Chem. Soc.* **87**, 4957 (1965).
14. D. Arigoni, E. L. Eliel, *Top. Stereochem.* **4**, 127 (1969).
15. M. M. Green *et al.*, *Angew. Chem. Int. Ed.* **38**, 3139 (1999).
16. K. Soai, T. Shibata, H. Morioka, K. Choji, *Nature* **378**, 767 (1995).
17. I. Sato, H. Urabe, S. Ishiguro, T. Shibata, K. Soai, *Angew. Chem. Int. Ed.* **42**, 315 (2003).
18. T. Shibata *et al.*, *J. Am. Chem. Soc.* **120**, 12157 (1998).
19. K. Soai *et al.*, *J. Am. Chem. Soc.* **121**, 11235 (1999).
20. T. Kawasaki *et al.*, *J. Am. Chem. Soc.* **128**, 6032 (2006).
21. D. G. Blackmond, C. R. McMillan, S. Ramdeehul, A. Schorm, J. M. Brown, *J. Am. Chem. Soc.* **123**, 10103 (2001).
22. D. Lavabre, J.-C. Micheau, J. R. Islas, T. Buhse, *Top. Curr. Chem.* **284**, 67 (2008).
23. Materials, methods, and additional experimental results of asymmetric autocatalysis are available as supporting material on *Science* Online.
24. O. Prieto, D. J. Ramón, M. Yus, *Tetrahedron Asymmetry* **14**, 1955 (2003).
25. T. Katsuki, K. B. Sharpless, *J. Am. Chem. Soc.* **102**, 5974 (1980).
26. O. Mitsunobu, M. Yamada, *Bull. Chem. Soc. Jpn.* **40**, 2380 (1967).
27. K. Soai, S. Niwa, *Chem. Rev.* **92**, 833 (1992).
28. G. Zhao, X. Li, X. Wang, *Tetrahedron Asymmetry* **12**, 399 (2001).
29. K. Soai *et al.*, *Tetrahedron Asymmetry* **14**, 185 (2003).
30. T. Kawasaki, K. Suzuki, M. Shimizu, K. Ishikawa, K. Soai, *Chirality* **18**, 479 (2006).
31. M. M. Green, C. Khatri, N. C. Peterson, *J. Am. Chem. Soc.* **115**, 4941 (1993).
32. T. Shibata, S. Yonekubo, K. Soai, *Angew. Chem. Int. Ed.* **38**, 659 (1999).
33. B. Barabás, L. Caglioti, K. Micskei, C. Zucchi, G. Pályi, *Orig. Life Evol. Biosph.* **38**, 317 (2008).

34. This work was supported by a Grant-in-Aid for Scientific Research from The Ministry of Education, Culture, Sports, Science and Technology (MEXT). The authors are grateful to the reviewers for helpful discussions.

Supporting Online Material

www.sciencemag.org/cgi/content/full/1170322/DC1
Materials and Methods
SOM Text
Figs. S1 to S11
Schemes S1 to S10
Tables S1 and S2

29 December 2008; accepted 3 March 2009
Published online 26 March 2009;
10.1126/science.1170322
Include this information when citing this paper.

A Global View of the Lithosphere-Asthenosphere Boundary

Catherine A. Rychert* and Peter M. Shearer

The lithosphere-asthenosphere boundary divides the rigid lid from the weaker mantle and is fundamental in plate tectonics. However, its depth and defining mechanism are not well known. We analyzed 15 years of global seismic data using *P*-to-*S* (*Ps*) converted phases and imaged an interface that correlates with tectonic environment, varying from 95 ± 4 kilometers beneath Precambrian shields and platforms to 81 ± 2 kilometers beneath tectonically altered regions and 70 ± 4 kilometers at oceanic island stations. High-frequency *Ps* observations require a sharp discontinuity; therefore, this interface likely represents a boundary in composition, melting, or anisotropy, not temperature alone. It likely represents the lithosphere-asthenosphere boundary under oceans and tectonically altered regions, but it may constitute another boundary in cratonic regions where the lithosphere-asthenosphere boundary is thought to be much deeper.

Mapping the depth and character of the lithosphere-asthenosphere boundary with existing seismic methods has proven to be a challenge. Global surface-wave studies (*1*–*4*) image rigid lithospheres that increase in thickness from oceans to continents at broad

wavelengths (~1000 km). However, both the absolute depth and the nature of the boundary are debated. Lateral variations in depth likely occur at finer scales, as seen in regional results [e.g., (*5*, *6*)]. Similarly, the depth resolution of most surface- and body-wave tomography studies is limited to >40 km, which is insufficient to determine the mechanism that defines the boundary. Finally, imaging of the boundary globally at higher resolution with regional and global stacks of body waves has not been possible (*7*). This could be because the boundary is not sharp enough to be detected at high frequencies, or because of small-scale variations in its depth and/or character. A growing number of regional observations of sharp velocity decreases with depth (*P*-to-*S* and *S*-to-*P* conversions; multibounce *S* waves) suggest the latter explanation in a variety of tectonic environments, such as beneath oceans (*8*), in hotspot regions (*9*, *10*), and in continental regions with thin lithosphere (<110 km) (*11*–*13*). Beneath continental interiors, boundaries interpreted to be the base of the lid have been imaged using converted, reflected, or refracted phases; in many cases these dip to greater depths (>200 km) toward the continental interior [e.g., (*14*)], although the sharpness of the associated velocity gradient in these locations has not been determined and results beneath cratonic interiors can be relatively complex [e.g., (*15*, *16*)]. Overall, sharp discontinuities associated with the tomographically defined lithosphere-asthenosphere boundary are detected in noncratonic regions, but they are not usually imaged beneath thick continental interiors. Therefore, although it is often assumed that the character of the boundary may vary, it has remained a puzzle as to why such a fundamental boundary would be so variable in its nature.

Here, we used *Ps* imaging to resolve the shear-wave velocity structure beneath individual seismic stations. We considered data in the IRIS (Incorporated Research Institutions for Seismology) FARM data set from 1990 to 2004 at single stations. We rotated the recorded wave field into its predicted *P* and *S* components before simultaneously deconvolving and migrating to depth (*17*) assuming a reference one-dimensional velocity model (IASP91). Our results are affected to some extent by crustal thicknesses and ratios of *P*-wave to *S*-wave velocity (V_P/V_S) that do not match IASP91, but reasonable variations in crustal parameters would change our results by <5 km in extreme cases and by <2.5 km generally (*18*). The same is the case for mantle V_P/V_S variations (*11*).

Of 745 stations, we focused on 334 with large quantities (>50 events) of high-quality (signal-to-noise ratio >5) data. This amount of data is required to attain high-resolution imaging (i.e., clear signals owing to data stacking rather than low-pass filtering). We eliminated additional locations where deconvolved signals are characterized by ringing caused by noise and/or shallow discontinuities, and selected 169 stations that have relatively simple crustal structure—that is, places where the Moho and its two first-order reverberations may be easily identified. This selection process was important for determining whether an observed phase is representative of discontinuity structure. An apparent phase in our deconvolved waveforms represents (i) the reverberation from a discontinuity at shallow depths, (ii) a side lobe of a crustal phase,

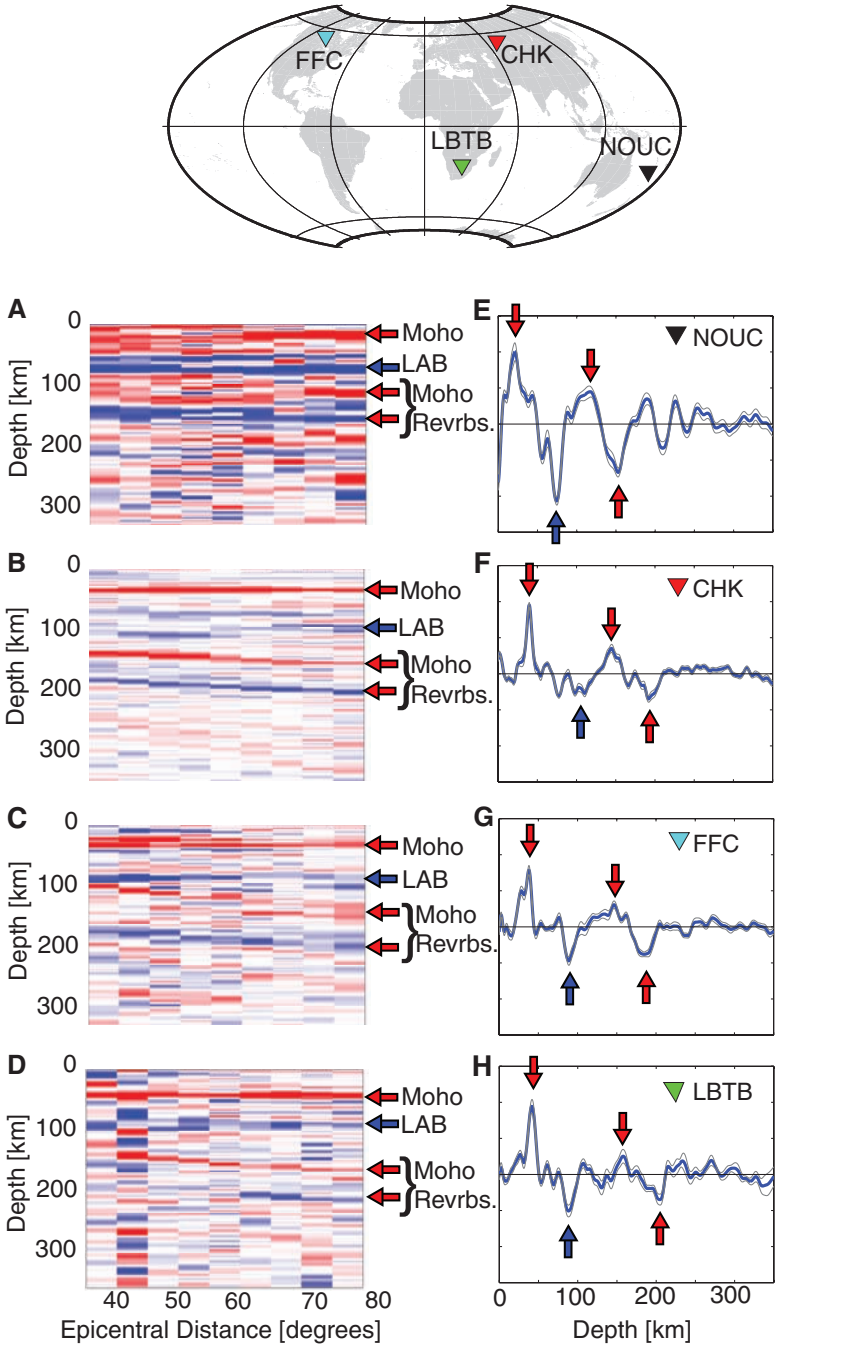

Fig. 1. Data examples for each tectonic region, after (*19*). Triangles on the map indicate station locations. Tectonic regions: NOUC, oceanic; CHK, Phanerozoic orogenic zones and magmatic belts; FFC, Phanerozoic platforms; LBTB, Precambrian shields and platforms. (**A** to **D**) Data binned by epicentral distance, with positive amplitude plotted in red and negative amplitude in blue. (**E** to **H**) All data from a given station deconvolved in a single bin (blue lines). Thin gray lines indicate 2σ error determined by bootstrap testing. Red arrows indicate crustal phases. Blue arrows indicate the phase we associate with the lithosphere-asthenosphere boundary (LAB).

Institute of Geophysics and Planetary Physics, Scripps Institution of Oceanography, University of California, San Diego, 9500 Gilman Drive, M/C 0225, La Jolla, CA 92093, USA.

*To whom correspondence should be addressed. E-mail: crychert@ucsd.edu

or (iii) a direct conversion from a discontinuity at that depth. To evaluate these possibilities, we examined data binned by epicentral distance, which enables easy detection of crustal reverberations because they migrate to increasing depth with respect to epicentral distance. Once crustal phases were identified, we searched for other phases that may be associated with discontinuity structure. We also analyzed data stacked from all distances along predicted *Ps* moveout curves to enhance the visibility of the *Ps* phases that we observed.

At all stations where crustal phases were reasonably identifiable, we also found the presence of negative phases (i.e., phases opposite in polarity to the *Ps* conversion from the velocity increase at the Moho). These phases are not reverberations, because they do not migrate to increasing depth with respect to epicentral distance. In addition, the direct conversions and positive-polarity reverberations that would be associated with negative reverberation phases are not apparent. Furthermore, inclusion of high frequencies and consideration of epicentral distance and single bin plots indicate that the phases are distinct from surrounding phases and do not represent side lobes. Therefore, the observed negative phases likely represent direct conversions from sharp velocity drops at associated depths.

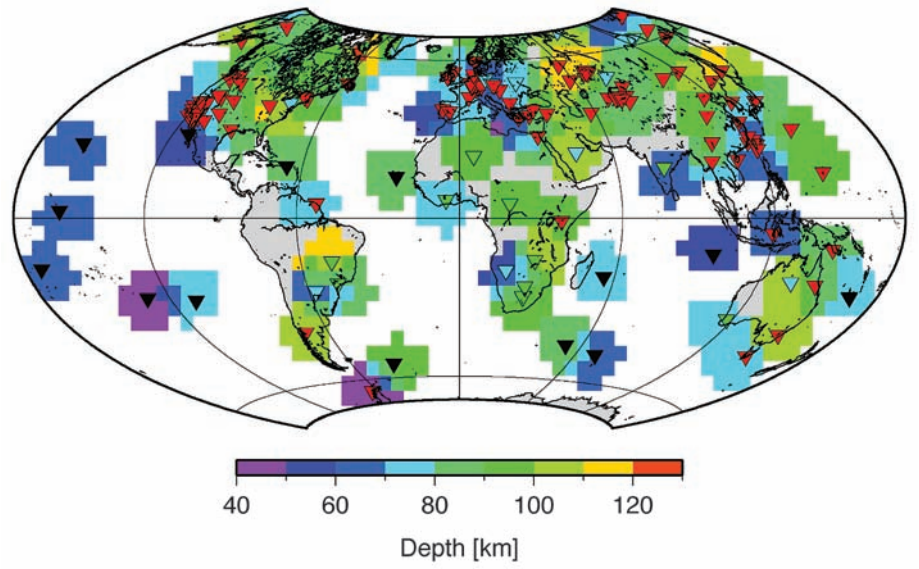

Fig. 2. Global map of the depth to the lithosphere-asthenosphere boundary imaged using *Ps*. Color indicates depth. Triangles show the 169 stations used in this study. Station color corresponds to tectonic regionalization, after (*19*); tectonic regions are colored as follows: black, oceanic; red, Phanerozoic orogenic zones and magmatic belts; cyan, Phanerozoic platforms; green, Precambrian shields and platforms. Although in (*19*) oceanic environments are divided into three age groupings, a single oceanic bin, encompassing all ages, is used here because sampling of this region is sparse.

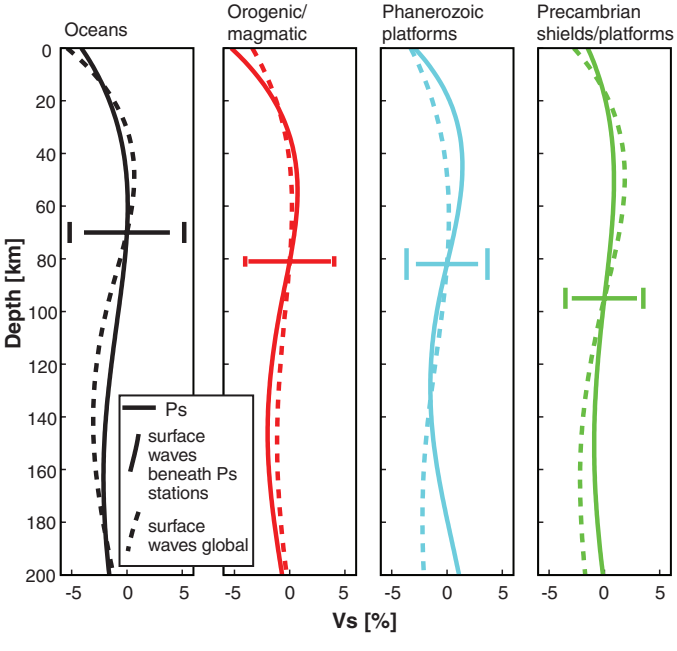

Fig. 3. Comparison of *Ps*-inferred average properties of the lithosphere-asthenosphere boundary and Voigt averaged *S*-wave velocity profiles from the surface-wave results of (*2*) for different tectonic regions. The surface-wave profiles (*2*) are averaged tectonically over the entire model (dashed line) and beneath the stations used in this study (solid line). Horizontal lines represent average *Ps* results. Short solid vertical lines show estimated standard errors in average *Ps* depths. Separation between horizontal bars and vertical bars indicates errors in the average *Ps* magnitudes. Percentages are calculated with respect to the average surface-wave velocity at the *Ps* conversion depth in each region. Each panel represents a tectonic region (*19*) from left to right: oceanic, Phanerozoic orogenic zones and magmatic belts, Phanerozoic platforms, and Precambrian shields and platforms.

Our total data set included 14 stations from oceanic sites, 123 from Phanerozoic orogenic zones and magmatic belts, 14 from Phanerozoic platforms, and 18 from Precambrian shields and platforms (*19*) (Fig. 1). We rated the clarity of the waveforms and the certainty of identifying the phase of interest at each station, assigning ratings from 1 (most obvious) to 5 (most ambiguous) (*18*). Restricting the analysis to only the higher-quality ratings produced similar results to those presented here, but with less complete global coverage (fig. S2). At some stations, multiple phases that may be associated with discontinuities were observed (e.g., Fig. 1B). In these cases it is assumed that the deeper phase is the phase of interest and the shallower phase represents internal lithospheric structure, because it is unlikely that there is a velocity drop with depth within the sublithospheric mantle. Crustal reverberations can impede our ability to detect discontinuities at depths of ~100 to 200 km, depending on the thickness of the crust. We did not observe *Ps* phases related to sharp negative discontinuities between 200 and 410 km. Strong discontinuities between 100 and 200 km depth cause some degree of interference with reverberations, but this type of interference pattern was not observed consistently, either globally or beneath cratonic environments.

Depths to the discontinuity exhibited wide variation among individual stations, but most were between 60 and 110 km. We found a correlation between the depth of the observed discontinuity and tectonic environment when the results were plotted globally and results for locations in close proximity were simply averaged (Fig. 2). The average depth to the discontinuity in each of the tectonic environments increased from ocean to craton: 70 ± 4 km (oceans), 81 ± 2 km (Phanerozoic orogenic zones and magmatic belts), 82 ± 6 km (Phanerozoic platforms), and 95 ± 4 km (Precambrian shields and platforms). Averages of only the most reliable results (ratings 1 to 3) were within the estimated errors of the results that include all ratings (1 to 5). Our sampling of the oceanic lithosphere consisted entirely of ocean island stations and therefore may not be representative of typical oceanic lithosphere. The existence of multiple boundaries, primarily beneath magmatic/orogenic zones in our observations, could be the effect of non-coincident dehydration and depletion boundaries. A similar double boundary was imaged in eastern North America (*12*). We did not find a

correlation between Moho depth and depth to this discontinuity.

The tectonically averaged *Ps* depths are similar to those of shear-wave velocity profiles from a recent surface-wave study (*2*) (Fig. 3). The *Ps* depths agree with the smooth decreases in surface-wave velocity beneath our stations: 70 ± 4 km versus a gradual decease from 61 to 164 km in oceanic environments, 81 ± 2 km versus 55 to 147 km beneath Phanerozoic orogenic zones and magmatic belts, 82 ± 6 km versus 46 to 130 km beneath Phanerozoic platforms, and 95 ± 4 km versus 51 to 152 km beneath Precambrian shields and platforms (Fig. 3). The surface-wave velocity drops in Fig. 3 are gradual, occurring over ~100 km, and a trend of increasing lithospheric thickness from ocean to craton is not apparent. However, surface waves average what is likely a more complicated velocity structure and can be relatively insensitive to the depth of the sharpest velocity contrast (*5*), which is the parameter to which *Ps* is sensitive. Our result is in agreement with the trend of increasing lithospheric thickness that is generally observed by global seismic results (*1*–*4*), although muted in magnitude.

The velocity contrast estimated for the *Ps* signal (*18*) is generally larger than the total drop in *S*-wave velocity from surface-wave studies (Fig. 3). The total *Ps* contrast decreases from 9 ± 1% beneath oceanic islands to 6 ± 0.3% beneath regions that have been tectonically altered to 6 ± 1% beneath both Phanerozoic and Precambrian platforms and shields, versus 2 to 6%, 3 to 4%, and 2 to 5% for the surface waves, respectively. However, strong, sharp contrasts are frequently observed on a regional scale. For instance, velocity drops of 3 to 9.6% over depths of less than 11 km at 60 to 110 km have been modeled beneath a variety of tectonic environments including fault zones, orogenic belts, passive continental margins, and oceanic plates (*8*, *11*–*13*, *20*). Global surface-wave results could be averaging a more complex structure consisting of lateral variations in the depth or character of this discontinuity, sharp negative vertical boundaries that occur within more gradual velocity increases with depth, or combinations of any or all of these phenomena.

Boundaries imaged by *Ps* at high frequency are sharp and cannot be explained by thermal gradients alone (*11*, *12*); hence, they likely require a mechanism such as composition, melting, or anisotropy. Beneath continents, a boundary in depletion can explain velocity contrasts up to ~1.5% (*21*, *22*) and a dehydration boundary may provide an additional ~4.5% (*18*), readily explaining the average *Ps* contrast (6%). Beneath oceans, a dehydration boundary may contribute up to 5.7% (*18*), slightly less than our observed 9%. However, the discrepancy could be caused by our sparse and biased sampling in oceanic regions (i.e., ocean islands only), a complex attenuation structure that is averaged by the global attenuation models (*23*) from which these numbers are derived, and/or the general low quality of the *Ps* ocean station results. Alternatively, a small amount of partial melting in the asthenosphere (*24*–*26*) could easily produce a strong, sharp boundary (*11*) that is consistent with our results, although maintaining this amount of partial melting may be difficult because of melt connectivity.

Overall, either melting or composition could readily account for our observations, and beneath oceans and magmatic/orogenic regions, a weak asthenosphere at ~70 to 81 km depth seems reasonable in the context of global and regional seismic and geochemical evidence. However, beneath cratonic interiors, a weak asthenosphere from hydration or melting at ~95 km depth would likely induce lithosphere-asthenosphere decoupling, eliminating the possibility of a thermal boundary layer that extends to greater depths beneath continents. It is commonly accepted (*27*–*29*) that such a boundary layer is required to explain seismic evidence (*1*–*4*) that continental regions are seismically faster than oceanic regions at ~150 to 200 km depth.

One explanation is that the majority of our stations located on Precambrian shields and platforms are not actually sampling cratonic interiors. Many stations in the Precambrian shield/platform environment are located close to the boundaries between tectonic environments. A few stations with high-quality results (ratings of 1 to 3) are near the centers of cratons. However, in general the exact locations of cratonic roots at depth are somewhat ambiguous owing to the broad resolution of tomographic results. Alternatively, the discontinuities illuminated by this study beneath continents may represent boundaries in seismic anisotropy orientation or strength. Although a boundary in frozen-in anisotropy would not necessarily be associated with the lithosphere-asthenosphere boundary, such a feature would have implications for the formation and evolution of the continents. A sharp change from stronger to weaker radial anisotropy (i.e., transverse isotropy, vertical symmetry axis) with depth would produce a *Ps* phase with the correct polarity to explain our observations. Indeed, recent surface-wave results (*2*) indicate a decrease (~3%) in radial anisotropy from the Moho to ~125 km depth beneath Precambrian shields and platforms; this constitutes strong evidence that the observed boundary could be related to anisotropic structure beneath cratons. The strength of the anisotropy in this model alone is insufficient to explain our observed *Ps* amplitudes. However, as noted above, surface waves likely average more complicated structure.

An anisotropic explanation for our observations beneath oceans and magmatic/orogenic zones is not as likely. First, decreases in radial anisotropy with depth occur at deeper depths (>125 km) beneath the remaining tectonic environments in global surface-wave results (*2*). In addition, although sharp variations in anisotropy may be preserved in ancient structures in cratons, another mechanism (such as hydration or melt) would still be required to create sharp variations in anisotropy beneath oceans and magmatic/orogenic zones. This same logic holds for creating a sharp boundary through variations in grain size (*11*).

A tectonically varying explanation for our globally pervasive *Ps* observations is not completely satisfying. However, in the context of global and regional tomography, this is the best explanation at the present time. Our results beneath oceans and Phanerozoic magmatic/orogenic zones likely represent a discontinuity in hydration or melting, and our results for shields and platforms either represent sampling at the edges of cratonic interiors or indicate that a sharp mid-lithospheric discontinuity in anisotropy is a global feature of cratonic roots.

References and Notes

1. M. Panning, B. Romanowicz, *Geophys. J. Int.* **167**, 361 (2006).
2. M. Nettles, A. M. Dziewonski, *J. Geophys. Res.* **113**, B02303 (2008).
3. S. Lebedev, R. D. van der Hilst, *Geophys. J. Int.* **173**, 505 (2008).
4. B. Kustowski, G. Ekstrom, A. M. Dziewonski, *J. Geophys. Res.* **113**, B06306 (2008).
5. A. B. Li, K. Burke, *J. Geophys. Res.* **111**, B10303 (2006).
6. F. J. Simons, A. Zielhuis, R. D. van der Hilst, *Lithos* **48**, 17 (1999).
7. P. M. Shearer, *J. Geophys. Res.* **96**, 18147 (1991).
8. Y. Tan, D. V. Helmberger, *J. Geophys. Res.* **112**, B08301 (2007).
9. X. Li, R. Kind, X. H. Yuan, I. Wolbern, W. Hanka, *Nature* **427**, 827 (2004).
10. X. Li *et al.*, *Nature* **405**, 938 (2000).
11. C. A. Rychert, S. Rondenay, K. M. Fischer, *J. Geophys. Res.* **112**, B08314 (2007).
12. C. A. Rychert, K. M. Fischer, S. Rondenay, *Nature* **436**, 542 (2005).
13. L. Chen, T. Y. Zheng, W. W. Xu, *J. Geophys. Res.* **111**, B09312 (2006).
14. P. Kumar, X. Yuan, R. Kind, G. Kosarev, *Geophys. Res. Lett.* **32**, L07305 (2005).
15. A. Levander, F. L. Niu, C. T. A. Lee, X. Cheng, *Tectonophysics* **416**, 167 (2006).
16. D. B. Snyder, *Tectonics* **27**, TC4006 (2008).
17. M. G. Bostock, *J. Geophys. Res.* **103**, 21183 (1998).
18. See supporting material on *Science* Online.
19. T. H. Jordan, *Bull. Seismol. Soc. Am.* **71**, 1131 (1981).
20. S. Oreshin, L. Vinnik, D. Peregoudov, S. Roecker, *Geophys. Res. Lett.* **29**, 1191 (2002).
21. C. T. A. Lee, *J. Geophys. Res.* **108**, 2441 (2003).
22. D. L. Schutt, C. E. Lesher, *J. Geophys. Res.* **111**, B05401 (2006).
23. C. A. Dalton, G. Ekstrom, A. M. Dziewonski, *J. Geophys. Res.* **113**, B09303 (2008).
24. H. Thybo, *Tectonophysics* **416**, 53 (2006).
25. D. L. Anderson, *Theory of the Earth* (Blackwell Science, Boston, 1989).
26. K. Mierdel, H. Keppler, J. R. Smyth, F. Langenhorst, *Science* **315**, 364 (2007).
27. C. T. A. Lee, A. Lenardic, C. M. Cooper, F. L. Niu, A. Levander, *Earth Planet. Sci. Lett.* **230**, 379 (2005).
28. S. D. King, *Earth Planet. Sci. Lett.* **234**, 1 (2005).
29. T. H. Jordan, *Nature* **274**, 544 (1978).

30. We thank J. Lawrence for preparing the seismogram data set, M. Nettles for providing her surface-wave model, and C. Dalton for providing her attenuation model.

Supporting Online Material

www.sciencemag.org/cgi/content/full/324/5926/495/DC1
Materials and Methods
Figs. S1 and S2
Table S1
References

15 December 2008; accepted 9 March 2009
10.1126/science.1169754

Seismic Evidence for Sharp Lithosphere-Asthenosphere Boundaries of Oceanic Plates

Hitoshi Kawakatsu,[1]* Prakash Kumar,[1]† Yasuko Takei,[1] Masanao Shinohara,[1] Toshihiko Kanazawa,[1] Eiichiro Araki,[2] Kiyoshi Suyehiro[2]

The mobility of the lithosphere over a weaker asthenosphere constitutes the essential element of plate tectonics, and thus the understanding of the processes at the lithosphere-asthenosphere boundary (LAB) is fundamental to understand how our planet works. It is especially so for oceanic plates because their relatively simple creation and evolution should enable easy elucidation of the LAB. Data from borehole broadband ocean bottom seismometers show that the LAB beneath the Pacific and Philippine Sea plates is sharp and age-dependent. The observed large shear wave velocity reduction at the LAB requires a partially molten asthenosphere consisting of horizontal melt-rich layers embedded in meltless mantle, which accounts for the large viscosity contrast at the LAB that facilitates horizontal plate motions.

Oceanic plates are created at mid-oceanic ridges and spread away as a rigid body (lithosphere) to move over a weaker asthenosphere. The age of oceanic plate is recorded by the magnetic lineation, and its evolution is well explained by thermal cooling of a moving plate. The bottom of an oceanic plate was thought to correspond to the top of the seismically observed low-velocity layer around a depth of 50 to 100 km, possibly indicating the presence of partially molten mantle rocks (*1*), and the thickening of oceanic plates with the age has been confirmed by using low-resolution surface waves (*2*). An alternative is that the oceanic lithosphere is hardened by water extraction at the mid-oceanic ridges (*3*, *4*), and once the lithosphere is created it does not evolve nor thicken. In this case, the observed age dependence is solely a thermal effect. This view predicts that the seismic lithosphere-asthenosphere boundary (LAB) signal should be small [~1 to 2% velocity reduction (*3*)].

We detected the bottom of oceanic plates beneath the normal ocean by using high-resolution body waves observed by the borehole broadband ocean bottom seismometry. A LAB has been observed beneath continents (*5*, *6*). Attempts to observe the oceanic LAB by using long-period body waves that traverse long distance in the mantle suffers from the large spatial averaging and the contamination from highly heterogeneous structure at the bottom of the mantle. Data beneath normal oceans have been lacking because of the lack of high-quality ocean bottom broadband seismic observatories. Under the Japanese Ocean Hemisphere network Project (OHP) (*7*), ocean bottom broadband seismic observatories were deployed, and two borehole stations, WP1 and WP2, were operated for a few years in the Philippine Sea and the Pacific Ocean, respectively (Figs. 1 and 2) (*8*–*10*). We applied P- and S-receiver function (RF) techniques to the teleseismic data (*5*, *11*–*13*). The RF technique uses compression-to-shear (*P*-to-*S*, P-RF) and shear-to-compression (*S*-to-*P*, S-RF) converted seismic waves to detect sharp velocity changes beneath stations. The S-RF method is especially powerful for detecting signatures like LAB at depths between 50 and 200 km, for which strong signal-generated interfering phases are present in the P-RF method (*5*, *13*). Because the seismological observatories were situated at a depth of ~500 m below the ocean floor and below ~5-km-thick water column, we also had to properly estimate the effect of water

[1]Earthquake Research Institute, University of Tokyo, 1-1-1 Yayoi, Bunkyo-ku, Tokyo 113-0032, Japan. [2]Japan Agency for Marine-Earth Science and Technology, 2-15 Natsushima, Yokosuka, Kanagawa 237-0061, Japan.

*To whom correspondence should be addressed. E-mail: hitosi@eri.u-tokyo.ac.jp

†On leave from National Geophysical Research Institute, Uppal Road, Hyderabad-500007, India.

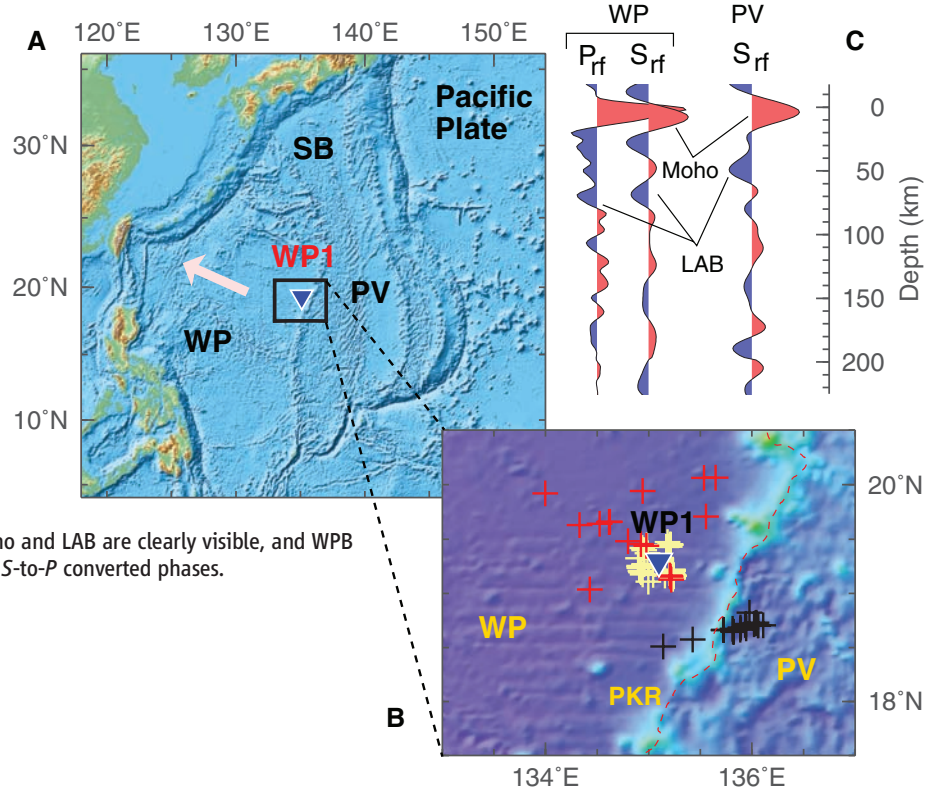

Fig. 1. Location of borehole broadband seismic observatory WP1 and the receiver functions. (**A**) The location of WP1 (inverted blue triangle) in the Philippine Sea plate. This station is at a depth of 561 m below seafloor with an ocean water thickness of 5710 m (*9*). (**B**) Zoomed version of the rectangular region around the station. Palau Kyushu Ridge (PKR) runs almost in the center of the Philippine Sea plate from north to south and divides the plate into two distinct geological provinces: PVB, Parece-Vela basin (15 to 27 My), and WPB, Western Philippine basin (33 to 49 My). Crosses in yellow and red are the piercing points for *P*-to-*S* and *S*-to-*P* converted waves, respectively, at 70 km depth falling in the WPB, whereas black crosses are the piercing points for *S*-to-*P* conversion falling mostly in the PVB. (**C**) Stacked radial P-RFs and S-RFs from WP1 for WPB and PVB. Red and blue colors indicate positive and negative values of RFs, respectively. Only *S*-to-*P* piercing points sample the PVB because of the larger *S*-wave slowness. Converted signals from Moho and LAB are clearly visible, and WPB shows the consistent structure with both *P*-to-*S* and *S*-to-*P* converted phases.

reverberations. Systematic modeling using synthetic waveforms show that S-RF is also an effective tool for such a case, whereas P-RF can be significantly disturbed by the presence of the ocean (*10*).

The results of RFs of two observatories show consistent findings (Figs. 1 to 3). The analyses reveal at least two prominent discontinuities present in the first 10 s of RFs (roughly corresponding to depths of 0 to 100 km beneath the station), one with positive polarity corresponding to the oceanic Moho, followed by a negative discontinuity, which we interpret as the LAB. Crustal phases in both regions are observed at a delay time of ~1 s, corresponding to 7- to 8-km-thick oceanic crusts that are close to the regionally determined estimates based on active seismic data (*9*) and to the global average.

The station WP1 in the central Philippine Sea is located near the Palau Kyushu Ridge (PKR), and observed S-RFs are grouped into two depending on the location relative to PKR of the piercing points of the LAB signals (Fig. 1B). The prominent phases corresponding to LAB occur at ~7.5 s (76 ± 1.8 km, 1 SE) for both P-RF and S-RF for piercing points located directly beneath the station, which is situated in the west of PKR with a plate age of ~49 million years (My). The same LAB phase was observed ~2 s earlier (~55 km LAB) for S-RF of eastern piercing points where the plate age is ~25 My. For WP2 in the northwestern Pacific ocean where the plate age is ~129 My, the data quality is slightly lower (*10*), but we still observe similar LAB phases at ~7–8 s for both P-RF and S-RF. The waveform modeling gives the best estimate for LAB depth of 82 ± 4.4 km (Fig. 3C). A deep LAB is also observed for the old Pacific plate beneath northeast Japan, where the highest quality seismic data are available from Japanese high-sensitivity seismograph network (Hi-net) to allow detailed imaging of subducting plate (*14*). The imaged thickness of the lithosphere is ~80 km (Fig. 2A) (*15*). Because the

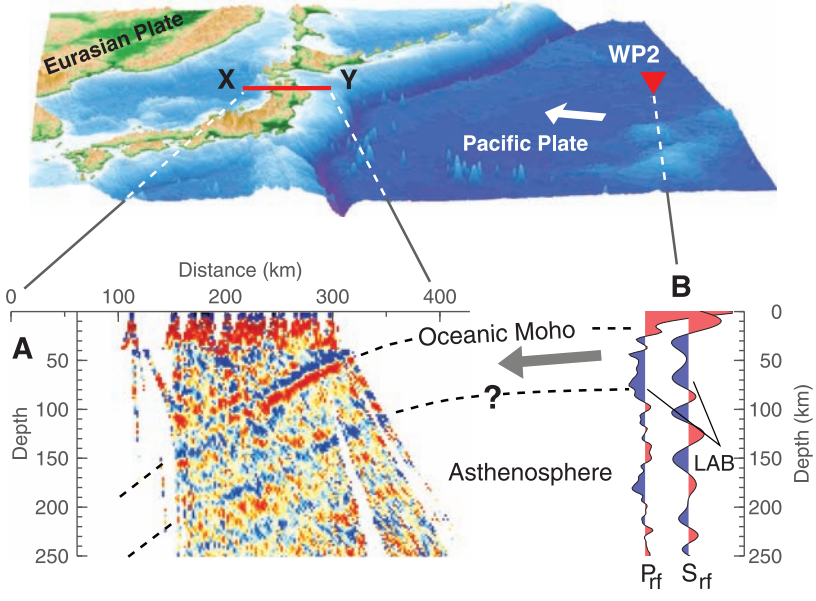

Fig. 2. RFs for WP2 and RF image of subducting Pacific plate beneath northeast Japan. In the topographic map, the inverted red triangle indicates the location of WP2, which is deployed at a depth of 460 m below the seafloor with a water column of 5566 m thick. (**A**) P-RF image along the profile XY using dense land seismic data of Hi-net from Japan (*10*). Red and blue colors indicate velocity increase (from shallow to deep) and decrease at the point, respectively. The top surface of the slab and the oceanic Moho are clearly imaged, as well as the bottom surface of the slab (i.e., subducting LAB). (**B**) P-RF and S-RF for WP2. Negative phases associated with a shear wave velocity drop marked as LAB appear to correspond to the strong negative (blue) signature of the subducting slab below Japan.

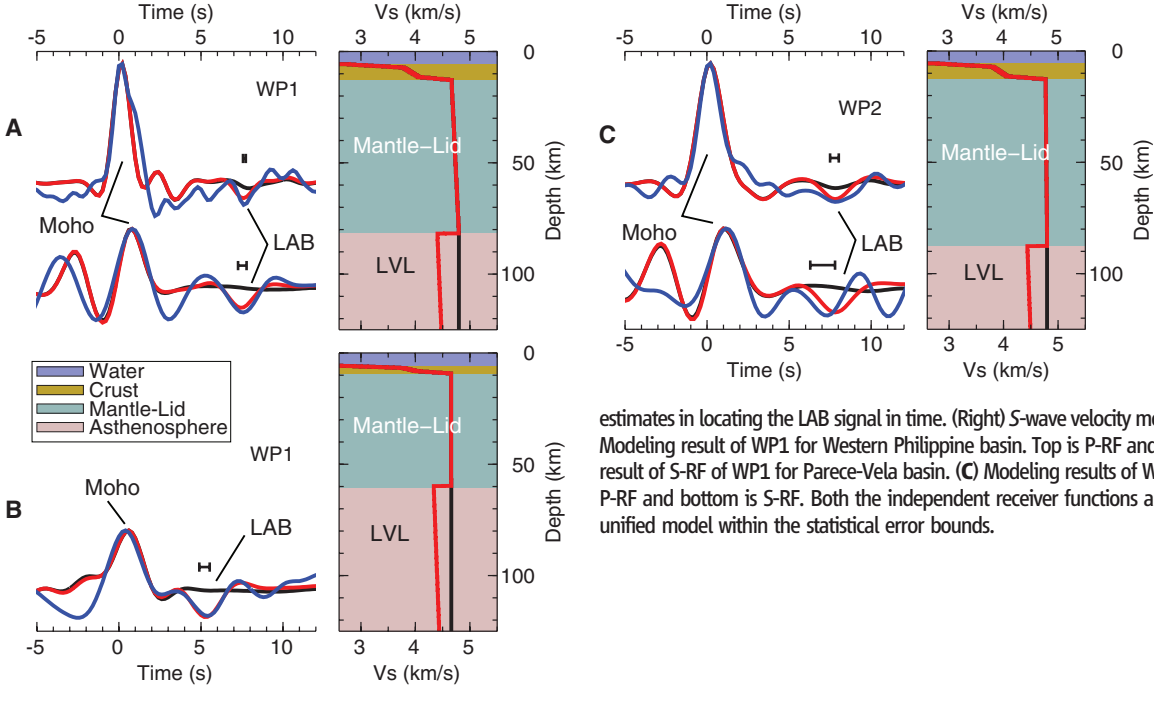

Fig. 3. Modeling of RFs for borehole seismological observatories. Blue lines indicate observed stacked receiver functions; black, the synthetic receiver functions for the model containing no low velocity layer (LVL); and red, synthetic receiver functions for the model shown on the right-hand graph with the same color. The horizontal lines just above the negative LAB phases are bootstrap error estimates in locating the LAB signal in time. (Right) *S*-wave velocity model used for synthetic RFs. (**A**) Modeling result of WP1 for Western Philippine basin. Top is P-RF and bottom is S-RF. (**B**) Modeling result of S-RF of WP1 for Parece-Vela basin. (**C**) Modeling results of WP2 for the Pacific plate. Top is P-RF and bottom is S-RF. Both the independent receiver functions are well matched with use of a unified model within the statistical error bounds.

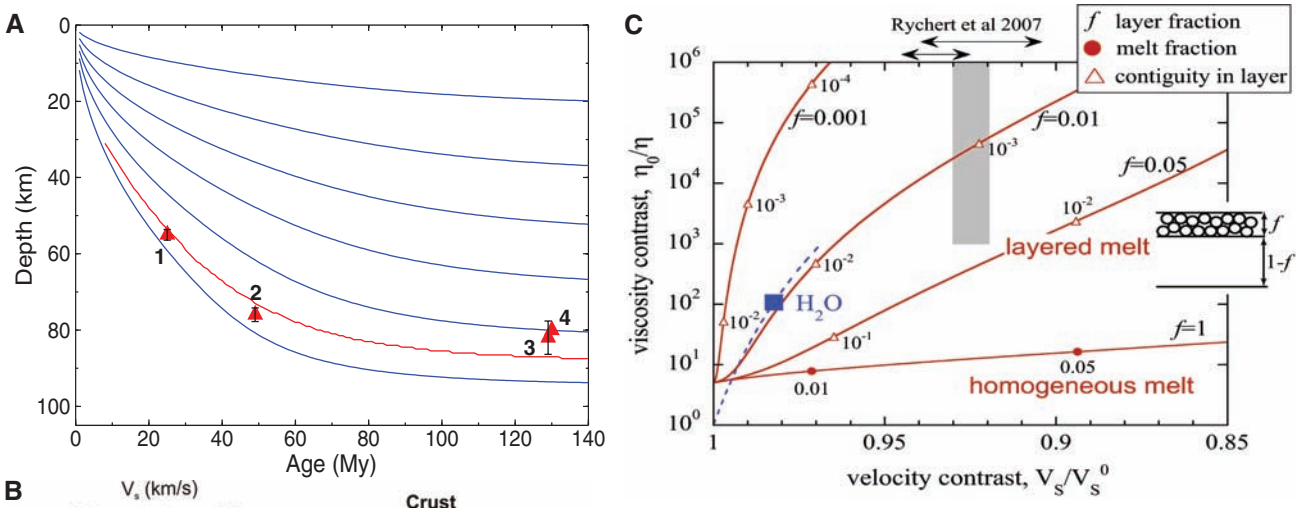

Fig. 4. Age dependence of observed LAB depths and a model for LAB and asthenosphere. (**A**) Observed LAB depths are plotted as a function of the plate age (red triangles; 1 indicates PVB; 2, WPB; 3, WP2; and 4, northeast Japan) over the isotherms given in a 200° intervals (blue lines) (*18*). Red line indicates the top of partial melting region calculated on the basis of the model of Mierdel *et al.* defined by the water solubility of 1000 parts per million H_2O (*16*). (**B**) A schematic illustration for the LAB and the asthenosphere. A schematic model for a *S*-wave seismic velocity structure of a radial anisotropy is superposed. (**C**) Viscosity (η) versus *S*-wave velocity (V_S) contrasts at LAB predicted from models of wet asthenosphere (bule) and partially molten asthenosphere (red), with seismological and geodynamical requirements (shaded) (*30*). Subscript 0 denotes lithospheric values. In the partially molten asthenosphere model, horizontal melt-rich layers are embedded in meltless mantle with various layer fractions from $f = 1$ (homogeneous) to $f = 0.001$. For $f = 1$ (homogeneous), melt has equilibrium geometry with variable melt fraction ϕ. For $f < 1$ (layered), ϕ in layers is close to the disaggregation melt fraction ϕ_c, and contiguity φ of grain-to-grain contact is small and variable [$\varphi = 1$ means melt-free and $\varphi = 0$ means disaggregation (*19*, *25*)]. Average ϕ in asthenosphere is given by $f\phi_c$.

age of subducting plate there is estimate to be ~130 My, the depth of 80 km for the LAB is consistent with that from the WP2 data.

The relative thickness of oceanic plates estimated above is consistent with the thermally controlled origin for the oceanic LAB (Fig. 4A), but the observation in short-period waves (~3 s) indicates that the LAB is a sharp boundary (the transition thickness of less than ~10 to 15 km) and thus has chemical or fabric origin. This apparent age dependence and the large LAB signal preclude the water-extraction model for the origin of oceanic LAB (*3*). One possibility to explain these features is partial melting in the asthenosphere. The depth of the initiation of the partial melting is estimated on the basis of the solubility of water in aluminous orthopyroxene component of mantle rocks (*16*–*18*). Although the fit is not perfect, this kind of model is capable of reproducing the basic trend in data (Fig. 4A).

Waveform modeling given in Fig. 3 indicates that the shear wave velocity is reduced at the LAB by ~7 to 8%. For a texturally equilibrated partially molten region, this translates into the melt fraction of ~3.5 to 4.0% (*19*), which is one order of magnitude larger than the commonly accepted amount of melt at mid-oceanic ridges (*20*) and may be unrealistically high. Therefore, some additional mechanism other than the conventional view of the partially molten asthenosphere is required.

Recent experimental and theoretical studies demonstrate that deformation can segregate melt into bands (*21*, *22*). On the basis of these results, we propose a model of partially molten asthenosphere consisting of horizontal melt-rich layers embedded in melt-less mantle (Fig. 4B). Such layered melt efficiently reduces vertically propagating shear wave velocities (*23*) and explains well the strong LAB signals reported here and elsewhere (*6*), as well as other properties expected for the asthenosphere. Figure 4C shows the velocity and viscosity contrasts at LAB predicted for a model of wet asthenosphere (blue), a conventional model of homogeneous partially molten asthenosphere (red line with layer fraction $f = 1$), and the present model of layered asthenosphere (red lines with $f < 1$). The strong seismological signals and a large viscosity contrast of $>10^3$ at LAB (*24*) can be explained quantitatively by the layered model, whereas the other two models cannot. The combination of both seismological and geodynamical constraints at the LAB (shaded) indicates that the melt-rich layers make up less than 5% by volume of the mantle here and that the melt fraction is close to the disaggregation melt fraction, ϕ_c, over which the partially molten rock loses grain-to-grain contacts (contiguity) and hence loses rigidity. Small but nonzero contiguity of the grains causing small rigidity of layers is important for the converted phases to be detectable. For $\phi_c = 0.25$ and $f = 0.05$ to 0.01, the average melt fraction in the asthenosphere is 1.25 to 0.25%, which is consistent with the petrological expectation (*20*). We describe the internal structure of the layers by grain-scale contiguity so that granular models developed recently to predict both elasticity and viscosity (*19*, *25*) can be applied. However, the obtained small rigidity of the layers might imply kinks and/or jogs, which may develop at much larger scales than grain size.

The layered model qualitatively explains other characteristics expected for the asthenosphere, such as radial anisotropy (transverse isotropy with a radial symmetry axis) inferred from long-period surface waves (*26*), high electrical conductivity (*27*), and high attenuation. The depth extent of this low-velocity asthenosphere is estimated to be ~210 km beneath WP2 on the basis of the travel-time analysis of WP2 data (*9*). Considering that LABs (*5*), the radial anisotropic layer (*28*), and the partially molten region (*16*) are all observed to be deeper (~200 km) beneath stable continents, the proposed model may be applicable to the continental asthenosphere to be an universal model for the asthenosphere.

References and Notes

1. B. Gutenberg, *Physics of the Earth's Interior* (Elsevier, New York, 1959).
2. H. Kanamori, F. Press, *Nature* **226**, 330 (1970).
3. S. Karato, H. Jung, *Earth Planet. Sci. Lett.* **157**, 193 (1998).
4. G. Hirth, D. Kohlstedt, *Earth Planet. Sci. Lett.* **144**, 93 (1996).
5. P. Kumar, X. Yuan, R. Kind, J. Ni, *J. Geophys. Res.* **111**, 10.1029/2005JB003930 (2006).
6. C. A. Rychert, K. M. Fischer, S. Rondenay, *Nature* **436**, 542 (2005).
7. Y. Fukao *et al.*, in *Workshop Report of OHP/ION Joint Symposium, Long-Term Observations in the Oceans* (Earthquake Research Institute, Univ. of Tokyo, Tokyo, Japan, 2001), pp. 13–29.
8. M. Shinohara *et al.*, *Ann. Geophys.* **49**, 625 (2006).
9. M. Shinohara *et al.*, *Phys. Earth Planet. Inter.* **170**, 95 (2008).
10. Materials and methods are available as supporting material on *Science* Online.
11. L. P. Vinnik, *Phys. Earth Planet. Inter.* **15**, 39 (1977).
12. C. A. Langston, *J. Geophys. Res.* **84**, 4749 (1979).
13. V. Farra, L. Vinnik, *Geophys. J. Int.* **141**, 699 (2000).
14. H. Kawakatsu, S. Watada, *Science* **316**, 1468 (2007).
15. T. Tonegawa, K. Hirahara, T. Shibutani, N. Fujii, *Earth Planet. Sci. Lett.* **247**, 101 (2006).
16. K. Mierdel, H. Keppler, J. R. Smyth, F. Langenhorst, *Science* **315**, 364 (2007).
17. S. Honda, D. A. Yuen, *Geophys. Res. Lett.* **28**, 351 (2001).
18. The thermal model is constructed incorporating the pressure and temperature effect on the thermal diffusivity; among the range of models that give similar fit to surface observables (*29*), one with the plate thickness of 104 km and the temperature at the base of plate 1358°C (corresponding to a potential temperature of 1315°C) is used.
19. Y. Takei, *J. Geophys. Res.* **107**, 10.1029/2001JB000522 (2002).
20. J. Langmuir, E. M. Klein, T. Plank, in *Mantle Flow and Melt Generation at Mid-Ocean Ridges* (American Geophysical Union, Washington, DC, 1992), pp. 183–200.
21. B. K. Holtzman *et al.*, *Science* **301**, 1227 (2003).
22. R. F. Katz, M. Spiegelman, B. Holtzman, *Nature* **442**, 676 (2006).
23. G. E. Backus, *J. Geophys. Res.* **67**, 4427 (1962).
24. M. Takaku, Y. Fukao, *Phys. Earth Planet. Inter.* **166**, 44 (2008).
25. Y. Takei, B. K. Holtzman, *J. Geophys. Res.*, in press.
26. G. Ekström, A. M. Dziewonski, *Nature* **394**, 168 (1998).
27. K. Baba, A. D. Chave, R. L. Evans, G. Hirth, R. L. Mackie, *J. Geophys. Res.* **111**, B02101 (2006).
28. Y. Gung, M. Panning, B. Romanowicz, *Nature* **422**, 707 (2003).
29. C. A. Stein, S. Stein, *Nature* **359**, 123 (1992).
30. In the wet asthenosphere model, the velocity contrast is estimated from the relation between η_0/η and V_S/V_S^0 (*3*) (blue dotted line) and $\eta_0/\eta \cong 100$ (*4*). In the partially molten asthenosphere model, viscosity of grain-boundary diffusion creep and elasticity are calculated for each layer by granular models (*19*, *25*), and effective properties of layered medium are calculated by the Backus average (*23*). In the layered model, η_0/η shows the contrast for horizontal shear flow, and V_S/V_S^0 shows the contrast of equivalent isotropic media, which give the same amplitude of *S*-to-*P* phase for the incident angle of 25° (typical for this study) (*10*).

31. B. Holtzman's drawing [figure 12 of (*25*)] was the inspiration for the proposed model of the melt-segregated shear zone in the asthenosphere. We thank S. Honda for the computer code to calculate the thermal structure and T. Inoue and K. Mibe for discussions. P.K. is supported by the JSPS fellowship provided by the Japan Society for the Promotion of Science. OHP was funded by the Ministry of Education, Culture, Sports, Science, and Technology of Japan.

Supporting Online Material

www.sciencemag.org/cgi/content/full/324/5926/499/DC1
Materials and Methods
Figs. S1 to S11
References

9 December 2008; accepted 26 February 2009
10.1126/science.1169499

Subducting Slab Ultra-Slow Velocity Layer Coincident with Silent Earthquakes in Southern Mexico

Teh-Ru Alex Song,[1]* Donald V. Helmberger,[2] Michael R. Brudzinski,[3] Robert W. Clayton,[2] Paul Davis,[4] Xyoli Pérez-Campos,[5] Shri K. Singh[5]

Great earthquakes have repeatedly occurred on the plate interface in a few shallow-dipping subduction zones where the subducting and overriding plates are strongly locked. Silent earthquakes (or slow slip events) were recently discovered at the down-dip extension of the locked zone and interact with the earthquake cycle. Here, we show that locally observed converted *SP* arrivals and teleseismic underside reflections that sample the top of the subducting plate in southern Mexico reveal that the ultra-slow velocity layer (USL) varies spatially (3 to 5 kilometers, with an *S*-wave velocity of ~2.0 to 2.7 kilometers per second). Most slow slip patches coincide with the presence of the USL, and they are bounded by the absence of the USL. The extent of the USL delineates the zone of transitional frictional behavior.

Silent earthquakes, or episodic slow slip events (SSEs), and nonvolcanic tremor have been observed in a few shallow subduction zones such as Cascadia (*1*–*3*), southwest Japan (*4*–*6*), and southern Mexico (*7*–*15*). In general, most slow slip and tremor activities take place at the transition zone down-dip of the strong coupling section, where great thrust earthquakes occur. In southern Mexico, the Cocos plate is subducting underneath the North America plate, where the slab is almost flat near Guerrero (*16*) and is at a low angle near Oaxaca (Fig. 1) (*17*). SSEs with moment magnitudes M_w of ~7 to 7.5 occur every 1 to 2 years (Fig. 1) (*7*–*11*, *18*, *19*). However, the locations of SSEs vary along-strike, extending about 150 km inland from the Guerrero coast (*7*–*10*, *18*) but are limited to within 100 km near Oaxaca (Fig. 1) (*11*, *15*). In addition, nonvolcanic tremor (NVT) concentrates near the down-dip end of the slow-slip zone (*12*–*14*). This along-strike variation in the location of SSEs and NVT can be compared with the seismic structure of the subducting plate to investigate if the location variation is structurally controlled. We examined locally converted *SP* waves from intraslab earthquakes to map out the seismic structure at the top of the subducting slab beneath southern Mexico (*20*).

SP waves start as shear waves radiated from intraslab earthquakes and convert to *P* waves at the sharp velocity contrast on the plate interface. They are particularly useful for examining a slab structure directly above the source (Fig. 2A) (*21*). The *SP* wave typically arrives 2 to 3 s after the direct *P* wave, depending on the depth of an earthquake (*20*). In this study, we model the first 7 s of the broadband *P* waveforms (0.01 to 0.6 Hz) to explain the interference between the direct *P* wave and the *SP* wave, which ultimately provides a high-resolution map of the upper slab structure (*20*). Our data include two moderate intraslab events recorded by the temporary Meso-American Subduction Experiment (MASE) (*17*) and 40 intraslab events from 1990 to 2008 [body wave magnitude (M_b) = 4.5 ~ 6.0] recorded by the permanent GEOSCOPE station UNM (Fig. 1 and fig. S1).

As an example, we display *P* waveforms recorded at station PTRP and station SAME farther to the north to illustrate how the waveform changes with position (Fig. 2B). The timing of the first negative pulse (pulse A) after the direct *P* wave is consistent with an *SP* arrival, but its amplitude is anomalously large at station PTRP. We can model the *SP* wave that was converted from the bottom of an ultra-slow velocity layer [USL; 3 km and a *S*-wave velocity (V_s) of ~2.7 km/s] directly above the source region. The pulse with a positive polarity (pulse B) immediately following the pulse A is an *SP* arrival converted from the top of the USL. A series of

[1]Department of Terrestrial Magnetism, Carnegie Institution of Washington, 5241 Broad Branch Road N.W., Washington, DC 20015, USA. [2]Seismological Laboratory, Division of Geological and Planetary Science, California Institute of Technology, 1200 East California Boulevard, Pasadena, CA 91125, USA. [3]Department of Geology, Miami University, 114 Shideler Hall, Oxford, OH 45056, USA. [4]Department of Earth and Space Sciences, Center of Embedded Network Systems (CENS), University of California, Los Angeles (UCLA), 595 Charles Young Drive East, Los Angeles, CA 90095–1567, USA. [5]Instituto de Geofísica, Universidad Nacional Autónoma de México, Circuito de la Investigación Científica s/n, Ciudad Universitaria, D.F. 04510 Distrito Federal, México.

*To whom correspondence should be addressed. E-mail: asong@ciw.edu

synthetic tests demonstrate that the amplitude of pulse A and pulse B and their relative timing are primarily determined by the *S* wave velocity and the thickness of the USL (fig. S2). However, the interpretation of the pulse C, which arrived about 1.5 s after the direct *P* wave, is less obvious (Fig. 2B). Synthetic tests demonstrate that introducing a low velocity layer [LVL; 22 km and a *P*-wave velocity (V_p) of ~7.5 km/s] directly below the USL can reproduce a turning *P* wave from the bottom of the LVL with correct timing and amplitude (Fig. 2B). The amplitude of the pulse C increases with the velocity contrast between the LVL and the underlying fast slab, whereas its timing is controlled by the separation between the source and the lower boundary of the LVL (fig. S2). In this report, we focus on the USL and its lateral variation.

About 30 events were recorded by station UNM that display waveforms similar to those recorded by station PTRP above (Fig. 1), demonstrating a similar slab structure above the various sources. We can reproduce the characteristics of these waveforms and their variability by moving the source location to match the differential behavior between the *P* wave and converted *SP* arrival (fig. S3). Our best-fitting model consists of a thin USL of ~3 to 5 km and shear velocity of about 2.0 to 2.7 km/s. The contrast in *S* wave velocity across the bottom of the USL is about 26 to 40%. In general, the data are well-explained (Fig. 1 and figs. S4 to S5).

Broadband waveforms from the other 13 events are similar [Fig. 1, black waveforms (far right) and white circles] but have much smaller *SP* arrivals. These data do not require the prominent USL described above (fig. S6). However, the amplitude of *SP* arrivals, particularly for pulse A, from events such as 13 and 21 are smaller than that of the 28 events but slightly larger than that of other events near Oaxaca. These data suggest that seismic velocity near the top of the slab varies both parallel and normal to the trench (Fig. 1). Cases without the USL are all farther inland than cases with the USL. Furthermore, the MASE data from an event located beneath west Guerrero display a systematic decrease in *SP* amplitude toward the north (Fig. 1, top left inset) over distances of <10 km. On the basis of these observations, it is clear that the USL is confined to within 150 km of the coast in Guerrero. Data from events such as 1, 2, 4, 5, and 7 near Oaxaca do not reveal the USL, suggesting that it extends probably no more than 100 km from the coast near Oaxaca.

If the spatial variation in the presence of the USL is reasonably constrained by the local *SP* arrival, our model should be able to explain other independent data from these same events. In particular, by stacking teleseismic *P* waves recorded by the Yellowknife array, we can identify the depth phases such as *pP* and *sP* (Fig. 3A and fig. S7). The prominence of the depth phase *sP* is favorable to further search for the underside reflection ($s_{USL}P$) from the USL (Fig. 3B). Indeed, an additional strong phase arrived about 3.5 to 4 s after the first *P* wave of event 27. Its timing and amplitude are consistent with the $s_{USL}P$ from the USL. Variations

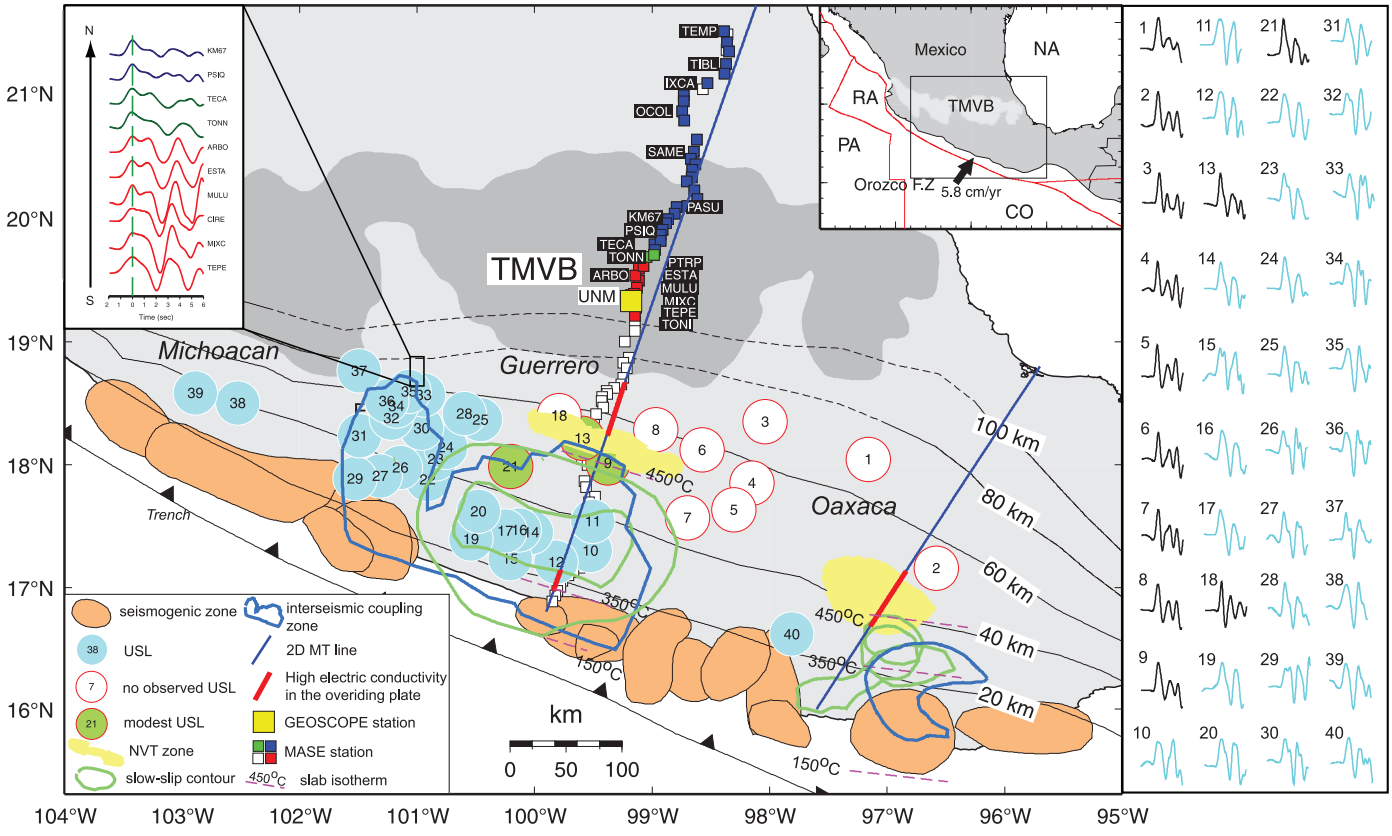

Fig. 1. Mapping of the USL beneath southern Mexico. The top right inset shows the regional tectonic setting where the Cocos plate (CO) is subducting beneath the North America plate (NA). RA, Rivera plate; PA, Pacific plate. The red line delineates the plate boundary. The enlarged map shows geophysical observables and seismic sampling. Shown is the nearly flat portion of the slab beneath the Guerrero province (*16*). *P* wave displacement data (0.01 to 0.6 Hz) recorded on the vertical component of the GEOSCOPE station UNM are displayed on the far right. Data associated with blue circles (blue traces) are characterized by a large converted *SP* wave arriving about 2 to 3 s after the first *P* wave, whereas data associated with white circles (black traces) are without such a strong negative pulse. Data associated with light green circles are with a converted *SP* arrival but are less strong. The spatial extent of the USL (blue circles) coincides with the location of large slow slip patches (green contours) and interseismic coupling (blue contours) (*18*). NVT occurs along the transition from blue circles to white circles where electric resistivity is relatively high (~ 200 ohm m) in the overriding plate (indicated by the red segments in the two-dimensional magnetotelluric lines (dark blue lines across Guerrero and Oaxaca) (*26*). Abrupt decrease in the amplitude of the *SP* arrival from stations ARBO to PSIQ (top left panel) also indicates the north limit of the USL (solid rectangle).

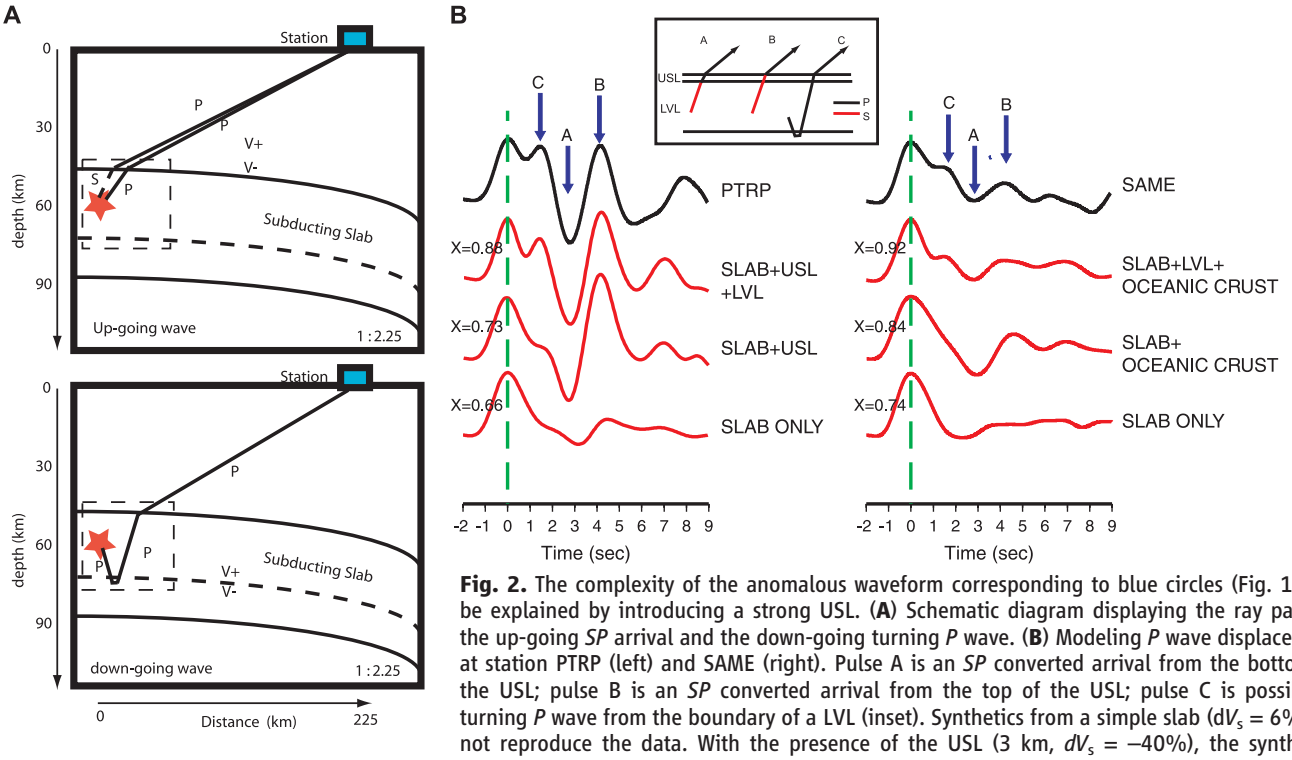

Fig. 2. The complexity of the anomalous waveform corresponding to blue circles (Fig. 1) can be explained by introducing a strong USL. (**A**) Schematic diagram displaying the ray path of the up-going *SP* arrival and the down-going turning *P* wave. (**B**) Modeling *P* wave displacement at station PTRP (left) and SAME (right). Pulse A is an *SP* converted arrival from the bottom of the USL; pulse B is an *SP* converted arrival from the top of the USL; pulse C is possibly a turning *P* wave from the boundary of a LVL (inset). Synthetics from a simple slab (dV_s = 6%) do not reproduce the data. With the presence of the USL (3 km, dV_s = −40%), the synthetics explain the pulse A and pulse B at station PTRP. But data recorded at station SAME to the north do not require the USL, and we can model it as a hydrated oceanic crust with dV_s = −20%. We assume $d\ln V_s/d\ln V_p$ = 2 in the USL and LVL. *X* is the coefficient of cross-correlation between data and synthetics.

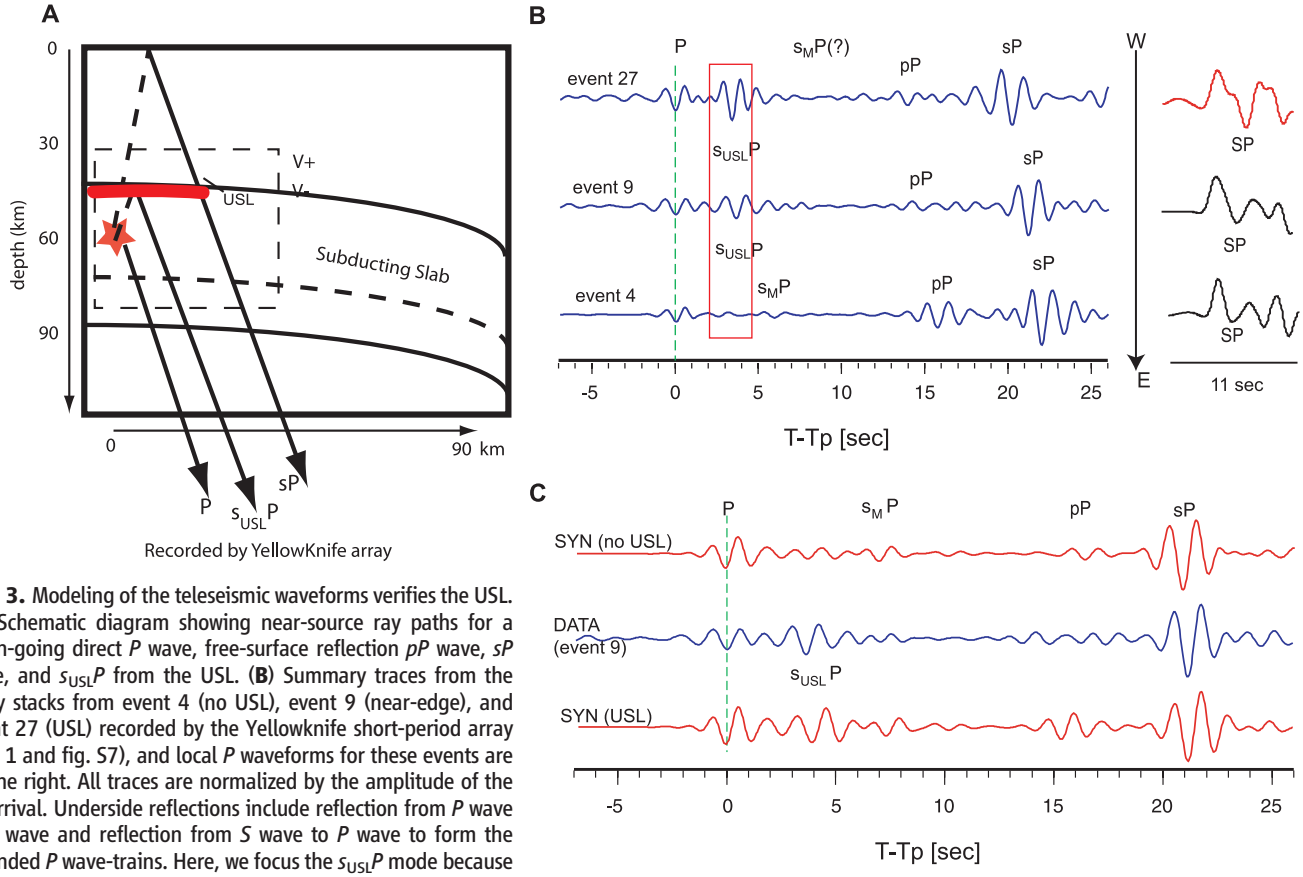

Fig. 3. Modeling of the teleseismic waveforms verifies the USL. (**A**) Schematic diagram showing near-source ray paths for a down-going direct *P* wave, free-surface reflection *pP* wave, *sP* wave, and $s_{USL}P$ from the USL. (**B**) Summary traces from the array stacks from event 4 (no USL), event 9 (near-edge), and event 27 (USL) recorded by the Yellowknife short-period array (Fig. 1 and fig. S7), and local *P* waveforms for these events are on the right. All traces are normalized by the amplitude of the *sP* arrival. Underside reflections include reflection from *P* wave to *P* wave and reflection from *S* wave to *P* wave to form the extended *P* wave-trains. Here, we focus the $s_{USL}P$ mode because of its large amplitude. s_MP is the underside reflection from the continental Moho arriving 7 to 9 s after the *P* wave, but it is not prominent. Data from event 27 beneath west Guerrero show the largest $s_{USL}P$ relative to *sP*, whereas the amplitude of the $s_{USL}P$ decreases toward the east. This observation is consistent with the amplitude of the local *SP* wave. (**C**) Predictions match the amplitude of the $s_{USL}P$ from event 9 when the USL has half the velocity reduction needed to model event 27. Synthetics computed from the model without the USL explain the data from event 4.

in the amplitude of the teleseismic $s_{USL}P$ are consistent with the amplitude of the local converted *SP* wave from the same intraslab events (Fig. 3B). Our model, which was derived from modeling local converted *SP* waves, can reasonably predict these teleseismic $s_{USL}P$, their along-strike variations, and teleseismic $s_{USL}S$ (Fig. 3C and fig. S8). Moreover, teleseismic receiver function analysis directly beneath the MASE line (*16*) also reveals strong evidence of an uneven but continuous LVL extending to the southern end of the Trans-Mexican Volcanic Belt (TMVB) and is generally consistent with the USL sampled by the regional *SP* waves near the array. A relatively weak receiver function pulse from 130 to 170 km from the coast (*16*) is also consistent with weaker *SP* waves (Fig. 1, green circles). Complexities do exist near event 13, possibly because of lateral variations in the down-dip extent of the USL near the MASE array.

The *S*-wave velocity of the USL (2.0 to 2.7 km/s) is 30 to 54% slower than that of the hydrated ocean crust at the depth of 25 to 50 km, which is typically in the 3.8 to 4.4 km/s range (*22*). The *S* wave velocity across the bottom of the USL (~26 to 40%) also exceeds the velocity contrast predicted for hydrated oceanic crust and oceanic mantle (*22*). Although partial melting of oceanic crust can drastically decrease *S* wave velocity, thermal modeling of the slab (*23*, *24*) suggested that temperatures probably are too low. Alternatively, the USL may represent the oceanic crust (or part of the oceanic crust) that is fluid-saturated, forming a high pore-fluid pressure layer (HPFP) with a porosity (ϕ) of ~2 to 3.5% and aspect ratio α of ~0.01 (*25*). These estimates are consistent with local electric resistivity of ~200 ohm m in the overriding plate that was obtained from magnetotelluric studies in southern Mexico (*26*).

We find that the spatial extent of the HPFP layer coincides well with the region close to the coast near Guerrero, where slow slip is well documented and the sampling of the slab is denser. Both seem to be located in a region bounded by the 350 and 450°C isotherms predicted for the plate interface (*23*, *24*), where there is interseismic coupling (*7*, *15*, *18*). The HPFP layer could potentially extend farther up-dip than observed before the plate interface reaches temperatures of >350°C. Most NVT locations are concentrated in the upper plate north of where the prominent HPFP layer occurs at the plate interface and where electric conductivity in the upper plate is relatively high (Fig. 1). Although the sampling of the slab near Oaxaca is sparse, we find similar relations there, supporting a direct spatial correlation of the HPFP layer and SSEs with NVT and high conductivity again to the north. Examining all of the events between 99°W and 102°W with evidence for the USL (Fig. 1), events 35, 37, 22, and 34 clearly show the HPFP layer is present during the SSEs (Fig. 1 and fig. S9). Although these events primarily occur west of the slow slip contour in Fig. 1, the western extent of slow slip is not well known. Furthermore, the HPFP layer also exists during the inter-SSE period (fig. S9), indicating that the HPFP layer is persistent over at least the 20 years of our data.

Our interpretation (Fig. 4) is that a transition zone at shallow depths on the plate interface lies below the region where interseismic coupling is strong. It is partially coupled during the interseismic period, resulting in episodic slow slip at the down-dip end of the seismogenic zone at regions with temperatures ranging from 350 to 450°C (*24*). NVT sources concentrate near the down-dip end of the transition zone around 450°C, where blueschist-eclogite dehydration reactions are predicted to occur at depths near 40 to 50 km (*22*). Fluid released from this reaction could percolate into the overriding plate, produce observed high electric conductivity, and probably trigger the NVT. Fluids appear to be trapped up-dip in a HPFP layer and it is probably controlled by material-dependent permeability and fluid generation processes near the interface (*20*). The spatial extent of the HPFP layer provides a natural explanation for the occurrence of SSEs and NVT because it would be expected to greatly reduce the effective normal stress on the plate interface, promoting episodic slow slip (*27*) and the dynamic triggering of tremors (*28*).

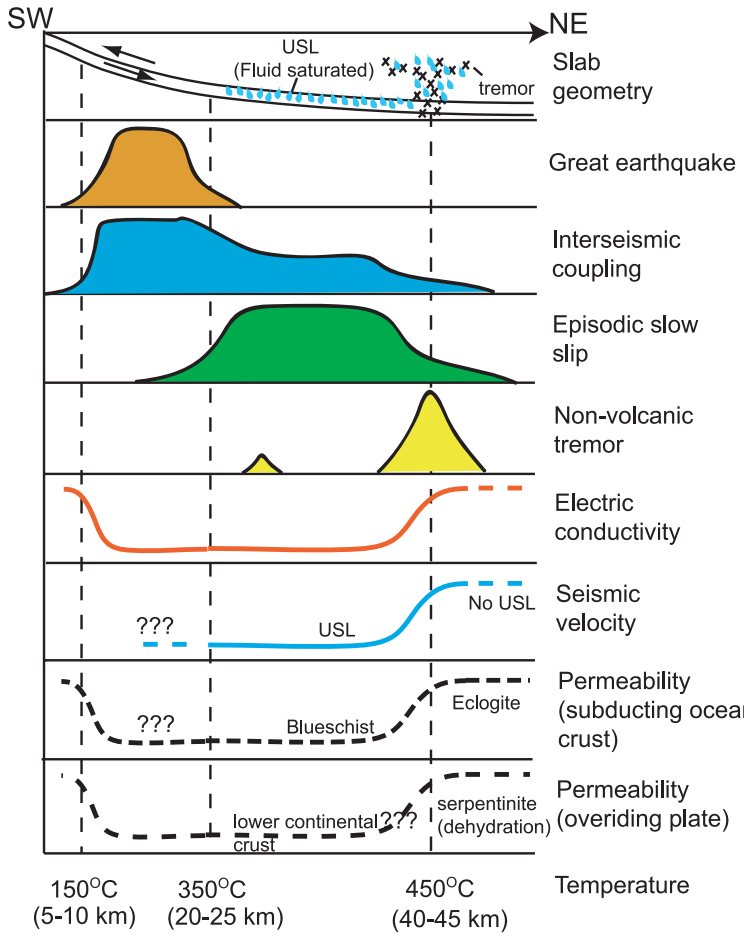

Fig. 4. A schematic cross section of the slab geometry along with observations that were used to make the interpretation. Dotted lines indicate the slab isotherm. The various panels include variations in the location of great earthquakes, interseismic coupling, SSEs, NVT, electric conductivity, seismic velocity, and inferred permeability (*20*). Blue drops indicate the presence of fluids, and x's indicate NVT cavities.

References and Notes

1. H. Dragert, K. Wang, T. S. James, *Science* **292**, 1525 (2001).
2. G. Rogers, H. Dragert, *Science* **300**, 1942 (2003).
3. H. Kao *et al.*, *Nature* **436**, 841 (2005).
4. K. Obara, *Science* **296**, 1679 (2002).
5. S. Zawa *et al.*, *Geophys. Res. Lett.* **31**, 10.1029/2003GL019381 (2004).
6. D. R. Shelly, G. C. Beroza, S. Ide, S. Nakamula, *Nature* **442**, 188 (2006).
7. V. Kostoglodov *et al.*, *Geophys. Res. Lett.* **30**, 10.1029/2003GL017219 (2003).
8. K. M. Larson *et al.*, *J. Geophys. Res.* **109**, 10.1029/2003JB002843 (2004).
9. A. R. Lowry, *Nature* **442**, 802 (2006).
10. K. M. Larson, V. Kostoglodov, S. Miyazaki, J. A. Santiago, J. A. *Geophys. Res. Lett.* **34**, 10.1029/2007GL029912 (2007).
11. M. Brudzinski, E. Cabral-Cano, F. Correa-Mora, C. DeMets, B. Márquez-Azúa, *Geophys. J. Int.* **171**, 523 (2007).
12. M. Brudzinski, E. Cabral-Cano, A. Arciniega-Ceballos, C. DeMets, O. Diaz-Molina, *Eos Trans. AGU* **88**(23), abstract G31A-02 (2007).
13. H. R. Hinojosa-Prieto *et al.*, *EOS Trans. AGU* **88**, abstract T21A-0350 (2007).

14. J. S. Payero *et al.*, *Geophys. Res. Lett.* **35**, 10.1029/2007GL032877 (2008).
15. F. Correa-Mora, C. DeMets, E. Cabral-Cano, B. Marquez-Azua, O. Diaz-Molina, *Geophys. J. Int.* **175**, 269 (2008).
16. X. Perez-Campos *et al.*, *Geophys. Res. Lett.* **35**, 10.1029/2008GL035127 (2008).
17. M. Pardo, G. Suárez, *J. Geophys. Res.* **100**, 12357 (1995).
18. S. Yoshioka *et al.*, *Phys. Earth Planet Inter.* **146**, 513 (2004).
19. A. Iglesias *et al.*, *Geofis. Int.* **43**, 309 (2004).
20. Materials and methods are available as supporting material on *Science* Online.
21. T. Matsuzawa, T. Kono, A. Hasegawa, A. Takagi, *Tectonophysics* **181**, 123 (1990).
22. B. R. Hacker, G. A. Abers, S. M. Peacock, *J. Geophys. Res.* **108**, 10.1029/2001JB001127 (2003).
23. V. Manea, M. Manea, V. Kostoglodov, C. A. Currie, G. Sewell, *Geophys. J. Int.* **158**, 775 (2004).
24. C. A. Currie, R. D. Hyndman, K. Wang, V. Kostoglodov, *J. Geophys. Res.* **107**, 10.1029/2001JB000886 (2002).
25. Y. Takei, *J. Geophys. Res.* **107**, 10.1029/2001JB000522 (2002).
26. H. Jödicke *et al.*, *J. Geophys. Res.* **111**, 10.1029/2005JB003739 (2006).
27. Y. Liu, J. R. Rice, *J. Geophys. Res.* **112**, 10.1029/2007JB004930 (2007).
28. J. L. Rubinstein *et al.*, *Nature* **448**, 579 (2007).
29. We thank S. Sacks, P. Silver, S. Shirey, M. Bostock, J.-P. Avouav, and V. Manea for helpful discussions; R. Engdahl provided the global relocated seismic catalog used in fig. S10. We thank CENS at UCLA for support and the entire MASE team for making the MASE data available. We thank H. Hinojosa-Prieto, E. Cabral-Cano, A. Arciniega, O. Diaz-Molina, and C. DeMets for sharing their work on episodic tremor and slip in Oaxaca. Incorporated Research Institutions for Seismology Data Management Center and Canadian National Data Centre provided the GEOSCOPE data and Yellowknife short-period data used in this analysis, respectively. Station UNM is operated and maintained by Servicio Sismológical Nacional. This work is partially supported by NSF grant EAR-0636012. This is Tectonic Observatory contribution 10015. T.-R.A.S. is supported by a Carnegie fellowship at the Department of Terrestrial Magnetism.

Supporting Online Material

www.sciencemag.org/cgi/content/full/324/5926/502/DC1
Materials and Methods
SOM Text
Figs. S1 to S11
Table S1
References

23 October 2008; accepted 20 February 2009
10.1126/science.1167595

$^{14}CH_4$ Measurements in Greenland Ice: Investigating Last Glacial Termination CH_4 Sources

Vasilii V. Petrenko,[1]*† Andrew M. Smith,[2] Edward J. Brook,[3] Dave Lowe,[4] Katja Riedel,[4] Gordon Brailsford,[4] Quan Hua,[2] Hinrich Schaefer,[4] Niels Reeh,[5] Ray F. Weiss,[1] David Etheridge,[6] Jeffrey P. Severinghaus[1]

The cause of a large increase of atmospheric methane concentration during the Younger Dryas–Preboreal abrupt climatic transition (~11,600 years ago) has been the subject of much debate. The carbon-14 (^{14}C) content of methane ($^{14}CH_4$) should distinguish between wetland and clathrate contributions to this increase. We present measurements of $^{14}CH_4$ in glacial ice, targeting this transition, performed by using ice samples obtained from an ablation site in west Greenland. Measured $^{14}CH_4$ values were higher than predicted under any scenario. Sample $^{14}CH_4$ appears to be elevated by direct cosmogenic ^{14}C production in ice. ^{14}C of CO was measured to better understand this process and correct the sample $^{14}CH_4$. Corrected results suggest that wetland sources were likely responsible for the majority of the Younger Dryas–Preboreal CH_4 rise.

Ice core records from Greenland and Antarctica show large and rapid variations in atmospheric methane (CH_4) concentrations ([CH_4]) in response to climate change (*1*). One such rapid [CH_4] increase occurred at the Younger Dryas (YD)–Preboreal (PB) [~11,600 years before present (B.P.), in which 0 B.P. = 1950 A.D.] abrupt warming event during the last deglaciation (Fig. 1). The causes of these rapid [CH_4] fluctuations have been the subject of intense debate. Several modeling studies suggest that glacial-interglacial changes in the atmospheric concentration of OH radicals (the main CH_4 sink) were small (*2*, *3*). It is thus likely that the observed rapid [CH_4] increases were driven mostly by increases in CH_4 sources.

Several hypotheses regarding such sources have been proposed, including increased emissions from wetlands (*4*), marine clathrates (*5*, *6*), and, more recently, thermokarst lakes (*7*). The possibility of CH_4 clathrate reservoir instability in response to climatic warming is particularly troubling in the light of present anthropogenic warming. If only 10% of CH_4 from the modern clathrate reservoir (which has ~5000 Pg of C) were to be released to the atmosphere in a few years, the radiative forcing would be equivalent to a 10-fold increase in [CO_2] (*8*).

In an attempt to better understand past changes in the CH_4 budget, two records of carbon-13/carbon-12 ratio ($\delta^{13}C$) (*9*, *10*) and one record of deuterium/hydrogen ratio (δD) (*11*) of CH_4 from ice cores spanning the last glacial termination have recently been produced. Unfortunately, $\delta^{13}CH_4$ of many major CH_4 sources is similar (*12*), imperfectly known (*13*), and influenced by climatic conditions (*14*), limiting the utility of $\delta^{13}CH_4$ for testing different hypotheses for the rapid [CH_4] increases. δD of CH_4 is a more promising tracer for this purpose, because the δD of clathrate CH_4 is much higher than that of wetland emissions (*11*). The Greenland Ice Sheet Project 2 (GISP2) ice core record (Fig. 1) showed no significant change in δD of CH_4 through the YD-PB transition, which is evidence against major clathrate involvement (*11*).

The best tracer for distinguishing between the clathrate and wetland hypotheses is arguably $^{14}CH_4$. The ultimate source of C for wetland-produced CH_4 is essentially contemporaneous atmospheric CO_2 (*15*). If wetlands were the only source of the rapid [CH_4] rise, there should be either no change or an increase in $^{14}CH_4$ after the abrupt warming event. In contrast, CH_4 clathrates are geologically old and contain little or no measurable ^{14}C (*16*). If clathrates were the only source of the [CH_4] rise, $^{14}CH_4$ over the transition would decrease (Fig. 1). In addition, paleoatmospheric $^{14}CH_4$ measurements should allow for straightforward quantification of the strength of the geologic CH_4 source, which may be an important term in the global CH_4 budget (*17*).

We used a surface outcrop named Pakitsoq on the west Greenland ice margin (*18*–*20*) to obtain ~1000-kg-sized glacial ice samples containing ancient air from the YD-PB transition and yielding ~ 20 μg of CH_4 carbon per sample for ^{14}C measurements. Air was melt-extracted from sample ice in the field (*20*, *21*). We dated the sampled ice and occluded air using a combination of $\delta^{15}N$ of N_2, $\delta^{18}O$ of O_2, $\delta^{18}O$ of ice ($\delta^{18}O_{ice}$), and [CH_4] measurements (*21*), which uniquely identified the age of the sampled section. Sample CH_4 was separated from bulk air by means of combustion to CO_2 on platinized quartz wool followed by cryogenic trapping (*20*, *22*). CH_4-derived CO_2 was converted to graphite and measured for ^{14}C by means of accelerator mass spectrometry (*20*, *22*).

$^{14}CH_4$ results are presented in Fig. 1 and table S1. Surprisingly, all values are higher than ^{14}C of contemporaneous CO_2; that is, above the highest expected paleoatmospheric $^{14}CH_4$. Procedural ^{14}C contamination was shown through extensive testing to be very small (<3% of sample

[1]Scripps Institution of Oceanography, University of California, San Diego, La Jolla, CA 92093, USA. [2]Australian Nuclear Science and Technology Organisation (ANSTO), Private Mail Box 1, Menai, NSW 2234, Australia. [3]Department of Geosciences, Oregon State University, Corvallis, OR 97331, USA. [4]National Institute of Water and Atmospheric Research Ltd., Post Office Box 14901, Kilbirnie, 301 Evans Bay Parade, Wellington, New Zealand. [5]DTU Space, National Space Institute, Technical University of Denmark, Ørsteds Plads, Building 348, DK-2800 Kongens Lyngby, Denmark. [6]Commonwealth Scientific and Industrial Research Organisation, Marine and Atmospheric Research, Private Mail Box 1, Aspendale, VIC 3195, Australia.

*Present address: Institute of Arctic and Alpine Research, University of Colorado, Boulder, CO 80309, USA.
†To whom correspondence should be addressed. E-mail: vasilii.petrenko@colorado.edu

^{14}C content) and has been corrected for (*22*). Therefore, at least one other mechanism must exist that elevates $^{14}CH_4$ in Pakitsoq ice.

$[CH_4]$ in Pakitsoq samples from the YD-PB transition agrees within uncertainties with expected values based on the GISP2 $[CH_4]$ record (table S1) (*21*). The mechanism that elevates sample $^{14}CH_4$ must therefore do so without significantly affecting sample $[CH_4]$. We carefully considered the following possibilities (*20*): (i) biological CH_4 production from CO_2 or methylphosphonate in the ice [ruled out because the substrate ^{14}C is insufficiently high (table S3)], (ii) cosmogenic $^{14}CH_4$ production in the deglacial atmosphere (ruled out for not having been observed today), (iii) addition of ^{14}C from ^{14}C-rich CO during sample air processing (ruled out through testing), (iv) CH_4 production from ^{14}C-rich CO during air extraction from ice (an unlikely reaction under extraction conditions), and (v) biological CH_4 production directly from ^{14}C-rich CO in the ice (unlikely because it is an unknown reaction pathway with an insufficient ^{14}C yield). We found that the only feasible mechanism is in situ cosmogenic production of $^{14}CH_4$ molecules in the ice.

Cosmogenic production of ^{14}C in glacial ice by way of neutron-induced spallation of ^{16}O atoms is well known, although all of the produced ^{14}C has been thought to form ^{14}CO or $^{14}CO_2$ (*23*). However, laboratory experiments in which water or ice were subjected to intensive irradiation by protons to produce hot ^{11}C atoms or by energetic $^{14}C^+$ or $^{14}CO^+$ beams found that a small fraction of the hot C atoms formed CH_4; other simple organics were also formed (*24*, *25*). This suggests the hypothesis that a small amount of $^{14}CH_4$ is also formed in natural ice via hot-atom chemistry after the nuclear reactions.

To better understand cosmogenic ^{14}C production in Pakitsoq ice, we measured ^{14}C of CO in remaining sample air (*20*). We found values in the range of 2 to 9 ^{14}CO molecules per gram of ice from cosmogenic production for most samples (table S4). Although considerable uncertainties exist regarding cosmogenic ^{14}CO production rates in ice, our results agree well with theoretical calculations of ablation-zone cosmogenic ^{14}CO production at Pakitsoq (*20*). We therefore applied a correction to sample $^{14}CH_4$ to account for cosmogenic production in the ablation zone (*20*). The correction uses a model to predict the total amount of cosmogenic ^{14}C produced in the ablation zone for each sample, which depends mainly on sample depth below the surface. The correction also assumes that the fraction of cosmogenic ^{14}C that forms $^{14}CH_4$ is the same for all samples. This allows for precise estimates of the ratios of cosmogenic $^{14}CH_4$ content between different samples (the uncertain parameters in the model affect the absolute values but not the ratios). The absolute magnitude of this correction is then adjusted so that the corrected $^{14}CH_4$ value for the YD sample average falls on the wetland/clathrate hypothesis line in Fig. 1. Individual corrected absolute $^{14}CH_4$ values are thus meaningless, but this approach allows meaningful comparisons between samples.

Although the applied correction represents the most likely scenario according to available evidence, it is imperfectly understood and therefore somewhat speculative. Corrected $^{14}CH_4$ values within each pair of replicate samples are still in agreement within ^{14}C measurement uncertainties [for age-corrected $\Delta^{14}C$ values, the average offset between replicates is 38 per mil (‰) versus an average measurement uncertainty of 44‰ (table S1)]. This is consistent

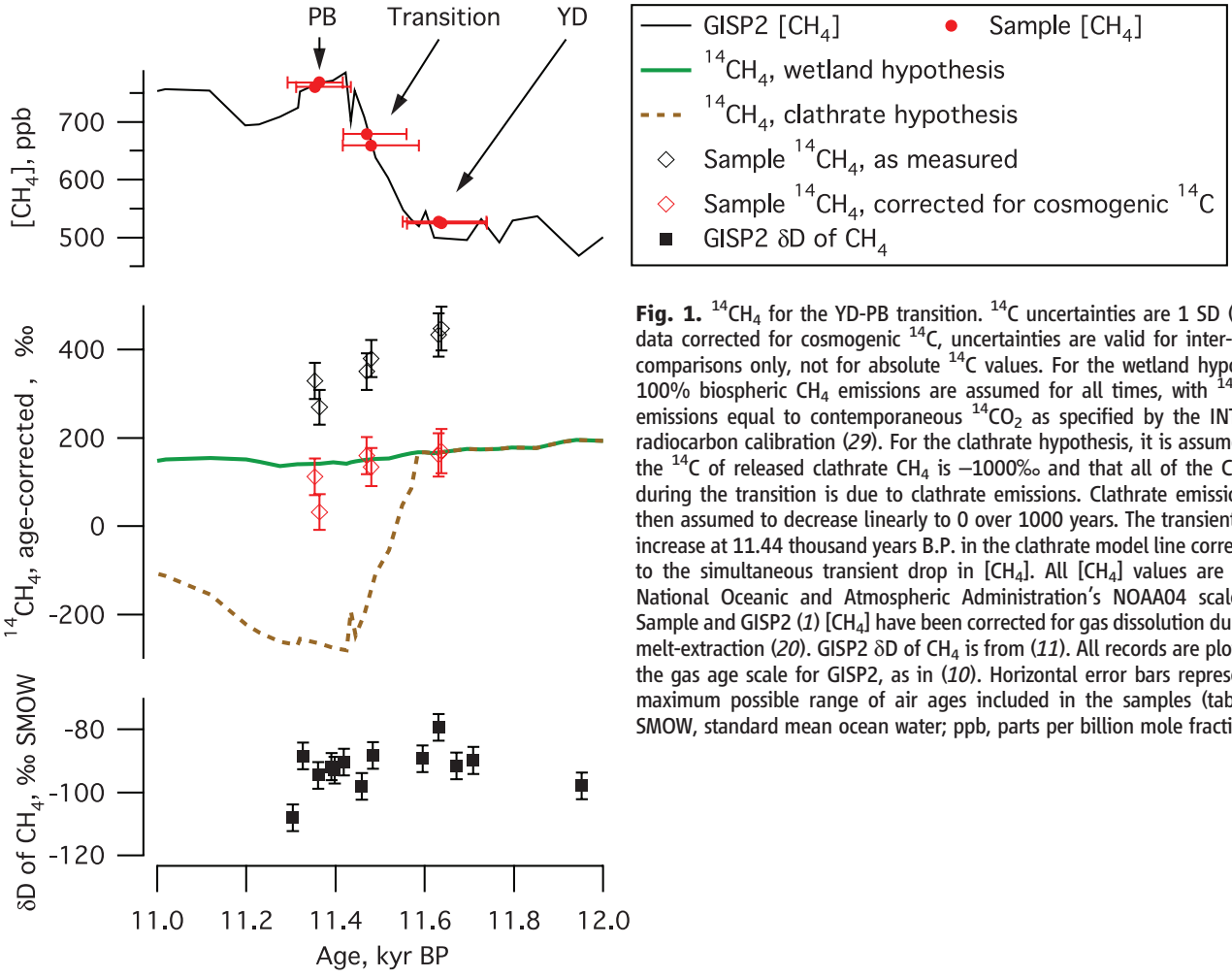

Fig. 1. $^{14}CH_4$ for the YD-PB transition. ^{14}C uncertainties are 1 SD (σ). For data corrected for cosmogenic ^{14}C, uncertainties are valid for inter-sample comparisons only, not for absolute ^{14}C values. For the wetland hypothesis, 100% biospheric CH_4 emissions are assumed for all times, with $^{14}CH_4$ of emissions equal to contemporaneous $^{14}CO_2$ as specified by the INTCAL04 radiocarbon calibration (*29*). For the clathrate hypothesis, it is assumed that the ^{14}C of released clathrate CH_4 is −1000‰ and that all of the CH_4 rise during the transition is due to clathrate emissions. Clathrate emissions are then assumed to decrease linearly to 0 over 1000 years. The transient $^{14}CH_4$ increase at 11.44 thousand years B.P. in the clathrate model line corresponds to the simultaneous transient drop in $[CH_4]$. All $[CH_4]$ values are on the National Oceanic and Atmospheric Administration's NOAA04 scale (*30*). Sample and GISP2 (*1*) $[CH_4]$ have been corrected for gas dissolution during air melt-extraction (*20*). GISP2 δD of CH_4 is from (*11*). All records are plotted on the gas age scale for GISP2, as in (*10*). Horizontal error bars represent the maximum possible range of air ages included in the samples (table S1). SMOW, standard mean ocean water; ppb, parts per billion mole fraction.

with the applied corrections accurately representing the real processes that elevated sample $^{14}CH_4$.

Corrected $^{14}CH_4$ results with their propagated uncertainties are presented in Fig. 1 and table S1. For the assessment of possible clathrate contribution to the [CH_4] increase, it is useful to consider the changes in $^{14}CH_4$ during the YD-PB transition in terms of the implied changes in the strength of the fossil (^{14}C-free) CH_4 source (ΔQ_{fossil}) (Table 1). The calculation of ΔQ_{fossil} is dependent on the initial Q_{fossil} value assumed for the YD. The corrected results presented in Fig. 1 assumed a Q_{fossil} of zero for YD for simplicity. However, there is now evidence for substantial ^{14}C-free geologic CH_4 emissions (*26*). We used the atmospheric $\delta^{13}CH_4$ record from Greenland ice (*10*) to estimate the maximum YD geologic CH_4 source at 50 Tg/year (*20*) and included a scenario with a Q_{fossil} of 50 Tg/year for the YD in Table 1.

Considering these end-member scenarios, the full suggested range of possible ΔQ_{fossil} between the intervals represented by YD and transition samples is –4 to + 7 Tg/year (as compared with a 38 Tg/year total CH_4 source increase). This argues against a substantial involvement of clathrate or other geologic CH_4 in the first half of the YD-PB transition and is consistent with evidence from δD (*11*). The results suggest a ΔQ_{fossil} of +7 to +30 Tg/year (as compared with a 64 Tg/year total CH_4 source increase) for the full YD-PB transition, pointing to wetland CH_4 emissions with contemporaneous $^{14}CH_4$ as the likely main source of the YD-PB [CH_4] rise. For the YD Q_{fossil} = 50 Tg/year scenario, the results further suggest that most of the fossil source increase took place in the later part of the transition. This scenario implies that wetland sources respond to the warming quickly, whereas ^{14}C-depleted sources have a time lag of at least ~100 years, which is consistent with estimated minimum response times for thermokarst lake (*20*) and clathrate emissions (*8*, *20*).

The +7 to +30 Tg/year increase in Q_{fossil} suggested by the $^{14}CH_4$ results for the full YD-PB transition can be explained by either thermokarst lake or clathrate/geologic CH_4 emissions, or some combination of the two, as follows. Measured thermokarst lake emissions today have a mean $\Delta^{14}CH_4$ of ~–740‰ (*27*). If we assume the same overall $\Delta^{14}CH_4$ for thermokarst lake emissions for the PB (*20*) and a maximum YD-PB thermokarst lake emission rate increase of ~15 Tg/year (*7*), then thermokarst lakes can explain a ΔQ_{fossil} of up to 12 Tg/year (*20*).

The YD-PB record of δD of CH_4 (*11*) can be used to illustrate some possible constraints on the magnitude of clathrate/geologic contributions to the CH_4 rise. δD of CH_4 in natural gas is very similar to the estimated clathrate value [–189 ± 27‰ (*11*)], whereas δD of wetland CH_4 is around –320 ± 20‰ (*9*, *11*). Results of a simple one-box model and isotopic mass balance calculations (*20*) show that for the case of zero Q_{fossil} for the YD, the δD record allows for only 1 Tg/year of clathrate/geologic emissions in the PB. However, if a Q_{fossil} of 50 Tg/year is assumed for the YD, then a YD-PB increase of up to 28 Tg/year of clathrate/geologic emissions is possible. These limits decrease if we assume that all of the fossil source increase is due to marine clathrates (rather than a combination of marine clathrate and terrestrial geologic sources, for example) (*20*). This is because CH_4 released from marine clathrates is partially oxidized in the sediments and the water column, resulting in even higher δD values for clathrate-derived CH_4 released to the atmosphere (*28*).

In summary, our $^{14}CH_4$ results, although somewhat uncertain because of the applied correction for cosmogenic ^{14}C, suggest that wetlands were the likely main driver of the YD-PB [CH_4] increase and that clathrates did not play a large role. This is in agreement with findings from previous ice core CH_4 isotopic studies (*10*, *11*).

Table 1. Inferred changes in the total CH_4 source (Q_{total}) and the fossil CH_4 source (Q_{fossil}) during the YD-PB transition. Q_{total} for the YD is as in (*1*); Q_{total} for the transition and PB was calculated based on the YD value and the average sample [CH_4] and assuming no changes in the CH_4 atmospheric lifetime. Q_{fossil} for the YD was assumed to be either zero (third column) or 50 Tg/year (fourth column); for other intervals it was calculated as

$$Q_{fossil} = Q_{total} \times \left(1 - \frac{^{14}CH_{4sample}}{^{14}CH_{4wetland}}\right)$$

$^{14}CH_{4wetland}$ is the expected value for wetland CH_4 emissions, set equal to contemporaneous $^{14}CO_2$ (*29*). Calculations were made with the corrected $^{14}CH_4$ results, averages of replicate samples, in pMC units and decay-corrected for the sample age. For the case of YD Q_{fossil} = 50 Tg/year, the cosmogenic ^{14}C corrections were recalculated accordingly for all samples.

Intervals compared	ΔQ_{total}, Tg/year	ΔQ_{fossil}, Tg/year*	ΔQ_{fossil}, Tg/year†
Younger Dryas (141 Tg/yr) → transition	+38	−4 − +5	−3 − +7
Transition → Preboreal	+26	+2 − +22	+12 − +33
Younger Dryas → Preboreal	+64	+7 − +18	+18 − +30

*Assuming Q_{fossil} = 0 Tg/year for YD; 1 σ range. †Assuming Q_{fossil} = 50 Tg/year for YD; 1 σ range.

References and Notes

1. E. J. Brook, S. Harder, J. Severinghaus, E. J. Steig, C. M. Sucher, *Global Biogeochem. Cycles* **14**, 559 (2000).
2. A. M. Thompson, J. A. Chappellaz, I. Y. Fung, T. L. Kucsera, *Tellus* **45B**, 242 (1993).
3. P. Martinerie, G. P. Brasseur, C. Granier, *J. Geophys. Res.* **100**, 14291 (1995).
4. J. Chappellaz *et al*., *Nature* **366**, 443 (1993).
5. J. P. Kennett, K. G. Cannariato, I. L. Hendy, R. J. Behl, *Science* **288**, 128 (2000).
6. E. G. Nisbet, *Can. J. Earth Sci.* **27**, 148 (1990).
7. K. M. Walter, M. E. Edwards, G. Grosse, S. A. Zimov, F. S. Chapin III, *Science* **318**, 633 (2007).
8. D. Archer, *Biogeosciences* **4**, 521 (2007).
9. H. Fischer *et al*., *Nature* **452**, 864 (2008).
10. H. Schaefer *et al*., *Science* **313**, 1109 (2006).
11. T. Sowers, *Science* **311**, 838 (2006).
12. P. Quay *et al*., *Global Biogeochem. Cycles* **13**, 445 (1999).
13. A. V. Milkov, *Org. Geochem.* **36**, 681 (2005).
14. H. Schaefer, M. J. Whiticar, *Global Biogeochem. Cycles* **22**, GB002889 (2008).
15. M. Wahlen *et al*., *Science* **245**, 286 (1989).
16. G. Winckler *et al*., *Geophys. Res. Lett.* **29**, 1423 (2002).
17. K. A. Kvenvolden, B. W. Rogers, *Mar. Pet. Geol.* **22**, 579 (2005).
18. V. V. Petrenko, J. P. Severinghaus, E. J. Brook, N. Reeh, H. Schaefer, *Quat. Sci. Rev.* **25**, 865 (2006).
19. N. Reeh, H. Oerter, A. Letreguilly, H. Miller, H. W. Hubberten, *Global Planet. Change* **90**, 373 (1991).
20. Materials and methods are available as supporting material on *Science* Online.
21. V. V. Petrenko *et al*., *J. Glaciol.* **54**, 233 (2008).
22. V. V. Petrenko *et al*., *Radiocarbon* **50**, 53 (2008).
23. D. Lal, A. J. T. Jull, D. J. Donahue, D. Burtner, K. Nishiizumi, *Nature* **346**, 350 (1990).
24. I. M. Evans, thesis, University of Cambridge, Cambridge, UK (1970).
25. K. Rossler, H. J. Jung, B. Nebeling, *Adv. Space Res.* **4**, 83 (1984).
26. G. Etiope, *Atmos. Environ.* **38**, 3099 (2004).
27. K. M. Walter, J. P. Chanton, F. S. Chapin, E. A. G. Schuur, S. A. Zimov, *J. Geophys. Res.* **113**, JG000569 (2008).
28. M. J. Whiticar, *Chem. Geol.* **161**, 291 (1999).
29. P. J. Reimer *et al*., *Radiocarbon* **46**, 1029 (2004).
30. E. J. Dlugokencky *et al*., *J. Geophys. Res.* **110**, JD006035 (2005).

31. This work was supported by NSF grants OPP0221470 (to J.P.S.) and OPP0221410 (to E.J.B.), a Packard Fellowship (to J.P.S.), an American Chemical Society grant PRF 42551-AC2 (to H.S. and E.J.B.), the ANSTO Cosmogenic Climate Archives of the Southern Hemisphere project, the New Zealand Foundation of Science and Technology (contract C01X0703), and the Australian Climate Change Science Program. We thank D. Ferretti and P. Franz for making $\delta^{13}CH_4$ measurements; the Keeling laboratory for the use of a CO_2 extraction line; G. Emanuel for advice with $^{14}CO_2$ processing; M. Headly for Kr/Ar and Xe/Ar measurements; D. Lal for valuable discussions; A. Williams, V. Levchenko, R. Moss, T. Bromley, and R. Martin for assistance with sample processing; J. Melton, M. Arsenault, P. Rose, N. Ness, and K. Ranke for help with field sampling; and Z. Wang and J. Mak for ^{13}C of CO measurements. The manuscript was improved by suggestions from E. Nesbit and one anonymous reviewer.

Supporting Online Material

www.sciencemag.org/cgi/content/full/324/5926/506/DC1
Materials and Methods
Tables S1 to S6
References

24 November 2008; accepted 5 March 2009
10.1126/science.1168909

Tuning the Activation Threshold of a Kinase Network by Nested Feedback Loops

Quincey A. Justman,[1,2]* Zach Serber,[3]† James E. Ferrell Jr.,[3] Hana El-Samad,[4]‡ Kevan M. Shokat[2]‡

Determining proper responsiveness to incoming signals is fundamental to all biological systems. We demonstrate that intracellular signaling nodes can tune a signaling network's response threshold away from the basal median effective concentration established by ligand-receptor interactions. Focusing on the bistable kinase network that governs progesterone-induced meiotic entry in *Xenopus* oocytes, we characterized glycogen synthase kinase–3β (GSK-3β) as a dampener of progesterone responsiveness. GSK-3β engages the meiotic kinase network through a double-negative feedback loop; this specific feedback architecture raises the progesterone threshold in correspondence with the strength of double-negative signaling. We also identified a marker of nutritional status, L-leucine, which lowers the progesterone threshold, indicating that oocytes integrate additional signals into their cell-fate decisions by modulating progesterone responsiveness.

To respond to environmental cues appropriately, biological systems establish precise response thresholds. It is unclear how metazoan signal transduction networks exert control over sensitivity because stimulus and response are separated in space and time: Rapid receipt of the signal often occurs extracellularly, whereas downstream responses occur on longer time scales and require cellwide coordination.

Maturation of *Xenopus* oocytes, the irreversible, progesterone-induced resumption of meiosis I (*1*, *2*), provides a classic example of a cell-fate decision with a well-defined threshold: Oocytes treated with a sufficient concentration of progesterone undergo maturation, whereas those treated with a lower concentration do not. Suprathreshold progesterone stimulus up-regulates the translation and gradual accumulation of the protein kinase Mos through a largely unidentified pathway. Mos is the essential initiator of meiosis (*3*); it signals through the mitogen-activated protein kinase (MAPK) cascade (composed of Mos, the MAPK kinase MEK1, and p42 MAPK) and promotes the activation of the cyclin-dependent kinase 1 (Cdk1)•cyclin B complex (Fig. 1A). Nonlinearity in the relationship between Mos concentration and MAPK activation conveys switchlike character to the decision to mature (*4*). In mature, M-phase cells, high Mos concentrations are maintained by continual Mos translation. Mos translation, in turn, is critically dependent on the activities of Mos, MEK, MAPK, and Cdk1, forming a positive feedback loop (*5*). The net effect of this nonlinearity and positive feedback is to enforce a stable separation of interphase and M phase at steady state. Thus, *Xenopus* oocyte maturation is bistable (*4*, *5*). An oocyte crosses its progesterone threshold when Mos concentrations are sufficient to initiate M-phase positive feedback, hours after the signal is received at the cell surface. We explain how oocytes specify the progesterone concentration that initiates M-phase entry.

Depending on environmental factors and a frog's physiology, the dose of hormone required

[1]Graduate Group in Biophysics, University of California, San Francisco, CA 94158, USA. [2]Howard Hughes Medical Institute and Department of Cellular and Molecular Pharmacology, University of California, San Francisco, CA 94158, USA. [3]Department of Chemical and Systems Biology, Stanford University School of Medicine, Stanford, CA 94305–5174, USA. [4]Department of Biochemistry and Biophysics, University of California, San Francisco, CA 94158, USA.

*Present address: Department of Molecular and Cellular Biology, Harvard University, Cambridge, MA 02138, USA.
†Present address: Amyris Biotechnologies, Incorporated, Emeryville, CA 94608, USA.
‡To whom correspondence should be addressed. E-mail: helsamad@biochem.ucsf.edu (H.E.); shokat@cmp.ucsf.edu (K.M.S.)

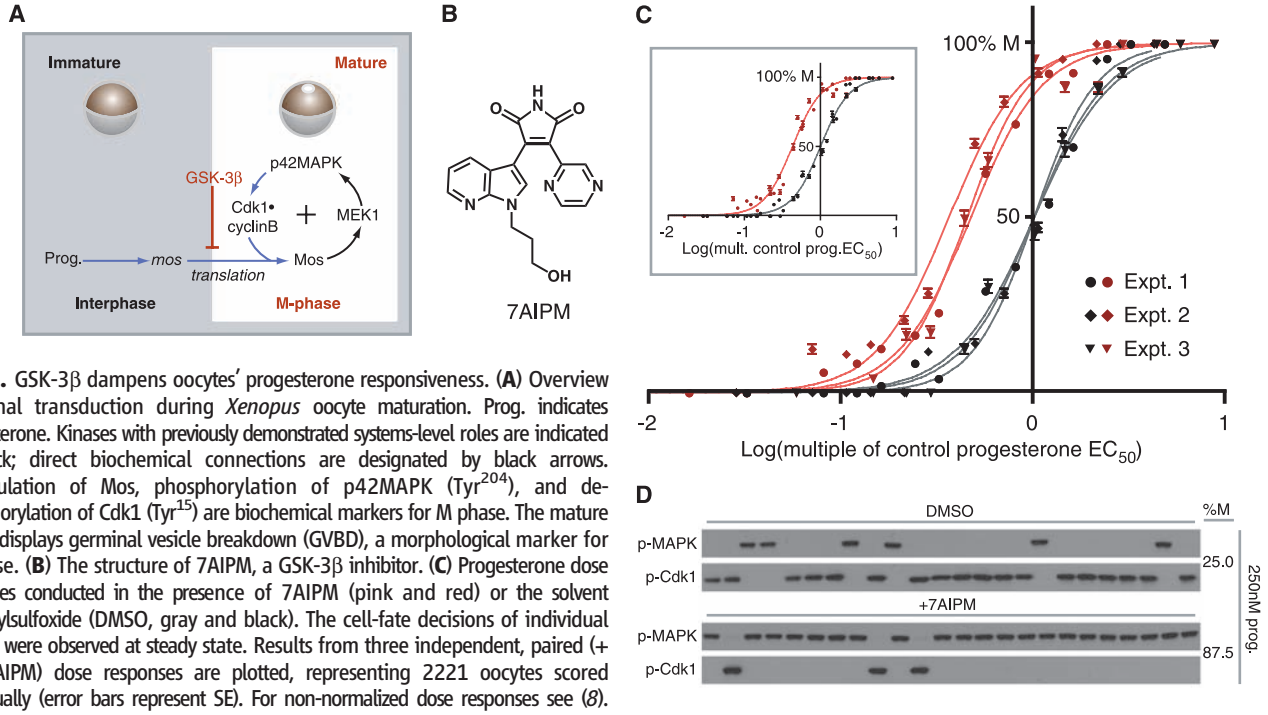

Fig. 1. GSK-3β dampens oocytes' progesterone responsiveness. (**A**) Overview of signal transduction during *Xenopus* oocyte maturation. Prog. indicates progesterone. Kinases with previously demonstrated systems-level roles are indicated in black; direct biochemical connections are designated by black arrows. Accumulation of Mos, phosphorylation of p42MAPK (Tyr^{204}), and dephosphorylation of Cdk1 (Tyr^{15}) are biochemical markers for M phase. The mature oocyte displays germinal vesicle breakdown (GVBD), a morphological marker for M phase. (**B**) The structure of 7AIPM, a GSK-3β inhibitor. (**C**) Progesterone dose responses conducted in the presence of 7AIPM (pink and red) or the solvent dimethylsulfoxide (DMSO, gray and black). The cell-fate decisions of individual oocytes were observed at steady state. Results from three independent, paired (+ or –7AIPM) dose responses are plotted, representing 2221 oocytes scored individually (error bars represent SE). For non-normalized dose responses see (*8*). (Inset) Composite progesterone dose responses from the three independent experiments shown in (C). For DMSO-treated oocytes (gray and black), EC_{50} = 1.00 (normalized) and n_H = 2.3. For 7AIPM-treated oocytes (pink and red), EC_{50} = 0.43 (normalized to DMSO control) and n_H = 2.3. (**D**) Representative single-oocyte Western blots. Each lane contains lysate prepared from one oocyte at steady state.

to induce ovulation can vary. We reasoned that, although receptor number and ligand affinity establish a basal median effective concentration (EC_{50}) for the system, specific intracellular kinases might tune the oocytes' progesterone thresholds. Progesterone-dependent inactivation of glycogen synthase kinase–3β (GSK-3β) (by phosphorylation on Ser^9) is an obligatory step in determining the cell-fate of the oocyte. Overexpression of GSK-3β can prevent progesterone-induced translation of Mos (*6*), and it uncoupled MAPK and Cdk1 activation, rendering M-phase entry incomplete (fig. S1). Because it regulates the transition between interphase and M phase, we tested whether GSK-3β also regulates the progesterone threshold of *Xenopus* oocytes. We measured progesterone dose responses in the presence and absence of 7-azaindolyl-pyrazinyl-maleimide (7AIPM), a specific GSK-3β inhibitor (*7*) (Fig. 1B), and observed that constant inhibition of GSK-3β doubled the system's responsiveness to progesterone (Fig. 1C and fig. S2) (*8*). Single-cell experiments indicated that maturation retained its all-or-none, irreversible character in 7AIPM-treated oocytes (Fig. 1D and fig. S3), suggesting that GSK-3β dampens overall progesterone responsiveness by raising the thresholds of individual oocytes. The 7AIPM treatment brought the oocytes' in vitro EC_{50} closer to the low nM progesterone concentrations measured in intact *Xenopus* ovaries (*9*, *10*).

We envisioned two possible threshold regulation mechanisms that center on two negative regulatory connections placed in series. First, GSK-3β could dampen interphase signaling until GSK-3β is inactivated by progesterone-dependent signaling in a feed-forward manner, before meiotic entry (Fig. 2A, top). Alternatively, M-phase feedback could inactivate GSK-3β and relieve its repression of Mos translation as the meiotic switch activates (Fig. 2A, bottom). To verify that these mechanisms can raise a bistable system's threshold, we modeled them mathematically and mimicked 7AIPM treatment by setting GSK-3β activity to zero (*11*). This analysis revealed that both mechanisms provide a general solution for dampening a system's responsiveness (Fig. 2A, far right). In an analytical treatment, we proved mathematically that a raised threshold is a structural feature of bistable systems con-

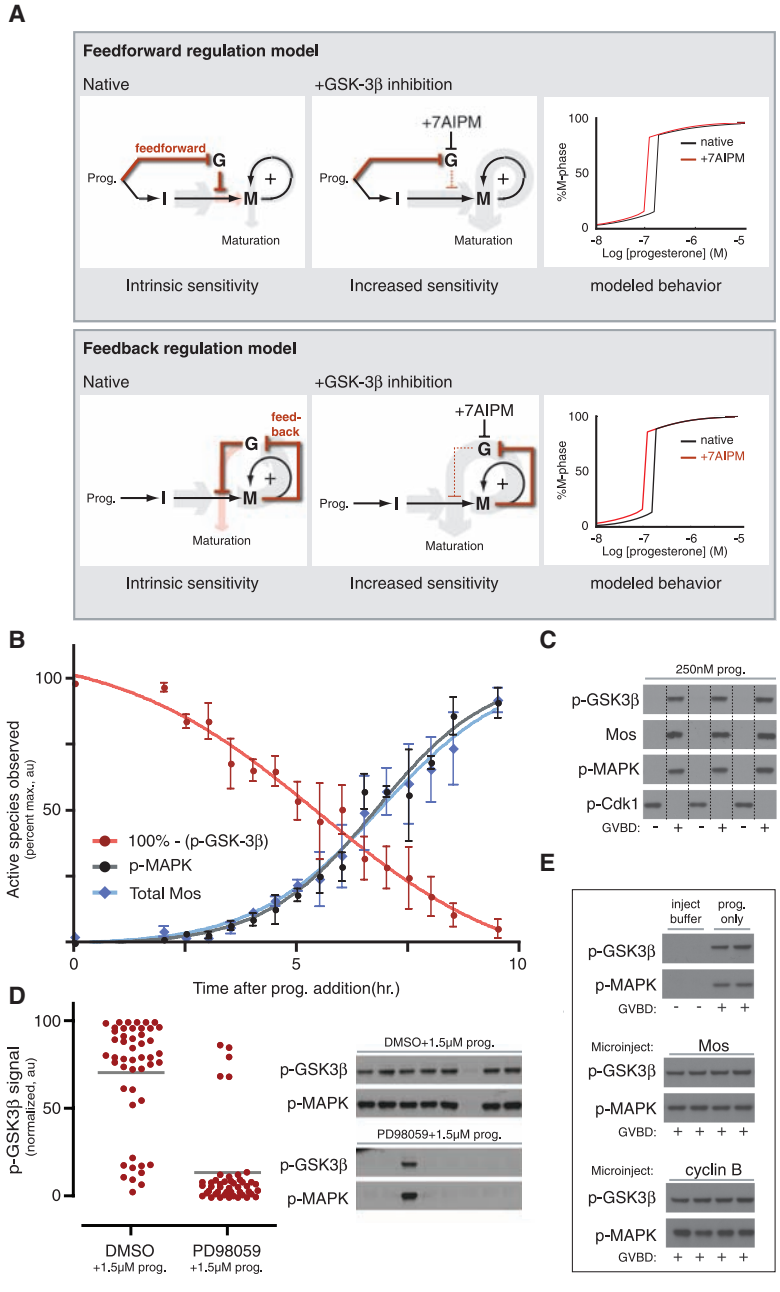

Fig. 2. GSK-3β inactivation is an M-phase event. (**A**) Feed-forward versus feedback models for GSK-3β–dependent progesterone desensitization, relating the activity of GSK-3β (G) to interphase (I) and M-phase (M) signaling. Relative signal strength (i.e., the amount of downstream, promeiosis signal per unit of progesterone) is indicated by the thickness of the gray and pink arrows. The pink arrow designates the threshold-regulation step. (Right) The black curve models the input dose-response curve of the native bistable system; the red curve models the response after 7AIPM treatment. (**B**) Time course of phospho-regulation and Mos accumulation during maturation. Average phospho-MAPK, phospho-GSK-3β, and total Mos were quantified by Western blotting (error bars are ±SD, n = approximately 24 oocytes per time point). At 9.5 hours, GVBD was 100%. (**C**) Single-oocyte Western blots at intermediate progesterone. Lysates were prepared from individual oocytes at steady state, then Western blotted. Lanes were assigned by cell morphology (+ indicates GVBD was observed; –, GVBD was not observed); lane lines are included for clarity. (**D**) MEK inhibition before progesterone stimulus. Lysate was prepared from individual oocytes at steady state. (Left) Phospho–GSK-3β signal quantitated by closed-circuit device (CCD) camera. Dots represent signal from single oocytes; lines indicate population average. PD98059 pretreatment reduces average GSK-3β Ser^9 phosphorylation significantly ($P < 0.0001$, Student's t test). (Right) Phospho-MAPK and phospho-GSK in representative single oocytes. Phospho-MAPK is a direct readout of MEK activity and M-phase entry. DMSO pretreatment: 71.2% M phase; PD98059 pretreatment: 10.9% M phase. Total n = 48 (DMSO) and 46 (PD98059). (**E**) Phospho–GSK-3β and phospho-MAPK in oocytes microinjected with Mos or nondegradable cyclin B1 (Δ90). Oocytes were lysed individually after GVBD; lysates were run on the same gel and Western blotted on a single blot. Microinjected oocytes were not stimulated with progesterone.

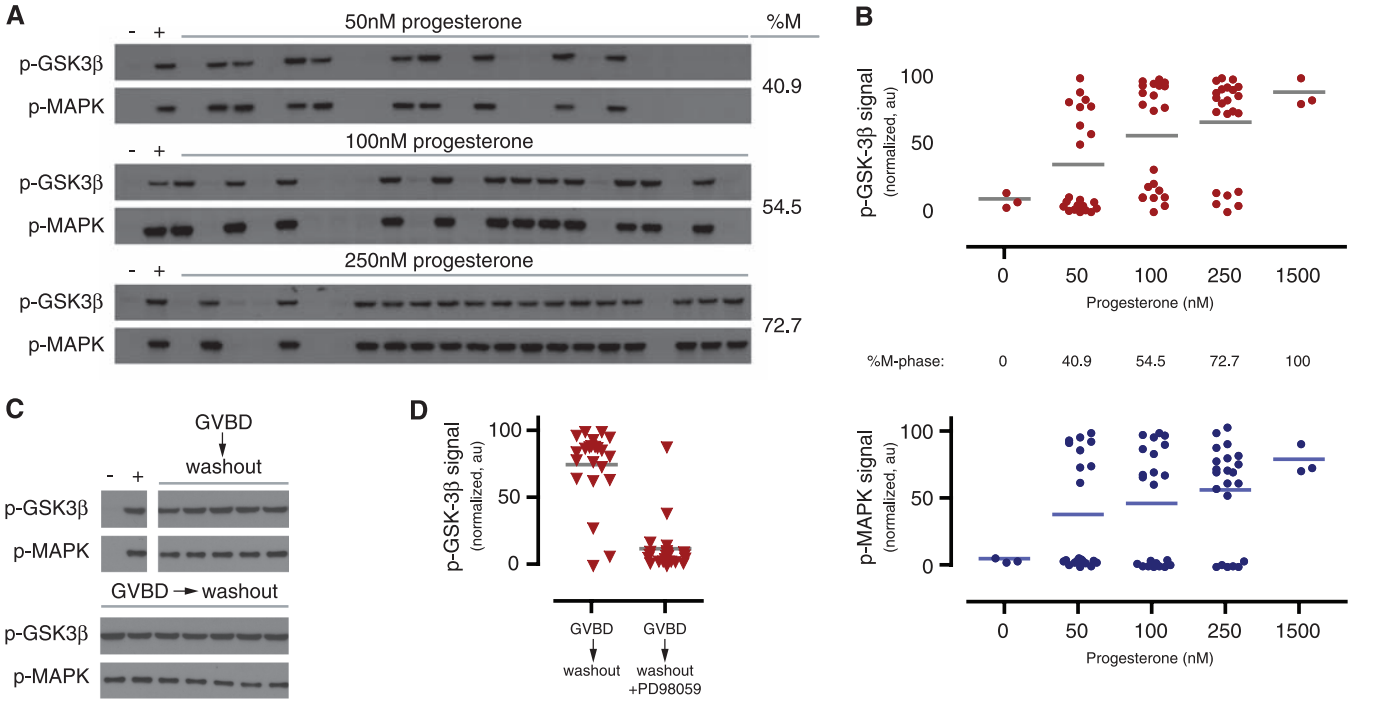

Fig. 3. M-phase GSK-3β inactivation is switchlike, MEK-dependent, and irreversible. (**A** and **B**). Phosphorylation of GSK-3β in single oocytes. Phospho–GSK-3β within each oocyte was scored by Western blot (A) then quantitated by CCD camera [(B), top, red]. Lanes indicated by "+" were treated with 1.5 μM progesterone. Dots represent the phospho–GSK-3β signal from individual oocytes; lines indicate the oocyte population's average phospho–GSK-3β signal. The single-cell quantitation of MAPK phosphorylation is included for reference [(B), bottom, blue]. (**C** and **D**) Progesterone removal. After GVBD, oocytes were washed extensively over 18 hours then lysed individually. Phospho–GSK-3β was scored by Western blot [(C), a representative oocyte, total $n = 23$]. In (D), PD98059 was added during the washout period. PD98059 treatment during M-phase arrest reduces average GSK-3β Ser^9 phosphorylation significantly ($P < 0.0001$, Student's t test). DMSO treatment: 86.4% M phase; PD98059 treatment: 4.2% M phase.

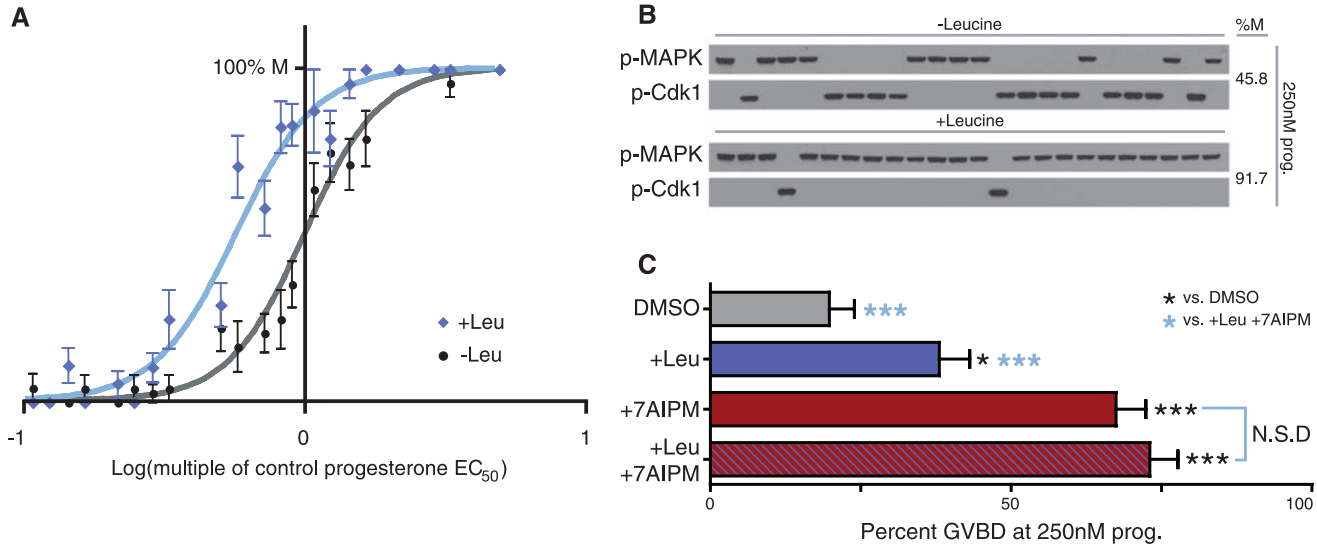

Fig. 4. Integration of progesterone and Leu signaling. (**A**) Progesterone dose responses of oocytes incubated in the presence of Leu (blue) or its absence (gray and black). The cell-fate decisions of individual oocytes were observed at steady state. Results plotted represent 1290 oocytes scored individually (error bars represent SE). For control (gray and black), EC_{50} = 1.00 (normalized) and n_H = 3.2. For Leu-treated oocytes (blue), EC_{50} = 0.57 (normalized to control) and n_H = 3.1. (**B**) Representative single-cell Western blots reveal response of individual oocytes to progesterone at steady state, + or −Leu. (**C**) Combined treatment with Leu and 7AIPM. Oocytes were treated with DMSO ($n = 91$), Leu ($n = 92$), 7AIPM ($n = 89$), or Leu plus 7AIPM ($n = 89$) before progesterone stimulus. Cell-fate decisions were scored at steady state. Error bars represent SE. Pairwise comparisons were made to the DMSO control (black asterisks) and the +Leu+7AIPM treatment (blue asterisks), $*P < 0.05$; $***P < 0.0001$; "N.S.D" indicates no significant difference (Student's t tests). More stringent χ^2 analysis reveals that all values are statistically different except 7AIPM and 7AIPM+Leu.

taining two negative regulatory connections placed in series; this is not dependent on parameter choice (fig. S8) (*8*).

To distinguish between these threshold regulation mechanisms, we experimentally defined GSK-3β's position in the progesterone-responsive signaling network relative to M-phase entry. Unlike most kinases, phosphorylation of GSK-3β on Ser^9 inhibits its activity; this occurs through pseudo-substrate inhibition (*12*). We conducted a time course of phospho-GSK-3β accumulation at high progesterone concentration and found that maximum GSK-3β phosphorylation occurred during M phase (Fig. 2B) (*13*). Accordingly, phosphorylation of GSK-3β correlated precisely with the decision to enter M phase in individual progesterone-stimulated oocytes (Fig. 2C). To determine whether M-phase signaling is necessary for phosphorylation of GSK-3β, we initiated maturation in the presence of PD98059, a specific MEK inhibitor. PD98059 treatment significantly reduced the population's average amount of phospho-GSK-3β (Fig. 2D, left); single-oocyte analysis revealed a precise correlation between MEK inhibition, very low amounts of phospho-GSK-3β, and failure of most cells to enter M phase (Fig. 2D, right). To verify that GSK-3β is not inactivated by progesterone-dependent interphase signals, we initiated meiosis in the absence of progesterone by microinjecting oocytes with Mos or nondegradable cyclin B1 (Δ90). In the microinjected cells, phospho-MAPK confirmed meiotic entry, and phosphorylation of GSK-3β was indistinguishable from progesterone-treated controls (Fig. 2E), suggesting that signals originating within the M-phase feedback loop are sufficient to inactivate GSK-3β. Given these data, we hypothesized that GSK-3β regulates oocytes' progesterone responsiveness by participating in M-phase network itself.

We tested whether phosphorylation of GSK-3β mirrors the hallmark characteristics of MAPK activation during *Xenopus* oocyte maturation: nonlinear progesterone dependence and hysteresis (*4*, *5*). In equivalently stimulated cells, phosphorylation of GSK-3β on Ser^9 was either nearly undetectable or maximal at steady state (Fig. 3, A and B top). No intermediate responses were observed in single cells, demonstrating that GSK-3β phosphorylation is ultrasensitive with respect to progesterone concentration. In mature oocytes, positive, Mos-dependent feedback is sufficiently strong to maintain meiotic commitment after progesterone is removed (*5*). If GSK-3β inactivation relies on the same M-phase feedback, GSK-3β's phosphoregulation should display the same extreme hysteresis. We observed that phosphorylation of GSK-3β was sustained at its maximum 18 hours after removal of progesterone (Fig. 3C). Moreover, this hysteresis depended on the activity of MEK: When PD98059 was added as progesterone was removed, phosphorylation of GSK-3β was significantly reduced (Fig. 3D). In total, our data show that induction and maintenance of GSK-3β inactivation requires feedback through the meiotic kinase network. GSK-3β also displays the same bistable behavior observed in MAPK and Cdk1. Taken together, these results define GSK-3β as a node in a MEK-dependent, double-negative feedback loop that is likely driven by the bistable, positive feedback within M-phase oocytes. These results provide experimental verification of our feedback regulation mechanism (Fig. 2A, bottom images).

GSK-3β–dependent desensitization might allow a cell to integrate several signals, an impossibility if it were maximally responsive to progesterone alone. The branched-chain amino acid L-leucine (Leu), a nutritional marker, regulates translation through kinases that require inhibition of GSK-3β for activity (*14*, *15*). To test whether Leu-dependent signals can be integrated into oocytes' decision to mature, we conducted progesterone dose-responses in the presence and absence of extracellular Leu. Although Leu does not alter oocytes' baseline response at low progesterone concentrations (Fig. 4A), Leu lowered the oocytes' progesterone threshold, demonstrating cooperation between nutritional signals and cell-cycle entry (Fig. 4, A and B). If Leu signaling and GSK-3β form a common pathway during maturation, simultaneous treatment with Leu and 7AIPM would have no greater effect on progesterone threshold than either 7AIPM or Leu alone. However, if nutrient signaling was mediated through a GSK-3β–independent pathway, the two stimuli would have an additive or synergistic effect. We observed that the effect of Leu and 7AIPM together on progesterone responsiveness was statistically indistinguishable from that of 7AIPM alone (Fig. 4C), suggesting that GSK-3β regulation is a point of signal integration during *Xenopus* oocyte maturation.

Much attention has focused on the ubiquity of simple dynamical motifs in biological systems (*16*–*23*). Here, we demonstrate that layering apparently redundant motifs (positive feedback and double-negative feedback) tunes a bistable system's response threshold. This illustrates a remarkable separation of functions in bistable systems: Input EC_{50} is regulated by relationships that are not strictly input-dependent. A striking number of biological networks contain nested feedback loops (*17*–*19*, *21*), suggesting that this may be a general mechanism for modulating biological responsiveness. If multiple stimuli act on components of linked feedback loops, cells may tune their responsiveness to respond appropriately to their environment.

References and Notes

1. A. R. Nebreda, I. Ferby, *Curr. Opin. Cell Biol.* **12**, 666 (2000).
2. T. Kishimoto, *Curr. Opin. Cell Biol.* **15**, 654 (2003).
3. F. Gebauer, J. D. Richter, *Bioessays* **19**, 23 (1997).
4. J. E. Ferrell Jr., E. M. Machleder, *Science* **280**, 895 (1998).
5. W. Xiong, J. E. Ferrell Jr., *Nature* **426**, 460 (2003).
6. M. Sarkissian, R. Mendez, J. D. Richter, *Genes Dev.* **18**, 48 (2004).
7. D. J. O'Neill *et al.*, *Bioorg. Med. Chem.* **12**, 3167 (2004).
8. Materials and methods are available as supporting material on *Science* Online.
9. L. B. Lutz *et al.*, *Proc. Natl. Acad. Sci. U.S.A.* **98**, 13728 (2001).
10. J. E. Fortune, *Dev. Biol.* **99**, 502 (1983).
11. The feed-forward model is given by

$$\frac{dM}{dt} = k_{off}^{M^*} M^* - \gamma_M M - k_{on}^{M} M + f_{pos}\frac{M^{*n_H}}{M^{*n_H} + EC_{50}^{n_H}} + \frac{stim^n}{stim^n + K_s^n}\frac{k_{stim}}{1 + \left(G^*/K_{G^*}\right)^{n_1}}$$

$$\frac{dM^*}{dt} = k_{on}^{M} M - k_{off}^{M^*} M^* - \gamma_{M^*} M^*$$

$$\frac{dG^*}{dt} = k_{on}^{G}\frac{(G_t - G^*)}{K_{M^*}^{n_2} + stim^{n_2}} - k_{off}^{G^*} G^*$$

The feedback model is given by

$$\frac{dM}{dt} = k_{off}^{M^*} M^* - \gamma_M M - k_{on}^{M} M + f_{pos}\frac{M^{*n_H}}{M^{*n_H} + EC_{50}^{n_H}} + \frac{stim^n}{stim^n + K_s^n}\frac{k_{stim}}{1 + \left(G^*/K_{G^*}\right)^{n_1}}$$

$$\frac{dM^*}{dt} = k_{on}^{M} M - k_{off}^{M^*} M^* - \gamma_{M^*} M^*$$

$$\frac{dG^*}{dt} = k_{on}^{G}\frac{(G_t - G^*)}{K_{M^*}^{n_2} + M^{*n_2}} - k_{off}^{G^*} G^*$$

stim is an aggregate of all interphase signaling; *M* is newly synthesized Mos; *M** is an aggregate of stabilized Mos and all Mos-dependent signaling; *G** is active GSK-3β; k_{on} designates activation terms; k_{off} designates inactivation terms; γ designates destruction; *n* terms are theoretical Hill coefficients. To model 7AIPM treatment (Fig. 2A), *G** was set to zero. See also (*8*).
12. R. Dajani *et al.*, *Cell* **105**, 721 (2001).
13. D. L. Fisher, N. Morin, M. Doree, *Development* **126**, 567 (1999).
14. D. H. Kim *et al.*, *Cell* **110**, 163 (2002).
15. K. Peyrollier, E. Hajduch, A. S. Blair, R. Hyde, H. S. Hundal, *Biochem. J.* **350**, 361 (2000).
16. T. S. Gardner, C. R. Cantor, J. J. Collins, *Nature* **403**, 339 (2000).
17. K. Amonlirdviman *et al.*, *Science* **307**, 423 (2005).
18. G. Lahav *et al.*, *Nat. Genet.* **36**, 147 (2004).
19. J. R. Pomerening, S. Y. Kim, J. E. Ferrell Jr., *Cell* **122**, 565 (2005).
20. M. Acar, A. Becskei, A. van Oudenaarden, *Nature* **435**, 228 (2005).
21. O. Brandman, J. E. Ferrell Jr., R. Li, T. Meyer, *Science* **310**, 496 (2005).
22. N. T. Ingolia, A. W. Murray, *Curr. Biol.* **17**, 668 (2007).
23. G. M. Suel, J. Garcia-Ojalvo, L. M. Liberman, M. B. Elowitz, *Nature* **440**, 545 (2006).

24. We thank J. Yue for providing Mos and cyclin protein; N. L. Salimi for help with statistics; J. J. Fleming and P. M. England for help with oocytes; and A. W. Murray, R. D. Mullins, J. A. Blair, and E. C. Garner for critical reading of the manuscript. Funding from NIH grant AI49006 (to K.M.S.), the Sandler Family Supporting Foundation (to H.E.), and NIH grant GM46383 (to J.E.F.).

Supporting Online Material

www.sciencemag.org/cgi/content/full/324/5926/509/DC1
Materials and Methods
Figs. S1 to S10
Tables S1 to S3
References

9 December 2008; accepted 17 March 2009
10.1126/science.1169498

Catalytic Core of a Membrane-Associated Eukaryotic Polyphosphate Polymerase

Michael Hothorn,[1,2] Heinz Neumann,[3]* Esther D. Lenherr,[1] Mark Wehner,[4] Vladimir Rybin,[1] Paul O. Hassa,[1] Andreas Uttenweiler,[3]† Monique Reinhardt,[3] Andrea Schmidt,[3] Jeanette Seiler,[1] Andreas G. Ladurner,[1] Christian Herrmann,[4] Klaus Scheffzek,[1]‡ Andreas Mayer[3,5]

Polyphosphate (polyP) occurs ubiquitously in cells, but its functions are poorly understood and its synthesis has only been characterized in bacteria. Using x-ray crystallography, we identified a eukaryotic polyphosphate polymerase within the membrane-integral vacuolar transporter chaperone (VTC) complex. A 2.6 angstrom crystal structure of the catalytic domain grown in the presence of adenosine triphosphate (ATP) reveals polyP winding through a tunnel-shaped pocket. Nucleotide- and phosphate-bound structures suggest that the enzyme functions by metal-assisted cleavage of the ATP γ-phosphate, which is then in-line transferred to an acceptor phosphate to form polyP chains. Mutational analysis of the transmembrane domain indicates that VTC may integrate cytoplasmic polymer synthesis with polyP membrane translocation. Identification of the polyP-synthesizing enzyme opens the way to determine the functions of polyP in lower eukaryotes.

Inorganic polyphosphate (polyP) occurs in all life forms. In prokaryotes, polyP is a store of phosphate and energy and augments stress responses (*1*). In eukaryotes, polyP also acts in phosphate transport between mycorrhizal fungi and symbiotic plants (*2*), in osmoregulation (*3*), and in bone calcification (*4*). Large quantities of plankton-generated polyP form marine sediments (*5*). PolyP kinase generates bacterial polyP (*6*), but in eukaryotes this enzyme has only been reported in slime mold (*7*). Genetic screens in yeast yielded ≥250 alternative candidates whose deletion decreases cellular polyP (*8*, *9*), but the identity of the polyP-synthesizing enzyme has remained elusive. Among the candidates is the yeast vacuolar transporter chaperone (VTC) complex, a membrane protein assembly whose deletion reduces polyP accumulation (*8*) but also affects membrane transport and vesicular traffic (*10*–*12*). We have used x-ray crystallography to identify a polyP polymerase in VTC.

Four *Saccharomyces cerevisiae* Vtc proteins form hetero-oligomeric complexes (*8*, *10*, *12*). Vtc1p is a small transmembrane protein. Vtc2p, 3p, and 4p contain the transmembrane domain and additional large and sequence-related cytoplasmic segments (*13*). Within these segments, we proteolytically defined 35-kD-sized domains. We determined the 2.1 Å crystal structure of the fragment Vtc2p$^{183\text{-}553}$ and the 2.6 Å structure of Vtc4p* (Vtc4p$^{189\text{-}480}$) in the presence of Li_2SO_4 or adenosine triphosphate (ATP)–$MnCl_2$, respectively (see supporting online material) (tables S1 and S2). The structures are similar (root mean square deviation ~ 1.7 Å between 241 corresponding C_α atoms) and structurally related to the RNA triphosphatase Cet1p (*14*). Like Cet1p, they comprise a tunnel-shaped domain formed by antiparallel β strands (fig. S1A) with the tunnel walls lined by conserved basic residues. Vtc2p$^{183\text{-}553}$ and Cet1p both have a sulfate coordinated in the tunnel center (fig. S1B). In the case of Cet1p, the sulfate mimics the γ-phosphate of nucleoside triphosphates (*14*), which Cet1p hydrolyzes in the presence of Mn^{2+} (*15*). The Vtc4p* structure contained a long chain of electron density winding through the tunnel domain (Fig. 1A), which suggests that this module had generated phosphate polymers from ATP during dialysis or crystallization. Difference density in our structure accounts for 29 phosphate units that are bound by two neighboring molecules in the asymmetric unit (fig. S2A). Consistently, Vtc4p*-synthesized polyP can be detected in solution (Fig. 1B). Vtc4p* generates polyP from ATP in a phosphotransfer reaction releasing adenosine diphosphate (ADP) (Fig. 1C) (*16*). Our results define Vtc4p* as a polyP-synthesizing

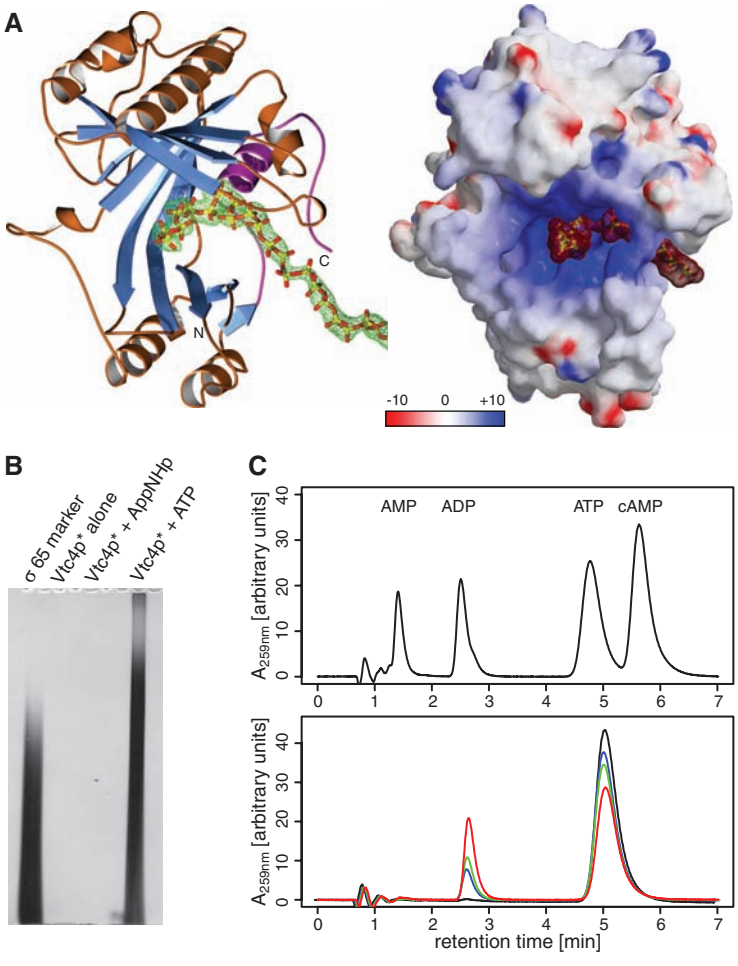

Fig. 1. Vtc4p* is a polyP polymerase. (**A**) Ribbon diagram of Vtc4p* with the phosphate polymer (in bonds representation) and an omit electron difference density map contoured at 4.5 σ included. The helical plug is shown in magenta. Mapping of the electrostatic potential [in kBT/e; as output by program GRASP (*24*)] on the surface of Vtc4p* highlights the basic tunnel center and the negatively charged polymer (**B**) Urea polyacrylamide gel electrophoresis of polyP generated by Vtc4p* from ATP and in the presence of Mn^{2+} ions. (**C**) High-performance liquid chromatography (HPLC) analysis of nucleotide products in the polymerization reaction. (Top) Elution profile showing the retention times for different nucleotides. (Bottom) HPLC analysis after incubating 30 μM Vtc4p* with 200 μM ATP for 0 (black line), 15 (blue), 45 (green), and 90 min (red).

[1]European Molecular Biology Laboratory, Structural and Computational Biology Unit, Meyerhofstrasse 1, 69117 Heidelberg, Germany. [2]Plant Biology Laboratory, Salk Institute for Biological Studies, 10010 North Torrey Pines Road, La Jolla, CA 92037, USA. [3]Département de Biochimie, Université de Lausanne, 1066 Epalinges, Switzerland. [4]Physikalische Chemie 1, Ruhr-Universität Bochum, 44780 Bochum, Germany. [5]Department of Biochemistry and Molecular Biology, Baylor College of Medicine, One Baylor Plaza, Houston, TX 77030, USA.

*Present address: Medical Research Council Laboratory of Molecular Biology, Hills Road, Cambridge CB2 0QH, UK.
†Present address: Novartis Pharma Schweiz AG, Monbijoustrasse 118, 3007 Bern, Switzerland.
‡To whom correspondence should be addressed: E-mail: scheffzek@embl.de

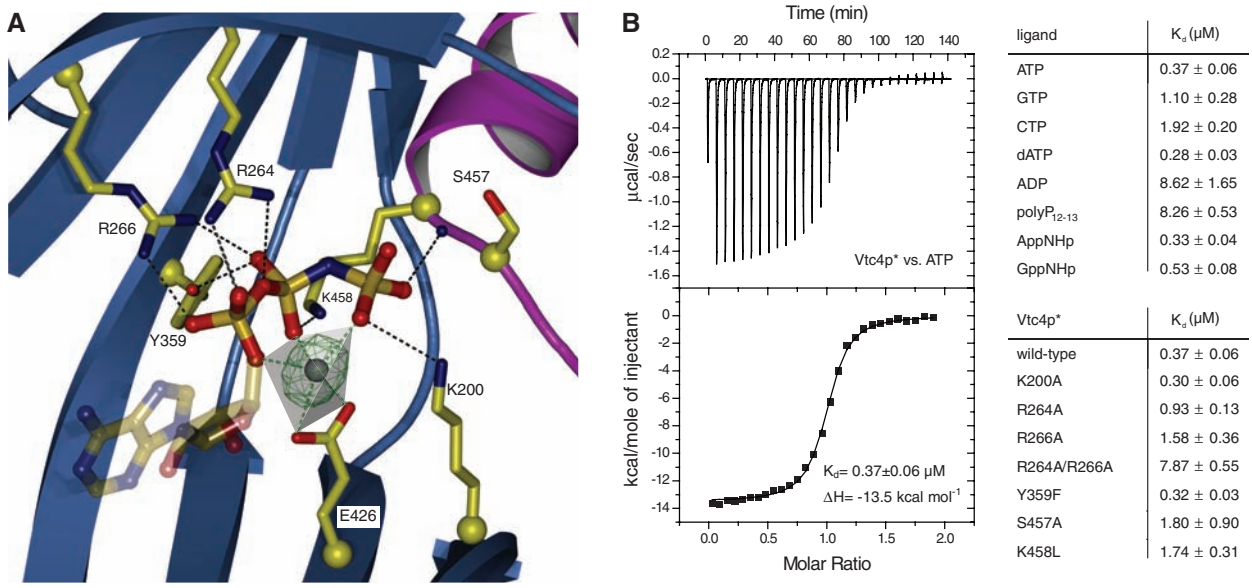

ligand	K_d (µM)
ATP	0.37 ± 0.06
GTP	1.10 ± 0.28
CTP	1.92 ± 0.20
dATP	0.28 ± 0.03
ADP	8.62 ± 1.65
$polyP_{12-13}$	8.26 ± 0.53
AppNHp	0.33 ± 0.04
GppNHp	0.53 ± 0.08

Vtc4p*	K_d (µM)
wild-type	0.37 ± 0.06
K200A	0.30 ± 0.06
R264A	0.93 ± 0.13
R266A	1.58 ± 0.36
R264A/R266A	7.87 ± 0.55
Y359F	0.32 ± 0.03
S457A	1.80 ± 0.90
K458L	1.74 ± 0.31

Fig. 2. Unusual modes of nucleotide and metal cofactor binding in Vtc4p*. (**A**) Close-up view of Vtc4p* tunnel center bound to AppNHp (in bonds representation) and Mn^{2+} (gray sphere). The sugar and base portions were modeled stereochemically. The pentavalent coordination of Mn^{2+} is distorted square-based pyramidal. A phased anomalous difference map calculated from data collected at the Mn K edge and contoured at 15 σ is shown in green. (**B**) Isothermal titration calorimetry of wild-type Vtc4p* versus ATP, together with table summaries for the binding constants for different ligands and Vtc4p* mutants (versus ATP). Shown are experimental values ± fitting errors.

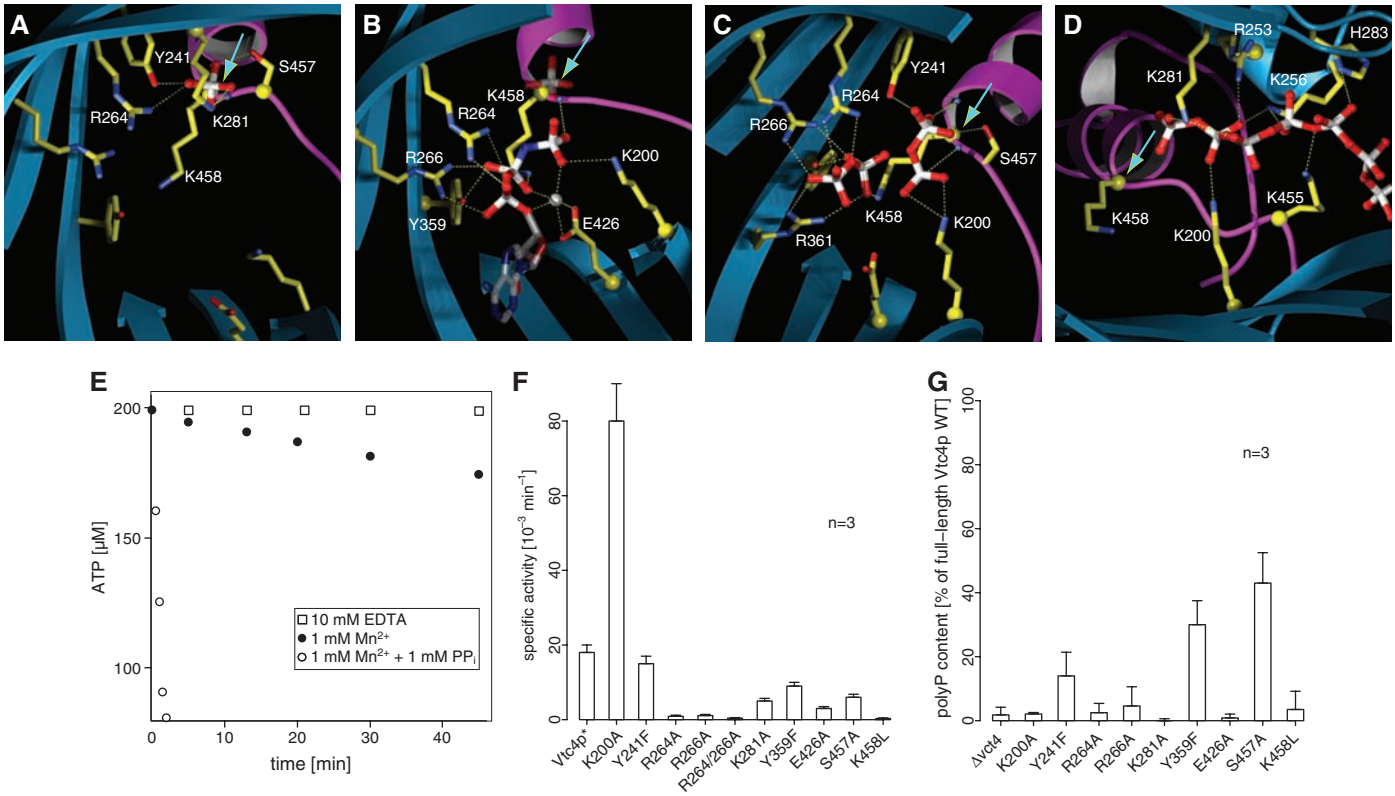

Fig. 3. Structural views of the Vtc4p* polymerase cycle. (**A**) Structure of Vtc4p* bound to orthophosphate. Coordinating residues are shown, along with the catalytic Lys^{458} (marked with an arrow) to facilitate comparison. (**B**) Structure of the AppNHp-Mn^{2+} complex. The Mn^{2+} ion is shown as a gray sphere; the position of the orthophosphate has been inferred from (A). (**C**) Rotated view of Vtc4p* bound to PP_i. One PP_i occupies the nucleotide binding site mimicking ADP; a second molecule occupies the acceptor pocket. (**D**) Close-up view of the polyP exit tunnel. (**E**) ATP turnover analyzed by HPLC at 30 µM Vtc4p* and 1 mM Mn^{2+} (filled circles), 1 mM additional PP_i (open circles), or 10 mM EDTA (squares). (**F**) ATP turnover rates for various Vtc4p* mutants at 30 µM. (**G**) Cellular polyP content for Vtc4p point mutants expressed under the control of their native promoter in yeast BY4742 Δ*vtc4*. Error bars represent the standard deviation derived from three independent measurements.

enzyme, an activity that rationalizes the loss of vacuolar polyP in yeast *vtc4* deletion strains (*8*) and the concomitant increase in cellular ATP (*9*).

We located the substrate binding site in the structure of Vtc4p* crystallized in the presence of the substrate analog adenosine-5′-[(β, γ)-imido] triphosphate (AppNHp) and $MnCl_2$. Difference electron density accounts for the Mn^{2+}-bound triphosphate moiety of AppNHp, which is coordinated by seven conserved basic residues and a tyrosine in the tunnel center (Fig. 2A, and fig. S3A). The nucleoside moiety appears disordered. We can define the directionality of the nucleotide by the topology of the tunnel domain that is closed by a helical segment on one end (Fig. 1A) (*17*). To validate the unusual substrate binding mode, we quantified interaction of Vtc4p* with different nucleotides by isothermal titration calorimetry. Vtc4p* tightly interacts with ATP, as well as with other nucleoside triphosphates [dissociation constant (K_d) ranging from 0.3 to 2 μM], with a 1:1 stoichiometry and high binding enthalpy (Fig. 2B). Vtc4p* does not discriminate ATP and its 2′-deoxy form, but the absence of a γ-phosphate substantially weakens the interaction (Fig. 2B). Mutation of Arg^{264} or Arg^{266}, which contact the ATP α- and β-phosphates, to alanine decreases nucleotide binding (by a factor of 2.5 to 4) (Fig. 2B) and Vtc4p activity (Fig. 3, F and G). Their simultaneous mutation substantially impairs binding (by a factor of 20) (Fig. 2B) and inactivates Vtc4p* (Fig. 3F). Consistent with these observations, our structure reveals extensive protein contacts only with the triphosphate moiety of the nucleotide substrate (Fig. 2A).

ATP turnover is impaired in the presence of EDTA (Fig. 3E), which indicates that Vtc4p* activity requires bivalent cations. There is moderate metal ion specificity with $Mn^{2+} > Zn^{2+} > Co^{2+} > Mg^{2+} > Fe^{2+} > Ni^{2+}$ (fig. S4). The nucleotide α-, β- and γ-phosphates coordinate the Mn^{2+}, which in turn makes a bidentate interaction with Glu^{426} (Fig. 2A). Mutation of Glu^{426} reduces ATP turnover and polyP synthesis (Fig. 3, F and G). Mn^{2+} coordination in Vtc4p* differs from the previously reported octahedral binding geometry in Cet1p and other tunnel enzymes (*14*, *18*) (fig. S4).

We next addressed the catalytic mechanism employed by Vtc4p. A structure of Vtc4p* crystallized from Na^+/K^+ phosphate reveals an orthophosphate (P_i) bound close to the nucleotide binding site (Fig. 3A). Superposition with the AppNHp-bound structure shows the phosphate in this "acceptor pocket" in a binding geometry compatible with an in-line transfer of the ATP γ-phosphate in a nucleophilic displacement reaction (Fig. 3B). Consistently, we found that ATP turnover can be stimulated by "priming" the reaction with either orthophosphate (by a factor of 3 at 10 mM P_i) or pyrophosphate (by a factor of 90 at 1 mM PP_i) (Fig. 3E and fig. S5). ATP cleavage is supported by Mn^{2+} that is positioned over the terminal scissile phosphoanhydride (Fig. 2A). Mutation of Lys^{458} originating from the "helical plug" and directly facing the γ-phosphate impairs ATP turnover (Fig. 3, B and F), which suggests a role in catalysis.

To further validate the key position of the acceptor phosphate, we solved the structure of Vtc4p* cocrystallized with PP_i. The structure reveals difference density peaks in the substrate binding pocket and in the acceptor pocket. It may thus mimic Vtc4p* after the first round of ATP cleavage (Fig. 3C). Lys^{200} contacts the γ-phosphate of AppNHp (Fig. 3B) and the transferred phosphate in the acceptor pocket (Fig. 3C). Mutation of this residue to alanine reduces polyP formation and substantially enhances ATP turnover (Fig. 3, F and G), seemingly uncoupling these steps.

The substrate-bound structures suggest that the polyP complex (Fig. 1A) represents a product-bound state in the polymerization process where polyP occupies the entire tunnel domain, including the substrate binding and acceptor pockets (fig. S2B). This structure defines a path along which polyP may be transported. Several conserved basic residues align like bristles, guiding the polymer away from the active site (Fig. 3D). Notably, the tunnel domain in Vtc4p* presents itself more closed in the nucleotide-bound state, when compared with the P_i-bound structure (fig. S2C). We speculate that substrate binding and polyP transport in Vtc4p* may be driven by similar conformational changes.

We next investigated Vtc4p-catalyzed polyP formation in vivo. Yeast *vtc4* deletion strains lack the entire vacuolar polyP pool (*8*) (Fig. 3G). Point mutations in the full-length Vtc4 protein that correspond to those found essential for Vtc4p* function in vitro (R264A, R266A, K281A, E426A, and K458L) (Fig. 3F) cannot complement this deficiency (Fig. 3G). In media with limiting phosphate concentration, where the internal polyP store is used, these point mutants also arrested growth clearly faster than wild-type cells (fig. S3B). Thus, VTC accounts for most of the polyP synthesis in yeast, and the catalytic activity resides in the tunnel domain of Vtc4p.

In fungi, polyP accumulates in the vacuole and in the extracellular space (*19*). Correspondingly, we detected two VTC subcomplexes composed of Vtc1/2/4p or of Vtc1/3/4p (fig. S6). Vtc2p and 3p are catalytically impaired and appear to be accessory subunits in VTC (fig. S7). We studied green fluorescent protein (GFP)–tagged Vtc2p and 3p in yeast cells by microscopy. GFP-Vtc3p predominantly stains vacuoles on P_i-rich media as well as under low P_i conditions (Fig. 4A). In contrast, GFP-Vtc2p is only partially on vacuoles but mainly around the nucleus and at the cell periphery along the plasma membrane, where it is highly enriched in patches. Upon transfer of cells to low-phosphate medium, these patches disappear and GFP-Vtc2p concentrates on vacuoles (Fig. 4A), perhaps to maximize synthesis of the vacuolar polyP store that buffers fluctuations in exogenous phosphate (*20*). We assume that the peripheral VTC pool may generate extracellular polyP (*19*). At both membranes, the catalytic tunnel domain in VTC faces the cytoplasm (*13*), and thus the polymer must pass the membrane. Notably, all Vtcs share related transmembrane domains that contain conserved basic residues. *Vtc1* point mutations targeting these residues drastically reduce cellular polyP levels (Fig. 4B and fig. S8), while leaving VTC complexes stable and correctly sorted (fig. S6). We thus speculate that Vtc transmembrane domains participate in the transport of polyP across the membrane. Phosphate polymerization and membrane translocation would thus be orchestrated functions of VTC. Purification and

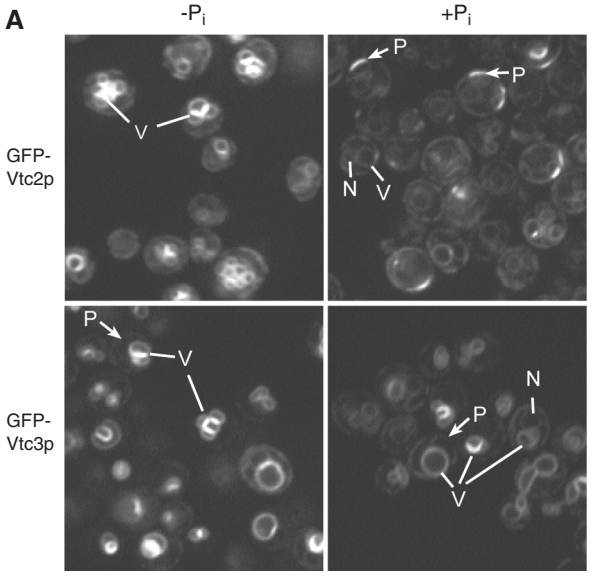

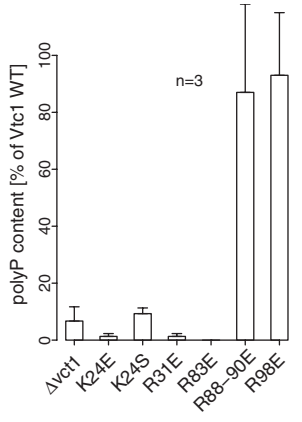

Fig. 4. Phosphate-dependent subcellular distribution of Vtc2p or 3p subcomplexes. (**A**) GFP-Vtc2p or GFP-Vtc3p integrated into strain BY4742 was expressed under the control of an ADH promoter. Logarithmically growing cells were transferred for 2 hours to phosphate-depleted yeast extract, peptone, and dextrose medium (YPD) replenished with 0 (-P_i) or 5 mM (+P_i) Na-phosphate pH 5.5 and analyzed by spinning disc microscopy. Nucleus (N), vacuole (V), and peripheral (P) concentrations are labeled. (**B**) Point mutations in the Vtc1p transmembrane domain impact cellular polyP levels. Vtc1 mutants were expressed under the control of the vtc1 promoter from pRS304 plasmids integrated into the TRP1 locus of BY4727 vtc1::HIS.

biochemical reconstitution of the entire VTC complex will be necessary to test this hypothesis.

Our identification of a eukaryotic polyP polymerase now allows investigating polyphosphate metabolism in fungi such as *Laccaria* (*21*) (fig. S9) that deliver polyP to the roots of their plant hosts, in diatoms such as *Thalassiosira* (*22*) (fig. S9), whose polyP pools form marine sediments (*5*), and in parasites where VTC is essential for osmoregulation (*23*). Because the VTC complex appears not to be conserved in animals or plants, another class of enzymes remains to be discovered that catalyzes phosphate polymerization in these organisms.

References and Notes

1. M. R. Brown, A. Kornberg, *Trends Biochem. Sci.* **33**, 284 (2008).
2. H. Javot, N. Pumplin, M. J. Harrison, *Plant Cell Environ.* **30**, 310 (2007).
3. R. Docampo, W. de Souza, K. Miranda, P. Rohloff, S. N. Moreno, *Nat. Rev. Microbiol.* **3**, 251 (2005).
4. S. J. Omelon, M. D. Grynpas, *Chem. Rev.* **108**, 4694 (2008).
5. J. Diaz *et al.*, *Science* **320**, 652 (2008).
6. K. Ahn, A. Kornberg, *J. Biol. Chem.* **265**, 11734 (1990).
7. H. Zhang, M. R. Gomez-Garcia, M. R. Brown, A. Kornberg, *Proc. Natl. Acad. Sci. U.S.A.* **102**, 2731 (2005).
8. N. Ogawa, J. DeRisi, P. O. Brown, *Mol. Biol. Cell* **11**, 4309 (2000).
9. F. M. Freimoser, H. C. Hurlimann, C. A. Jakob, T. P. Werner, N. Amrhein, *Genome Biol.* **7**, R109 (2006).
10. O. Muller *et al.*, *EMBO J.* **21**, 259 (2002).
11. J. M. Murray, D. I. Johnson, *Genetics* **154**, 155 (2000).
12. A. Cohen, N. Perzov, H. Nelson, N. Nelson, *J. Biol. Chem.* **274**, 26885 (1999).
13. O. Muller, H. Neumann, M. J. Bayer, A. Mayer, *J. Cell Sci.* **116**, 1107 (2003).
14. C. D. Lima, L. K. Wang, S. Shuman, *Cell* **99**, 533 (1999).
15. C. K. Ho, Y. Pei, S. Shuman, *J. Biol. Chem.* **273**, 34151 (1998).
16. Using recombinant Vtc4p* in vitro, we did not detect regeneration of ATP from ADP and either a polyP 3-, ~12-, or ~65-nucleotide oligomer.
17. Modeling of the nucleotide substrate in the opposite direction leads to severe clashes of the ribose and base portions with main chain atoms in the C-terminal helix in Vtc4p*. The position of this helical plug appears invariant in all crystal forms analyzed, making the helix unlikely to move upon substrate binding. Further, our assigned directionality of the nucleotide is consistent with the positions of the acceptor pocket and the polyP exit tunnel, respectively (Fig. 3, A and D, and fig. S3B).
18. N. Keppetipola, R. Jain, S. Shuman, *J. Biol. Chem.* **282**, 11941 (2007).
19. T. P. Werner, N. Amrhein, F. M. Freimoser, *Fungal Genet. Biol.* **44**, 845 (2007).
20. M. R. Thomas, E. K. O'Shea, *Proc. Natl. Acad. Sci. U.S.A.* **102**, 9565 (2005).
21. F. Martin *et al.*, *Nature* **452**, 88 (2008).
22. E. V. Armbrust *et al.*, *Science* **306**, 79 (2004).
23. J. Fang, P. Rohloff, K. Miranda, R. Docampo, *Biochem. J.* **407**, 161 (2007).
24. A. Nicholls, K. A. Sharp, B. Honig, *Proteins* **11**, 281 (1991).

25. With the exception of the AppNHp-Mn^{2+} and PP_i complexes (determined at the Salk Institute), all crystallographic work was carried out at the European Molecular Biology Laboratory. We thank J. Noel, T. Gibson, and T. A. Steitz for discussion and J. Chory for generous support. This work was funded by the Peter and Traudl Engelhorn Foundation (Penzberg, Germany) and a European Molecular Biology Organization long-term fellowship (M.H), the Boehringer Ingelheim Fonds (A.U.), the German Science Foundation and the Landesstiftung Baden-Württemberg (K.S.), the Swiss National Science Foundation (A.M, P.O.H), and the National Science Foundation (IOS-0649389 to J. Chory). We thank the staff at the European Synchrotron Radiation Facility, Grenoble, France, at the Deutsches Elektronen Synchrotron, Hamburg, Germany, and at the Advanced Light Source, Berkeley, for technical support; and C. Müller and S. Cusack for sharing beam time. Coordinates and structure factors for $Vtc2p^{183\text{-}553}$ (PDB-ID 3g3o), Vtc4p*-polyP (3g3q), Vtc4p*-AppNHp-Mn^{2+} (3g3r), Vtc4p*-P_i (3g3t), and Vtc4p*- PP_i (3g3u) have been deposited with the Protein DataBank (www.rcsb.org).

Supporting Online Material

www.sciencemag.org/cgi/content/full/324/5926/513/DC1
Materials and Methods
Figs. S1 to S9
Tables S1 and S2
References

5 November 2008; accepted 9 March 2009
10.1126/science.1168120

Homeostatic Sleep Pressure and Responses to Sustained Attention in the Suprachiasmatic Area

Christina Schmidt,[1,2*] Fabienne Collette,[1,2] Yves Leclercq,[1] Virginie Sterpenich,[1] Gilles Vandewalle,[1] Pierre Berthomier,[3] Christian Berthomier,[3] Christophe Phillips,[1] Gilberte Tinguely,[1] Annabelle Darsaud,[1] Steffen Gais,[1] Manuel Schabus,[1] Martin Desseilles,[1] Thien Thanh Dang-Vu,[1] Eric Salmon,[1] Evelyne Balteau,[1] Christian Degueldre,[1] André Luxen,[1] Pierre Maquet,[1] Christian Cajochen,[4] Philippe Peigneux[1,5*]

Throughout the day, cognitive performance is under the combined influence of circadian processes and homeostatic sleep pressure. Some people perform best in the morning, whereas others are more alert in the evening. These chronotypes provide a unique way to study the effects of sleep-wake regulation on the cerebral mechanisms supporting cognition. Using functional magnetic resonance imaging in extreme chronotypes, we found that maintaining attention in the evening was associated with higher activity in evening than morning chronotypes in a region of the locus coeruleus and in a suprachiasmatic area (SCA) including the circadian master clock. Activity in the SCA decreased with increasing homeostatic sleep pressure. This result shows the direct influence of the homeostatic and circadian interaction on the neural activity underpinning human behavior.

Maintaining optimal performance levels during evening hours may become difficult because increasing sleep propensity progressively overrides the wake-promoting circadian signal (*1*–*3*). Morning-type individuals wake up early and find it difficult to maintain performance in the evening (*4*). In contrast, evening types perform well in the evening hours (*4*) and seem to tolerate elevated sleep pressure in the evening better than morning types. Besides differences in circadian phase (*5*–*8*), morning types differ from evening types by a faster build-up of homeostatic sleep pressure during daytime (*9*) and by its faster dissipation during sleep (*10*, *11*). Taken together, these results support the notion that the circadian variation in waking performance also depends on homeostatic sleep pressure (*2*, *12*, *13*). Using functional magnetic resonance imaging (fMRI) in extreme chronotypes, we investigated the neural correlates of performance in the psychomotor vigilance task (PVT) (*14*–*16*), a simple reaction-time task that probes the ability to maintain sustained attention (*14*), which is modulated by circadian and sleep homeostatic regulatory processes (*17*).

Young, healthy participants of extreme morning (n = 16) or evening (n = 15) typology (*18*) were matched at the group level according to age, sex, and educational level and did not differ in their anxiety and depression levels or in sleep quality and daytime sleepiness (all P values > 0.1) (table S1). Participants were instructed to live according to their own preferred sleep-wake schedule for at least 1 week before the study (*16*). Afterwards, they reported to the sleep laboratory for two consecutive nights, where they were monitored by polysomnography at their preferred bedtimes (Fig. 1). The laboratory protocol started 7 hours before their habitual sleep time, which allowed for hourly assessments of subjective sleepiness (*19*) and objective vigilance (*14*), as well as hourly collections of saliva samples for assessment of circadian melatonin phase (*16*).

On average, bedtime, wake time, and circadian phase [estimated by the melatonin midrange crossing (MRC) time (*16*)] were about 4 hours earlier in morning than in evening types (all P values < 0.05) (table S1). These results indicate circadian phase entrainment with a similar phase angle (i.e., similar distance between MRC and bedtimes, P > 0.2) (table S1) in both chronotypes. One and a half hours (morning session) after scheduled awaken-

[1]Cyclotron Research Centre, University of Liège, 4000 Liège, Belgium. [2]Cognitive and Behavioral Neuroscience Centre, University of Liège, 4000 Liège, Belgium. [3]PHYSIP S.A., 75011 Paris, France. [4]Centre for Chronobiology, Psychiatric Hospital of the University of Basel, CH-4025 Basel, Switzerland. [5]Neuropsychology and Functional Neuroimaging Research Unit (UR2NF), Université Libre de Bruxelles, B-1050 Brussels, Belgium.

*To whom correspondence should be addressed. E-mail: Christina.Schmidt@ulg.ac.be and Philippe.Peigneux@ulb.ac.be

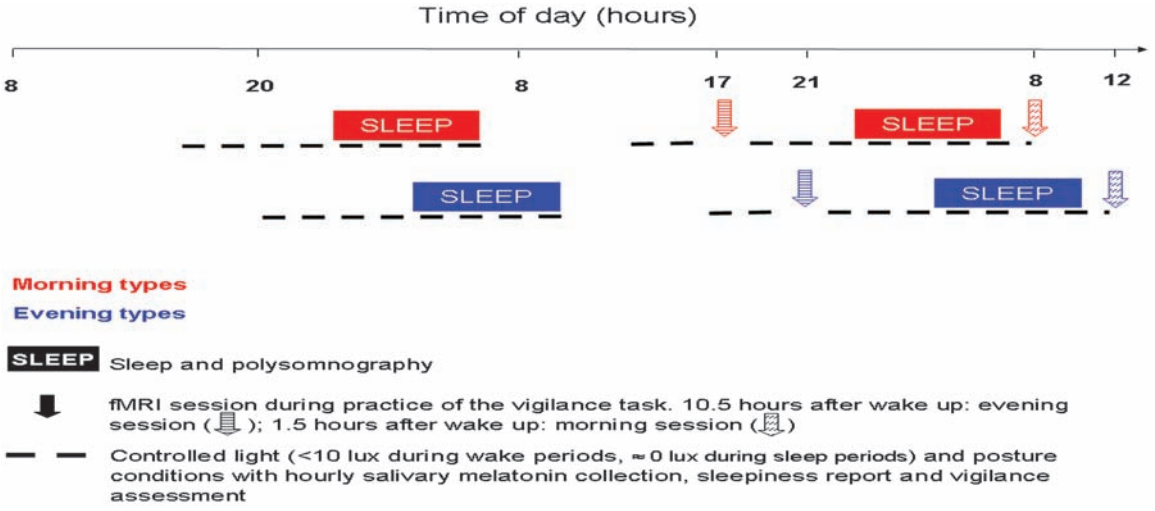

Fig. 1. Overview of the experimental design with sample time schedule for morning (red) and evening (blue) types. Subjects came to the laboratory 7 hours before scheduled sleeping time and stayed for two consecutive nights monitored via polysomnography. They stayed under controlled light (dashed line, <10 lux for wake periods, ≈ 0 lux for sleep periods) conditions and body posture. During the wake periods, sleepiness and vigilance measures were collected at hourly intervals and hourly saliva samples were assessed for melatonin. One and a half (morning session) and 10 and a half (evening session) hours after scheduled wake-up time and in a counterbalanced order, subjects underwent an fMRI session during the performance of the PVT task.

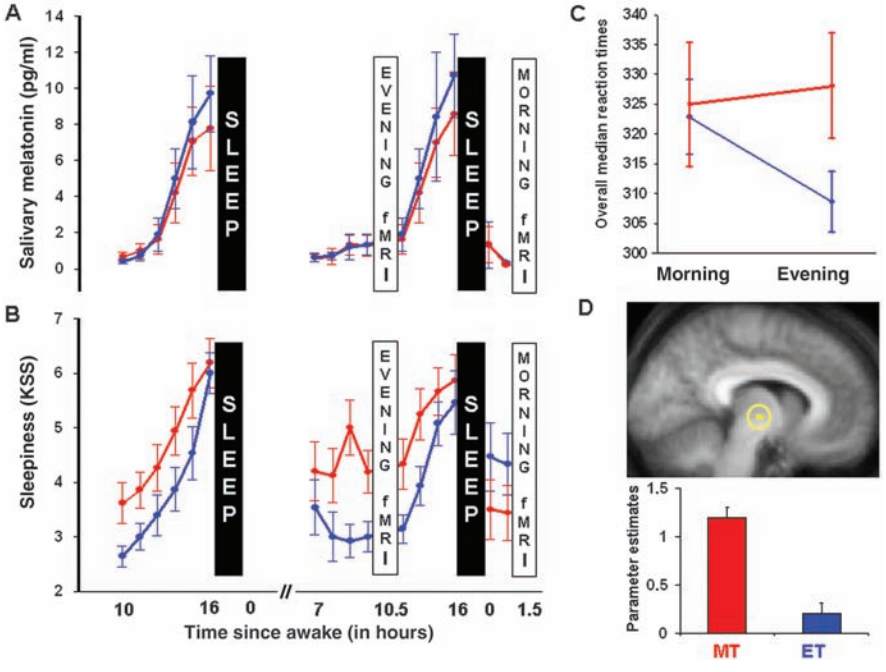

Fig. 2. (**A**) Time course of salivary melatonin in morning (red line) and evening (blue line) chronotypes. Hours spent since waking up throughout the protocol versus salivary melatonin as assessed by direct double-antibody radioimmunoassay. (**B**) Time course of daytime sleepiness (±SEMs) in morning (red line) and evening (blue line) chronotypes. Hours spent since waking up throughout the protocol versus self-reported values of sleepiness on the Karolinska Sleepiness Scale (KSS; higher scores correspond to increased sleepiness levels). (**C**) Overall median reaction times (±SEMs) according to time of day (morning versus evening) and chronotype (blue line: evening types, red line: morning types). (**D**) Increased thalamic response in morning as compared with evening types during the evening session. Display shows areas where blood oxygen level–dependent (BOLD) response is associated with the main effect of chronotype during the evening session for global alertness. Functional results are displayed at $P > 0.001$, uncorrected threshold, over the mean normalized structural magnetic resonance (MR) image of the population. Corresponding parameter estimates (arbitrary units) are plotted below the display [red, morning types (MT); blue, evening types (ET)].

ing, participants underwent a fMRI session during which they performed a PVT. The same protocol was administered 10.5 hours (evening session) after wake up on the other day (Fig. 1). This individually tailored design ensured equal amounts of time spent awake across chronotypes for the morning and the evening fMRI sessions, respectively.

The time course of salivary melatonin showed similar profiles according to the time spent awake in both morning and evening types (Fig. 2A) (interaction chronotype × melatonin profile: $P > 0.5$), which indicated comparable entrainment to the 24-hour cycle. Previously reported shorter circadian cycle length in morning than evening types (*20*) could potentially lead to a more advanced point of their circadian cycle after 10.5 hours of time spent awake, which would lead to a decreased circadian countersignal in morning types during the subjective evening hours. Although we cannot rule out such a possibility, our data do not indicate this, and we assume that both morning and evening types were tested at similar circadian phases during the morning and evening sessions.

The order of the morning and evening sessions was counterbalanced across subjects, and each scanning session was preceded by dim light conditions for at least 4 hours (<10 lux) (Fig. 1) to avoid the effects of bright light on circadian entrainment (*21*). During the evening fMRI session, evening types were less sleepy ($P < 0.05$) (Fig. 2B) (*16*) and tended to perform faster than morning types (overall median reaction times (RTs) ($P = 0.06$) (Fig. 2C) (*16*). No significant group differences in subjective sleepiness and sustained attention performance were observed for the morning session [all P values > 0.5 (*16*)]. These data indicate that under conditions of self-selected sleep-wake schedules, behavioral differences between chronotypes mostly prevail in the subjective evening hours, when the circadian wake-promoting signal has to counteract the homeostatic sleep pressure achieved after a normal waking day (*3*).

Our analyses of fMRI data tried to determine the neural correlates of successful sustained attention during the evening session, based on two behavioral measures that reflect different facets of attention. Trials associated with intermediate RTs (percentile 10 < RTs < percentile 90) corresponded to an average alertness level required to perform the task in a satisfactory manner, which is not compromised by the slowest RTs or by lapses associated with momentary task disengagement (*15*). We will refer to it as global alertness, deemed to be particularly sensitive to detect early effects of growing sleep pressure (*22*). In contrast, trials associated with fastest RTs reflect optimum response capabilities (*15*) that can be phasically recruited

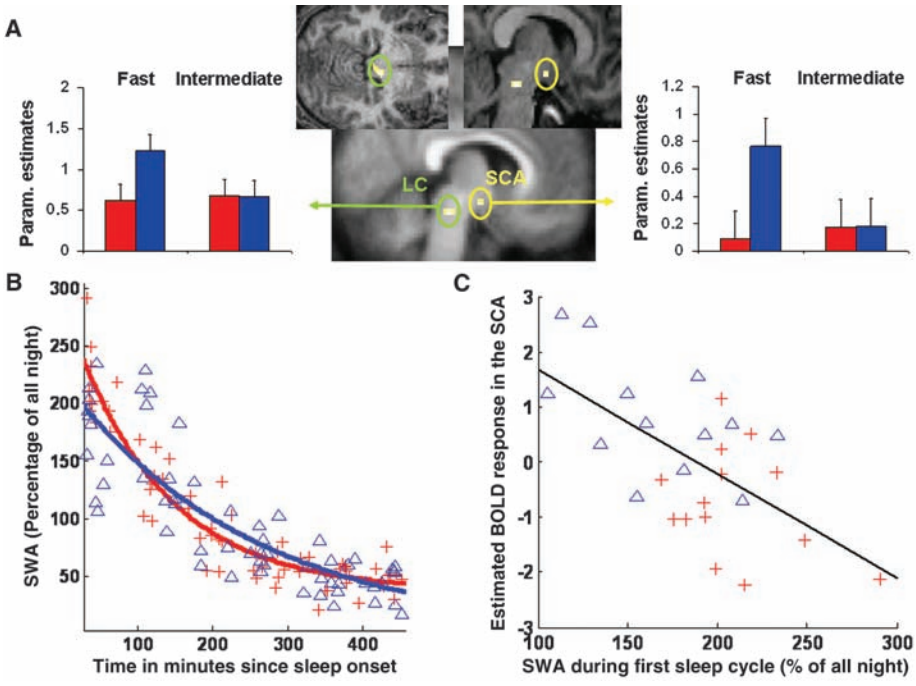

Fig. 3. (**A**) Increased task-related response in the dorsal pontine tegmentum and the anterior hypothalamus, compatible with the LC and SCA, respectively, in evening as compared with morning chronotypes during the subjective evening. Display shows areas where BOLD activity is associated with the main effect of chronotype during the evening session for optimal alertness. Functional results are displayed at $P > 0.001$, uncorrected threshold, over the mean normalized structural MR image of the population. Corresponding parameter estimates (arbitrary units) are displayed for event indicators of fast and intermediate reaction times (red, morning types; blue, evening types). (**B**) Exponential decay function [$SWA_t = SWA_\infty + SWA_0 \times e^{-rt}$ (*16*)] adjusted on relative SWA in sleep cycles (NREM sleep) measured from the central frontal derivation for all-night EEG of the night preceding the evening scan acquisition. Red crosses, morning types; blue triangles, evening types. SWA0 and *r* values are significantly higher in morning relative to evening types ($P > 0.05$). (**C**) Regression analysis of the relation between estimated BOLD responses during optimal task performance in the SCA region and the amount of SWA during the first sleep cycle in the preceding night ($r = 0.54$, $P < 0.05$, $n = 27$). Red crosses, morning types; blue triangles, evening types.

above and beyond the baseline cognitive level set by global alertness. To characterize this optimal vigilance component, fastest RTs (< percentile 10) were contrasted with intermediate RTs, which constituted an adequate global vigilance baseline.

Global alertness during the evening session was associated with larger responses in the thalamus in morning than in evening types (Fig. 2D, and table S4) (see table S3 for main effects of the task during the evening session). A similar enhancement of thalamic response by attention has been observed after sleep deprivation [e.g., (*23, 24*)]. No brain responses related to global alertness were significantly larger in evening than morning types during the subjective evening. In contrast, responses associated with optimal alertness were enhanced in evening relative to morning types, in a dorsal pontine tegmentum area and an anterior hypothalamic region. These areas encompass the locus coeruleus (LC) and the suprachiasmatic area (SCA), respectively (Fig. 3A, and table S4), two anatomically connected structures deeply involved in the circadian signal that promotes wakefulness and potentially regulates cognitive output during the waking state (*25*). These responses might result from differences in the ability to cope with increasing time spent awake during the subjective evening hours of a normal waking day, as already suggested by differences in subjective sleepiness levels (Fig. 2B). To test this hypothesis, we computed the slow wave activity (SWA; power spectral activity between 1 and 4 Hz) during non–rapid eye movement (NREM) sleep on the night preceding the evening scan session (*16*). The SWA observed during the first NREM sleep episode was considered to be a reliable estimate of the homeostatic sleep pressure (*26*, *27*) faced by the participant while performing the PVT during the fMRI evening session (see SOM (*16*)). In the frontal derivation, known to be most sensitive to variations in homeostatic sleep pressure (*28*), relative SWA was higher in morning than evening types at the beginning of the night (Fig. 3B) ($P < 0.05$) (*16*). SWA dissipation in the course of the night was also faster in morning than evening types (Fig. 3B) ($P < 0.05$) (*16*) resulting in similar SWA levels at the end of the night for both chronotypes ($P > 0.5$) (Fig. 3B) (*16*).

These findings confirm that morning and evening chronotypes differ in important parameters of sleep homeostasis. Furthermore, homeostatic sleep pressure turned out to be related to regional brain responses elicited by the PVT during the evening session, which might account for observed behavioral differences between groups. An independent regression analysis revealed that activity in the SCA was inversely proportional to the mean SWA recorded during the first NREM sleep episode (table S4 and Fig. 3C). This result suggests that activity in an area that includes the circadian master clock has a negative relation with indicators of sleep homeostatic pressure. It echoes similar findings obtained using long-term multiunit recordings of the suprachiasmatic nucleus (SCN) in rodents, which reported a decrease in SCN neuronal activity under conditions of increased sleep pressure (*29*). Conversely, lesions of the SCN in nonhuman primates resulted in an increase in total sleep time (*3*). These results indicate a direct interaction between sleep homeostasis and circadian rhythms in anterior hypothalamic areas. Consequently, we suggest that one of the key mechanisms accounting for behavioral differences between extreme chronotypes is that optimal alertness of morning-type individuals is jeopardized in the evening, because of a more pronounced negative influence of sleep homeostasis onto anterior hypothalamic structures involved in circadian regulation. Alternatively, it may be due to a lower circadian influence on sleep homeostasis arising from anterior hypothalamic areas. The ensuing decrease in local SCA activity is associated with decreased activity in brainstem structures promoting wakefulness, such as the LC, thereby diminishing their activating influence on the whole forebrain.

References and Notes

1. S. Daan, D. G. M. Beersma, A. A. Borbély, *Am. J. Physiol.* **246**, R161 (1984).
2. D. J. Dijk, J. F. Duffy, C. A. Czeisler, *J. Sleep Res.* **1**, 112 (1992).
3. D. M. Edgar, W. C. Dement, C. A. Fuller, *J. Neurosci.* **13**, 1065 (1993).
4. J. A. Horne, C. G. Brass, A. N. Pettitt, *Ergonomics* **23**, 29 (1980).
5. G. A. Kerkhof, H. P. Van Dongen, *Neurosci. Lett.* **218**, 153 (1996).
6. J. F. Duffy, D. J. Dijk, E. F. Hall, C. A. Czeisler, *J. Investig. Med.* **47**, 141 (1999).
7. E. K. Baehr, W. Revelle, C. I. Eastman, *J. Sleep Res.* **9**, 117 (2000).
8. V. Mongrain, S. Lavoie, B. Selmaoui, J. Paquet, M. Dumont, *J. Biol. Rhythms* **19**, 248 (2004).
9. J. Taillard, P. Philip, O. Coste, P. Sagaspe, B. Bioulac, *J. Sleep Res.* **12**, 275 (2003).
10. G. A. Kerkkof, *Electroencephalogr. Clin. Neurophysiol.* **78**, 197 (1991).
11. V. Mongrain, J. Carrier, M. Dumont, *Eur. J. Neurosci.* **23**, 497 (2006).
12. J. K. Wyatt, A. Ritz-De Cecco, C. A. Czeisler, D. J. Dijk, *Am. J. Physiol. Regul. Integr. Comp. Physiol.* **277**, R1152 (1999).
13. C. Cajochen, S. B. Khalsa, J. K. Wyatt, C. A. Czeisler, D. J. Dijk, *Am. J. Physiol.* **277**, R640 (1999).
14. D. F. Dinges, J. W. Powell, *Behav. Res. Methods Instrum. Comput.* **17**, 625 (1985).
15. S. P. Drummond *et al.*, *Sleep* **28**, 1059 (2005).
16. Supplementary methods and results are available as supporting material on *Science* Online.
17. J. Lim, D. F. Dinges, *Ann. N. Y. Acad. Sci.* **1129**, 305 (2008).
18. J. A. Horne, O. Östberg, *Int. J. Chronobiol.* **4**, 97 (1976).
19. T. Akerstedt, M. Gillberg, *Int. J. Neurosci.* **52**, 29 (1990).
20. J. F. Duffy, D. W. Rimmer, C. A. Czeisler, *Behav. Neurosci.* **115**, 895 (2001).
21. C. Gronfier, K. P. Wright Jr., R. E. Kronauer, C. A. Czeisler, *Proc. Natl. Acad. Sci. U.S.A.* **104**, 9081 (2007).
22. P. Graw, K. Krauchi, V. Knoblauch, A. Wirz-Justice, C. Cajochen, *Physiol. Behav.* **80**, 695 (2004).
23. C. M. Portas *et al.*, *J. Neurosci.* **18**, 8979 (1998).

24. D. Tomasi *et al.*, *Cereb. Cortex* **19**, 233 (2009).
25. G. Aston-Jones, S. Chen, Y. Zhu, M. L. Oshinsky, *Nat. Neurosci.* **4**, 732 (2001).
26. D. J. Dijk, D. G. Beersma, S. Daan, *J. Biol. Rhythms* **2**, 207 (1987).
27. L. A. Finelli, H. Baumann, A. A. Borbely, P. Achermann, *Neuroscience* **101**, 523 (2000).
28. C. Cajochen, R. Foy, D. J. Dijk, *Sleep Res. Online* **2**, 65 (1999).
29. T. Deboer, L. Detari, J. H. Meijer, *Sleep* **30**, 257 (2007).
30. This study was supported by the Belgian Fonds National de la Recherche Scientifique (FNRS), the Fondation Médicale Reine Elisabeth, and the University of Liège. C.S., F.C., Y.L., V.S., G.V., C.P., G.T., A.D., M.D., T.T.D.V., E.S., E.B., and P.M. were supported by the FNRS. M.S. was supported by and Austrian Science Fund Erwin-Schrödinger Fellowship J2470-B02. C.S. was supported by the LUNDBECK-BCNBP grant, P.B. and C.B. are cofounders, employees, and shareholders of PHYSIP company, which setup Aseega software, C.C. was supported by grants from the Swiss National Science Foundation and the Daimler-Benz Foundation. P.P. was supported until 2006 by the Pôle d'Attraction Interuniversitaire (PAI/P504).

Supporting Online Material
www.sciencemag.org/cgi/content/full/324/5926/516/DC1
Materials and Methods
SOM Text
Fig. S1
Tables S1 to S5
References

17 October 2008; accepted 6 March 2009
10.1126/science.1167337

Intuition and Deliberation: Two Systems for Strategizing in the Brain

Wen-Jui Kuo,[1]* Tomas Sjöström,[2]* Yu-Ping Chen,[3] Yen-Hsiang Wang,[4] Chen-Ying Huang[3]†

Dual-process theories distinguish between intuition (fast and emotional) and reasoning (slow and controlled) as a basis for human decision-making. We contrast dominance-solvable games, which can be solved by step-by-step deliberative reasoning, with pure coordination games, which must be solved intuitively. Using functional magnetic resonance imaging, we found that the middle frontal gyrus, the inferior parietal lobule, and the precuneus were more active in dominance-solvable games than in coordination games. The insula and anterior cingulate cortex showed the opposite pattern. Moreover, precuneus activity correlates positively with how "effortful" a dominance-solvable game is, whereas insula activity correlates positively with how "effortless" a coordination game is.

There are games in which, given sufficient computational capacity, each player can determine an optimal strategy using only the mathematical structure of the game. Checkers is a typical example; if each player plays optimally, then checkers must end in a draw (*1*). There are other games, though, in which players are required to coordinate their actions, and this requires a "meeting of the minds" that is not amenable to mathematical analysis. In this study, we contrast dominance-solvable games, where finding an optimal strategy is purely a mathematical problem, with pure coordination games, where successful play requires the players to go beyond the mathematics of the game (*2*).

A strategy is "dominated" if it is always worse than another strategy. Rational players eliminate all dominated strategies from consideration, creating a new game with fewer strategies, some of which may again be dominated. If this process can be iterated until a unique strategy remains for each player, then the game is dominance-solvable. Implementing this game-theoretic textbook procedure of step-by-step deliberation would likely require neural structures underlying cognitive processing, reasoning, and memory maintenance.

In a pure coordination game, each player's objective is simply to match the action of the other player (without communicating) (*3*). In "Nash equilibrium," both players choose the same action, but it is not possible to determine mathematically which action to choose, that is, on which Nash equilibrium to coordinate. In (*4*), participants were asked to name (among other things) a color, a number, and a year. When rewards did not depend on their answers, blue and red were about equally popular colors; the most popular numbers were 7, 2, and 10; and only 6.8% named the current year. However, when the game was turned into a pure coordination game, by rewarding those who matched the choices of others, red became by far the most frequent color, 1 the most frequent number, and 61.1% named the current year. Red, 1, and the current year had become "focal points," objects with "symbolic or connotative characteristics that transcend the mathematical structure of the game" (*5*). Automatic (fast, effortless) recognition of salient characteristics of complex high-dimensional objects is typical of intuitive judgments (*6*). Focal points must have properties that each participant recognizes as being salient not only to herself but also to others, but this too may be at least partly an intuitive judgment, using salience to oneself as an input. In general, intuition and deliberative reasoning are mental processes with very different properties. Intuition is fast, automatic, emotional, and effortless. Reasoning is slow, rule-governed, controlled, and effortful (*7*).

We designed two kinds of games, number games and box games. A dominance-solvable number game is shown at the top of Fig. 1A. Two players, X ("you") and Y ("other"), simultaneously pick a number from 0, 1, 2, or 3, without communicating. Each player's objective is to be as close as possible to a "target number." The instruction "other: you" means Y's target is "the number chosen by X," so Y wants to match X's choice. The instruction "you: other+1" means X's target is "one plus the number chosen by Y." A player who achieves her objective receives a reward [supporting online material (SOM), S1.2].

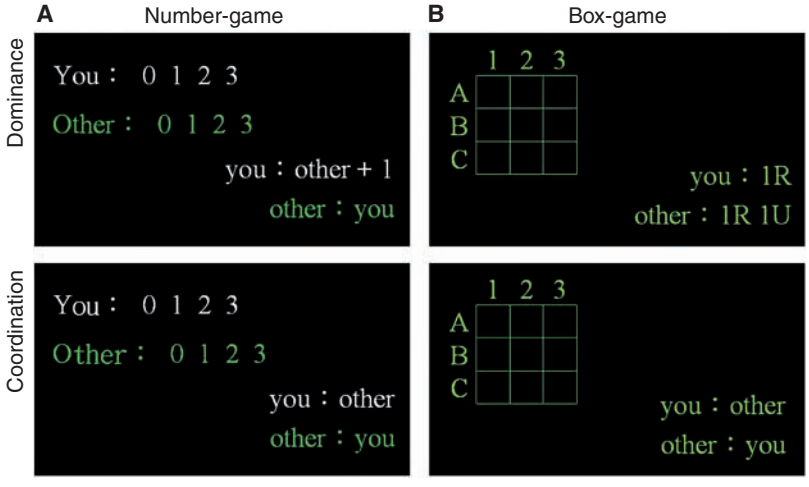

Fig. 1. Sample screens from the experiment. There are two conditions in the experiment: dominance-solvable games and pure coordination games. The condition in the top row is the dominance-solvable game and that in the bottom row is the pure coordination game. Targets of both players are shown in the lower right corner of each screen. In each game, each participant's objective is to be as close as possible to her target, which in turn depends on the choice of the other player (SOM, S1.2). There are two treatments. (**A**) In the number-game treatment, participants have to choose one number. (**B**) In the box-game treatment, participants have to choose one box.

[1]Institute of Neuroscience, National Yang-Ming University, Taipei, Taiwan. [2]Department of Economics, Rutgers University, New Brunswick, NJ 08901, USA. [3]Department of Economics, National Taiwan University, Taipei, Taiwan. [4]Department of Electrical Engineering, National Taiwan University, Taipei, Taiwan.

*These authors contributed equally to this work.
†To whom correspondence should be addressed. E-mail: chenying@ntu.edu.tw

For example, if X chooses 1 and Y chooses 0, then only X is rewarded. Because X's target is at least 1, choosing 0 is dominated for X and should be eliminated. This makes 0 dominated for Y, who wants to match X's choice. Eliminating 0 for Y makes X's target at least 2, so eliminates 1 for X. Three more steps lead to the formal game-theoretic solution: Each player chooses 3 (SOM, S1.3). To obtain a pure coordination game, we modify the rules slightly to make each player's target the other player's chosen number (Fig. 1A, bottom). In the new game, there is no formal game-theoretic reason to choose one number over another.

A dominance-solvable box game is displayed at the top of Fig. 1B. Two players, X ("you") and Y ("other"), simultaneously choose a box in a 3 by 3 matrix by picking a letter indicating row A, B, or C and a number indicating column 1, 2, or 3. For example, A3 is the box in the northeast corner of the matrix. The instruction "you: 1R" means X's target is "the box to the right of Y's choice." Similarly, the instruction "other: 1R 1U" means Y's target is "the box to the right of and above player X's choice" (SOM, S1.2). For example, if X chooses B1 and Y chooses A2, then only Y gets a reward. The game-theoretic solution is A3 for each player (SOM, S1.3). To obtain a pure coordination game, we make each player's target the box chosen by the other player (Fig. 1B, bottom).

Using functional magnetic resonance imaging (fMRI), we scanned 21 participants when they played games against a pool of students (SOM, S1). We used two experimental treatments: number game and box game. Each treatment had two conditions: dominance-solvable and pure coordination. All games were slight variations of the games shown in Fig. 1 (table S1). Each participant played 40 dominance-solvable and 40 pure coordination games. Response times were significantly faster in coordination games than in dominance-solvable games, consistent with the idea that intuitive decisions are faster than step-by-step deliberations (*8*) (SOM, S2.7). The games were displayed using the intuitive graphics of Fig. 1, which we hoped would help the comprehension of the games. The behavioral results are consistent with this (SOM, S2). In dominance-solvable games, our participants picked the game-theoretic solution 79.26% of the time. In coordination games, when participants' choices were paired with the modal responses from the pool of students, coordination was achieved 69.92% of the time. When randomly paired with a pool student, participants chose the "best response" (the strategy which yielded a reward) in 66.97% of the dominance-solvable games and in 46.10% of the pure coordination games. If choice had been completely random, participants would have earned rewards in only 21.24% of the dominance-solvable games and in only 18.66% of the pure coordination games. The P value of Pearson's chi-square test on whether participants' choices were uniformly random is 0.00 for both dominance-solvable and pure coordination games. Previous experiments have suggested that players do not complete more than two or three steps of iterated elimination of dominated strategies (*9*). Our participants did better, perhaps due to the intuitive displays. The impressive feats of tacit coordination are consistent with (*4*).

Comparing dominance-solvable games with coordination games, higher activation was found bilaterally in the frontal and parietal regions. In the frontal cortex, the most prominent area of activation lies in the middle frontal gyrus, extending upward to the superior frontal gyrus. In the parietal cortex, activation was observed in precuneus and inferior parietal lobule. In the left inferior parietal activation, it reaches downward to the angular gyrus (Fig. 2 and table S2). Previous studies found frontoparietal activity when tasks required attention, conscious perception, reasoning, or memorizing (*10*). For instance, frontoparietal activation is observed when contrasting logical reasoning with tasks in which reasoning is not required (*11*), contrasting challenging reasoning tasks with straightforward ones (*12*), or contrasting a meaningful middle game position with a random game position in chess (*13*). The higher frontoparietal activation in dominance-solvable games squares well with these previous studies, because the textbook solution procedure requires a sequence of reasoning steps. In each step, the player eliminates dominated strategies, holds remaining strategies in mind, and then iterates.

Working memory is crucial for problem solving, reasoning, and planning (*14*, *15*). It allows the temporary retention and manipulation of information in a system of limited capacity (*16*). The working memory model contains a central executive system for control and two subsystems for maintaining verbal and visuospatial information. Frontoparietal activation in dominance-solvable games can be interpreted according to this model. First, the participant must verbally encode and hold in mind the targets of both players (*17*). The inferior parietal lobule has been implicated in verbal memory storage and may serve this purpose (*18*, *19*). Eliminating dominated strategies presumably engages the central executive, which is hypothe-

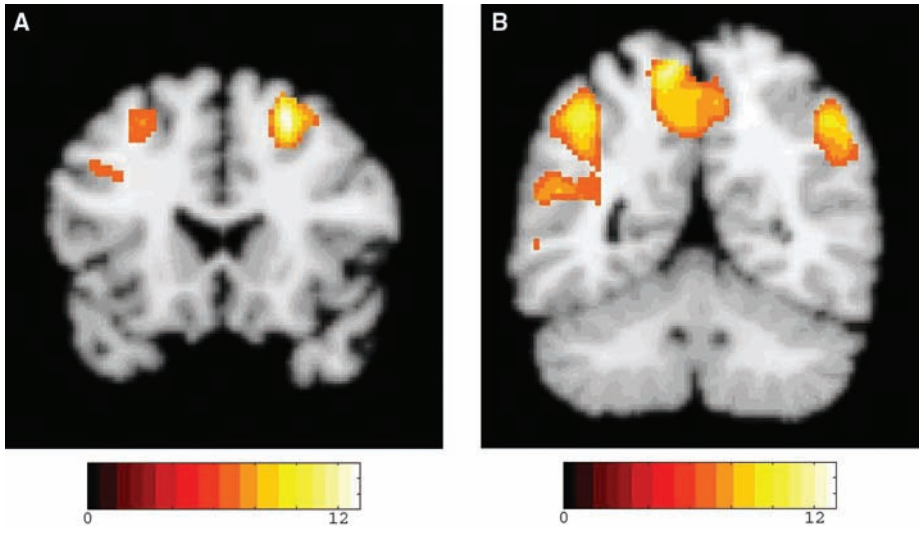

Fig. 2. Regions showing greater activation in dominance-solvable games than in pure coordination games [$P < 0.05$, corrected (family-wise)] (SOM, S4.1 and table S2). (**A**) Activation in bilateral middle frontal gyri ($y = 19$). (**B**) Activation in bilateral inferior parietal lobules and precuneus ($y = -54$).

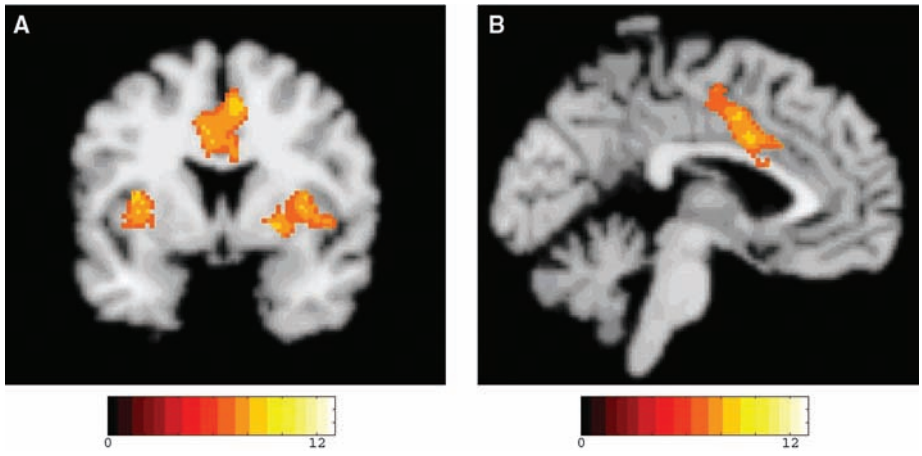

Fig. 3. Regions showing greater activation in pure coordination games than in dominance-solvable games [$P < 0.05$, corrected (family-wise)] (SOM, S4.1 and table S3). (**A**) Activation in bilateral insulae ($y = 4$). (**B**) Activation in ACC ($x = -2$).

sized to manipulate the contents of storage. The activation of the middle frontal gyrus may relate to this, as it is thought to execute goal-directed operations (*18*, *20*, *21*). Posterior parietal cortex plays a role in visuospatial working memory (*18*, *21*). The precuneus, the medial portion of the posterior parietal cortex, may be related to imagery (mental representations of objects that are not perceptually present) and memory retrieval (*22*–*25*). Keeping track of eliminated strategies may require generating and keeping in mind a mental image which must be retrieved in each step of elimination. We caution that the iterated elimination is a complex algorithm, and neatly mapping it onto the working memory model is speculative. Also, some participants may have deviated from the algorithm. However, working memory may still have been important. Post-scan interviews strongly suggested that the participants used deliberative mathematical reasoning in dominance-solvable games (SOM, S6). Most explicitly stated that they would keep in mind both targets, going back and forth, and eliminating strategies.

Among the areas showing greater activation for coordination games than for dominance-solvable games were bilateral insulae and anterior cingulate cortex (ACC) (Fig. 3 and table S3). The activation in the insular cortex lies in the middle insula, extending mostly toward the posterior insula. In the cingulate, the activation extends from the caudal ACC to the cingulate motor area (CMA) and the supplementary motor area (SMA). The insula has previously been implicated in subjective prereflective and reflective representations of ongoing changes in internal bodily and feeling states (*26*). The ACC seems to act as a conflict monitor when tasks require attention, novel or open-ended responses, or when cognitive uncertainty exists (*27*). These areas are also activated in many paradigms with strong social content or emotions, such as when participants contemplate cooperating instead of competing with another person (*28*), when they judge other persons to be trustworthy instead of being untrustworthy (*29*), or when they experience social emotions such as empathy (*30*) or love (*31*). These emotions might have evolved to ensure quick response to the factors arousing them in the presence of many stimuli. Many social interactions involve myriad stimuli but demand immediate decisions. Rapid processing and extraction of the most salient aspects of complex situations is characteristic of intuitive decision-making. Deciding within the context of a coordination game which Nash equilibrium has the most salient characteristics requires rapid processing of various cultural connotations as well as geometric symmetry, centrality or even mathematical oddity (SOM, S7.2). The insula and ACC might be part of a general network contributing to a quick and flexible evaluation of complex multidimensional experiences, and this may be the common denominator between our coordination games and the earlier experiments on social decision-making (*32*).

The key to coordination may be the ability to make judgments of salience common to both. That is, the participant must identify features that are likely to be salient not only to herself but also to the pool student. Nevertheless, mentally simulating the pool student's judgment of salience may require the participant to use her own intuitive judgment of salience as an input. A model suggests that the middle insula receives inputs about the physiological condition of the body from the posterior insula and integrates this with salient environmental stimuli (*33*). It has also been suggested that insula and ACC are a part of a general network that responds to varied forms of personal salience (*34*). For instance, the posterior insula and the SMA/CMA are shown to be responsive to changes of many sensory modalities (*35*), whereas the anterior insula and ACC are sensitive to novelty (*36*). A study using single-cell recording in the caudal ACC indicates that neurons in caudal ACC respond differentially to high-conflict and low-conflict tasks (*37*). These studies all point to a possible role of insula and ACC in identifying salience and provide support for the hypothesis that the higher activation we observe is due to participants extracting salient features in order to coordinate. A recent study of functional connectivity between the insula and the cingulate also agrees with our finding (*38*).

The textbook procedure for dominance-solvable games requires a well-defined number of steps (SOM, S2.3). If participants use this procedure, then the activation of the frontoparietal network might correlate with the required number of steps. For coordination games, the normalized coordination index (NCI) measures how well coordination is achieved (*39*) (SOM, S2.5). A high NCI may reflect the existence of an obvious focal point. If activation of the insula or ACC reflects the "gut feeling" aroused by a salient focal point, then it might correlate with the NCI. To investigate these hypotheses at the trial-by-trial level, a second model was built. We divided the 40 dominance-solvable games into 20 "hard" and 20 "easy" games, depending on the number of steps required. Similarly, 20 coordination games with high NCI were classified as "highly focal," and 20 games with low NCI were "less focal." In the

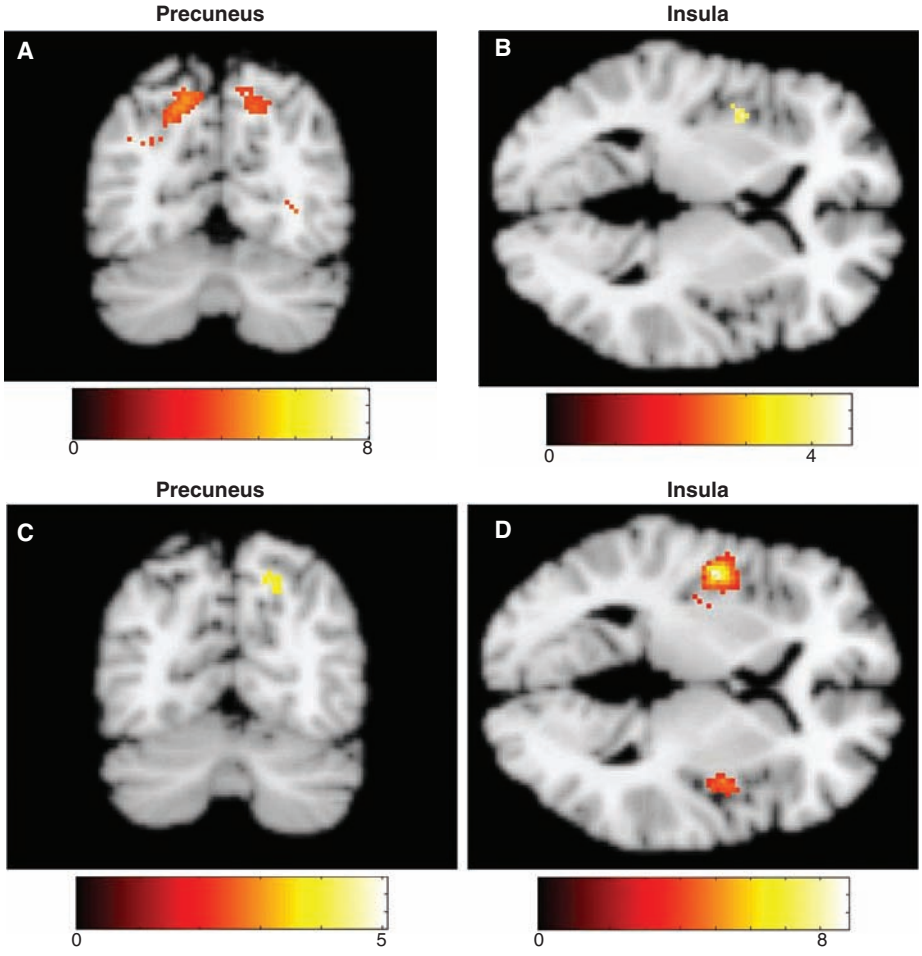

Fig. 4. Activations related to classifications within a condition ($P < 0.001$, uncorrected; cluster size greater than 10 voxels) (SOM, S5). (**A**) Activation in precuneus (y = −66) for the contrast of hard dominance-solvable games with easy dominance-solvable games (table S10). (**B**) Activations in insula ($z = 4$) for the contrast of highly focal coordination games with less focal coordination games (table S11). (**C**) Activation in precuneus ($y = -68$) is negatively correlated with a participant's probability of obtaining a reward in dominance-solvable games (table S12). (**D**) Activation in insula ($z = 4$) is positively correlated with a participant's probability of obtaining a reward in pure coordination games (table S13).

second model, the two main conditions were parametrically modulated by the two categories, respectively (SOM, S5.1). The activation of the precuneus was higher for hard dominance-solvable games than for easy ones (Fig. 4A and table S10). The activation of the insula was higher for the highly focal coordination games than for less focal ones (Fig. 4B and table S11). Previous studies also found that precuneus activity increased when the number of planned moves increased (*40*, *41*). The higher demand for memory-related imagery and memory retrieval may explain the greater precuneus activation in hard dominance-solvable games. In highly focal coordination games, the participants may have felt quite strongly that the pool students must notice the same salient feature. This may explain why insula activation correlates with NCI.

Participants might have disagreed about which games were difficult. We built a third model to investigate whether the frontoparietal activation correlates with how hard a dominance-solvable game is and whether the activation in insula and ACC correlates with how easy a coordination game is. Here, the two main conditions were parametrically modulated by each participant's probability of obtaining a reward in each game (SOM, S2.2 and S5.2). We found a negative correlation between the activation of the precuneus and the participant's probability of obtaining a reward in dominance-solvable games (Fig. 4C and table S12), which suggests that dominance-solvable games that yielded lower payoffs presented harder mental challenges. In a previous study on working memory, precuneus activity positively correlated with response times, a measure of mental effort (*24*). Both findings are consistent with the interpretation that subjective measures reflecting harder tasks (higher efforts) correlate with activation in precuneus. A positive correlation between insula activation and the participant's probability of obtaining a reward again suggests that coordination games with a highly salient feature strongly activated the "gut feeling" reported by many participants (Fig. 4D and table S13). A previous study found that the subjective rating of "chills intensity" in music correlates with activation of insula (*42*). Both findings are consistent with the interpretation that the subjective intensity of how salient a stimulus is correlates with activation in insula.

As mentioned, choices were made significantly faster in coordination games than in dominance-solvable games. The results of the second and third models provide additional support for the idea that intuitive and deliberative mental processes have quite different properties. The "slow and effortful" process was more heavily taxed when the dominance-solvable games were harder. The "fast and effortless" process was more strongly activated when coordination was easy.

References and Notes

1. J. Schaeffer *et al.*, *Science* **317**, 1518 (2007).
2. Previous fMRI studies of game-playing include Gallagher et al. (*43*) and Bhatt and Camerer (*44*), but they address different issues. In particular, Bhatt and Camerer found higher insula and ACC activity when comparing choices to first-order beliefs in dominance-solvable games.
3. We are considering here coordination without visual or other contact. Nonhuman primates seem able to coordinate their actions (simultaneously pulling on bars to obtain food) when they are in visual contact (*45*).
4. J. Mehta, C. Starmer, R. Sugden, *Am. Econ. Rev.* **84**, 658 (1994).
5. T. Schelling, *J. Conflict Resolution* **2**, 203 (1958), p. 211.
6. D. Kahneman, *Am. Psychol.* **58**, 697 (2003).
7. K. Stanovich, R. West, *Behav. Brain Sci.* **23**, 645 (2000).
8. A. Rubinstein, *Econ. J.* **117**, 1243 (2007).
9. See (*46*). In our experiment, the average number of steps required to find out the game-theoretic solution for all 40 dominance-solvable games is 3.675.
10. R. Jung, R. Haier, *Behav. Brain Sci.* **30**, 135 (2007).
11. V. Goel, R. Dolan, *Neuropsychologia* **39**, 901 (2001).
12. I. Noveck, V. Goel, K. Smith, *Cortex* **40**, 613 (2004).
13. M. Atherton *et al.*, *Brain Res. Cogn. Brain Res.* **16**, 26 (2003).
14. P. Kyllonen, R. Christal, *Intelligence* **14**, 389 (1990).
15. M. D'Esposito, *Philos. Trans. R. Soc. London Ser. B* **362**, 761 (2007).
16. A. Baddeley, *Nat. Rev. Neurosci.* **4**, 829 (2003).
17. In coordination games, the participant has to encode and hold this information as well. However, because the targets of both players are the same, the demand on this capacity should be smaller.
18. E. Smith, J. Jonides, *Proc. Natl. Acad. Sci. U.S.A.* **95**, 12061 (1998).
19. N. Müller, R. Knight, *Neuroscience* **139**, 51 (2006).
20. E. Smith, J. Jonides, *Science* **283**, 1657 (1999).
21. T. Wager, E. Smith, *Cogn. Affect. Behav. Neurosci.* **3**, 255 (2003).
22. M. Berryhill, I. Olson, *Neuropsychologia* **46**, 1775 (2008).
23. A. Cavanna, M. Trimble, *Brain* **129**, 564 (2006).
24. M. Wallentin, A. Roepstorff, R. Glover, N. Burgess, *Neuroimage* **32**, 1850 (2006).
25. M. Wallentin, E. Weed, L. Østergaard, K. Mouridsen, A. Roepstorff, *Hum. Brain Mapp.* **29**, 524 (2008).
26. A. D. Craig, *Nat. Rev. Neurosci.* **3**, 655 (2002).
27. A. MacDonald III, J. Cohen, A. Stenger, C. Carter, *Science* **288**, 1835 (2000).
28. J. Decety *et al.*, *Neuroimage* **23**, 744 (2004).
29. J. S. Winston *et al.*, *Nat. Neurosci.* **5**, 277 (2002).
30. T. Singer *et al.*, *Science* **303**, 1157 (2004).
31. A. Bartels, S. Zeki, *Neuroreport* **11**, 3829 (2000).
32. J. Woodward, J. Allman, *J. Physiol. (Paris)* **101**, 179 (2007).
33. A. D. Craig, *Nat. Rev. Neurosci.* **10**, 59 (2009).
34. W. Seeley *et al.*, *J. Neurosci.* **27**, 2349 (2007).
35. J. Downar, A. Crawley, D. Mikulis, K. Davis, *Nat. Neurosci.* **3**, 277 (2000).
36. J. Downar, A. Crawley, D. Mikulis, K. Davis, *J. Neurophysiol.* **87**, 615 (2002).
37. K. Davis *et al.*, *J. Neurosci.* **25**, 8402 (2005).
38. K. Taylor, D. Seminowicz, K. Davis, *Hum. Brain Mapp.*, in press; published online 15 December 2008; 10.1002/hbm.20705.
39. See (*47*). The NCI can be interpreted as the probability that two randomly chosen individuals make the same choice relative to the probability of successful coordination if all choose randomly (SOM, S2.5).
40. S. Newman, P. Carpenter, S. Varma, M. Just, *Neuropsychologia* **41**, 1668 (2003).
41. J. Fincham *et al.*, *Proc. Natl. Acad. Sci. U.S.A.* **99**, 3346 (2002).
42. A. Blood, R. Zatorre, *Proc. Natl. Acad. Sci. U.S.A.* **98**, 11818 (2001).
43. H. Gallagher, A. Jack, A. Roepstorff, C. Frith, *Neuroimage* **16**, 814 (2002).
44. M. Bhatt, C. Camerer, *Games Econ. Behav.* **52**, 424 (2005).
45. K. Mendres, F. de Waal, *Anim. Behav.* **60**, 523 (2000).
46. C. Camerer, *Behavioral Game Theory: Experiments in Strategic Interaction* (Princeton Univ. Press, Princeton, NJ, 2003), Chap. 5.
47. N. Bardsley, J. Mehta, C. Starmer, R. Sugden, CeDEx Discussion Paper No. 2008-17 (Centre for Decision Research and Experimental Economics, Nottingham, UK, 2008); available at www.nottinghamnetlearning.com/economics/cedex/papers/2008-17.pdf.

48. We thank M. Hsu for helpful comments on the manuscript and J.-Y. Leu, J.T.-Y. Wang, D. Niddam, and participants at many seminars for discussions. Technical assistance from C.-R. Chou, C.-T. Chen, C.-H. Lan, S.-C. Lin, K.-L. Chen, Y.-Y. Chung, W.-Y. Lin, S. Hsu, R. Chen, and the National Taiwan University Hospital MRI Laboratory is greatly appreciated. This work was supported by the National Science Council of Taiwan (grant NSC 94-2415-H-002-004).

Supporting Online Material

www.sciencemag.org/cgi/content/full/324/5926/519/DC1
Materials and Methods
Figs. S1 to S9
Tables S1 to S18
References

8 September 2008; accepted 24 February 2009
10.1126/science.1165598

The Genome Sequence of Taurine Cattle: A Window to Ruminant Biology and Evolution

The Bovine Genome Sequencing and Analysis Consortium,* Christine G. Elsik,[1] Ross L. Tellam,[2] Kim C. Worley[3]

To understand the biology and evolution of ruminants, the cattle genome was sequenced to about sevenfold coverage. The cattle genome contains a minimum of 22,000 genes, with a core set of 14,345 orthologs shared among seven mammalian species of which 1217 are absent or undetected in noneutherian (marsupial or monotreme) genomes. Cattle-specific evolutionary breakpoint regions in chromosomes have a higher density of segmental duplications, enrichment of repetitive elements, and species-specific variations in genes associated with lactation and immune responsiveness. Genes involved in metabolism are generally highly conserved, although five metabolic genes are deleted or extensively diverged from their human orthologs. The cattle genome sequence thus provides a resource for understanding mammalian evolution and accelerating livestock genetic improvement for milk and meat production.

Domesticated cattle (*Bos taurus* and *Bos taurus indicus*) provide a significant source of nutrition and livelihood to nearly 6.6 billion humans. Cattle belong to a clade phylogenetically distant from humans and rodents, the Cetartiodactyl order of eutherian mammals, which

first appeared ~60 million years ago (*1*). Cattle represent the Ruminantia, which occupy diverse terrestrial environments with their ability to efficiently convert low-quality forage into energy-dense fat, muscle, and milk. These biological processes have been exploited by humans since domestication, which began in the Near East some 8000 to 10,000 years ago (*2*). Since then, over 800 cattle breeds have been established, representing an important world heritage and a scientific resource for understanding the genetics of complex traits.

The cattle genome was assembled with methods similar to those used for the rat and sea urchin genomes (*3*, *4*). The most recent assemblies, Btau3.1 and Btau4.0, combined bacterial artificial chromosome (BAC) and whole-genome shotgun (WGS) sequences. Btau3.1 was used for gene-specific analyses. Btau4.0, which includes finished sequence data and used different mapping methods to place the sequence on chromosomes, was used for all global analyses other than gene prediction. The contig N50 (50% of the genome is in contigs of this size or greater) is 48.7 kb for both assemblies; the scaffold N50 for Btau4.0 is 1.9 Mb. In the Btau4.0 assembly, 90% of the total genome sequence was placed on the 29 autosomes and X chromosome and validated (*3*). Of 1.04 million expressed sequence tag (EST) sequences, 95.0% were contained in the assembled contigs. With an equivalent gene distribution in the remaining 5% of the genome, the estimated genome size is 2.87 Gbp. Comparison with 73 finished BACs and single-nucleotide polymorphism (SNP) linkage data (*5*, *6*) confirmed this assembly quality with greater than 92% genomic coverage, and fewer than 0.8% of SNPs were incorrectly positioned at the resolution of these maps (*3*, *4*).

We used the cattle genome to catalog protein-coding genes, microRNA (miRNA) genes, and ruminant-specific interspersed repeats, and we manually annotated over 4000 genes. The consensus protein-coding gene set for Btau3.1 (OGSv1), from six predicted gene sets (*4*), consists of 26,835 genes with a validation rate of 82% (*4*). On this basis, we estimate that the cattle genome contains at least 22,000 protein-coding genes. We identified 496 miRNA genes of which 135 were unpublished miRNAs (*4*). About half of the cattle miRNA occur in 60 genomic miRNA clusters, containing two to seven miRNA genes separated by less than 10 kbp (fig. S2). The overall GC content of the cattle genome is 41.7%, with an observed-to-expected CpG ratio of 0.234, similar to that of other mammals.

The cattle genome has transposable element classes like those of other mammals, as well as large numbers of ruminant-specific repeats (table S4) that compose 27% of its genome. The

[1]Department of Biology, 406 Reiss, Georgetown University, 37th and O Streets, NW, Washington, DC 20057, USA. E-mail: ce75@georgetown.edu [2]CSIRO Livestock Industries, 306 Carmody Road, St. Lucia, QLD 4067, Australia. E-mail: ross.tellam@csiro.au [3]Human Genome Sequencing Center, Department of Molecular and Human Genetics, Baylor College of Medicine, MS BCM226, One Baylor Plaza, Houston, TX 77030, USA. E-mail: kworley@bcm.edu

*All authors with their affiliations and contributions are listed at the end of this paper.

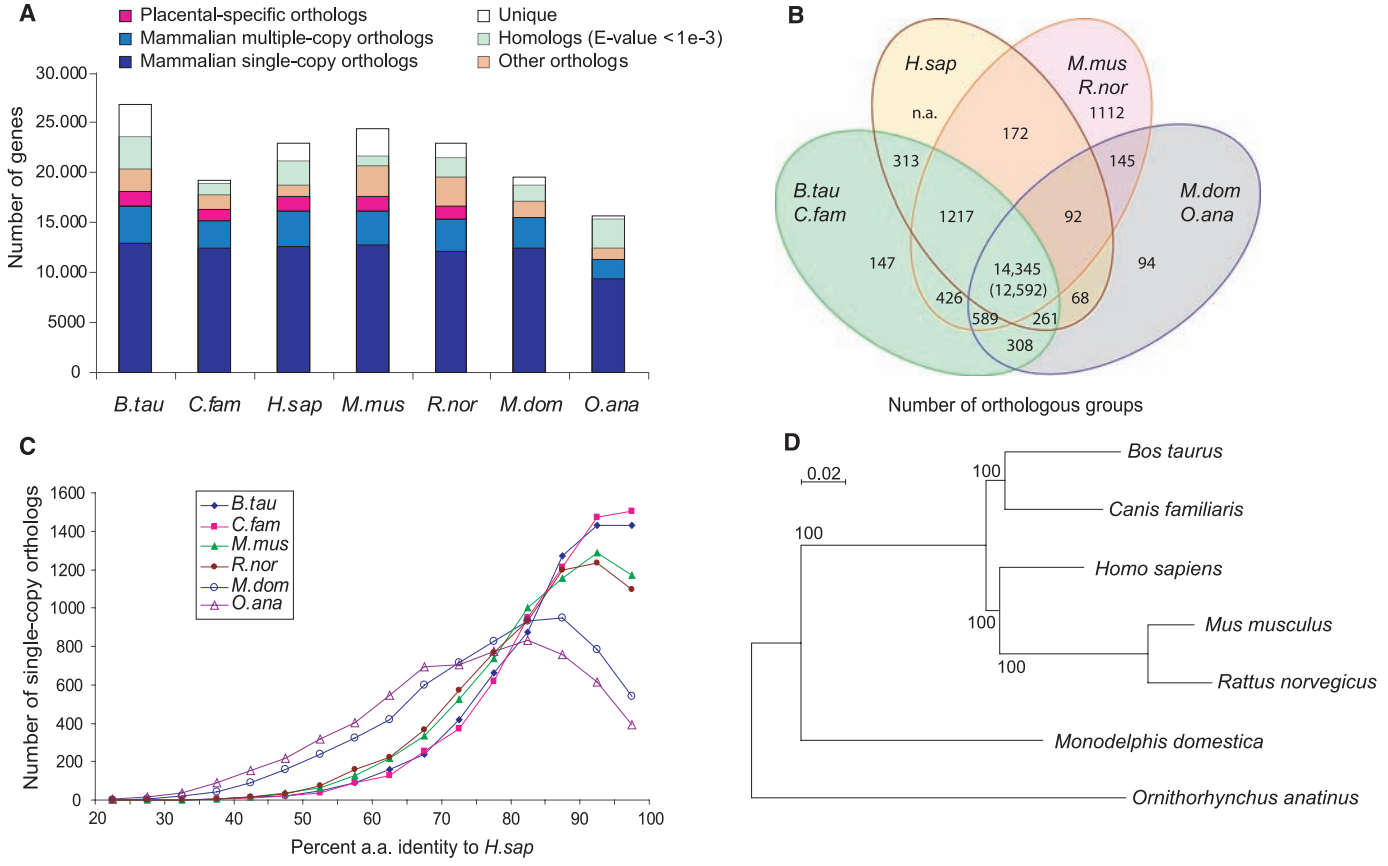

Fig. 1. Protein orthology comparison among genomes of cattle, dog, human, mouse, and rat (*Bos taurus*, *Canis familiaris*, *Homo sapiens*, *Mus musculus*, *Rattus norvegicus*, representing placental mammals), opossum (*Monodelphis domestica*, marsupial), and platypus (*Ornithorhynchus anatinus*, monotreme). (**A**) The majority of mammalian genes are orthologous, with more than half preserved as single copies (dark blue); a few thousand have species-specific duplications (blue); another few thousand have been lost in specific lineages (orange). We also show those lacking confident orthology assignment (green), and those that are apparently lineage specific [unique (white)]. Placental-specific orthologs are shown in pink. Single- or multiple-copy genes were defined on the basis of representatives in human, bovine, or dog; mouse or rat; and opossum or platypus. (**B**) Venn diagram showing shared orthologous groups (duplicated genes were counted as one) between laurasiatherians (cattle and dog), human, rodents (mouse and rat), and nonplacental mammals (opossum and platypus) on the basis of the presence of a representative gene in at least one of the grouped species [as in (A)]. (**C**) Distribution of ortholog protein identities between human and the other species for a subset of strictly conserved single-copy orthologs. (**D**) A maximum likelihood phylogenetic tree using all single-copy orthologs supports the accepted phylogeny and quantifies the relative rates of molecular evolution expressed as the branch lengths.

consensus sequence of Bov-B, a long interspersed nuclear element (LINE) lacked a functional open reading frame (ORF), which suggested that it was inactive (*7*). However, Bov-B repeats with intact ORF were identified in the genome, and their phylogeny (fig. S4) indicates that some are still actively expanding and evolving. Mapping chromosomal segments of high- and low-density ancient repeat content, L2/MIR [a LINE/SINE (short interspersed nuclear element) pair] and Bov-B, and more recent repeats, Bov-B/ART2A (Bov-B–derived SINE pair), revealed that the genome consists of ancient regions enriched for L2/MIR and recent regions enriched for Bov-B/ART2A (fig. S7). Exclusion of Bov-B/ART2A from contiguous blocks of ancient repeats suggests that evolution of the ruminant or cattle genome experienced invasions of new repeats into regions lacking ancient repeats. Alternatively, older repeats may have been destroyed by insertion of ruminant- or cattle-specific repeats. AGC trinucleotide repeats, the most common simple-sequence repeat (SSR) in artiodactyls (which include cattle, pigs, and sheep), are 90- and 142-fold overrepresented in cattle compared with human and dog, respectively (fig. S10). Of the AGC repeats in the cattle genome, 39% were associated with Bov-A2 SINE elements.

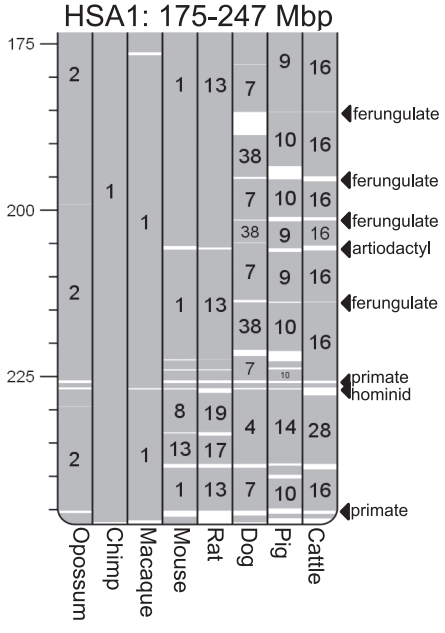

Fig. 2. Examples of EBRs. Ferungulate-, artiodactyl-, and primate-specific EBRs on HSA1 at 175 to 247 Mbp (other lineage-specific EBRs not shown). Homologous synteny blocks constructed for the macaque, chimp, cattle, dog, mouse, rat, and pig genomes were used for pairwise comparisons (*4*). White areas correspond to EBRs. Arrows to the right of the chromosome ideogram indicate positions of representative cattle-specific; artiodactyl-specific (specific to the chromosomes of pigs and cattle); ferungulate-specific (cattle, dog, and pig); primate-specific (human, macaque, and chimp); and hominoid-specific (human and chimp) rearrangements. Opossum is shown as an outgroup to the eutherian clade, which allows classification of ferungulate-specific EBRs.

A comparative analysis examined the rate of protein evolution and the conservation of gene repertoires among orthologs in the genomes of dog, human, mouse, and rat (representing placental mammals); opossum (marsupial); and platypus (monotreme). Orthology was resolved for >75% of cattle and >80% of human genes (Fig. 1A). There were 14,345 orthologous groups with representatives in human, cattle, or dog; mouse or rat; and opossum or platypus, which represent 16,749 cattle and 16,177 human genes, respectively, of which 12,592 are single-copy orthologs. We also identified 1217 placental mammal–specific orthologous groups with genes present in human, cattle, or dog; mouse or rat; but not opossum or platypus. About 1000 orthologs shared between rodents and laurasiatherians (cattle and dog), many of which encode G protein–coupled receptors, appear to have been lost or may be misannotated in the human genome (Fig. 1B). Gene repertoire conservation among these mammals correlates with conservation at the amino acid–sequence level (Fig. 1C). The elevated rate of evolution in rodents relative to other mammals (*8*) was supported by the higher amino acid sequence identity between human and dog or cattle proteins relative to that between human and rodent proteins. However, maximum-likelihood analysis of amino acid substitutions in single-copy orthologs supports the accepted sister lineage relation of primates and rodents (*1*) (Fig. 1D).

Table 1. Changes in the number of genes in innate immune gene families. Many of the β-defensin genes are present in unassigned scaffolds, i.e., they are not yet part of the current assembly. The exact number of β-defensin genes is uncertain. Interferon subfamily pseudogenes predicted on the basis of frame-shift mutations or stop codons within the first 100 amino acids of the coding sequence have been excluded from the table. The IFNX genes represent a newly discovered subfamily of IFN and are so named for convenience. BPI, Bactericidal and/or permeability-increasing; RNase, ribonuclease; LBP, lipopolysaccharide-binding protein; ULBP, UL16-binding protein.

Gene family	Bovine	Human	Murine
Cathelicidin	10	1	1
RNase	21	13	25
BPI-like	13	9	11
BPI/LBP	3	2	2
β-Defensin	~106	39	52
Interferon subfamilies			
IFNK	1	1	1
IFNE	1	1	1
IFNB	6	1	1
IFNA	13	13	14
IFNW	24	1	0
IFNT	3	0	0
IFNX	3	0	0
IFNL	0	3	2
IFNZ	0	0	2
C-type lysozyme	10	1	3
ULBP[1]	30	3	1

[1](*31*).

Alternative splicing is a major mechanism for transcript diversification (*9*), yet the extent of its evolutionary conservation and functional impact remain unclear. We used the cattle genome to analyze the conservation of the most common form of alternative splicing, exon skipping, defined as a triplet of exons in which the middle exon is absent in some transcripts, in a set of 1930 exon-skipping events across human, mouse, dog, and cattle (*4*). We examined 277 cases, with different conservation patterns between human and mouse, in 16 different cattle tissues with reverse transcription polymerase chain reaction (*4*). These splicing events were divided into a shared set (163 in both human and mouse) and a nonshared set (114 in human but not in mouse). Of the 277, we detected exon-skipping for 188 cases in cattle (table S5), which suggested that the majority of genes with exon-skipping in human were present and regulated in cattle and that, if an event is shared between human and mouse, it was more likely to be found in cattle. It was estimated that at most 40% of exon-skipping is conserved among mammals; thus, our data agree with the upper bound from previous analyses with human and rodents [e.g., (*10*)].

We constructed a cattle-human Oxford grid (fig. S12) (*4*) to conduct synteny-based chromosomal comparisons, which reinforced that human genome organization is more similar to cattle's than rodents' because most cattle chromosomes primarily correspond to part of one human chromosome, albeit with multiple rearrangements [e.g., (*11*)]. In contrast, the cattle-mouse Oxford grid shows poorer chromosomal correspondence. Lineage-specific evolutionary breakpoints were identified for cattle, artiodactyls, and ferungulates (a group encompassing artiodactyls and carnivores, represented by cattle, pig, and dog) and are shown with cattle (fig. S11) and human sequence coordinates (Fig. 2) (*4*). Primate, dog, rodent, mouse, and rat lineage-specific breakpoint positions were similarly identified. A total of 124 evolutionary breakpoint regions (EBRs) were identified in the cattle lineage, of which 100 were cattle- or ruminant-specific and 24 were artiodactyl-specific (e.g., Fig. 2). Nine additional EBRs represent presumptive ferungulate-specific rearrangements. *Bos taurus* chromosome 16 (BTA16) is populated with four ferungulate-specific EBRs, which suggests that this region was rearranged before the Artiodactyla and Carnivora divergence (Fig. 2). Such conserved regions demonstrate that many inversions that occurred before the divergence of the carnivores and artiodactyls have probably been retained in the ancestral form within the human genome. In contrast to the cattle genome, a pig physical map identified only 77 lineage-specific EBRs. Interchromosomal rearrangements and inversions characterize most of the lineage-specific rearrangements observed in the cattle, dog, and pig genomes.

An examination of repeat families and individual transposable elements within cattle-, artiodactyl- and ferungulate-specific EBRs showed a significantly higher density of LINE-L1 elements and the ruminant-specific LINE-RTE repeat family (*12*) in cattle-specific EBRs relative to the remainder of the cattle genome (table S6). In contrast, the SINE-BovA repeat family and the more ancient $tRNA^{Glu}$-derived SINE repeats (*13*) were present in lower density in cattle-specific EBRs, similar to other LINEs and SINEs (table S7). The differences in repeat densities were generally consistent in cattle-, artiodactyl- and ferungulate-specific EBRs, with the exception of the $tRNA^{Glu}$-derived and LTR-ERVL repeats, which are at higher densities in artiodactyl EBRs compared with the rest of the genome.

The $tRNA^{Glu}$-derived SINEs originated in the common ancestor of Suina (pigs and peccaries), Ruminantia, and Cetacea (whales) (*13*), which suggests that $tRNA^{Glu}$-derived SINEs were involved in ancestral artiodactyl chromosome rearrangements. Furthermore, the lower density of the more ancient repeat families in cattle-specific EBRs suggests that either more recently arising repeat elements were inserted into regions lacking ancient repeats or that older repeats were destroyed by this insertion (table S7). The repeat elements differing in density in EBRs were also found in regions of homologous synteny, which suggests that repeats may promote evolutionary rearrangements (see below). Differences in repeat density in cattle-specific EBRs are thus unlikely to be caused by the accumulation of repeats in EBRs after such rearrangements occur. We identified a cattle-specific EBR associated with a bidirectional promoter (figs. S14 and S15) that may affect control of the expression of the *CYB5R4* gene, which has been implicated in human diabetes and, therefore, may be important in the regulation of energy flow in cattle (*4*).

We identified 1020 segmental duplications (SDs) corresponding to 3.1% (94.4 Mbp) of the cattle genome (*4*). Duplications assigned to a chromosome showed a bipartite distribution with respect to length and percent identity (fig. S16), and interchromosomal duplications were shorter (median length 2.5 kbp) and more divergent (<94% identity) relative to intrachromosomal duplications (median length 20 kbp, ~97% identity) and tended to be locally clustered (fig. S17). Twenty-one of these duplications were >300 kbp and located in regions enriched for tandem duplications (e.g., BTA18) (fig. S18). This pattern is reminiscent of the duplication pattern of the dog, rat, and mouse but different from that of primate and great-ape genomes (*14*, *15*). On average, cattle SDs >10 kbp represent 11.7% of base pairs in 10-kbp intervals located within cattle-specific EBRs and 23.0% of base pairs located within the artiodactyl-specific EBRs. By contrast, in the remainder of the genome sequence assigned to chromosomes the fraction of SDs was 1.7% ($P < 1 \times 10^{-12}$). These data indicate that SDs play a role in promoting chromosome rearrangements by nonallelic homologous recombination [e.g., (*16*)] and suggest that either a significant fraction of the SDs observed in cattle occurred before the Ruminant-Suina split, and/or that the sites for accumulation of SDs are nonrandomly distributed in artiodactyl genomes.

SDs involving genic regions may give rise to new functional paralogs. Seventy-six percent (778 out of 1020) of the cattle SDs correspond to complete or partial gene duplications with high sequence identity (median 98.7%). This suggests that many of these gene duplications are specific to either the artiodactyla or the *Bos* lineage and tend to encode proteins that often interface with the external environment, particularly immune proteins and sensory and/or olfactory receptors. Several of these gene duplications are also duplicated in other mammalian lineages (e.g., cytochrome P-450, sulfotransferase, ribonuclease A, defensins, and pregnancy-associated glycoproteins). Paralogs located in segmental duplications that are present exclusively in cattle may have functional implications for the unique physiology, environment, and diet of cattle.

An overrepresentation of genes involved in reproduction in cattle SDs (tables S8 and S9) is associated with several gene families expressed in the ruminant placenta. These families encode the intercellular signaling proteins pregnancy-associated glycoproteins (on BTA29), trophoblast Kunitz domain proteins (on BTA13), and interferon tau (*IFNT*) (on BTA8). A gene family encoding prolactin-related proteins (on BTA23) was only identified in the assembly-dependent analysis of SDs. These genes regulate ruminant-specific aspects of fetal growth, maternal adaptations to pregnancy, and the coordination of parturition (*17*, *18*). Although type I interferon (IFN) genes are primarily involved in host defense (*19*), *IFNT* prevents regression of the corpus luteum during early pregnancy, which results in a uterine environment receptive to early conceptus development (*20*).

Signatures of positive selection (obtained by measurement of their rates of synonymous and nonsynonymous substitutions) identified 71 genes (*4*), including 10 immune-related genes (i.e., *IFNAR2*, *IFNG*, *CD34*, *TREM1*, *TREML1*, *FCER1A*, *IL23R*, *IL24*, *IL15*, and *LEAP2*). As previously mentioned, immune genes are overrepresented in SDs (see Table 1 and fig. S20). Examples of genes varying in cattle relative to mouse include a cluster of β-defensin genes, which encode antimicrobial peptides; the antimicrobial cathelicidin genes [which show increased sequence diversity of the mature cathelicidin peptides (*21*)]; and changes in the numbers of interferon genes (*22*) and the number and organization of genes involved in adaptive immune responses in cattle compared with human and mouse (*4*). This extensive duplication and divergence of genes involved in innate immunity may be because of the substantial load of microorganisms present in the rumen of cattle, which increases the risk of opportunistic infections at mucosal surfaces and positive selection for the traits that enabled stronger and more diversified innate immune responses at these locations. Another possibility is that immunity may have been under selection due to the herd structure, which can promote rapid disease transmission. Also, immune function–related duplicated genes have gained nonimmune functions, e.g., *IFNT* (see above), and the C-class lysozyme genes, which are involved in microbial degradation in the abomasum (see below).

There has been substantial reorganization of gene families encoding proteins present in milk. One such rearrangement affecting milk composition involves the histatherin (*HSTN*) gene within the casein gene cluster on BTA6 (fig. S21). In the cattle genome, *HSTN* is juxtaposed to a regulatory element (*BCE*) important (*23*) for β-casein (*CSN2*) expression, and as a probable consequence, *HSTN* is regulated like the casein genes during the lactation cycle. This rearrangement that led to the juxtaposition of *HSTN* next to the *BCE* is also the probable cause of deletion of one of the two copies of α-S2–like casein genes (*CSN1S2A*) present in other mammalian genomes (*24*). The biological implications of this change in casein gene copy number are not yet clear.

Additionally, the cattle serum amyloid A (*SAA*) gene cluster arose from both a laurasiatherian SD and a cattle-specific EBR, which resulted in two mammary gland–expressed *SAA3*-like genes, *SAA3.1* and *SAA3.2* on BTA29, and an *SAA3*-like gene on BTA15 (fig. S21). SAA3.2 has been shown to inhibit microbial growth (*25*). Two additional milk protein genes were associated with SDs: cathelicidin (*CATHL1*) and β_2-microglobulin (*B2M*)—part of the neonatal Fc receptor (FcRn) that transfers immunoglobulin IgG across epithelial cells of many tissues including the gut and mammary gland (*26*, *27*). IgG is the predominant immunoglobulin in cow's milk compared with IgA in human milk (*28*). Unlike humans, who acquire passive immunity from the mother via placental transfer of immunoglobulins during pregnancy, calves acquire passive immunity by ingestion of IgG in milk (*28*). *B2M* is also redistributed in epithelial cells upon calving, and it protects IgG from degradation (*26*). A genetic variant of *B2M* has negative effects on passive immune transfer (*29*). The additional copy of the gene encoding *B2M* might be associated with the abundance of IgG in cows' milk and an increased capacity for uptake in the neonatal gut. Considering that the passive transfer of immunity to the calf is one of the important functions of milk, it is striking that lactation-related genes affected by genomic rearrangements often encode immune-related proteins in milk.

Cattle metabolic pathways demonstrated a strong degree of conservation among the comprehensive set of genes involved in core mammalian metabolism (*4*) and permitted an examination of unique genetic events that may be related to ruminant-specific metabolic adaptations. However, among 1032 genes examined from the human metabolic pathways, five were deleted or extensively diverged in cattle: *PLA2G4C* (phospholipase A2, group IVC), *FAAH2* (fatty acid amide hydrolase 2), *IDI2* (isopentenyl-diphosphate delta isomerase 2), *GSTT2* (glutathione *S*-transferase

theta 2), and *TYMP* (thymidine phosphorylase), which may be adaptations that impact on fatty acid metabolism (*PLA2G4C* and *FAAH2)*; the mevalonate pathway (synthesis of dolichols, vitamins, steroid hormones, and cholesterol) (*IDI2*); detoxification (*GSTT2*); and pyrimidine metabolism (*TYMP*). Phylogenetic analysis shows that *PLA2G4C* was deleted ~87 to 97 million years ago in the laurasiatherian lineages (fig. S22). Strikingly, ~20% of the sequences from two abomasum (last chamber of the cattle stomach) EST libraries (a total of 2392 sequences) correspond to three C-type lysozyme genes. Lysozyme primarily functions in animals as an antibacterial protein, which suggests that they probably function in the abomasum (similar to the monogastric stomach) to degrade the cell walls of bacteria entering from the foregut (*30*). The cattle genome contains 10 C-type lysozyme genes (table S14 and fig. S23), and EST evidence (fig. S23) shows that six of the seven remaining C-type lysozyme genes are expressed primarily in the intestinal tract, which suggests additional roles for the encoded proteins in ruminant digestion.

In summary, the biological systems most affected by changes in the number and organization of genes in the cattle lineage include reproduction, immunity, lactation, and digestion. We highlighted the evolutionary activity associated with chromosomal breakpoint regions and their propensity for promoting gene birth and rearrangement. These changes in the cattle lineage probably reflect metabolic, physiologic, and immune adaptations due to microbial fermentation in the rumen, the herd environment and its influence on disease transmission, and the reproductive strategy of cattle. The cattle genome and associated resources will facilitate the identification of novel functions and regulatory systems of general importance in mammals and may provide an enabling tool for genetic improvement within the beef and dairy industries.

References and Notes

1. W. J. Murphy, P. A. Pevzner, S. J. O'Brien, *Trends Genet.* **20**, 631 (2004).
2. R. L. Willham, *J. Anim. Sci.* **62**, 1742 (1986).
3. Y. Liu *et al*., *BMC Genomics* **10**, 180 (2009).
4. Materials, methods, and additional discussion are available on *Science* online.
5. H. Nilsen *et al*., *Anim. Genet.* **39**, 97 (2008).
6. A. Prasad *et al*., *BMC Genomics* **8**, 310 (2007).
7. H. S. Malik, T. H. Eickbush, *Mol. Biol. Evol.* **15**, 1123 (1998).
8. C. I. Wu, W. H. Li, *Proc. Natl. Acad. Sci. U.S.A.* **82**, 1741 (1985).
9. B. Modrek, C. J. Lee, *Nat. Genet.* **34**, 177 (2003).
10. R. Sorek, R. Shamir, G. Ast, *Trends Genet.* **20**, 68 (2004).
11. A. Everts-van der Wind *et al*., *Proc. Natl. Acad. Sci. U.S.A.* **102**, 18526 (2005).
12. D. Kordis, F. Gubensek, *Gene* **238**, 171 (1999).
13. M. Shimamura, H. Abe, M. Nikaido, K. Ohshima, N. Okada, *Mol. Biol. Evol.* **16**, 1046 (1999).
14. J. A. Bailey, E. E. Eichler, *Nat. Rev. Genet.* **7**, 552 (2006).
15. J. A. Bailey *et al*., *Science* **297**, 1003 (2002).
16. W. J. Murphy *et al*., *Science* **309**, 613 (2005).
17. K. Hashizume *et al*., *Reprod. Fertil. Dev.* **19**, 79 (2007).
18. J. H. Larson *et al*., *Physiol. Genomics* **25**, 405 (2006).
19. S. Y. Zhang *et al*., *Immunol. Rev.* **226**, 29 (2008).
20. R. M. Roberts, Y. Chen, T. Ezashi, A. M. Walker, *Semin. Cell Dev. Biol.* **19**, 170 (2008).
21. M. Scocchi, S. Wang, M. Zanetti, *FEBS Lett.* **417**, 311 (1997).
22. M. G. Katze, Y. He, M. Gale Jr., *Nat. Rev. Immunol.* **2**, 675 (2002).
23. C. Schmidhauser *et al*., *Mol. Biol. Cell* **3**, 699 (1992).
24. M. Rijnkels, L. Elnitski, W. Miller, J. M. Rosen, *Genomics* **82**, 417 (2003).
25. A. J. Molenaar *et al*., *Biomarkers* **14**, 26 (2009).
26. B. Mayer *et al*., *J. Dairy Res.* **72** (suppl. S1), 107 (2005).
27. D. C. Roopenian, S. Akilesh, *Nat. Rev. Immunol.* **7**, 715 (2007).
28. T. J. Newby, C. R. Stokes, F. J. Bourne, *Vet. Immunol. Immunopathol.* **3**, 67 (1982).
29. M. L. Clawson *et al*., *Mamm. Genome* **15**, 227 (2004).
30. D. M. Irwin, *J. Mol. Evol.* **41**, 299 (1995).
31. J. H. Larson *et al*., *BMC Genomics* **7**, 227 (2006).

32. Funded by the National Human Genome Research Institute (NHGRI U54 HG003273); the U.S. Department of Agriculture's Agricultural Research Service (USDA-ARS agreement no. 59-0790-3-196) and Cooperative State Research, Education, and Extension Service National Research Initiative (grant no. 2004-35216-14163); the state of Texas; Genome Canada through Genome British Columbia; the Alberta Science and Research Authority; the Commonwealth Scientific and Industrial Research Organization of Australia (CSIRO); Agritech Investments Ltd., Dairy Insight, Inc., and AgResearch Ltd., all of New Zealand; the Research Council of Norway; the Kleberg Foundation; and the National, Texas, and South Dakota Beef Check-off Funds. The master accession for this WGS sequencing project is AAFC03000000. The individual WGS sequences are AAFC03000001 to AAFC03131728, and the scaffold records are CM000177 to CM000206 (chromosomes) and DS490632 to DS495890 (unplaced scaffolds).

The Bovine Genome Sequencing and Analysis Consortium

Principal Investigator: Richard A. Gibbs[1]
Analysis project leadership: Christine G. Elsik,[2,3] Ross L. Tellam[4]
Sequencing project leadership: Richard A. Gibbs,[1] Donna M. Muzny,[1] George M. Weinstock[5,1]
Analysis group organization: David L. Adelson,[6] Evan E. Eichler,[7,8] Laura Elnitski,[9] Christine G. Elsik,[2,3] Roderic Guigó,[10] Debora L. Hamernik,[11] Steve M. Kappes,[12] Harris A. Lewin,[13,14] David J. Lynn,[15] Frank W. Nicholas,[16] Alexandre Reymond,[17] Monique Rijnkels,[18] Loren C. Skow,[19] Ross L. Tellam,[4] Kim C. Worley,[1] Evgeny M. Zdobnov[20,21,22]
Sequencing project white paper: Richard A. Gibbs,[1] Steve M. Kappes,[12] Lawrence Schook,[13] Loren C. Skow,[19] George M. Weinstock,[5,1] James Womack[23]
Gene prediction and consensus gene set: Tyler Alioto,[10] Stylianos E. Antonarakis,[20] Alex Astashyn,[24] Charles E. Chapple,[10] Hsiu-Chuan Chen,[24] Jacqueline Chrast,[17] Francisco Câmara,[10] Christine G. Elsik[2,3] (leader), Olga Ermolaeva,[24] Roderic Guigó,[10] Charlotte N. Henrichsen,[17] Wratko Hlavina,[24] Yuri Kapustin,[24] Boris Kiryutin,[24] Paul Kitts,[24] Felix Kokocinski,[25] Melissa Landrum,[24] Donna Maglott,[24] Kim Pruitt,[24] Alexandre Reymond,[17] Victor Sapojnikov,[24] Stephen M. Searle,[25] Victor Solovyev,[26] Alexandre Souvorov,[24] Catherine Ucla,[20] George M. Weinstock,[5,1] Carine Wyss[20]
Experimental validation of gene set: Tyler Alioto,[10] Stylianos E. Antonarakis,[20] Charles E. Chapple,[10] Jacqueline Chrast,[17] Francisco Câmara,[10] Roderic Guigó[10] (leader), Charlotte N. Henrichsen,[17] Alexandre Reymond,[17] Catherine Ucla,[20] Carine Wyss[20]
MicroRNA analysis: Juan M. Anzola,[3] Daniel Gerlach,[20,21] Evgeny M. Zdobnov[20,21,22] (leader)
GC composition analysis: Eran Elhaik,[27,28] Christine G. Elsik[2,3] (leader), Dan Graur,[27] Justin T. Reese[2]
Repeat analysis: David L. Adelson[6] (leader), Robert C. Edgar,[29] John C. McEwan,[30] Gemma M. Payne,[30] Joy M. Raison[31]
Protein ortholog analysis: Thomas Junier,[19,20] Evgenia V. Kriventseva,[32] Evgeny M. Zdobnov[20,21,22] (leader)
Exon-skipping analysis: Jacqueline Chrast,[17] Eduardo Eyras,[33,34] Charlotte N. Henrichsen,[17] Mireya Plass,[34] Alexandre Reymond[17] (leader)
Evolutionary breakpoint analysis and Oxford grid: Ravikiran Donthu,[13] Denis M. Larkin,[13,14] Harris A. Lewin[13,14] (leader), Frank W. Nicholas[16]
Bidirectional promoter analysis: Laura Elnitski[9] (leader), Denis M. Larkin,[13,14] Harris A. Lewin,[13,14] James Reecy,[35] Mary Q. Yang[9]
Segmental duplication analysis: David L. Adelson,[6] Lin Chen,[7] Ze Cheng,[7] Carol G. Chitko-McKown,[36] Evan E. Eichler[7,8] (leader), Laura Elnitski,[9] Christine G. Elsik,[2,3] George E. Liu,[37] Lakshmi K. Matukumalli,[38,37] Jiuzhou Song,[39] Bin Zhu[39]
Analysis of gene ontology in segmental duplications: Christine G. Elsik,[2,3] David J. Lynn[15] (leader), Justin T. Reese[2]
Adaptive evolution: Daniel G. Bradley,[40] Fiona S.L. Brinkman,[15] Lilian P.L. Lau,[40] David J. Lynn[15] (leader), Matthew D. Whiteside[15]
Innate immunity: Ross L. Tellam[4] (leader), Angela Walker,[41] Thomas T. Wheeler[42]
Lactation: Theresa Casey,[43] J. Bruce German,[44,45] Danielle G. Lemay,[45] David J. Lynn,[15] Nauman J. Maqbool,[46] Adrian J. Molenaar,[42] Monique Rijnkels[18] (leader)
Metabolism: Harris A. Lewin[13,14] (leader), Seongwon Seo,[47] Paul Stothard[48]
Adaptive immunity: Cynthia L. Baldwin,[49] Rebecca Baxter,[50] Candice L. Brinkmeyer-Langford,[19] Wendy C. Brown,[51] Christopher P. Childers,[2] Timothy Connelley,[52] Shirley A. Ellis,[53] Krista Fritz,[19] Elizabeth J. Glass,[50] Carolyn T.A. Herzig,[49] Antti Iivanainen,[54] Kevin K. Lahmers,[51] Loren C. Skow[19] (leader)
Annotation data management: Anna K. Bennett,[2] Christopher P. Childers,[2] C. Michael Dickens,[3] Christine G. Elsik[2,3] (leader), James G.R. Gilbert,[25] Darren E. Hagen,[2] Justin T. Reese,[2] Hanni Salih[3]
Manual annotation organization: Jan Aerts,[55] Alexandre R. Caetano,[56] Brian Dalrymple,[4] Christine G. Elsik,[2,3] Jose Fernando Garcia,[57] Richard A. Gibbs,[1] Clare A. Gill,[3,58] Debora L. Hamernik,[11] Stefan G. Hiendleder,[59] Erdogan Memili,[60] Frank W. Nicholas,[16] James Reecy,[35] Monique Rijnkels,[18] Loren C. Skow,[19] Diane Spurlock,[35] Paul Stothard,[48] Ross L. Tellam,[4] George M. Weinstock,[5,1] John L. Williams,[61] Kim C. Worley[1]
cDNA tissues, libraries, and sequencing: Lee Alexander,[62] Michael J. Brownstein,[63] Leluo Guan,[48] Robert A. Holt[64] (leader), Steven J.M. Jones[64] (leader), Marco A. Marra[64] (leader), Richard Moore,[64] Stephen S. Moore[48] (leader), Andy Roberts,[62] Masaaki Taniguchi,[65,48] Richard C. Waterman[62]
Genome sequence production: Joseph Chacko,[1] Mimi M. Chandrabose,[1] Andy Cree[1] (leader), Marvin Diep Dao,[1] Huyen H. Dinh[1] (leader), Ramatu Ayiesha Gabisi,[1] Sandra Hines,[1] Jennifer Hume[1] (leader), Shalini N. Jhangiani,[1] Vandita Joshi,[1] Christie L. Kovar[1] (leader), Lora R. Lewis,[1] Yih-shin Liu,[1] John Lopez,[1] Margaret B. Morgan,[1] Donna M. Muzny[1] (leader), Ngoc Bich Nguyen,[1] Geoffrey O. Okwuonu,[1] San Juana Ruiz,[1] Jireh Santibanez,[1] Rita A. Wright[1]
Sequence finishing: Christian Buhay[1] (leader), Yan Ding,[1] Shannon Dugan-Rocha[1] (leader), Judith Herdandez,[1] Michael Holder,[1] Aniko Sabo[1]
Automated BAC assembly: Amy Egan,[1] Jason Goodell,[1] Katarzyna Wilczek-Boney[1]
Sequence production informatics: Gerald R. Fowler[1] (leader), Matthew Edward Hitchens,[1] Ryan J. Lozado,[1] Charles Moen,[1] David Steffen,[66,1] James T. Warren,[1] Jingkun Zhang[1]
BAC mapping: Readman Chiu,[64] Steven J.M. Jones,[64] Marco A. Marra[64] (leader), Jacqueline E. Schein[64]
Genome assembly: K. James Durbin,[67,1] Paul Havlak,[68,1] Huaiyang Jiang,[1] Yue Liu,[1] Xiang Qin,[1] Yanru Ren,[1] Yufeng Shen,[1,69] Henry Song,[1] George M. Weinstock,[5,1] Kim C. Worley[1] (leader)
Sequence library production: Stephanie Nicole Bell,[1] Clay Davis,[1] Angela Jolivet Johnson,[1] Sandra Lee,[1] Lynne V. Nazareth[1] (leader), Bella Mayurkumar Patel,[1] Ling-Ling Pu,[1] Selina Vattathil,[1] Rex Lee Williams Jr.[1]
BAC production: Stacey Curry,[1] Cerissa Hamilton,[1] Erica Sodergren[5,1] (leader)
Sequence variation detection: Lynne V. Nazareth,[1] David A. Wheeler[1]
Markers and mapping: David L. Adelson,[6] Jan Aerts,[55] Wes Barris,[4] Gary L. Bennett,[36] Brian Dalrymple,[4] André Eggen,[70] Clare A. Gill,[3,58] Ronnie D. Green,[71] Gregory P. Harhay,[36] Matthew Hobbs,[72] Oliver Jann,[50] Steve M. Kappes[12] (leader), John W. Keele,[36] Matthew P. Kent,[73] Denis M. Larkin,[13,14] Harris A. Lewin,[13,14] Sigbjørn Lien,[73] John C. McEwan,[30] Stephanie D. McKay,[74] Sean McWilliam,[4] Stephen S. Moore,[48] Frank W. Nicholas,[16] Gemma M. Payne,[30] Abhirami Ratnakumar,[75,4] Hanni Salih,[3] Robert D. Schnabel,[74] Timothy Smith,[36] Warren M. Snelling,[36] Tad S. Sonstegard,[37] Roger T. Stone,[36] Yoshikazu Sugimoto,[76] Akiko Takasuga,[76] Jeremy F. Taylor,[74] Ross L. Tellam,[4] Curtis P. Van Tassell,[37] John L. Williams[61]
Genomic DNA: Michael D. MacNeil[62]
Manual annotation: Antonio R.R. Abatepaulo,[77] Colette A. Abbey,[3] Jan Aerts,[55] Virpi Ahola,[78] Iassudara G. Almeida,[57] Ariel F. Amadio,[79] Elen Anatriello,[77] Suria M. Bahadue,[2] Cynthia L. Baldwin,[49] Rebecca Baxter,[50] Anna K. Bennett,[2] Fernando H. Biase,[13] Clayton R. Boldt,[3] Candice L. Brinkmeyer-Langford,[19] Wendy C. Brown,[51] Alexandre R. Caetano,[56] Jeffery A. Carroll,[80] Wanessa A. Carvalho,[77] Theresa Casey,[43] Eliane P. Cervelatti,[57] Elsa Chacko,[81] Jennifer E. Chapin,[3] Ye Cheng,[35] Christopher P. Childers,[2] Jungwoo Choi,[3] Adam J. Colley,[82] Timothy Connelley,[52] Tatiana A. de Campos,[56] Marcos De Donato,[83]

Isabel K.F. de Miranda Santos,[56,77] Carlo J.F. de Oliveira,[77] Heather Deobald,[84] Eve Devinoy,[85] C. Michael Dickens,[3] Kaitlin E. Donohue,[2] Peter Dovc,[86] Annett Eberlein,[87] Shirley A. Ellis,[53] Carolyn J. Fitzsimmons,[59] Alessandra M. Franzin,[77] Krista Fritz,[19] Gustavo R. Garcia,[77] Jose Fernando Garcia,[57] Sem Genini,[61] J. Bruce German,[44,45] James G.R. Gilbert,[25] Clare A. Gill,[3,58] Cody J. Gladney,[3] Elizabeth J. Glass,[50] Jason R. Grant,[48] Marion L. Greaser,[88] Jonathan A. Green,[74] Darryl L. Hadsell,[18] Darren E. Hagen,[2] Hatam A. Hakimov,[89] Rob Halgren,[43] Jennifer L. Harrow,[25] Elizabeth A. Hart,[25] Nicola Hastings,[90,50] Marta Hernandez,[91] Carolyn T.A. Herzig,[49] Stefan G. Hiendleder,[59] Matthew Hobbs,[72] Zhi-Liang Hu,[35] Antti Iivanainen,[54] Aaron Ingham,[4] Terhi Iso-Touru,[78] Catherine Jamis,[2] Oliver Jann,[50] Kirsty Jensen,[50] Dimos Kapetis,[61] Tovah Kerr,[51] Sari S. Khalil,[2] Hasan Khatib,[92] Davood Kolbehdari,[48,93] Charu G. Kumar,[13] Dinesh Kumar,[94,35] Richard Leach,[50] Justin C-M Lee,[2] Danielle G. Lemay,[45] Changxi Li,[95,48] George E. Liu,[37] Krystin M. Logan,[96] Roberto Malinverni,[61] Nauman J. Maqbool,[46] Elisa Marques,[48] William F. Martin,[45] Natalia F. Martins,[56] Sandra R. Maruyama,[77] Raffaele Mazza,[97] Kim L. McLean,[84] Juan F. Medrano,[98] Erdogan Memili,[60] Adrian J. Molenaar,[42] Barbara T. Moreno,[57] Daniela D. Moré,[77] Carl T. Muntean,[3] Hari P. Nandakumar,[19] Marcelo F.G. Nogueira,[99] Ingrid Olsaker,[100] Sameer D. Pant,[82] Francesca Panzitta,[61] Rosemeire C.P. Pastor,[57] Mario A. Poli,[101] Nathan Poslusny,[2] Satyanarayana Rachagani,[35] Shoba Ranganathan,[81,102] Andrej Razpet,[86] James Reecy,[35] Penny K. Riggs,[3,58] Monique Rijnkels,[18] Gonzalo Rincon,[98] Nelida Rodriguez-Osorio,[60,103] Sandra L. Rodriguez-Zas,[13] Natasha E. Romero,[3] Anne Rosenwald,[2] Lillian Sando,[4] Sheila M. Schmutz,[84] Seongwon Seo,[47] Libing Shen,[2] Laura Sherman,[48] Loren C. Skow,[19] Bruce R. Southey,[104] Diane Spurlock,[35] Ylva Strandberg Lutzow,[4] Jonathan V. Sweedler,[104] Imke Tammen,[72] Masaaki Taniguchi,[65,48] Ross L. Tellam,[4] Bhanu Prakash V.L. Telugu,[74] Jennifer M. Urbanski,[2] Yuri T. Utsunomiya,[57] Chris P. Verschoor,[82] Ashley J. Waardenberg,[4,105] Angela Walker,[41] Zhiquan Wang,[48] Robert Ward,[106] Rosemarie Weikard,[87] Thomas H. Welsh Jr.,[3,58] Thomas T. Wheeler,[42] Stephen N. White,[51,107] John L. Williams,[61] Laurens G. Wilming,[25] Kris R. Wunderlich,[3] Jianqi Yang,[108] Feng-Qi Zhao[109]

[1]Human Genome Sequencing Center, Department of Molecular and Human Genetics, Baylor College of Medicine, One Baylor Plaza, Houston, TX 77030, USA. [2]Department of Biology, 406 Reiss, Georgetown University, 37th & O Streets NW, Washington, DC 20057, USA. [3]Department of Animal Science, Texas A&M University, 2471 TAMU, College Station, TX 77843–2471, USA. [4]Livestock Industries, Commonwealth Scientific and Industrial Research Organization (CSIRO), 306 Carmody Road, St. Lucia, Queensland, 4067, Australia. [5]The Genome Center at Washington University, Washington University School of Medicine, 4444 Forest Park Avenue, St. Louis, MO 63108, USA. [6]School of Molecular and Biomedical Science, School of Agriculture, Food and Wine, The University of Adelaide, Adelaide, SA, 5005, Australia. [7]Department of Genome Sciences, University of Washington, 1705 NE Pacific Street, Seattle, WA 98195–5065, USA. [8]Howard Hughes Medical Institute, Seattle, WA 98195, USA. [9]National Human Genome Research Institute, National Institutes of Health, 5625 Fishers Lane, Rockville, MD 20878, USA. [10]Center for Genomic Regulation and Grup de Recerca en Informática Biomédica, Institut Municipal d'Investigació Mèdica, Universitat Pompeu Fabra, 08003 Barcelona, Catalonia, Spain. [11]U.S. Department of Agriculture (USDA), Cooperative State Research, Education, & Extension Service, 1400 Independence Avenue SW, Stop 2220, Washington, DC 20250–2220, USA. [12]National Program Staff, USDA–Agricultural Research Service, 5601 Sunnyside Avenue, Beltsville, MD 20705, USA. [13]Department of Animal Sciences, University of Illinois at Urbana–Champaign, 1201 West Gregory Drive, Urbana, IL 61801, USA. [14]Institute for Genomic Biology, University of Illinois at Urbana–Champaign, 1201 West Gregory Drive, Urbana, IL 61801, USA. [15]Department of Molecular Biology and Biochemistry, Simon Fraser University, 8888 University Drive, Burnaby, BC, V5A 1S6, Canada. [16]Faculty of Veterinary Science, University of Sydney, Sydney, NSW, 2006, Australia. [17]Center for Integrative Genomics, University of Lausanne, Lausanne, 1015, Switzerland. [18]Children's Nutrition Research Center, USDA–Agricultural Research Service, Department of Pediatrics–Nutrition, Baylor College of Medicine, 1100 Bates Street, Houston, TX 77030–2600, USA. [19]Department of Veterinary Integrative Biosciences, Texas A&M University, College Station, TX 77843, USA. [20]Department of Genetic Medicine and Development, University of Geneva Medical School, 1 rue Michel-Servet, Geneva, 1211, Switzerland. [21]Swiss Institute of Bioinformatics, 1 rue Michel-Servet, Geneva, 1211, Switzerland. [22]Division of Molecular Biosciences, Imperial College London, South Kensington Campus, London, SW7 2AZ, UK. [23]Department of Veterinary Pathobiology, Texas A&M University, College Station, TX 77843, USA. [24]National Center for Biotechnology Information, National Library of Medicine, National Institutes of Health, Bethesda, MD 20892, USA. [25]Informatics Department, Wellcome Trust Sanger Institute, Hinxton, Cambridge, CB10 1HH, UK. [26]Department of Computer Science, University of London, Royal Holloway, Egham, Surrey, TW20 0EX, UK. [27]Department of Biology and Biochemistry, University of Houston, Houston, TX 77204, USA. [28]McKusick—Nathans Institute of Genetic Medicine, BRB 579, Johns Hopkins University School of Medicine, 733 North Broadway, Baltimore, MD 21205, USA. [29]45 Monterey Drive, Tiburon, CA 94920, USA. [30]Animal Genomics, AgResearch, Invermay, PB 50034, Mosgiel, 9053, New Zealand. [31]eResearch SA, University of Adelaide, North Terrace, Adelaide, SA, 5005, Australia. [32]Department of Structural Biology and Bioinformatics, University of Geneva Medical School, 1 rue Michel-Servet, Geneva, 1211, Switzerland. [33]Catalan Institution for Research and Advanced Studies, 08010 Barcelona, Catalonia, Spain. [34]Computational Genomics, Universitat Pompeu Fabra, 08003 Barcelona, Catalonia, Spain. [35]Department of Animal Science, Iowa State University, 2255 Kildee Hall, Ames, IA 50011–3150, USA. [36]Meat Animal Research Center, USDA–Agricultural Research Service, Clay Center, NE 68933, USA. [37]Bovine Functional Genomics Laboratory, USDA–Agricultural Research Service, Beltsville Agricultural Research Center (BARC)–East, Beltsville, MD 20705, USA. [38]Department of Bioinformatics and Computational Biology, George Mason University, 10900 University Blvd, Manassas, VA 20110, USA. [39]Department of Bioengineering, University of Maryland, College Park, MD 20742, USA. [40]Smurfit Institute of Genetics, Trinity College Dublin, Dublin 2, Ireland. [41]Department of Veterinary Pathobiology, 245 Bond Life Sciences Center, University of Missouri, Columbia, MO 65211, USA. [42]Dairy Science and Technology Section, AgResearch, Ruakura Research Centre, East Street, Private Bag 3123, Hamilton, 3240, New Zealand. [43]Department of Animal Science, Michigan State University, East Lansing, MI 48824–1225, USA. [44]Nestlé Research Centre, Vers chez les Blanc CH, Lausanne 26, 1000, Switzerland. [45]Department of Food Science and Technology, University of California–Davis, Davis, CA 95616, USA. [46]Bioinformatics, Mathematics and Statistics, AgResearch, Ruakura Research Centre, East Street, Private Bag 3123, Hamilton, 3240, New Zealand. [47]Division of Animal Science and Resource, Chungnam National University, Daejeon, 305-764, Korea. [48]Department of Agricultural, Food and Nutritional Science, University of Alberta, 410 AgFor Centre, Edmonton, AL, T6G 2P5, Canada. [49]Department of Veterinary and Animal Sciences, University of Massachusetts, Amherst, MA 01003, USA. [50]The Roslin Institute and Royal (Dick) School of Veterinary Studies, University of Edinburgh, Roslin, Midlothian, EH25 9PS, UK. [51]Department of Veterinary Microbiology and Pathology, Washington State University, Pullman, WA 99164, USA. [52]Division of Infection and Immunity, The Roslin Institute, Royal (Dick) School of Veterinary Science, University of Edinburgh, Roslin, Midlothian, EH25 9RG, UK. [53]Immunology Division, Institute for Animal Health, Compton, RG20 7NN, UK. [54]Department of Basic Veterinary Sciences, University of Helsinki, Post Office Box 66, Helsinki, FIN-00014, Finland. [55]Genome Dynamics and Evolution, Wellcome Trust Sanger Institute, Hinxton, Cambridge, CB10 1SA, UK. [56]Embrapa Recursos Genéticos e Biotecnologia, Final Avenida W/5 Norte, Brasilia, DF, 70770-900, Brazil. [57]Animal Production and Health Department, UNESP—Sao Paulo State University, Aracatuba, SP, 16050-680, Brazil. [58]Texas AgriLife Research, College Station, TX 77843, USA. [59]JS Davies Epigenetics and Genetics Group, School of Agriculture, Food & Wine and Research Centre for Reproductive Health, The University of Adelaide, Roseworthy Campus, Roseworthy, SA, 5371, Australia. [60]Department of Animal and Dairy Sciences, Mississippi Agricultural and Forestry Experiment Station, Mississippi State University, Mississippi State, MS 39762, USA. [61]Parco Tecnologico Padano, Via Einstein, Polo Universitario, Lodi, 26900, Italy. [62]Fort Keogh Livestock and Range Research Laboratory, USDA-Agricultural Research Service, Miles City, MT 59301, USA. [63]Laboratory of Genetics, National Institute of Mental Health, NIH, Building 49, B1EE16, 49 Convent Drive, Bethesda, MD 20892, USA. [64]Genome Sciences Centre, British Columbia Cancer Agency, 675 West 10th Avenue, Vancouver, BC, V5Z 1L3, Canada. [65]Division of Animal Sciences, National Institute of Agrobiological Sciences, Tsukuba, Ibaraki, 305-8602, Japan. [66]Bioinformatics Research Center, Baylor College of Medicine, One Baylor Plaza, Houston, TX 77030, USA. [67]Department of Biomolecular Engineering, University of California at Santa Cruz, Santa Cruz, CA 95064, USA. [68]Department of Computer Science, University of Houston, Houston, TX 77204–3010, USA. [69]Department of Computer Science and Center for Computational Biology and Bioinformatics, Columbia University, New York, NY 10032, USA. [70]INRA, Animal Genetics and Integrative Biology, Bovine Genetics and Genomics, 78350 Jouy-en-Josas, France. [71]Pfizer Animal Genetics, Pfizer Animal Health, New York, NY 10017, USA. [72]Faculty of Veterinary Science, University of Sydney, Camden, NSW, 2570, Australia. [73]Centre for Integrative Genetics and Department of Animal and Aquacultural Sciences, Norwegian University of Life Sciences, Arboretveien 6, Ås, 1432, Norway. [74]Division of Animal Sciences, University of Missouri, 920 East Campus Drive, Columbia, MO 65211, USA. [75]Department of Medical Biochemistry and Microbiology, Uppsala University, Uppsala Biomedical Centre Husargatan 3, Uppsala, 75 123, Sweden. [76]Shirakawa Institute of Animal Genetics, Nishigo, Fukushima 961-8061, Japan. [77]Department of Biochemistry and Immunology, Ribeirão Preto Medical School, University of São Paulo, Av Bandeirantes 3900, Ribeirão Preto, SP, 14049-900, Brazil. [78]Biotechnology and Food Research, MTT Agrifood Research Finland, Jokioinen, FI-31600, Finland. [79]EEA Rafaela, Instituto Nacional de Tecnología Agropecuaria (INTA), Ruta 34 Km 227, Rafaela, Santa Fe, 2300, Argentina. [80]Livestock Issues Research Unit, USDA–Agricultural Research Service, Lubbock, TX 79403, USA. [81]Department of Chemistry and Biomolecular Sciences & ARC Centre of Excellence in Bioinformatics, Macquarie University, Sydney, 2109, NSW, Australia. [82]Department of Animal and Poultry Science, University of Guelph, Guelph, ON, N1G2W1, Canada. [83]Instituto de Investigaciones en Biomedicina y Ciencias Aplicadas, Universidad de Oriente, Avenida Universidad, Cumana, Sucre, 6101, Venezuela. [84]Department of Animal and Poultry Science, University of Saskatchewan, Saskatoon, SK, S7N 5A8, Canada. [85]INRA–UR1196, Génomique et Physiologie de la Lactation, F78352 Jouy-en-Josas, France. [86]Department of Animal Science, University of Ljubljana, Groblje 3, Domzale, SI-1230, Slovenia. [87]Research Unit Molecular Biology, Research Institute for the Biology of Farm Animals (FBN), Dummerstorf, 18196, Germany. [88]Department of Animal Sciences, University of Wisconsin–Madison, 1805 Linden Drive, Madison, WI 53706, USA. [89]Department of Molecular and Cellular Biology, University of Guelph, Guelph, ON, N1G 2W1, Canada. [90]Cell Biology and Biophysics, European Molecular Biology Laboratory (EMBL)–Heidelberg, Meyerhofstrasse 1, Heidelberg, Germany. [91]Laboratory of Molecular Biology, Instituto Tecnologico Agrario de Castilla y Leon (ITACyL), Carretera de Burgos km 119, Valladolid, 47071, Spain. [92]Department of Dairy Science, University of Wisconsin, Madison, WI 53706, USA. [93]Monsanto Company, 3302 SE Convenience Blvd, Ankeny, IA 50021, USA. [94]Genes & Genetic Resources Molecular Analysis Lab, National Bureau of Animal Genetic Resources, Baldi Bye Pass, Karnal, Haryana, 132001, India. [95]Lacombe Research Centre, Agriculture and Agri-Food Canada, Lacombe, AL, T4L 1W1, Canada. [96]Biomedical Sciences, University of Guelph, Guelph, ON, N1G 2W6, Canada. [97]Zootechnics Institute, Università Cattolica del Sacro Cuore, via Emilia Parmense 84, Piacenza, 29100, Italy. [98]Department of Animal Science, University of California at Davis, One Shields Avenue, Davis, CA 95616, USA. [99]Departamento de Ciências Biológicas, Faculdade de Ciências e Letras, UNESP–São Paulo State University, Av Dom Antônio 2100, Vila Tênis Clube, Assis, SP, 19806-900, Brazil. [100]Department of Basic Sciences and Aquatic Medicine, Norwegian School of Veterinary Science, Post Office Box 8146 Dep, Oslo, NO-0033, Norway. [101]Instituto de Genética Ewald Favret, Instituto Nacional de Tecnología Agropecuaria (INTA), Las Cabañas y de Los Reseros s/n CC25, Castelar, Buenos Aires, B1712WAA, Argentina. [102]Department of Biochemistry, Yong Loo Lin School of Medicine, National University of Singapore, 8 Medical Drive, Singapore, 117597, Singapore. [103]Grupo CENTAURO, Universidad de Antioquia, Medellín, Colombia. [104]Department of Chemistry, University of Illinois, Urbana, IL 61801, USA. [105]Eskitis Institute for Cell and Molecular Therapies, Griffith University, Nathan, QLD, 4111, Australia.

[106]Nutrition and Food Sciences, Utah State University, Logan, UT 84322, USA. [107]Animal Disease Research Unit, USDA–Agricultural Research Service, Pullman, WA 99164, USA. [108]Department of Pharmacology, 2-344 BSB, University of Iowa, 51 Newton Road, Iowa City, IA 52242, USA. [109]Department of Animal Science, 211 Terrill, University of Vermont, 570 Main Street, Burlington, VT 05405, USA.

Supporting Online Material
www.sciencemag.org/cgi/content/full/324/5926/522/DC1
Materials and Methods
Figs. S1 to S23
Tables S1 to S14
References

10 December 2008; accepted 16 March 2009
10.1126/science.1169588

Genome-Wide Survey of SNP Variation Uncovers the Genetic Structure of Cattle Breeds

The Bovine HapMap Consortium*

The imprints of domestication and breed development on the genomes of livestock likely differ from those of companion animals. A deep draft sequence assembly of shotgun reads from a single Hereford female and comparative sequences sampled from six additional breeds were used to develop probes to interrogate 37,470 single-nucleotide polymorphisms (SNPs) in 497 cattle from 19 geographically and biologically diverse breeds. These data show that cattle have undergone a rapid recent decrease in effective population size from a very large ancestral population, possibly due to bottlenecks associated with domestication, selection, and breed formation. Domestication and artificial selection appear to have left detectable signatures of selection within the cattle genome, yet the current levels of diversity within breeds are at least as great as exists within humans.

The emergence of modern civilization was accompanied by adaptation, assimilation, and interbreeding of captive animals. In cattle (*Bos taurus*), this resulted in the development of individual breeds differing in, for example, milk yield, meat quality, draft ability, and tolerance or resistance to disease and pests. However, despite mapping and diversity studies (*1*–*5*) and the identification of mutations affecting some quantitative phenotypes (*6*–*8*), the detailed genetic structure and history of cattle are not known.

Cattle occur as two major geographic types, the taurine (humpless—European, African, and Asian) and indicine (humped—South Asian, and East African), which diverged >250 thousand years ago (Kya) (*3*). We sampled individuals representing 14 taurine (n = 376), three indicine (n = 73) (table S1), and two hybrid breeds (n = 48), as well as two individuals each of *Bubalus quarlesi* and *Bubalus bubalis*, which diverged from *Bos taurus* ~1.25 to 2.0 Mya (*9*, *10*). All breeds except Red Angus (n = 12) were represented by at least 24 individuals. We preferred individuals that were unrelated for ≥4 generations; however, each breed had one or two sire, dam, and progeny trios to allow assessment of genotype quality.

Single-nucleotide polymorphisms (SNPs) that were polymorphic in many populations were primarily derived by comparing whole-genome sequence reads representing five taurine and one indicine breed to the reference genome assembly obtained from a Hereford cow (*10*) (table S2). This led to the ascertainment of SNPs with high minor allele frequencies (MAFs) within the discovery breeds (table S5). Thus, as expected, with trio progeny removed, SNPs discovered within the taurine breeds had higher average MAFs

*The full list of authors with their contributions and affiliations is included at the end of the manuscript.

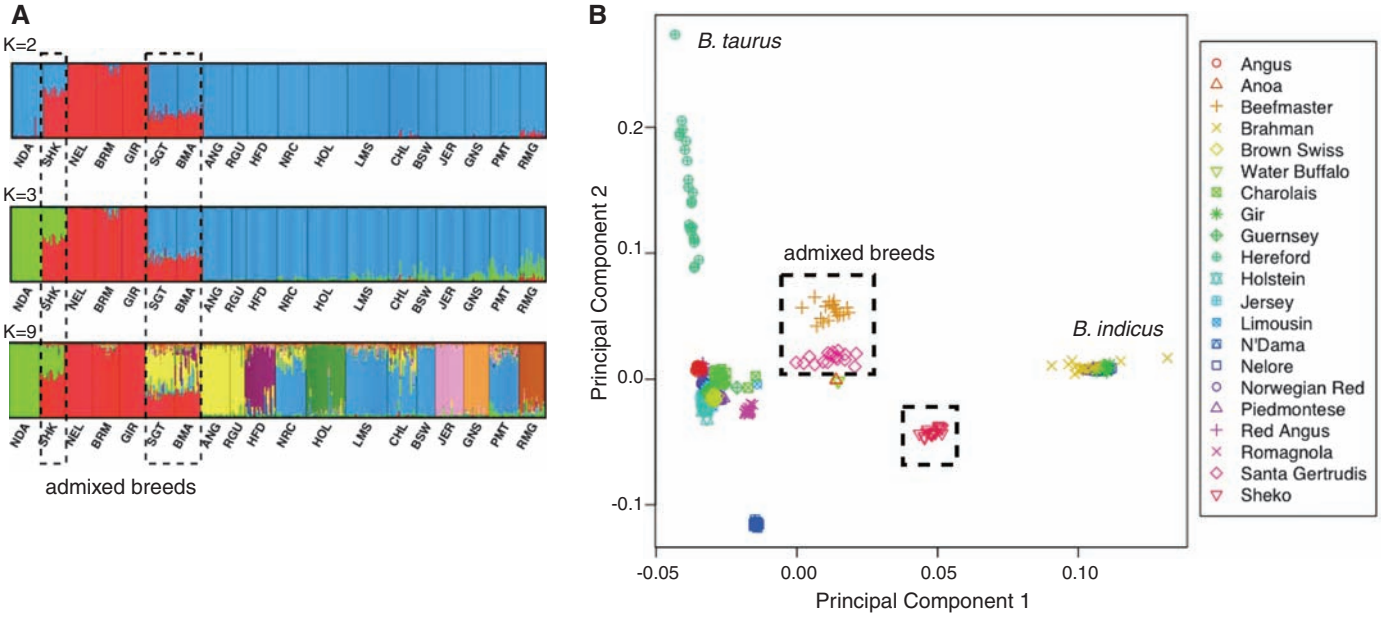

Fig. 1. (**A**) Population structure assessed by InStruct. Bar plot, generated by DISTRUCT, depicts classifications with the highest probability under the model that assumes independent allele frequencies and inbreeding coefficients among assumed clusters. Each individual is represented by a vertical bar, often partitioned into colored segments with the length of each segment representing the proportion of the individual's genome from K = 2, 3, or 9 ancestral populations. Breeds are separated by black lines. NDA, N'Dama; SHK, Sheko; NEL, Nelore; BRM, Brahman; GIR, Gir; SGT, Santa Gertrudis; BMA, Beefmaster; ANG, Angus; RGU, Red Angus; HFD, Hereford; NRC, Norwegian Red; HOL, Holstein; LMS, Limousin; CHL, Charolais; BSW, Brown Swiss; JER, Jersey; GNS, Guernsey; PMT, Piedmontese; RMG, Romagnola. (**B**) Principal components PC1 and PC2 from all SNPs. Taurine breeds remain separated from indicine breeds, and admixed breeds are intermediate.

within the taurine than the indicine breeds, and vice versa (table S5); about 30% of SNPs had MAFs >0.3 within the taurine breeds, whereas only about 19% had MAFs >0.3 within the indicine breeds (table S4). The proportions of SNPs in intergenic, intronic, and exonic regions were 63.74, 34.9, and 1.35%, respectively, similar to their representation within the genome. We found that as few as 50 SNPs were necessary for parentage assignment and proof of identity (table S9). Additionally, when we compared ancestries based on pedigree and allele-sharing between individuals, we were able to predict accurately the extent of ancestry when the pedigree was not known (fig. S24), which could be a useful tool for the management of endangered bovine populations.

To examine relatedness among breeds, we analyzed SNP genotype frequencies with InSTRUCT (*11*) and performed principal component analysis (PCA) using Eigenstrat (*12*) (Fig. 1 and fig. S27). Varying the number of presumed ancestral populations (K) within InSTRUCT revealed clusters consistent with the known history of cattle breeds (Fig. 1A). The first level of clustering (K = 2) reflects the primary, predomestication division of taurine from indicine cattle. Consequently, breeds derived from indicine and taurine crosses (Beefmaster, Santa Gertrudis, and Sheko) show signatures of admixture with both approaches. At K = 3, the African breeds N'Dama and Sheko separate from the European breeds—a division that reflects an early, possibly predomestication, divergence. PCA recapitulated these findings (Fig. 1B). At higher levels of K, we observed clusters that identify single breeds as closed endogamous breeding units. For example, at K = 9, Jersey, Hereford, Romagnola, and Guernsey each form unique clusters.

If modern breeds arose from bottlenecks from a large ancestral population, we should detect bottleneck signatures within patterns of linkage disequilibrium (LD) and effective population size. We found that the decline of r^2 with genetic distance varied among breeds, although the decline was generally rapid (fig. S10). The extent of LD in cattle is greater than human (*13*) but less than dog (*14*). The Jersey and Hereford breeds had higher r^2 than other breeds across the range of distances separating loci. N'Dama had the highest r^2 values at short distances and the lowest r^2 at long distances, which suggested that they were derived from a relatively small ancestral population not subjected to very narrow bottlenecks. The indicine breeds had lower r^2 values at short distances and intermediate r^2 values at longer distances, which indicated that their ancestral popula-

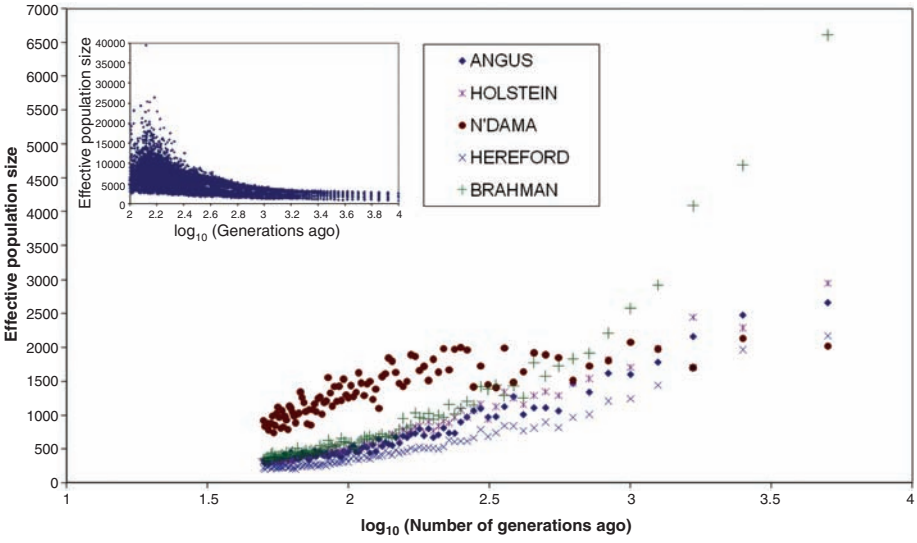

Fig. 2. Effective population size in the past estimated from linkage disequilibrium data. Inset graph shows effective population size for the European humans over the same period; from (*13*). Breeds as in Fig. 1.

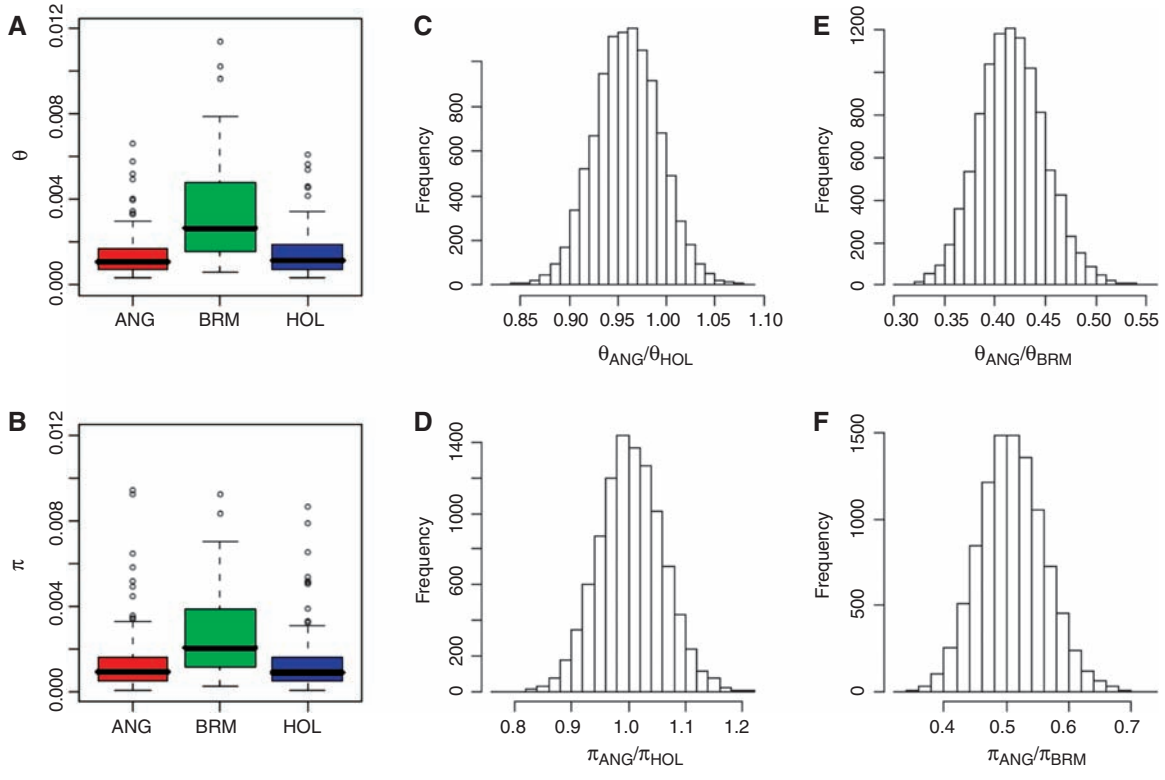

Fig. 3. Nucleotide diversity across five ENCODE regions resequenced in 47 animals from ANG, Angus; BRM, Brahman; and HOL, Holstein. (**A**) Watterson's estimate (θ) of the population mutation rate per base pair (pooled across regions). (**B**) Average pairwise nucleotide distance (π) within breeds. (**C** and **E**) Nonparametric bootstrap estimates of diversity ratios among the three populations on the basis of θ. (**D** and **F**) Nonparametric bootstrap estimates of diversity ratios among the three populations on the basis of π.

tion was much larger than that from which taurine cattle were domesticated (Fig. 2). As the MAFs for utilized SNPs were generally high and the estimates of LD did not require phased chromosomes, these results should be robust.

When breeds were combined, the decline in LD was more rapid, which reflected a lack of conserved phase relations across breeds. We characterized the extent of haplotype-sharing among breeds between pairs of adjacent SNPs using the *r* statistic. A high correlation between *r* values between two breeds indicates that the same haplotypes tend to persist within both breeds. Correlations between *r* values for SNPs separated by 10 kb were high among the taurine and indicine breeds but were low between these groups (fig. S11). Once SNPs are separated by 100 to 250 kb, we found little haplotype sharing between breeds. Clearly, phase relations dissipated as populations diverged despite the relatively young origin of all breeds. Breeds known to have a recent shared ancestry, notably, Angus and Red Angus; Holstein and Norwegian Red; and Beefmaster and Santa Gertrudis, showed a high correlation among *r* values for SNPs separated by 100 to 250 kb.

Breeds were expected to differ for effective population sizes (N_e) on the basis of differences in the decline of r^2 with genetic distance (*13*). We estimated N_e at various times in each breed's history by setting average r^2 values equal to their expectation (*15*) (Fig. 2 and table S1). N_e has recently declined for all breeds, which reflects bottlenecks associated with domestication, breed formation, and, in some breeds, recent intense selection for milk or beef production. In contrast, human N_e has expanded exponentially over the same period (inset to Fig. 2).

A smaller N_e suggests lower genetic diversity, which is of concern for species viability. To assess genetic diversity free from SNP ascertainment bias, we used the polymerase chain reaction to amplify and sequence 119 closely spaced fragments from five genomic regions on two chromosomes. Two of these regions were known to harbor quantitative trait loci (QTL). Following the amplification of these regions from 18 Angus, 16 Holstein, and 5 Brahman, the individual segments were Sanger-sequenced to detect SNPs. Of the 1201 discovered SNP, only 258 were common to taurine and indicine breeds, consistent with their age of divergence. Remarkably, 569 SNP (47.4%) were unique to Brahman, and 365 SNP (30.4%) were found only in Angus or Holstein, with 169 SNP (46.3%) common to both breeds. This suggests that breeds represent partly overlapping subsamples within the taurine diversity. However, seven times as many taurine animals had to be sequenced to uncover 75.3% as many SNPs as were discovered in indicine animals. Estimates of the unascertained genomic distributions of SNPs by MAFs within taurine and indicine breeds are in fig. S19.

Diversities as measured by the population mutation rate (θ) and pairwise nucleotide heterozygosity (π) were also estimated for the 119 fragments and compared between the three breeds (Fig. 3). Angus and Holstein have similar levels of nucleotide diversity measured by both statistics ($\sim 1.4 \times 10^{-3}$) and have ~40% more nucleotide variation than is found in human populations ($\sim 1.0 \times 10^{-3}$). Brahman variation was even higher, with average estimates of θ and π of 3.35×10^{-3} and 2.74×10^{-3}, respectively. These correspond to densities of 1 SNP every 714 bp for pairs of Angus or Holstein chromosomes and 1 SNP every 285 bp for pairs of Brahman chromosomes. These results demonstrate that genetic diversity in cattle is not low despite the decline in N_e.

The lower genetic diversity within modern taurine cattle could reflect a lower diversity within the predomestication ancestral population, and/or postdomestication effects of stronger bottlenecks at breed formation and stronger selection for docility and productivity. Selection is unlikely to be the primary cause, because the diversity distributions for θ and π were similar for all five sequenced regions, and only one region revealed a signature of selection. On the other hand, Fig. 2 suggests that the predomestication N_e of indicine cattle, which originated in southern Asia, a center of species diversity, was much larger than that of taurine cattle. Finally, the process of breed formation in European taurine cattle involved sequential limited migrations from the center of domestication in west Asia (*5*). Diversity declines with distance from primary sites of domestication (*4*) and ancient DNA from domesticated cattle and aurochs in Europe show that there was essentially no gene flow from the aurochs into domesticated cattle (*5*). Therefore, the evidence suggests that the current difference in diversity is mainly due to progenitor population diversity and bottleneck effects at, and before, breed formation rather than differences in the intensity of natural or artificial selection postdomestication.

Cattle have been marked by selection during domestication, breed formation, and ongoing selection to enhance performance and productivity. We utilized three methods to detect genomic selection in cattle: (i) the iHS statistic, which identifies regions of increased local LD (*16*) suggestive of directional selection; (ii) the F_{ST} statistic, a measure of the degree of differentiation between subpopulations (*17*); and (iii) the composite likelihood ratio test (*CLR*) (*18*), which assumes a selective sweep model (*10*). The iHS method was limited by low SNP density and our inability to completely specify ancestral SNP allele states (*10*). However, despite these limitations, we found evidence for selective sweeps on chromosomes 2, 6, and 14 (table S8 and fig. S20). We identified selection near *MSTN*, in which mutations can cause double muscling (*6*). Similarly, high iHS values were found in the region near *ABCG2* in which mutations cause differences in milk yield and composition (*8*). A peak in iHS values was also identified within a gene poor region of chromo-

Table 1. Genomic regions associated with extreme F_{ST} values with gene content consistent with domestication. F_{ST} values averaged over eight adjacent SNP. Gene functions from OMIM and NCBI Gene database, except for *R3HDM1* described in (*2*).

Genes	Index SNP	F_{ST}	BTA	Location	Effect or important phenotypes
High values					
ZRANB3, *R3HDM1*	rs29021800	0.31	2	64740286...64931017	Feed efficiency
WIF1	BTA-27454	0.29	5	52696749...53098507	Mammalian mesoderm segmentation
SPOCK1	BTA-142690	0.30	7	47501122...47899778	Proteoglycan—synaptic fields of the developing CNS
NBEA	BTA-153392	0.34	12	25884192...26189285	Human idiopathic autism
NMT1, *DCAKD*, *C1QL1*	BTA-45533	0.31	19	46088946...46157261	Activator of serum complement system
DACH2, *CHM*, *POU3F4*, *BRWD3*	BTA-161991	0.39	X	41471338...44478564	Human mental retardation
NLGN3 to *DGAT2L6*	BTA-164256	0.36	X	49279035...50192452	Severe combined immunodeficiency
Low values					
PPARGC1A, *DHX15*, *SOD3*	BTC-039516	0.04	6	45354707...45415844	Antioxidative extracellular protection
No known gene	BTC-049723	0.05	14	4569804...5204473	
DNAH9	rs29018632	0.05	19	30943404...31220868	Multisubunit molecular motor
POU5F1, MHC	BTA-55856	0.05	23	27895932...28145846	Major histocompatibility complex
ZNF187	rs29024230	0.04	23	30241236...30502690	Expressed in olfactory tissues
AUTS2	BTC-074065	0.04	25	31773107...32498861	Human autism susceptibility candidate
RYR2	rs29011563	0.05	28	8736599...8772178	Stress- and exercise-induced sudden cardiac death

some 14 adjacent to a region containing genes from *KHDRBS3* to *TG*, associated with intramuscular fat content in beef (*19*).

Calculation of F_{ST} across all populations for each SNP detected both balancing and divergent selection (fig. S20). Some of the highest and lowest average F_{ST} values were found in genes associated with behavior, the immune system, and feed efficiency (Table 1). Domestication most likely required the selection of smaller and more docile animals that could resist pathogens and adapt to a human-controlled environment (*20*). One region under selection contains *R3HDM1* and is associated with efficient food conversion and intramuscular fat content in some breeds (*2*). In addition to the *R3HDM1* gene (*21*), this region is also under selection in Europeans, most likely because it contains *LCT,* mutations of which allow the digestion of lactose in adults (*22*). These results suggest that mutations in this region may affect energy homeostasis. Furthermore, we detected selection between beef and dairy breeds with both CLR and iHS, represented by a broad, high F_{ST} peak across the region, centered on *SPOCK1* (Table 1). As several QTL have been mapped to this region, multiple loci could be under divergent selection (*1*), although this peak does not encompass *CAST*, which affects meat quality (*23*).

Our high resolution examination of cattle shows that unlike the dog—which has restricted diversity and high levels of inbreeding—domesticated cattle had a large ancestral population size and that more aurochs must have been domesticated than wolves; reducing the severity of the domestication bottleneck. SNP diversity within taurine breeds was similar to that of humans, but was significantly less than diversity within indicine breeds, which suggested that the Indian subcontinent was a major site of cattle domestication and predomestication diversity. Selection first for domestication and then for agricultural specialization have apparently reduced breed effective population sizes to relatively small numbers. The recent decline in diversity is sufficiently rapid that loss of diversity should be of concern to animal breeders. Despite this, population levels of LD are unexpectedly low considering the relatively small N_e, which indicates that effective population sizes were much larger in the very recent past.

References and Notes

1. S. M. Kappes *et al*., *J. Anim. Sci.* **78**, 3053 (2000).
2. W. Barendse *et al*., *Genetics* **176**, 1893 (2007).
3. D. G. Bradley *et al*., *Proc. Natl. Acad. Sci. U.S.A.* **93**, 5131 (1996).
4. R. T. Loftus *et al*., *Mol. Ecol.* **8**, 2015 (1999).
5. C. J. Edwards *et al*., *Proc. R. Soc. London B. Biol. Sci.* **274**, 1377 (2007).
6. L. Grobet *et al*., *Nat. Genet.* **17**, 71 (1997).
7. B. Grisart *et al*., *Genome Res.* **12**, 222 (2002).
8. M. Cohen-Zinder *et al*., *Genome Res.* **15**, 936 (2005).
9. A. Schreiber *et al*., *J. Hered.* **90**, 165 (1999).
10. Materials and methods are available as supporting materials on *Science* Online.
11. H. Gao, S. Williamson, C. D. Bustamante, *Genetics* **176**, 1635 (2007).
12. N. Patterson, A. L. Price, D. Reich, *PLoS Genet.* **2**, e190 (2006).
13. A. Tenesa *et al*., *Genome Res.* **17**, 520 (2007).
14. K. Lindblad-Toh *et al*., *Nature* **438**, 803 (2005).
15. J. A. Sved, *Theor. Popul. Biol.* **2**, 125 (1971).
16. B. F. Voight, S. Kudaravalli, X. Wen, J. K. Pritchard, *PLoS Biol.* **4**, e72 (2006).
17. J. M. Akey, G. Zhang, K. Zhang, L. Jin, M. D. Shriver, *Genome Res.* **12**, 1805 (2002).
18. R. Nielsen *et al*., *Genome Res.* **15**, 1566 (2005).
19. W. Barendse *et al*., *Aust. J. Exp. Agric.* **44**, 669 (2004).
20. J. Clutton-Brock, *A Natural History of Domesticated Mammals* (Cambridge Univ. Press, Cambridge, 2nd ed., 1999), 238 pp.
21. P. C. Sabeti *et al*., *Nature* **449**, 913 (2007).
22. S. A. Tishkoff *et al*., *Nat. Genet.* **39**, 31 (2007).
23. W. Barendse *et al*., *Genetics* **176**, 2601 (2007).

24. The Bovine Hapmap Consortium funded by the National Human Genome Research Institute of the National Institutes of Health, U.S. Department of Agriculture's Agricultural Research Service (USDA-ARS) and Cooperative State Research, Education and Extension Service (USDA CSREES), the Research Council of Norway, as well as: American Angus Association, American Hereford Association, American Jersey Cattle Association, AgResearch (New Zealand), Beef CRC and Meat and Livestock Australia for the Australian Brahman Breeders Association, Beefmaster Breeders United, The Brazilian Agricultural Research Corporation (Embrapa), Brown Swiss Association, Commonwealth Scientific and Industrial Research Organization, Dairy InSight, GENO Breeding and Artificial Insemination Association—Norway, Herd Book/France Limousin Selection, Holstein Association USA, International Atomic Energy Agency (IAEA)—United Nations Food and Agriculture Organization (FAO)/IAEA Vienna, International Livestock Research Institute—Kenya, Italian Piedmontese Breeders—Parco Tecnologico Padano, Italian Romagnola Society—Università Cattolica del Sacro Cuore, Livestock Improvement Corporation, Meat and Wool New Zealand. North American Limousin Foundation, Red Angus Association of America, Roslin Institute for UK Guernsey, and Sygen (now Genus). See SOM for additional acknowledgements. The genome sequence (AAFC03000000) and SNPs (SOM) are available from NCBI.

The Bovine HapMap Consortium

Overall project leadership: Richard A. Gibbs,[1,2]* Jeremy F. Taylor,[3]* Curtis P. Van Tassell[4]*

HapMap project group leaders: William Barendse,[5,6] Kellye A. Eversole,[7] Richard A. Gibbs,[1,2] Clare A. Gill,[8] Ronnie D. Green,[9] Debora L. Hamernik,[10] Steven M. Kappes,[9] Sigbjørn Lien,[11] Lakshmi K. Matukumalli,[12,4] John C. McEwan,[13] Lynne V. Nazareth,[1,2] Robert D. Schnabel,[3] Jeremy F. Taylor,[3] Curtis P. Van Tassell,[4] George M. Weinstock,[1,2] David A. Wheeler[1,2]

Breed champions: Paolo Ajmone-Marsan,[14] William Barendse,[5,6] Paul J. Boettcher,[15] Alexandre R. Caetano,[16] Jose Fernando Garcia,[15,17] Clare A. Gill,[8] Ronnie D. Green[9] (leader), Olivier Hanotte,[18] Sigbjørn Lien,[11] Paola Mariani,[19] John C. McEwan,[13] Loren C. Skow,[20] Tad S. Sonstegard,[4] Curtis P. Van Tassell,[4] John L. Williams[19,21]

Pedigree analysis and breed sampling: Alexandre R. Caetano,[16] Boubacar Diallo,[22] Ronnie D. Green,[9] Lemecha Hailemariam,[23] Olivier Hanotte,[18] Mario L. Martinez,[24]† Chris A. Morris,[25] Luiz O. C. Silva,[26] Richard J. Spelman,[27] Jeremy F. Taylor[3] (leader), Curtis P. Van Tassell[4,28] (leader), Woudyalew Mulatu,[28] Keyan Zhao[29]

Sample acquisition and DNA preparation: Colette A. Abbey,[8] Morris Agaba,[18] Flábio R. Araujo,[26] Rowan J. Bunch,[5,6] James Burton,[30] Clare A. Gill[8] (leader), Chiara Gorni,[19] Ronnie D. Green,[9] Hanotte Olivier,[18] Blair E. Harrison,[5,6] Sigbjørn Lien,[11] Bill Luff,[31] Marco A. Machado,[24] Paola Mariani,[19] John C. McEwan,[13] Chris A. Morris,[25] Joel Mwakaya,[18] Graham Plastow,[32] Warren Sim,[5,6] Loren C. Skow,[20] Timothy Smith,[33] Tad S. Sonstegard,[4] Richard J. Spelman,[27] Jeremy F. Taylor,[3] Merle B. Thomas,[5,6] Alessio Valentini,[34] Curtis P. Van Tassell,[4] Paul Williams,[5] James Womack,[35] John A. Woolliams[21]

Genome assembly: Yue Liu,[1,2] Xiang Qin,[1,2] Kim C. Worley[1,2] (leader)

SNP discovery: Chuan Gao,[8] Clare A. Gill,[8] Huaiyang Jiang,[1,2] Yue Liu,[1,2] Stephen S. Moore,[32] Lynne V. Nazareth,[1,2] Yanru Ren,[1,2] Xing-Zhi Song,[1,2] David A. Wheeler[1,2] (leader), Kim C. Worley[1,2]

ENCODE resequencing: Carlos D. Bustamante,[29] Ryan D. Hernandez,[29] Donna M. Muzny,[1,2] Lynne V. Nazareth,[1,2] Shobha Patil,[1,2] Yanru Ren,[1,2] Anthony San Lucas,[1,2] David A. Wheeler[1,2] (leader)

Genotyping: Qing Fu,[1,2] Matthew P. Kent,[11] Sigbjørn Lien,[11] Stephen S. Moore,[32] Lynne V. Nazareth[1,2] (leader), Richard Vega,[1,2] David A. Wheeler[1,2] (leader)

Database & Web site development: Colette A. Abbey,[8] Chuan Gao,[8] Clare A. Gill,[8] Ronnie D. Green,[9] Lakshmi K. Matukumalli[12,4] (leader), Aruna Matukumalli,[4] Sean McWilliam,[5,6] Curtis P. Van Tassell[4]

QA/QC: Colette A. Abbey,[8] Clare A. Gill,[8] Matthew P. Kent,[11] Sigbjørn Lien,[11] Lakshmi K. Matukumalli[12,4] (leader), Robert D. Schnabel[3] (leader), Gert Sclep,[19] Jeremy F. Taylor[3]

Allele frequency analysis: Paolo Ajmone-Marsan,[14] Katarzyna Bryc,[29] Carlos D. Bustamante[29] (leader), Jungwoo Choi,[8] Hong Gao,[29] John J. Grefenstette,[12] Lakshmi K. Matukumalli[12,4] (leader), Brenda Murdoch,[32] Stephen S. Moore,[32] Lynne V. Nazareth[1,2] (leader), Alessandra Stella,[19] Curtis P. Van Tassell,[4] Rafael Villa-Angulo,[12] David A. Wheeler[1,2] (leader), Mark Wright[29]

Map data provision and analysis: Jan Aerts,[21,36] Oliver Jann,[21] Lakshmi K. Matukumalli,[12,4] Riccardo Negrini,[14] Tad S. Sonstegard,[4] John L. Williams[19,21]

Haplotype estimation: Paolo Ajmone-Marsan,[14] John J. Grefenstette[12] (leader), Lakshmi K. Matukumalli,[12,4] Riccardo Negrini,[14] Robert D. Schnabel,[3] Jeremy F. Taylor,[3] Rafael Villa-Angulo[12]

Long-range LD analysis: John J. Grefenstette,[12] Lakshmi K. Matukumalli,[12,4] Curtis P. Van Tassell[4] (leader), Rafael Villa-Angulo[12]

LD persistence across breeds: Mike E. Goddard,[37,38] Ben J. Hayes[37] (leader)

Selective sweeps: William Barendse[5,6] (leader), Daniel G. Bradley,[39] Paul J. Boettcher,[15] Carlos D. Bustamante,[29] Jungwoo Choi,[8] Marcos Barbosa da Silva,[4,24] Clare A. Gill,[8] Lilian P. L. Lau,[39] George E. Liu,[4] David J. Lynn,[39,40] Francesca Panzitta,[19] Gert Sclep,[19] Mark Wright[29]

Applications: Carlos D. Bustamante[29] (leader), Ken G. Dodds,[13] John C. McEwan[13] (leader), Jeremy F. Taylor[3] (leader), Curtis P. Van Tassell[4]

[1]Human Genome Sequencing Center, Baylor College of Medicine, One Baylor Plaza, Houston, TX 77030, USA. [2]Department of Molecular and Human Genetics, Baylor College of Medicine, One Baylor Plaza, Houston, TX 77030, USA. [3]Division of Animal Sciences, University of Missouri, 920 East Campus Drive, Columbia, MO 65211–5300, USA. [4]Bovine Functional Genomics Laboratory, U.S. Department of Agriculture (USDA) Agricultural Research Service (USDA–ARS), Beltsville Agricultural Research Center (BARC)–East, Beltsville, MD 20705, USA. [5]Commonwealth Scientific and Industrial Research Organization (CSIRO), Livestock Industries, 306 Carmody Road, St. Lucia, Queensland 4067, Australia. [6]Cooperative Research Center (CRC) for Beef Genetic Technologies, University of New England, Armidale, NSW 2351, Australia. [7]Alliance for Animal Genome Research, 5207 Wyoming Road, Bethesda, MD 20816, USA. [8]Department of Animal Science, Texas A&M University, 2471 TAMU, College Station, TX 77843–2471, USA. [9]National Program Staff, USDA–ARS, 5601 Sunnyside Avenue, Beltsville, MD 20705, USA. [10]USDA Cooperative State Research, Education, and Extension Service, 1400 Independence Avenue, SW, Washington, DC 20250–2220, USA. [11]Centre for Integrative Genetics and Department of Animal and Aquacultural Sciences, Norwegian University of Life Sciences, Arboretveien 6, Ås 1432, Norway. [12]Department of Bioinformatics and Computational Biology, George Mason University, 10900 University Boulevard, Manassas, VA 20110, USA. [13]Animal Genomics, AgResearch, Invermay, Post Box 50034, Mosgiel 9053, New Zealand. [14]Istituto di Zootecnica, Università Cattolica del Sacro Cuore, via East Parmense, 84, Piacenza 29100, Italy. [15]Joint United Nations Food and Agriculture Organization (FAO)–International Atomic Energy Agency (IAEA), Division of Nuclear Techniques in Food and Agriculture, IAEA, Post Office Box 100, Wagramerstrasse 5, Vienna A1400, Austria. [16]Embrapa Genetic Resources and Biotechnology Center, Final Avenida W/5 Norte, Brasília, DF 70770-900, Brazil. [17]Universidade Estadual Paulista (UNESP), Department of Animal Production and Health, IAEA Collaborating Centre in Animal Genomics and Bioinformatics, Aracatuba, SP 16050-680, Brazil. [18]Animal Genetics Resources Characterization, International Livestock Research Institute, Post Office Box 30709, Nairobi 00100, Kenya. [19]Parco Tecnologico Padano, Via Einstein, Polo Universitario, Lodi 26900, Italy. [20]Department of Veterinary Integrative Biological Sciences, College of Veterinary Medicine and

Biomedical Sciences, Texas A&M University, College Station, TX 77843–4461, USA. [21]The Roslin Institute, Royal (Dick) School of Veterinary Studies, The University of Edinburgh, Roslin, Midlothian, E25 9PS, UK. [22]Direction Nationale de l'Élevage, Post Office Box 559, Conakry, Guinea. [23]Ethiopian Institute of Agricultural Research, Post Office Box 2003, Addis Ababa, Ethiopia. [24]Embrapa Dairy Cattle Center, Rua Eugênio do Nascimento, 610, Juiz de Fora, MG 36038-330, Brazil. [25]Animal Genomics, AgResearch, Ruakura, Post Box 3123, Hamilton 3240, New Zealand. [26]Embrapa Beef Cattle Center, Rod. BR 262, km 4, Campo Grande, MS 79002-970, Brazil. [27]Research and Development, LIC, Post Box 3016, Hamilton 3240, New Zealand. [28]Animal Genetics Resources Characterization, International Livestock Research Institute, Post Office Box 5689, Addis Ababa, Ethiopia. [29]Department of Biological Statistics and Computational Biology, Cornell University, 101 Biotechnology Building, Ithaca, NY 14853, USA. [30]Veterinary Biomedical Sciences, Royal (Dick) School of Veterinary Studies, The University of Edinburgh Summerhall, Edinburgh, EH9 1QH Scotland. [31]World Guernsey Cattle Federation, The Hollyhocks, 10 Clos des Goddards, Rue des Goddards, Castel, Guernsey, GY5 7JD, Channel Islands, UK. [32]Agricultural Food and Nutritional Science, University of Alberta, 410 AgFor Centre, Edmonton, AB, T6G 2P5, Canada. [33]Molecular Genetics Research Unit, USDA–ARS, U.S. Meat Animal Research Center, Post Office Box 166, Clay Center, NE 68933, USA. [34]Dipartimento di Produzioni Animali, Universita della Tuscia, via de Lellis, Viterbo 01100, Italy. [35]Department of Veterinary Pathobiology, College of Veterinary Medicine and Biomedical Sciences, Texas A&M University, College Station, TX 77843–4461, USA. [36]Genome Dynamics and Evolution, Wellcome Trust Sanger Institute, Hinxton, CB10 1SA, UK. [37]Animal Genetics and Genomics, Department of Primary Industries, 475 Mickelham Road Attwood, VIC 3031, Australia. [38]Faculty of Land and Food Resources, University of Melbourne, Royal Parade, Parkville, VIC 3010, Australia. [39]Smurfit Institute of Genetics, Trinity College, Dublin 2, Ireland. [40]Department of Molecular Biology and Biochemistry, Simon Fraser University, 8888 University Drive, Burnaby, BC, V5A 1S6, Canada.

*To whom correspondence and requests for materials should be addressed. E-mail: curt.vantassell@ars.usda.gov (C.P.V.T.), taylorjerr@missouri.edu (J.F.T.), and agibbs@bcm.tmc.edu (R.A.G.)
†In memoriam.

Supporting Online Material
www.sciencemag.org/cgi/content/full/324/5926/528/DC1
Materials and Methods
Figs. S1 to S27
Tables S1 to S9
References

31 October 2008; accepted 16 March 2009
10.1126/science.1167936

Revealing the History of Sheep Domestication Using Retrovirus Integrations

Bernardo Chessa,[1,2] Filipe Pereira,[3] Frederick Arnaud,[1] Antonio Amorim,[3] Félix Goyache,[4] Ingrid Mainland,[5] Rowland R. Kao,[1] Josephine M. Pemberton,[6] Dario Beraldi,[6] Michael J. Stear,[1] Alberto Alberti,[2] Marco Pittau,[2] Leopoldo Iannuzzi,[7] Mohammad H. Banabazi,[8] Rudovick R. Kazwala,[9] Ya-ping Zhang,[10] Juan J. Arranz,[11] Bahy A. Ali,[12] Zhiliang Wang,[13] Metehan Uzun,[14] Michel M. Dione,[15] Ingrid Olsaker,[16] Lars-Erik Holm,[17] Urmas Saarma,[18] Sohail Ahmad,[19] Nurbiy Marzanov,[20] Emma Eythorsdottir,[21] Martin J. Holland,[22,23] Paolo Ajmone-Marsan,[24] Michael W. Bruford,[25] Juha Kantanen,[26] Thomas E. Spencer,[27] Massimo Palmarini[1]*

The domestication of livestock represented a crucial step in human history. By using endogenous retroviruses as genetic markers, we found that sheep differentiated on the basis of their "retrotype" and morphological traits dispersed across Eurasia and Africa via separate migratory episodes. Relicts of the first migrations include the Mouflon, as well as breeds previously recognized as "primitive" on the basis of their morphology, such as the Orkney, Soay, and the Nordic short-tailed sheep now confined to the periphery of northwest Europe. A later migratory episode, involving sheep with improved production traits, shaped the great majority of present-day breeds. The ability to differentiate genetically primitive sheep from more modern breeds provides valuable insights into the history of sheep domestication.

The first agricultural systems, based on the cultivation of cereals, legumes, and the rearing of domesticated livestock, developed within Southwest Asia ~11,000 years before present (yr B.P.) (*1*, *2*). By 6000 yr B.P., agro-pastoralism introduced by the Neolithic agricultural revolution became the main system of food production throughout prehistoric Europe, from the Mediterranean north to Britain, Ireland, and Scandinavia (*3*); south into North Africa (*4*); and east into West and Central Asia (*5*).

Sheep and goats were the first livestock species to be domesticated (*6*). Multiple domestication events, as inferred by multiple mitochondrial lineages, gave rise to domestic sheep and similarly other domestic species (*7*–*10*). Initially, sheep were reared mainly for meat but, during the fifth millennium B.P. in Southwest Asia and the fourth millennium B.P. in Europe, specialization for "secondary" products such as wool became apparent. Sheep selected for secondary products appear to have replaced more primitive domestic populations. Whether specialization for secondary products occurred first in Southwest Asia or occurred throughout Europe is not known with certainty, owing to the lack of definitive archaeological evidence for the beginning of wool production (*6*, *11*, *12*).

For this study, we used a family of endogenous retroviruses (ERVs) as genetic markers to examine the history of the domestic sheep. ERVs result from the stable integration of the retrovirus genome ("provirus") into the germline of the host (*13*) and are transmitted vertically from generation to generation in a Mendelian fashion. The sheep genome contains at least 27 copies of ERVs related to the exogenous and pathogenic Jaagsiekte sheep retrovirus (enJSRVs) (*14*–*16*). Most enJSRVs loci are fixed in domestic sheep, but some are differentially distributed between breeds and individuals (i.e., they are insertionally polymorphic) (*14*). enJSRVs can be used as highly informative genetic markers because the presence of each endogenous retrovirus in the host

[1]Institute of Comparative Medicine, Faculty of Veterinary Medicine, University of Glasgow, Glasgow G61 1QH, UK. [2]Dipartimento di Patologia e Clinica Veterinaria, Universita' degli Studi di Sassari, 07100 Sassari, Italy. [3]Instituto de Patologia e Imunologia Molecular da Universidade do Porto (IPATIMUP), Faculdade de Ciências da Universidade do Porto, 4200-465 Porto, Portugal. [4]Área de Genética y Reproducción Animal, SERIDA-Somió, E-33203 Gijón, Spain. [5]Division of Archaelogical, Geographical and Environmental Sciences, University of Bradford, Bradford BD7 1DP, UK. [6]Institute of Evolutionary Biology, School of Biological Sciences, University of Edinburgh, Edinburgh EH9 3JT, UK. [7]National Research Council (CNR), ISPAAM, 80147 Naples, Italy. [8]Department of Biotechnology, Animal Science Research Institute of Iran (ASRI), 3146618361 Karaj, Iran. [9]Department of Veterinary Medicine and Public Health, Sokoine University of Agriculture, Morogor, Tanzania. [10]State Key Laboratory of Genetic Resources and Evolution, Kunming Institute of Zoology, Chinese Academy of Sciences, Kunming 650223, China. [11]Departamento de Producción Animal, Facultad de Veterinária, Universidad de León, 24071 León, Spain. [12]Genetic Engineering and Biotechnology Research Institute, Mubarak City for Scientific Research and Technology Applications, New Borg El-Arab City, 21934, Alexandria, Egypt. [13]National Diagnostic Center for Exotic Animal Diseases, China Animal Health and Epidemiology Centers, Qingdao 266032, China. [14]School of Health Science, Canakkale Onsekiz Mart University, 17100 Canakkale, Turkey. [15]International Trypanotolerance Centre, Banjul, Gambia. [16]Department of Basic Sciences and Aquatic Medicine, Norwegian School of Veterinary Science, 0033 Oslo, Norway. [17]Department of Genetics and Biotechnology, Faculty of Agricultural Sciences, University of Aarhus, 8830 Tjele, Denmark. [18]Department of Zoology, Institute of Ecology and Earth Sciences, University of Tartu, 51014 Tartu, Estonia. [19]NWFP Agricultural University, Peshwar, Pakistan. [20]All-Russian Research Institute of Animal Husbandry, Russian Academy of Agricultural Sciences, Dubrovitsy 142132, Russia. [21]Agricultural University of Iceland, Hvanneyri, IS-311 Borgarnes, Iceland. [22]Medical Research Council Laboratories, Fajara, Banjul, Gambia. [23]London School of Hygiene and Tropical Medicine, London WC1E 7HT, UK. [24]Istituto di Zootecnica, Universita' Cattolica del Sacro Cuore, 29100 Piacenza, Italy. [25]School of Biosciences, Cardiff University, Cardiff CF10 3AX, UK. [26]Biotechnology and Food Research, MTT Agrifood Research Finland, 31600 Jokioinen, Finland. [27]Center for Animal Biotechnology and Genomics, Texas A&M University, College Station, TX 77843, USA.

*To whom correspondence should be addressed. E-mail: m.palmarini@vet.gla.ac.uk

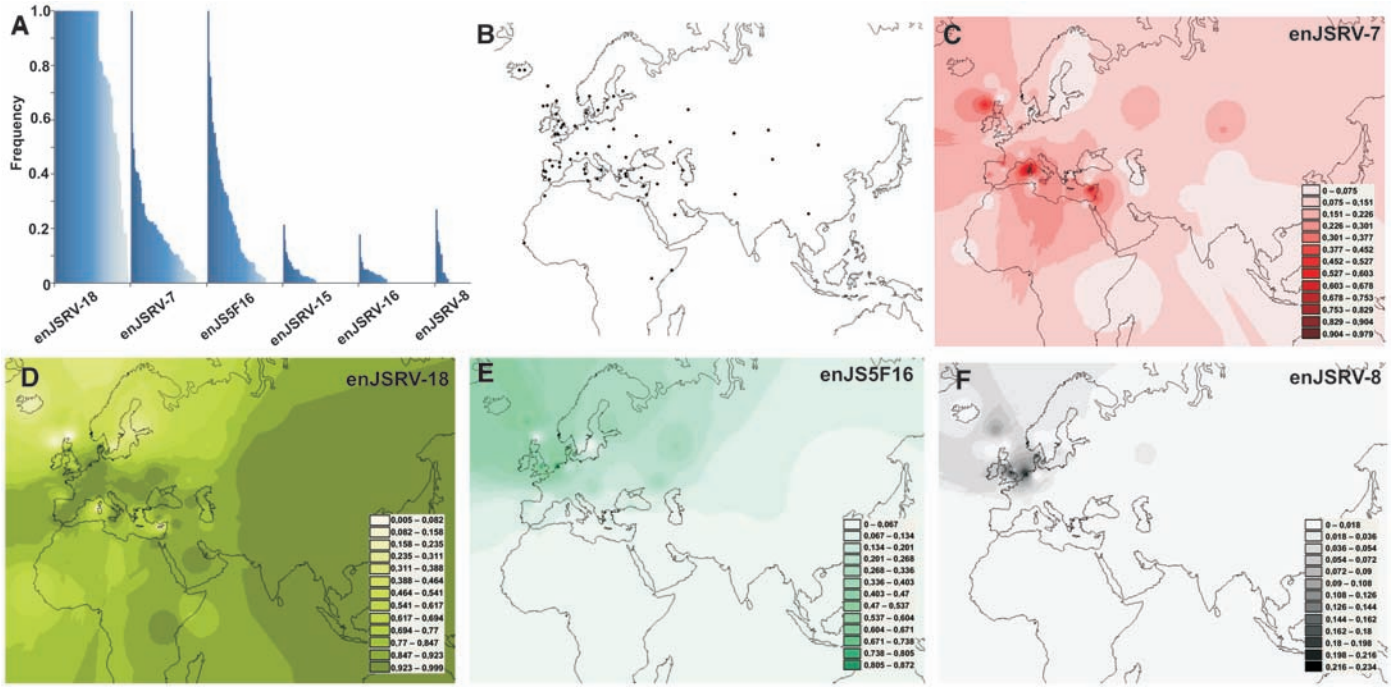

Fig. 1. Worldwide distribution of insertionally polymorphic enJSRVs. Distribution of the insertionally polymorphic enJSRV loci analyzed in this study in 65 sheep populations representing local breeds from the Old World. (**A**) Frequencies of each enJSRV locus in each population are represented by a vertical bar and arranged in descending order. Insertion frequencies were obtained with the software Arlequin 3.11 (*27*); the absence of a specific enJSRV provirus was treated as a recessive allele. (**B**) Locations of sheep populations sampled. (**C** to **F**) Interpolation maps displaying the spatial distribution of estimated enJSRVs frequencies. The geographical variation was visualized with the "Spatial Analyst Extension" of ArcView GIS 3.2 software (ESRI, Redlands, California, USA). Interpolated map values were calculated by using the inverse distance weighted with 12 nearest neighbors and a power of 2, and interpolation surfaces were divided into 13 classes with higher insertion frequencies indicated by darkest shading. The central point of the sampling area was used as geographic coordinates for each population (table S1).

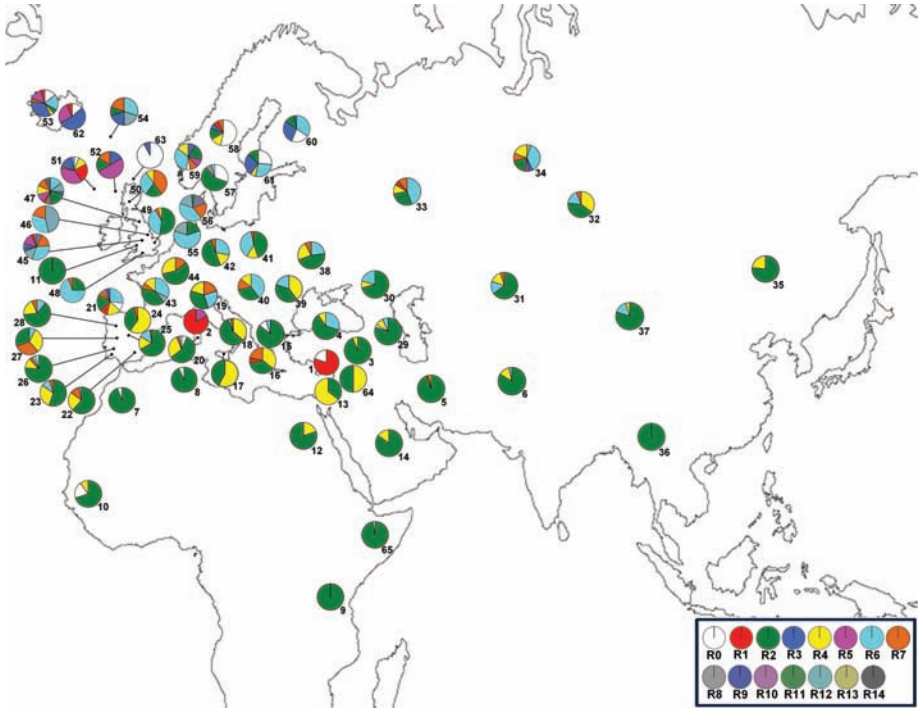

Fig. 2. Combination of enJSRV proviruses (retrotypes) in the domestic sheep. Pie charts in the figure represent the frequency of each retrotype in the 65 populations tested. Each sheep tested was assigned a retrotype on the basis of the combination of insertionally polymorphic enJSRV proviruses present in their genome. Retrotypes R0 to R14 were defined as follows: R0 = no insertionally polymorphic enJSRVs; R1 = enJSRV-7; R2 = enJSRV-18; R3 = enJS5F16; R4 = enJSRV-7 + enJSRV-18; R5 = enJSRV-7 + enJS5F16; R6 = enJSRV-18 + enJS5F16; R7 = enJSRV-7 + enJSRV-18+ enJS5F16; R8 = enJSRV-8; R9 =enJS5F16 + enJSRV-8; R10 = enJSRV-7 + enJS5F16 + enJSRV-8; R11 = enJSRV-18 + enJSRV-8; R12 = enJSRV-18 + enJS5F16 + enJSRV-8; R13 = enJSRV-7 + enJSRV-18 + enJSRV-8; R14 = enJSRV-7 + enJSRV-18 + enJS5F16 + enJSRV-8. Each retrotype is represented with a different color (and pattern) as indicated in the figure. Numbers beside each pie chart indicate each of the 65 populations tested as indicated in table S1. Most of the populations in Southwest Asia, Central Asia, Southern Europe, and Africa possess R2 (i.e., presence of enJSRV-18 only, shown in green) as the predominant retrotype. Around the Mediterranean basin there is also a high proportion of R4 given by the contemporary presence of enJSRV-7 and enJSRV-18 (shown in yellow). The primitive breeds are characterized by a high proportion of animals with R0 (no insertionally polymorphic proviruses, shown in white) or R1 (presence of enJSRV-7 only, shown in red). A "Nordic" retrotype, R3 (shown in blue), was characterized by a low frequency of enJSRV-18 and a high frequency of enJS5F16; Nordic populations also had a relatively high frequency of sheep with none of the insertionally polymorphic proviruses tested.

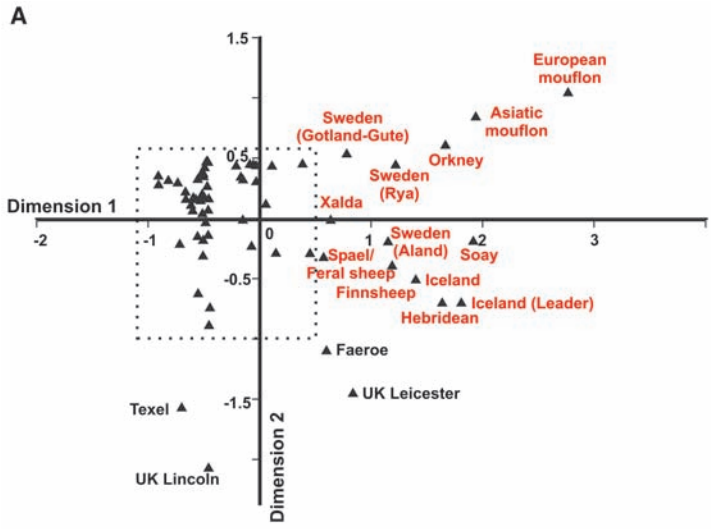

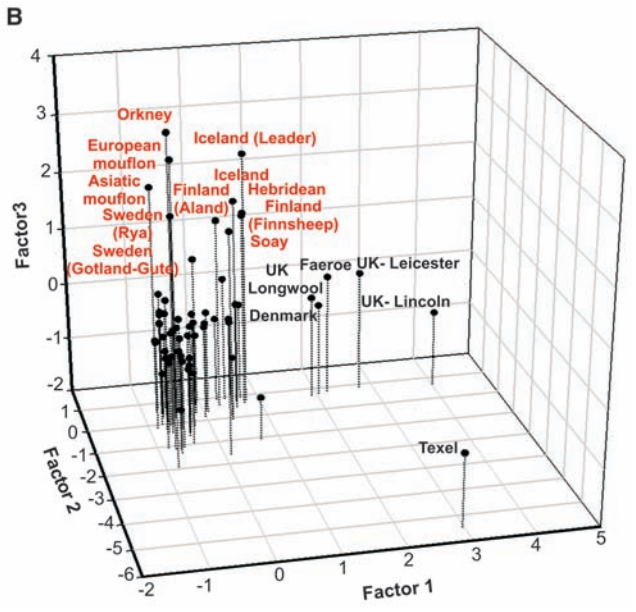

Fig. 3. Genetic distances between sheep populations on the basis of enJSRVs insertion frequencies. (**A**) Multidimensional (MDS) scaling plot computed from the matrix of Nei's unbiased genetic distances (TFPGA 1.3 software) (*28*). The dominant nature of the enJSRVs as genetic markers was considered in all analyses. The matrix of interpopulation distances was summarized in two dimensions by use of MDS analysis as implemented by STATISTICA '99 software (StatSoft, Tulsa, Oklahoma, USA). Each triangle represents one of the 65 populations tested. In the graph, only those populations outside the main cluster (enclosed within the square with the broken line and including most breeds from Africa, Asia, and Europe) have been named. (**B**) Tridimensional plot summarizing data obtained by PCA of the insertionally polymorphic enJSRV proviruses in the 65 sheep populations tested with the Proc Factor of the statistical package SAS/STAT (SAS Institute, Cary, North Carolina, USA) according to the recommendations by Cavalli-Sforza *et al*. (*29*). Four factors, accounting for 86.66% of variation, with eigenvalue ≥ 1 were identified. Factor 1 (on the *x* axis) explained 30.09% of variation and can be interpreted as the "Northern Sea factor," distinguishing between a group of populations formed from some United Kingdom and continental European (including Denmark and Texel) sheep populations and the others. Factor 2 (on the *y* axis) explained 23.58% of variation separating the Texel population from the rest. Factor 3 (on the *z* axis) explained 22.92% of variation and can be interpreted as the "primitive breed factor," distinguishing the group of populations formed by the Mouflon and Scandinavian populations (including the Hebridean, Orkney, and Soay populations) from the rest. For clarity, the populations that form the main cluster have not been named.

Fig. 4. Morphological characteristics of primitive breeds. Breeds identified in this study as remnants of the first sheep migrations possess morphological characteristics (such as darker, coarser fleece; moulting coat; frequent presence of horns in females) similar to those of wilder sheep and the Mouflon. (**A**) Urial sheep; (**B**) Cyprus Mouflon; (**C**) Mediterranean Mouflon; (**D**) Orkney sheep; (**E**) Soay sheep; (**F**) Gute sheep; (**G**) Åland sheep; (**H**) Icelandic sheep; and (**I**) Hebridean sheep.

genome is the result of a single integration event in a single animal and is irreversible, so populations sharing the same provirus in the same genomic location are de facto phylogenetically related.

We analyzed genomic DNA samples collected from 1362 animals belonging to 133 breeds of the domestic sheep (*Ovis orientalis aries*, usually referred to as *Ovis aries*) and closest wild relatives (see below) divided into 65 groups formed by one or more breeds sharing a common geographical location and/or breeding links (table S1) (*17*). Samples tested also included the Urial sheep (*Ovis vignei*) and the Mediterranean and Asiatic Mouflon (*Ovis orientalis musimon*, *Ovis orientalis ophion*, and *Ovis orientalis orientalis*). Most of the breeds that we studied are local, historically related to specific geographical areas, and not subjected to the intensive breeding programs of commercial flocks.

Samples were tested for the presence or absence of six independently inherited insertionally polymorphic enJSRVs (enJSRV-18, enJSRV-7, enJSRV-8, enJSRV-15, enJSRV-16, and enJS5F16) by polymerase chain reaction with two sets of primers that amplify, respectively, the 5′ and 3′ long terminal repeats (LTRs) of each provirus (including the flanking genomic DNA sequences of the host) as described (*14*, *17*). Provirus enJSRV-18 had by far the highest frequency in our data set (85%); enJSRV-7 and enJS5F16 were detected in 27% and 30% of the samples, respectively; and enJSRV-15, enJSRV-16, and enJSRV-8 were present in only 3 to 5% of the samples (Fig. 1A).

We inferred the distribution of the insertionally polymorphic enJSRV loci in the earliest domesticated sheep by determining their occurrence in the Urial sheep and in the Mediterranean/Asiatic Mouflon, and then by verifying the molecular signatures indicative of the age of a provirus. The estimated divergence between the Urial (one of the closest living relatives of the domestic sheep) and the domestic sheep is ~800,000 yr B.P. (*18*). Consequently, any provirus that is shared between these two species will predate the process of domestication. The same is true for the Asiatic Mouflon, which is believed to be the direct ancestor of the domestic sheep (*19*–*21*), whereas the closely related Mediterranean Mouflon is thought to be the remnant of the first domesticated sheep readapted to feral life (*19*, *22*, *23*). Despite its widespread distribution in the samples tested, enJSRV-18 was absent from the Urial sheep (n = 5), the Mediterranean Mouflon (n = 17), and the Asiatic Mouflon (n = 15). By contrast, the relatively rarer enJSRV-7 was detected in three of five Urial sheep, in most (86%) Asiatic Mouflons, and in all Mediterranean Mouflons. These data suggest that the integration of enJSRV-7 in the germline of the host predates the integration of enJSRV-18. Differences between the proximal (5′) and distal (3′) LTRs of enJSRV-7 confirm its antecedence. The divergence between the 5′ and 3′ LTR gives an estimate of the "age" of an endogenous provirus because upon infection, retroviruses reverse transcribe their genome from RNA into DNA, and during this process they duplicate the genomic ends, giving rise to two identical LTRs. Proximal and distal LTRs of an endogenous retrovirus must be identical upon integration, but can diverge over time at the same rate as noncoding sequences (~2.3×10^{-9} to 5×10^{-9} substitutions per site per year). enJSRV-7 appears to be the oldest provirus in our samples because it displays five nucleotide (nt) substitutions between 5′ and 3′ LTRs (445 nt long), whereas all the other insertionally polymorphic proviruses (including enJSRV-18) have identical LTRs. These data suggest that the populations originating from the earliest domesticated sheep did not carry any of the insertionally polymorphic enJSRVs used in this study or carried enJSRV-7.

To visualize the geographical variation of all enJSRV loci, we constructed interpolation maps from their insertion frequency values (Fig. 1, B to F). The highest frequency of enJSRV-7 was found in the Mediterranean Mouflon and in Soay sheep now inhabiting the island of St. Kilda off northwest Scotland (Fig. 1C). enJSRV-18 was uniformly distributed at very high frequencies throughout the Old World. Low frequencies of enJSRV-18 were observed in the islands inhabited by the Mediterranean Mouflon and in peripheral regions of northwest Europe (Fig. 1D). Two enJSRV proviruses, enJS5F16 and enJSRV-8, showed a similar geographical pattern with a high frequency in the British Isles and Scandinavia (Fig. 1, E and F). The less common enJSRV-15 and enJSRV-16 had less obvious geographical patterns (fig. S1).

We then analyzed the combination of insertionally polymorphic enJSRVs (which we call "retrotype") in each of the populations analyzed (Fig. 2). The R2 retrotype (representing the presence of enJSRV-18 only) was the predominant retrotype in most of the populations tested. The R4 retrotype, indicating presence of enJSRV-18 and enJSRV-7 together (Fig. 2), was another common retrotype in the area corresponding to the historical Phoenicia and in southern Europe, suggesting that maritime trade and colonization had a major influence on sheep movement in the Mediterranean, as confirmed by studies using sheep mitochondrial DNA variation (*24*, *25*). Additional enJSRV insertions accounted for more complex retrotypes of populations in northern Europe (see also supporting online text). Sheep populations in Africa, Pakistan, and China displayed a similarly homogeneous R2 retrotype pattern common to the populations in Southwest Asia, suggesting direct migratory links of domestic sheep between these areas. Most of the populations from Scandinavia displayed retrotypes similar to those of Icelandic and the Faeroe Island populations, supporting the historically registered movements of the Norse settlers during the later first millennium C.E. (*26*). To visualize the genetic relationship of the tested populations, we analyzed the data using two different approaches: a multidimensional scaling (MDS) plot obtained from the interpopulation matrix of Nei's unbiased genetic distances and principal component analysis (PCA) computed from the correlation matrix among enJSRV insertion frequencies.

The MDS analysis revealed a marked separation (particularly evident in the first dimension) between the great majority of domestic breeds and an outer group formed by the Mouflon, Soay sheep, Hebrideans, Orkney sheep, Icelandic, and Nordic breeds (Fig. 3A). Similar results were obtained by PCA (Fig. 3B).

Collectively, the data we obtained indicate that relicts of the first migrations are still present in the Mouflon of Sardinia, Corsica, and Cyprus and in breeds in peripheral north European areas. On the basis of their retrotypes, these primitive populations are characterized by the absence of enJSRV-18 (fixed in most of the modern breeds) and either the presence of enJSRV-7 in high frequency or the lack of insertionally polymorphic enJSRVs (including enJSRV-7). By contrast, the retrotypes of the great majority of sheep breeds cluster together and are characterized by the high frequency or fixation of enJSRV-18.

The homogeneous retrotypes (R2 only, or both R2 and R4) that we observed in the sheep of modern-day Turkey, Iran, Saudi Arabia, Syria, Israel, and Egypt, combined with available archaeological evidence, suggest that selection of domestic sheep with the desired secondary characteristics common to the modern breeds occurred first in Southwest Asia and then spread successfully into Europe and Africa, and the rest of Asia. This may provide genetic support to the theory that specialized wool production arose in Southwest Asia and then spread throughout Europe (*11*). The primitive breeds survived the second migrations of improved breeds from Southwest Asia by returning to a feral or semi-feral state in islands without predators or by occupying inaccessible areas less prone to commercial exchanges and associated introgression. Most, if not all, of the breeds we identified as of ancient origin were already considered primitive on the basis of morphological traits such as a darker and coarser hair (instead of a whiter woolly fleece), a moulting coat, and the frequent presence of horns in females as well as males (Fig. 4).

Our study also provides genetic evidence supporting the anecdotal origin of some less common sheep breeds. For example, one of the 10 populations analyzed from the British Isles, the Jacob sheep, displayed a homogeneous R2 retrotype very different from that of the other British populations and more similar to that of the southwestern Asiatic and African breeds. The origins of the Jacob are unknown. This breed owes its name to the Biblical story of Jacob who took "every speckled and spotted sheep" as a wage from his father-in-law Laban (Genesis 30:25–43; probably the first recorded use of selective breeding in livestock). Our retrotype analysis supports a direct link between the Jacob

sheep and breeds in Southwest Asia or Africa rather than other British breeds. Our study also firmly links the Soay sheep with the Mediterranean and Asiatic Mouflon.

In conclusion, the polymorphic nature of enJSRVs revealed a remarkable secondary population expansion of improved domestic sheep, most likely out of Southwest Asia, providing valuable insights into the history of pastoralist societies whose economy included sheep husbandry. By differentiating genetically primitive breeds from modern ones, our study offers a rationale for identifying and preserving rare gene pools. Finally, we demonstrate the utility of ERVs as a new class of genetic markers used to unravel the history of a domesticated species.

References and Notes

1. M. A. Zeder, *Proc. Natl. Acad. Sci. U.S.A.* **105**, 11597 (2008).
2. S. Colledge, J. Conolly, S. Shennan, *Eur. J. Archaeol.* **8**, 137 (2005).
3. T. D. Price, *Europe's First farmers* (Cambridge Univ. Press, Cambridge, 2000).
4. G. Barker, in *Examining the Farming/Language Dispersal Hypothesis*, P. Bellwood, C. Renfrew, Eds. (McDonald Institute Monographs, Cambridge, 2002), pp. 151–162.
5. D. R. Harris, C. Gosden, in *The Origins and Spread in Agriculture and Pastoralism in Eurasia*, D. Harris, Ed. (UCL Press, London, 1996), pp. 370–389.
6. M. L. Ryder, *Sheep & Man* (Duckworth, London, 1983).
7. S. Pedrosa *et al*., *Proc. Biol. Sci.* **272**, 2211 (2005).
8. M. Tapio *et al*., *Mol. Biol. Evol.* **23**, 1776 (2006).
9. J. R. Meadows, I. Cemal, O. Karaca, E. Gootwine, J. W. Kijas, *Genetics* **175**, 1371 (2007).
10. S. Naderi *et al*., *Proc. Natl. Acad. Sci. U.S.A.* **105**, 17659 (2008).
11. A. Sherratt, in *Patterns of the Past: Studies in Honour of David Clark*, I. Hodder, G. Isaacs, N. Hammond, Eds. (Cambridge Univ. Press, Cambridge, 1981), pp. 261–306.
12. D. Helmer, L. Gourichon, E. Vila, *Anthropozoologica* **42**, 41 (2007).
13. J. D. Boeke, J. P. Stoye, in *Retroviruses*, J. M. Coffin, S. H. Hughes, H. E. Varmus, Eds. (Cold Spring Harbor Laboratory Press, Plainview, NY, 1997), pp. 343–436.
14. F. Arnaud *et al*., *PLoS Pathog.* **3**, e170 (2007).
15. M. Palmarini, J. M. Sharp, M. De las Heras, H. Fan, *J. Virol.* **73**, 6964 (1999).
16. F. Arnaud, M. Varela, T. E. Spencer, M. Palmarini, *Cell. Mol. Life. Sci.* **65**, 3422 (2008).
17. Materials and Methods are available as supporting material on *Science* Online.
18. M. Hernández Fernández, E. S. Vrba, *Biol. Rev. Camb. Philos. Soc.* **80**, 269 (2005).
19. S. Hiendleder, B. Kaupe, R. Wassmuth, A. Janke, *Proc Biol Sci* **269**, 893 (2002).
20. J. Clutton-Brock, *A Natural History of Domesticated Mammals* (Cambridge Univ. Press, Cambridge, ed. 2, 1999).
21. D. Zohary, E. Tchernov, L. Horwitz, *J. Zool.* **245**, 129 (1998).
22. F. Poplin, *Ann. Genet. Sel. Anim.* **11**, 133 (1979).
23. J.-D. Vigne, in *The Holocene History of the European Vertebrate Fauna. Modern Aspects of Research*, N. Benecke, Ed. (Verlag Marie Leidorf GmbH, Rahden/Westf, Germany, 1999), pp. 295–322.
24. S. Pedrosa *et al*., *Genet. Sel. Evol.* **39**, 91 (2007).
25. F. Pereira *et al*., *Mol. Biol. Evol.* **23**, 1420 (2006).
26. T. H. McGovern, *Annu. Rev. Anthropol.* **19**, 331 (1990).
27. L. Excoffier, G. Laval, S. Schneider, *Evol. Bioinform. Online* **1**, 47 (2005).
28. M. P. Miller, Department of Biological Sciences, Northern Arizona University, Flagstaff, AZ (1997).
29. L. L. Cavalli-Sforza, P. Menozzi, A. Piazza, *The History and Geography of Human Genes* (Princeton Univ. Press, Princeton, NJ, 1994).

30. We thank the ECONOGENE, North-SheD, and NordGen consortia, and C. Leroux, J. DeMartini, J. Trafford, S. Haywood, V. Andresdottir, S. Thorgeirsdottir, M. Ganter, M. Reichert, Y. Bayon Gonzalez, K. Voigt, V. Feinstein, F. San Primitivo, and P. Halstead for help in obtaining some of the samples used in this study and for useful comments. We thank P. Murcia for coining the term "retrotypes." We are grateful to G. P. Di Meo and A. Perucatti for fluorescence in situ hybridization analysis. We also thank B. Huffman (www.ultimateungulate.com), NordGen, A. Ozgul, S. Jeppson, and K. Headspeath for images reproduced in Fig. 4. This study was supported by the Biotechnology and Biological Sciences Research Council, the Wellcome Trust and in part by NIH grant HD05274, the Scottish Funding Council through a Strategic Research Developmental Grant, Fundação para a Ciência e a Tecnologia, "Misura P5 Biodiversita' animale," from the Regione autonoma della Sardegna, the Chinese Academy of Sciences, the National Natural Science Foundation of China, and the European Regional Fund (Centre of Excellence FIBIR). The Soay sheep project in St. Kilda is supported by the Natural Environment Research Council. IPATIMUP is partially supported by "Programa Operacional Ciência e Inovação 2010" (POCI 2010), VI Programa Quadro (2002–2006). M.P. is a Wolfson–Royal Society Research Merit awardee. The GenBank accession numbers of the enJSRV loci described in this paper are as follows: EE680319 (enJSRV-6), EF680306 (enJSRV-8), EF680298 (enJSRV-7), EF680299 (enJSRV-15), EF680300 (enJSRV-16), EF680301 (enJSRV-18), and AF136224 (enJS5F16).

Supporting Online Material

www.sciencemag.org/cgi/content/full/324/5926/532/DC1
Materials and Methods
SOM Text
Figs. S1 to S3
Tables S1 and S2
References

7 January 2009; accepted 17 March 2009
10.1126/science.1170587

Hot and Stirring Plates

The rugged EchoTherm Models HP51 and HS51 Digital Hot Plates and Digital Stirring Hot Plates are designed for large samples. The units feature membrane keyboards and full-function liquid crystal displays where all parameters are continuously visible. They can store two settings in memory for instant recall and use at any time. They are suitable for use with large samples in chemical, pharmaceutical, environmental, biochemical, electronic, and other laboratories where temperature accuracy, ease of use, and reproducible sample preparations are a must. Tops are available in a choice of chemically resistant ceramic and milled-flat cast aluminum. Both tops are 12-inch squares. Temperatures can be set up to 450°C on the ceramic tops and to 400°C on the cast aluminum, which are recommended for working with solids directly on the heater plate surface. Stirrer speeds can be set from 100 rpm to 1,500 rpm.

Torrey Pines Scientific
For information 866-573-9104
www.torreypinesscientific.com

Laser Scanning Microscopes

The LSM 700 laser scanning microscope for materials research allows precise, three-dimensional imaging of surfaces. The combination of fluorescence and reflection techniques enables high-precision examinations of semiconductors, metal, glass, and polymers with high information content. The integrated detection of fluorescence signals on and in the materials provides additional information. The easy-to-use system permits precise capture of three-dimensional topography or the determination of finest roughness, for example, without damaging the surface.

Carl Zeiss MicroImaging
For information +49-(0)-3641/642770
www.zeiss.de/micro

Fluorescence Detection

A patented new ultramicrovolume fluorescence lens cell is designed to address the need for researchers to carry out clinical, biochemical, and pharmaceutical studies cost-effectively by performing ultraviolet/visible light spectrofluorometer analysis on samples of 5 microliters or less. It provides a practical solution when samples cannot be prepared in or diluted to larger volumes. Because it offers good sensitivity even in very small volumes, the Type 19FL ultramicro cell is suited for molecular biology and forensic applications, as well as proteomics applications in which the sensitivity of the cell is sufficiently high to measure native fluorescence of proteins prepared in microliter quantities. The cell design also allows most of the sample to be recovered.

Starna
For information 800-228-4482
www.starna.com

Custom Protein Expression Services

A new custom service, baculoXPRESS is a suite of comprehensive baculovirus expression services that can be tailored to individual requirements. The new services can provide customers with multiple recombinant viruses quickly and cost-effectively. Services include gene synthesis; polymerase chain reaction cloning; subcloning; production of recombinant viruses using flashBAC, flashBACGOLD, or flashBACULTRA virus DNA; expression optimization; protein production and purification; and next-day virus titration using baculoQUANT methodology.

Oxford Expression Technologies
For information +44-(0)1865-483-236
www.oetltd.com

Automatic Melting Point Detection

The SMP40 automatic melting point detection apparatus incorporates the latest digital video imaging technology to detect and capture the melting point of up to three samples simultaneously. With a color VGA screen to view the melting process in real time or retrospectively, the SMP40 introduces an innovative split-design concept for maximum footprint flexibility. For example, the sample side of the apparatus can be located at the back of the bench or even in a fume cupboard, while the control side detects which way the unit is being used and adjusts the screen orientation accordingly. Around 200 results can be stored in the form of AVI video files. Features include a safety hood to protect samples and act as a light shield, a capillary storage drawer with integral glass cutter, and a sample storage area.

Bibby Scientific
For information +44-(0)-844-936-0234
www.bibby-scientific.com

Fast Image Capture

Version 4.7.2 of AxioVision software enables fast image capture using the CellObserver SD and Laser TIRF 3 microscope systems. AxioVision now enables the combination of high-speed image capture under physiological conditions (such as incubation) and fast confocal microscopy, enhancing three-dimensional living cell imaging. The new software also permits the analysis of near-membrane processes at a high temporal resolution.

Carl Zeiss
For information +49-(0)-3641-642770
www.zeiss.de/micro

Flow Cytometer System

The Accuri C6 Flow Cytometer System includes two lasers and six detectors in only 2 square feet. The system includes blue and red lasers (488 nm and 640 nm), four fluorescence detectors, and two scatter detectors (forward and side). It features simple setup, with no detector voltage or gain adjustment required. Its software has an intuitive user interface designed with the researcher in mind. This cytometer works with current reagents and protocols, and data can be exported to popular third-party packages.

Accuri Cytometers
For information 734-994-8000
www.accuricytometers.com

Electronically submit your new product description or product literature information! Go to **www.sciencemag.org/products/newproducts.dtl** for more information.

Newly offered instrumentation, apparatus, and laboratory materials of interest to researchers in all disciplines in academic, industrial, and governmental organizations are featured in this space. Emphasis is given to purpose, chief characteristics, and availabilty of products and materials. Endorsement by *Science* or AAAS of any products or materials mentioned is not implied. Additional information may be obtained from the manufacturer or supplier.

Science Careers
Classified Advertising

For full advertising details, go to **ScienceCareers.org** and click **For Advertisers**, or call one of our representatives.

UNITED STATES & CANADA
E-mail: advertise@sciencecareers.org
Fax: 202-289-6742

Joribah Able
Industry – US & Canada
Phone: 202-326-6572

Alexis Fleming
Northeast Academic
Phone: 202-326-6578

Tina Burks
Southeast Academic
Phone: 202-326-6577

Daryl Anderson
Midwest/Canada Academic
Phone: 202-326-6543

Nicholas Hintibidze
West Academic
Phone: 202-326-6533

EUROPE & INTERNATIONAL
E-mail: ads@science-int.co.uk
Fax: +44 (0) 1223 326532

Tracy Holmes
Associate Director, *Science* Careers
Phone: +44 (0) 1223 326525

Alex Palmer
Phone: +44 (0) 1223 326527

Dan Pennington
Phone: +44 (0) 1223 326517

Susanne Kharraz Tavakol
Phone: +44 (0) 1223 326529

Louise Moore
Phone: +44 (0) 1223 326528

JAPAN
Mashy Yoshikawa
Phone: +81 (0) 3 3235 5961
E-mail: myoshikawa@aaas.org

To subscribe to *Science*:
In US/Canada call 202-326-6417 or 1-800-731-4939.
In the rest of the world call +44 (0) 1223 326515.

Science makes every effort to screen its ads for offensive and/or discriminatory language in accordance with US and non-US law. Since we are an international journal, you may see ads from non-US countries that request applications from specific demographic groups. Since US law does not apply to other countries we try to accommodate recruiting practices of other countries. However, we encourage our readers to alert us to any ads that they feel are discriminatory or offensive.

Science Careers
From the journal *Science* AAAS

POSITIONS OPEN

GENPATH

DIRECTOR OF CYTOGENETICS

The successful candidate will review and analyze patient test results to aid diagnosis in a clinical laboratory setting. Candidate will be analyzing cytogenetics and array comparative genomic hybridization–based diagnostic cases to review chromosomal and genetic abnormalities. Candidate should be well versed with oncology-, microarray-, and cytogenetics-based literature.

Qualifications: M.D. and/or Ph.D. in a relevant field and Board-certified in cytogenetics and/or molecular genetics.

Please send your resume to **e-mail: genpath@genpathdiagnostics.com.** For more information, please visit us at **website: http://wwwgenpathdiagnostics.com.**

DIRECTOR OF THE SUPERCOMPUTING INSTITUTE FOR ADVANCED COMPUTATIONAL RESEARCH and Tenured Faculty Member at the University of Minnesota

The University of Minnesota–Twin Cities invites applications for the position of Director of the University of Minnesota Supercomputing Institute for Advanced Computational Research (MSI). The Director will also hold a tenured faculty position in an appropriate academic department.

MSI has a long and distinguished history in promoting high-performance computational research and serving the high-end computational needs of the University's physical science and engineering community, while more recently expanding its scope to address the growing importance of computation in the biomedical and life sciences as well as emerging informatics demands across the disciplines. The mission of MSI spans both compute-intensive applications and data-intensive applications across the full spectrum of high-performance research computing at the University.

We offer a very competitive salary and benefits package, including an excellent retirement package.

Please see the employment section at **website: http://www.msi.umn.edu** for details on this position, including application instructions, as well as detailed information about the Supercomputing Institute.

The University of Minnesota is an Equal Opportunity Educator and Employer; women and members of underrepresented minorities are strongly encouraged to apply.

RESEARCH AND TECHNICAL STAFF POSITIONS, NORTHWESTERN UNIVERSITY

The Keck Inorganic Signatures of Life Program in collaboration with the Quantitative Bioelement Imaging Center (QBIC) (**website: http://www.clp.northwestern.edu**) and Northwestern University Atomic- and Nanoscale Characterization Experimental (NUANCE) Center (**website: http://www.nuance.northwestern.edu**) at Northwestern University have openings for two Keck Fellows and one technical staff member with backgrounds in cryobiological sample preparation, electron microscopy, element specific characterization, and/or oocyte maturation and fertilization. The Fellows, appointed at a Postdoctoral or Research Assistant Professor level, depending on qualifications, will work as part of a collaborative team with **Professors Vinayak Dravid, Teresa Woodruff, and Thomas O'Halloran** using a variety of S/TEMs including customized Hitachi STEM configured with HAADF, EELS, and dual EDS. The technical staff position is primarily for biological sample preparation, especially oocytes, for SEM/TEM. Send applications and three references to: **Mr. Kim Mccumber, e-mail: ohalloran-ofc@northwestern.edu.** *Northwestern University is Equal Employment Opportunity Commission compliant.*

POSITIONS OPEN

CONSERVATION INTERNATIONAL

SENIOR VICE PRESIDENT, SCIENCE + KNOWLEDGE, CONSERVATION INTERNATIONAL

Conservation International seeks a Senior Vice President (SVP) with full responsibility for developing and implementing CI's science-to-action agenda to support CI's new mission of delivering human well-being through conservation of healthy ecosystems and their goods and services. SVP will lead strategic, programmatic, and financial operations of CI's Science + Knowledge, global staff, and will play a prominent leadership role in communications, fund raising, and partnerships throughout the local, national, and international communities where we work. SVP will bring internationally significant credentials, a proven track record of successful leadership, fund raising at the multimillion dollar level, management of people, fiscal oversight of large programs, outstanding communication skills, and the ability to set priorities and achieve aggressive results as a change agent. Experience establishing the linkage between ecosystem services and human welfare of particular interest. A background in biodiversity and/or conservation ecology science is a plus. Requires Ph.D. and 12-plus years of experience. Review of applications will start immediately and continue until the position is filled, ideally on or before July 1, 2009. To view full job description and submit your required material, please visit **website: http://www.conservation.org/discover/careers/Pages/default.aspx.**

Worldwide candidates welcome. *Equal Opportunity Employer.*

SCIENCE DIRECTOR, ENERGY CENTER Utah State University

Applications are sought from highly qualified individuals to direct the science operations of the Energy Center (EC) on the Utah State University campus. The EC is supported by the Utah Science Technology and Research Initiative (USTAR) and is a high-energy, team-oriented organization that is pioneering the development of novel technologies for the use of algae in the production of liquid fuels and high-value compounds. Qualified applicants will have a Ph.D. in a relevant field and a demonstrated research program in some area related to phototrophic microbes. A strong record of coordinating science programs is preferred. A tenured or tenure-track faculty position in a USU department is available depending on qualifications. Applicants shall possess effective oral, written, and interpersonal communication skills. Postdoctoral or industrial research experience is desirable. USU is classified as a Carnegie Doctoral/Research University-Extensive, and is located in a rapidly growing region of northeastern Utah. A letter of application, curriculum vitae, a one-page statement of research interests, a one-page statement of teaching interests, and a list of four professional references must be submitted through the online system at **website: http://jobs.usu.edu/applicants/Central?quickFind=54019.** Review of applications will begin on May 18, 2009, and will continue until the position is filled. *USU is an Equal Opportunity Employer. USU is a National Science Foundation ADVANCE Gender Faculty Program recipient and is dedicated to recruiting stellar candidates from a diverse pool including women and minorities. Women and minority candidates are encouraged to apply, and spousal accommodation may be possible for dual-career couples.*

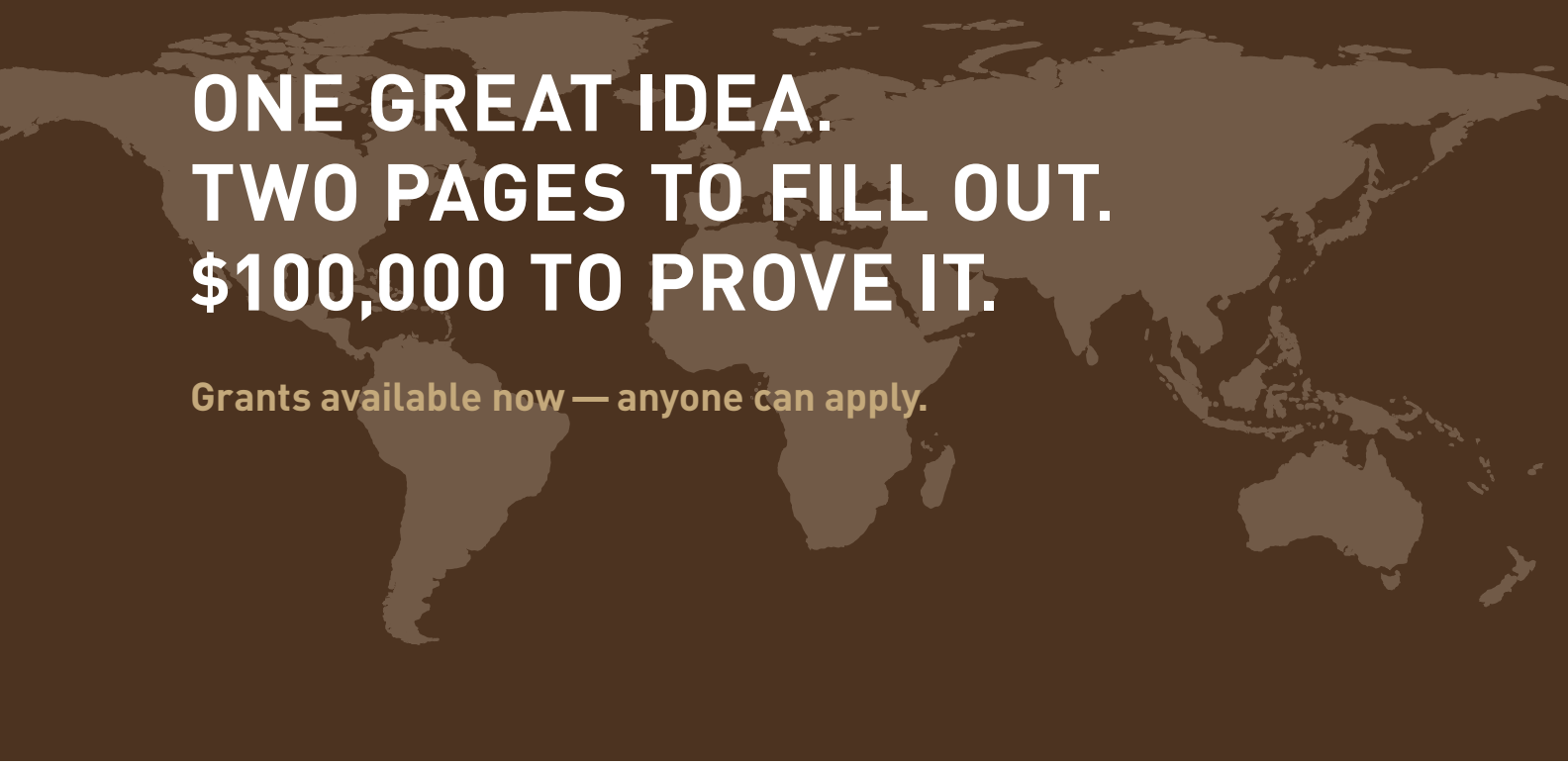

ONE GREAT IDEA.
TWO PAGES TO FILL OUT.
$100,000 TO PROVE IT.

Grants available now — anyone can apply.

The Bill & Melinda Gates Foundation seeks bold ideas from innovative thinkers to solve the greatest challenges in global health.

As part of our Grand Challenges Explorations initiative, grants of $100,000 are awarded two times a year. Projects that show great promise have the opportunity to receive a subsequent grant of $1 million or more.

Proposals will be accepted March 31 through May 28, 2009.

Please visit www.grandchallenges.org/explorations for Round 3 topics and complete application materials.

BILL & MELINDA GATES *foundation*

Grand Challenges | EXPLORATIONS

THE ROAD TO DIVERSITY:
ARE WE THERE YET?

On January 20, Barack Obama became the first African American to be sworn in as President of the United States. On that day television screens carried images of African American men and women moved to tears as they watched the historical event—one that many of them thought they would never witness in their lifetimes. **By Laura Bonetta**

Women, together with African American, Hispanic American, and Native American men, constitute almost two-thirds of the US population. Yet, too few from these groups hold professional leadership positions—and that is certainly the case in academic science. But the situation is changing.

"Over the past 20 years the position of women in science has changed dramatically. It is not where it needs to be. But women have reached a critical mass in many areas. They now have influence on committees for awarding tenure and hiring faculty," says **Linette Watkins,** former chair of the American Chemical Society (ACS) Committee on Minority Affairs. "We are going that way for ethnic and racial minorities as well, but for people with disabilities or of different sexual orientations, it may take even longer."

Women Scientists Reaching Critical Mass

Women's share of science, technology, engineering, and math (STEM) faculty positions has increased steadily. A study by the US National Science Foundation (NSF), published in July 2008, shows that tenured and tenure-track women faculty increased from less than 10 percent in 1979 to 28 percent in 2006, with distributions varying considerably by field. In 2006, women's share of tenured or tenure-track faculty was 17.4 percent in mathematics and 17 percent in physics but 32 percent in the life sciences and 33.9 percent in social sciences.

"The first tenure-track woman faculty in my department was hired three years before me," says Watkins, currently associate professor in the department of chemistry and biochemistry at Texas State University–San Marcos. "I was the second hire in 1997, and now we have five tenure-track women faculty."

Broadly, most women hold instructor and assistant professor positions (42 percent), with fewer of them at the associate (34 percent) and full professor (19 percent) levels. According to a 2007 report by the National Academies of Science, "Beyond Bias and Barriers: Fulfilling the Potential of Women in Academic Science and Engineering," women face several barriers to hiring and promotion in research universities in many fields of science and engineering, including having to contend with questioning of their abilities and commitment to their careers, and arbitrary evaluation systems that favor men. In addition the report found that "structural constraints and expectations built into academic institutions assume that faculty members have substantial support from their spouses."

Faculty members like Watkins agree that it is not easy to balance career demands with starting a family. "I found my way to do it," says Watkins, who has a six-month-old son whom she sometimes takes to work with her. "But I waited to have a child until I was tenured. Women who are coming along after me won't have to wait." That's in part because many universities and medical schools are putting in place more family-friendly policies, such as ones to "slow" the tenure clock, extending the time until tenure review.

Underrepresented Minorities Looking for Role Models

At ACS, Watkins oversaw the ACS Scholars Program, which provides financial assistance as well as mentors to undergraduate underrepresented minority (URM) students to encourage them to pursue degrees in the chemical sciences. (Most programs, including the ACS Scholars Program, define URMs as US citizens or permanent US residents who are African American, Hispanic American, or Native American). Launched in the fall of 1995, the ACS program boasts 45 scholars who have earned their Ph.D.s. "We are probably approaching 10-12 of its alumni who are now faculty," says Watkins. continued »

> "To increase representation of women, people of color, and of different sexual orientation, things have to change in terms of attitudes as well as policy."

Top: **Tuajuanda Jordan**; Bottom: **Richard Tapia**

UPCOMING FEATURES

Careers in Biotech and Pharma — May 8

Diversity Feature: Asian American Scientists — May 29

Focus on Cambridge/Oxford/London — June 26

CREDITS: (TOP) PAUL FETTERS FOR HHMI; (MIDDLE) ISTOCKPHOTO.COM/AVTG; (BOTTOM) PHOTOGRAPH BY THOMAS LAVERGNE, RICE PHOTOGRAPHER

"Over the past 20 years the position of women in science has changed dramatically"
—Linette Watkins

One person who benefited from the program is **Thomas Epps III.** "The scholarship allowed me to perform laboratory research for credit during the semester rather than find a separate job. It also helped me decide that I wanted to do research," says Epps, who completed his undergraduate degree at the Massachusetts Institute of Technology (MIT) in Cambridge, Massachusetts, under the mentorship of chemical engineering professor Paula Hammond. "She counseled me through some of my struggles. She was one of the few minority faculty who I interacted with at MIT, so it was helpful to speak with her about the pressures at a top-tier institution. We are still in regular contact."

Epps became assistant professor in the Department of Chemical Engineering at the University of Delaware in 2006. He is amongst the just 5.6 percent of faculty at the top 50 departments of chemical engineering who are URM individuals, according to a 2007 study by **Donna Nelson** at the University of Oklahoma.

Having a mentor who shares a similar background is critical, says Epps, but URM students should not limit their pool of mentors to only minority faculty. "It's important to have a range of mentors. I find that sometimes if I am not available, minority students choose not to ask anyone else in the faculty for help and so they end up not getting any assistance," says Epps. "But in many cases, their questions can be addressed by any faculty member."

Although URM students and junior faculty can benefit from having nonminority faculty mentors, the importance of having role models cannot be overstated. "If I see someone who looks like me, I think I can make it too. If you are a woman and you think you should be faculty, but everyone on the faculty is male, you don't see the feasibility," says **Richard Tapia,** professor of engineering and director of the Center for Excellence and Equality in Education at Rice University.

Math is one of the disciplines most resistant to change. In 2007, within the top 50 math departments less than 2.3 percent of members of the faculty were URMs, compared to 3.8 percent in biology. "In an ideal world we would like to see 30 percent of all science faculty URM, but I would be pretty happy to see even 5 percent or 10 percent," says Tapia. "Anything below these numbers does not provide the leadership, guidance, or role models that the country needs."

Waiting for a Sea Change

Although the number of minority students in science fields, according to Nelson's study, has increased dramatically in recent years, especially at the undergraduate level, the proportion of URM faculty has not kept pace. In 2005, 16.7 percent of the students graduating with a B.S. in chemistry were URMs but in 2007 only 3.9 percent of faculty at the top 100 chemistry departments were URMs. For women those numbers are 51.7 percent and 13.7 percent, respectively. In contrast, for white males the percentages are 37 percent and 74.2 percent, respectively.

Featured Participants

American Association for the Advancement of Science
www.aaas.org

American Chemical Society (ACS)
www.acs.org

California Polytechnic State University
www.calpoly.edu

EntryPoint! Program
www.entrypoint.org

Howard Hughes Medical Institute (HHMI)
www.hhmi.org

Massachusetts Institute of Technology
www.mit.edu

National Federation of the Blind
www.nfb.org

Penn State University
www.psu.edu

Rice University
www.rice.edu

University of Delaware
www.udel.edu

University of Oklahoma
www.ou.edu

US National Science Foundation (NSF)
www.nsf.gov

Web Accessibility Initiative (WAI)
www.w3.org/WAI/

"I went to college in the 1960s, and at that time I never saw a minority faculty member. Today it is still possible to have that experience," says **Shirley Malcom,** head of the Directorate for Education and Human Resources Programs at the American Association for the Advancement of Science (AAAS), publisher of *Science*. "The student body looks so much different than when I went to school. But the faculty is not moving at the same pace."

Part of the problem, says Malcom, is that the "current faculty selects the next faculty. Most often that means they look at research productivity alone." Instead, faculty should view themselves as a unit "and evaluate what that unit is missing in terms of experiences and perspectives, and not just in research," says Malcom. "The faculty job is not just research. It is also about mentoring, teaching, and larger issues of service to the community."

But although change may be slow to come, Malcom believes there is reason to be optimistic. "I see many programs reaching into institutions," she says. "There has been a strong focus on advancing women faculty, and the same will happen for other groups. Things are happening."

Supporting Minority Students

NSF is one government agency that has made a strong commitment to increasing diversity in the sciences by providing funds to universities willing to establish programs to recruit and retain URM students, as well as by establishing several scholarships and fellowship programs for students. Other agencies and organizations are making similar efforts, albeit on a smaller scale.

The Howard Hughes Medical Institute's (HHMI) Gilliam Fellowships, for example, provide full support for up to five years of study toward a Ph.D. for outstanding students who are from groups underrepresented in the sciences or from disadvantaged backgrounds. "We give them the means where they can be successful in graduate school. The expectation is that they will someday be really good faculty," says **Tuajuanda Jordan,** director of HHMI's Science Education Alliance. continued »

CREDIT: PHOTO BY CHANDLER PRUDE

PRIFYSGOL ABERYSTWYTH UNIVERSITY

IBERS

Institute of Biological, Environmental and Rural Sciences

The Institute of Biological, Environmental and Rural Sciences (IBERS) is a world class research, enterprise and education centre at Aberystwyth University. IBERS is now seeking to fill a number of key academic appointments to join an already thriving research and teaching community. The positions below are the first of a number of new academic opportunities that will be advertised over the coming months. These appointments are part of a major new £55 million investment in IBERS to further advance Aberystwyth University's standing as a major force in the biosciences underpinning Agriculture and the Environment.

- **Chair in Sustainable Agriculture** – to develop and lead world class research to integrate social/economic drivers with sustainable agriculture in the face of environmental change. Opportunities exist to lead a new Agro-ecology research centre with a focus on upland farming. Information enquiries to Professor Chris Thomas (cjt@aber.ac.uk; tel: +44 (0)1970 622265).
- **Chair in Quantitative Genetics** – to develop and lead a world class programme on the use of modern genomics methods focusing on the genetics and breeding of outbreeding species. Informal enquiries to Dr Michael Abberton (mla@aber.ac.uk; tel: +44 (0)1970 823180). (Salary negotiable).
- **Chair in Statistical/Population Genomics** – to develop a world class population genomics programme to better understand the evolutionary processes influencing how organisms and species adapt to different and changing environments. Informal enquiries to Professor Wayne Powell (wap@aber.ac.uk; tel. +44 (0)1970 823001).
- **Chair in Aquatic Molecular Ecology** – to lead a growing team of aquatic biologists in the study of marine and/or freshwater ecosystems. Significant experience in applying genomic approaches to research areas involving how aquatic species and populations adapt to environmental and climatic stresses is sought. Informal enquiries to Professor Karl Hoffmann (krh@aber.ac.uk; tel. +44 (0)1970 622237).
- **Senior Lectureship in Microbial Genomics (£44,930- £52,086)** – to develop a world class genomic/metagenomic program to better understand the interaction of microorganisms with their environment. Informal enquiries to Professor Jamie Newbold (cjn@aber.ac.uk; tel. +44 (0)1970 622242).
- **Lectureship in Animal Genomics (£32,458 - £43,622)** – to help develop a novel program investigating the linkage between animal genomics and microbial population within the digestive tract. Informal enquiries to Professor Jamie Newbold (cjn@aber.ac.uk; tel. +44 (0)1970 622242).
- **Lectureship in Ancient Bio-molecules (£32,458 - £35,469)** – to establish a new research initiative aimed at studying evolutionary and environmental change using preserved genetic material. Research areas could include: plants, animals, pathogens or human evolution. Informal enquiries to Professor Chris Thomas (cjt@aber.ac.uk; tel. +44 (0)1970 622265).

Closing date for applications: 30 April 2009

Inquiries : For more information see http://www.aber.ac.uk/en/hr/jobs/vacancies-external/. For further particulars, applications forms etc. please contact the Human Resources Operations Team: vacancies@aber.ac.uk / Tel: 01970 621572 / Fax: 01970 622975.

FOCUS ON DIVERSITY

VISITING ASSISTANT PROFESSOR (to teach Human Physiology) FORDHAM UNIVERSITY

Individuals are invited to apply for a one year non tenure-track Visiting Assistant Professor position to teach Human Physiology and Lab to undergraduate Biology and Pre-Medical students for both Fall 2009 and Spring 2010. Candidates are expected to have experience in teaching a similar Lecture/Lab course and the position will be open until a candidate is identified.

Please submit a curriculum vitae, including teaching experience, and the names and addresses of three references by **May 15, 2009** to: **Dr. William B. Thornhill, Chair, Department of Biological Sciences, Fordham University, Bronx, NY 10458** and/or by email to **thornhill@fordham.edu**. Candidates will be reviewed when their applications are received.

Fordham is an independent, Catholic university in the Jesuit tradition that welcomes applications from men and women of diverse backgrounds. Fordham is an AA/EOE.

UMass | Dartmouth

Careers with **Mass Appeal**

Assistant/Associate Professor Fisheries Oceanography

The School for Marine Science and Technology (SMAST)

The Department of Fisheries Oceanography/SMAST, University of Massachusetts Dartmouth, invites applications for two faculty positions to be filled at the Assistant or Associate Professor level.

For a complete job description, visit: http://www.umassd.edu/hr/asstprofsmast3-31-09.cfm

MUST MEET MINIMUM REQUIREMENTS

To apply, please send a statement of interest, resume, and three names of references via email to: dfmttp09@umassd.edu. Review of applications begins April 30, 2009 and continues until the positions are filled.

The University of Massachusetts is an EEO/AA employer.

Do you have a passion for cutting-edge science and protecting the public health?

Unleash your passion into a rewarding career as a Physician, Scientist or Consumer Safety Officer at the Center for Biologics Evaluation and Research!

The Center for Biologics Evaluation and Research's mission is to protect and enhance the public health through the regulation of biological products including blood, vaccines, allergenics, tissues, and cellular and gene therapies. Biologics, in contrast to drugs that are chemically synthesized, are derived from living sources (such as human, animals, and microorganisms) and are not easily identified or characterized, and many are manufactured using biotechnology. These products often represent cutting-edge biomedical research and, in time, may offer the most effective means to treat a variety of medical illnesses and conditions that presently have few or no other treatment options.

For details on qualifications and salary, please visit our Hiring Opportunities page at **http://www.fda.gov/cber/inside/hiring.htm**.

How to Apply: Applications are being accepted for current and future vacancies. Submit electronic resume or curriculum vitae with cover letter by **September 30, 2009** to: **CBER.Employment@fda.hhs.gov Attn: Job Code: Gen**

The Center for Biologics Evaluation and Research is part of the Food and Drug Administration, Department of Health and Human Services.

EQUAL OPPORTUNITY EMPLOYER. SMOKE FREE ENVIRONMENT.

"It's important to have a range of mentors."
—Thomas Epps III

But Jordan points out that these grass-root efforts will go only so far. "Unless someone up top makes a definite commitment to this type of training, current efforts will remain small and are going to take a long time to have an effect," she says. "One of the main problems I see is that the way we *teach* science in this country is counter to how we *do* science. What I see is that if a student is even remotely interested in science, we get them into college and lecture to them—a completely passive experience. This is the exact opposite of what we should be doing. Science is about mental and physical engagement. It is truly a holistic experience that we, as scientists and educators, can do a better job communicating."

Early Research Exposure

Jordan and others believe that providing opportunities for students to be exposed to research early on will increase the number of students—from all walks of life and backgrounds—entering scientific careers. To this end, AAAS established the EntryPoint! program for students with disabilities. "Our primary goal is to introduce students to internship opportunities using and expanding the skills they have and to promote them to employers," says **Virginia Stern,** director of the Project on Science, Technology and Disability at AAAS.

According to NSF figures, 20 percent of the population in 1993 had some form of disability and persons with disabilities were 13 percent of all employed persons and around 5 percent of the science and engineering labor force. In 2006, 18 percent of the population reported some kind of disability and scientists and engineers with disabilities made up 7 percent of all scientists and engineers. Although there has been only a slight increase in employment status among scientists and engineers with disabilities, in a span of 10 years the number of students with disabilities in STEM fields has increased.

"There is a definite increase in students with disabilities at the undergraduate level. Students realize that STEM fields are interesting and very marketable. Counselors may be the biggest barrier because they themselves often have not had math or science training, and they think these are too hard for their clients with disabilities," says Stern.

One of the biggest developments in the past 15 to 20 years that has helped students with disabilities enter STEM fields has been the availability of assistive technologies. "Legislation and assistive technologies have helped tremendously," says Stern. They include text and video relay services for people who are deaf, speech recognition software for people who may not be able to use a keyboard, text-to-speech software and spelling programs for people with some learning disabilities, and refreshable Braille displays and Braille printers for people who are blind.

When **Cary Supalo** started his Ph.D. in chemistry at Penn State University, he had to find individuals who could follow his directions, acting as his eyes and hands in carrying out experiments. He also had to employ, with financial assistance from his university, people capable of reading scientific papers to him. "At the time, that was the only way to get timely access to the scientific literature," says Supalo. Today, screen reader technology makes it possible to read some scientific information online. This has been one of the most important developments in the past decade for people who are blind. But "the technology is not where it should be," says Supalo. "Reading math equations is difficult and so is accessing organic chemistry molecular structures."

Making STEM Careers Accessible

Supalo learned what he needed to do to pursue a Ph.D. in chemistry through the National Federation of the Blind. By participating in the organization he met blind scientists and mathematicians who shared their strategies and advice. "Meeting scientists who were blind like me was tremendously inspirational. I don't know if I would have stuck it out in chemistry without those role models," says Supalo. "Knowing that someone had done it before me, that it was possible to do—that was very empowering."

Without the needed resources to pursue STEM careers, people with disabilities are cut off from these fields. "To increase representation of women, people of color, and of different sexual orientation, things have to change in terms of attitudes as well as policy," says **Trey Duffy,** director of the Disability Resource Center at the California Polytechnic State University. "But for people who have disabilities, you have to change the world physically. In a way it is harder because you can't stop at eliminating discriminatory beliefs and policy, you have to take the extra step of modifying material and tangible aspects of the environment. It is not just a matter of welcoming people, which is in itself difficult; there is an infrastructure that goes with it."

Although technological advances and laws requiring facilities and employers to make the workplace more accessible have removed some roadblocks, many remain. For example, "There are no required standards for building web pages; therefore, some designs inhibit accessibility by people who are blind," says Duffy. There are, however, signs that some of these obstacles will eventually be removed. The Web Accessibility Initiative (WAI) works with organizations around the world to develop strategies, guidelines, and resources to help make the web accessible to people with disabilities. "Programs by NSF for technology development, initiatives to make the web more accessible, and the focus on science under the new Obama administration are all positive things," says Duffy. "We are definitely heading in the right direction."

Most people share this optimism. Science fields are not yet representative of the diversity in the US population, but already more women have made their way into leadership positions in many STEM disciplines, and the student body in the life sciences is heavily female. There are also many minority undergraduates in STEM fields. Individuals with disabilities and of different sexual orientation are still few and far between. However, many government agencies, including NSF, as well as several private entities have made strong commitments to make science more inclusive.

Laura Bonetta is a scientist turned freelance writer based in the Washington, D.C., area.

DOI: 10.1126/science.opms.r0900070

CREDIT: PHOTO COURTESY OF JON COX

WWW.NIH.GOV
Positions NIH
THE NATIONAL INSTITUTES OF HEALTH

DEPARTMENT OF HEALTH AND HUMAN SERVICES (DHHS)
NATIONAL INSTITUTES OF HEALTH (NIH)
National Institute of Arthritis and Musculoskeletal and Skin Diseases (NIAMS)
Director, Division of Extramural Research Activities (DERA)

The Department of Health and Human Services (DHHS) and the National Institutes of Health (NIH) are seeking exceptional candidates for the position of Director, Division of Extramural Research Activities (DERA), National Institute of Arthritis and Musculoskeletal and Skin Diseases (NIAMS) to support research into the causes, treatment, and prevention of arthritis and musculoskeletal and skin diseases, the training of basic and clinical scientists to carry out this research, and the dissemination of information on research progress in these diseases, while promoting public health and addressing issues of health disparities. This position offers a unique opportunity to direct, manage, and provide oversight to the Grants Management Branch (GMB) and the Scientific Review Branch (SRB), as well as, to oversee human subject protection and clinical trial activities under the extramural programs of NIAMS.

The DERA Director manages and directs all DERA program activities, which includes developing and justifying the yearly budget request. The DERA Director provides guidance and leadership to the GMB and SRB Chiefs on the development of new programs and projects, directs collaboration with Federal organizations, grantees, contractors, and private industry to develop models for DERA programs, and best practice models for providing DERA services, and provide leadership and advice to the Director, NIAMS, on developing, implementing, and coordinating extramural research contract, grant, and training program policies. The DERA Director maintains ongoing analysis and evaluation of the review of applications and the management of grants and contracts to support overall policy research, development and reporting for the extramural activities of the Institute. In addition, the DERA Director will collaborate with leading figures in the scientific community at NIH and other government organizations, representatives of academic institutions, and members of foreign governments and scientific organizations to exchange information on scientific research and coordinate projects of mutual interest. The DERA Director is a full partner in the executive leadership of the NIAMS.

Applicants may browse the NIAMS Home Page at http://www.niams.nih.gov/ for additional information on the Institute. Applicants must possess an M.D., Ph.D., or equivalent degree in a biomedical field related to the mission of NIAMS and have professional experience with a broad national programmatic or scientific background; be able to interact with the Scientific Program Division with equal authority; have the demonstrated capability to plan and direct programs of national and international importance; and have the ability to communicate with and obtain the cooperation of public, private and national and international organizations and individuals. Salary is commensurate with his/her qualifications and experience. Full Federal benefits including leave, health and life insurance, long-term care insurance, retirement, and a savings plan (401k equivalent). A detailed vacancy announcement that includes application procedures is available at: **http://www.jobs.nih.gov (under vacancy announcement NIAMS-09-327761)**. Questions may be addressed to **Ms. Ruth Fritz, 301-496-6051 e-mail: fritzr@mail.nih.gov. A CV and bibliography, including a statement addressing the qualifications and interest in the position, should be received by April 30, 2009**. *Applications received after this date will be considered until the position is filled.*

National Heart Lung and Blood Institute

Postdoctoral Fellowship Program

Bioinformatics or Statistical Genetics

RESEARCH FELLOWSHIPS: Center for Population Studies and Framingham Heart Study, Division of Intramural Research, National Heart, Lung, & Blood Institute, NIH, DHHS.

Three fellowship positions are available in bioinformatics or statistical genetics: Mentored research with NHLBI scientists and bioinformaticians from the Division of Intramural Research in the development/analysis of population-based genetic/genomic research involving (a) genome-wide association study (GWAS) database of over 550,000 SNPs, (b) targeted resequencing of candidate gene regions, (c) whole genome sequencing or sequencing of all exons (the 'exome') in the human genome, or (d) gene expression transcript profiling in up to 8,000 carefully characterized Framingham Heart Study (FHS) participants with tens of thousands of phenotypes for cardiovascular disease and other disorders. Some research opportunities include development of computational methods for genotype-phenotype analysis using high-throughput sequence or expression data, genotype-phenotype analysis of structural variation, and use of systems biology approaches for integrative genomics. Fellows will be located at the Framingham Heart Study in Framingham, MA (working with Drs. O'Donnell, Levy, and Johnson) , or the NIH Campus (working with bioinformaticians at the National Library of Medicine, or with Dr. Munson at the NHLBI, Bethesda, MD).

Applicants must have a Ph.D. or M.D. degree with research experience in computational or molecular biology, statistical genetics, or informatics, particularly in the area of genetics and genomics.

Program Leaders: Christopher J. O'Donnell MD MPH, Daniel Levy MD, Andrew D. Johnson PhD, Peter Munson PhD

To apply, submit CV, cover letter and 3 letters of reference to: **Sandra Stoddard, 73 Mt. Wayte Avenue, Suite 2, Framingham, MA 01702, E-mail: nhlbi_researchfellowcps-fhs@mail.nih.gov**

The NIH Director's Wednesday Afternoon Lecture Series

Biomedical scientists around the world are invited to join us online to hear leading investigators present their latest results to the NIH Intramural Research community. Lectures may be viewed live at 3:00 p.m., EDT (20:00 GMT) on Wednesdays, from September through June. Live webcasts can be viewed under "Today's Events" at: <http://videocast.nih.gov/>

The current schedule of lectures is available at: <http://www1.od.nih.gov/wals/schedule.htm

Upcoming Lectures:

- **April 29:** Erkki Ruoslahti, Burnham Institute for Medical Research, (former President and CEO) *"Vascular Zip Codes in Targeted Delivery of Multifunctional Nanodevices"*
- **May 6:** Eric Nestler, *University of Texas Southwestern Medical Center, "Transcriptional Mechanisms of Drug Addiction"*
- **May 13:** James Collins, Boston University, *"Engineering Gene Networks: Integrating Synthetic Biology & Systems Biology"*
- **May 20:** Tom Rapoport, Harvard Medical School, *"Mechanisms of Protein Translocation Across Membranes"*

FLORIDA INTERNATIONAL UNIVERSITY

TENURE TRACK POSITION
ASSISTANT AND/OR ASSOCIATE/FULL PROFESSOR
ROBERT STEMPEL COLLEGE OF PUBLIC HEALTH AND SOCIAL WORK

Florida International University is ranked as a Research University in the High Research Activity category of the Carnegie Foundation's prestigious classification system. Our mission is to enhance the public's health by conducting innovative research, training future leaders and health professionals from diverse backgrounds, translating research into policy and practice, and serving our local communities as well as communities around the world, especially Latin America and the Caribbean.

Qualifications: Candidate must possess a Ph.D., M.D. or the equivalent and postdoctoral experience in environmental genomics, molecular epidemiology, human genetics, or a related area. Extensive experience in the broad field of genomics including proteomics and bioinformatics is desired. The Search Committee is especially interested in receiving applications from individuals experienced in interdisciplinary collaborative research with interests in assessment of gene-environment interactions, molecular epidemiology and toxicogenomics of human diseases. We welcome candidates with experience in evaluating intermediate biomarkers of effect and in examining the health, especially respiratory, cardiovascular, diabetes, reproductive/developmental, and cancer endpoints.

Duties and Responsibilities: The candidate will be expected to develop his/her own research program in environmental genomics, obtain competitive research funding, and engage in collaborative research with other faculty in the department as well as within the College of Public Health & Social Work and College of Medicine. Responsibilities also include teaching, advising graduate students, and serving on doctoral committees. The selected candidate will have the opportunity to participate in ongoing research with multidisciplinary researchers, and will be expected to develop and maintain an original, creative and independent research program in genetic or molecular environmental epidemiology with evidence of high quality and productivity. This requires publications in high impact peer-reviewed journals and demonstrating the potential for successful submission and management of investigator-initiated grant proposals.

Applications and Nominations: Applicants must submit the following material: letter of application that confirms applicant's interest in the position and addresses qualifications, including description of research; complete curriculum vitae; undergraduate and graduate transcripts, and documentation of the doctoral degree; representative publications, and at least three letters of recommendation.

The selection and review process will begin on April 2, 2009, and will remain open until the position is filled. To apply please visit us on-line at www.fiujobs.org and reference position #41663.

FIU is an Equal Opportunity/Equal Access Employer and Institution.

FACULTY POSITION IN PHYSIOLOGY AND PHARMACOLOGY

The Department of Physiology and Pharmacology at Des Moines University seeks to fill a tenure track faculty position. Successful candidates must have demonstrated a commitment to and expertise in the discipline of physiology or pharmacology. Additionally, it is expected that the individual develop an innovative and extramurally funded research program utilizing contemporary approaches. Highly desirable applicants would be able to teach in one or more of the following areas: cardiovascular, renal, or respiratory physiology/pharmacology for the medical, podiatric, and allied health curricula. Applicants must have an earned Ph.D. and relevant postdoctoral experience. Please visit **www.dmu.edu/employment** for a complete job description.

For full consideration, candidates are invited to submit a letter of application stating their interest along with their curriculum vitae, a concise statement of teaching and research interests, educational philosophy and contact information for three references using the online applicant tracking system at **www.dmu.edu/employment**. Review of applications will begin immediately and continue until a successful candidate is identified and hired to start prior to early Fall 09.

DMU is an EOE EMPLOYER.

University of Massachusetts Medical School
UMASS

Brudnick Neuropsychiatric Research Institute
bnri

TENURE-TRACK NEUROSCIENCE POSITION

The Brudnick Neuropsychiatric Research Institute (BNRI), established as part of the unprecedented research expansion at the University of Massachusetts Medical School, invites applications for a tenure-track position at the level of Assistant, Associate or Full Professor. The BNRI, a division of the Department of Psychiatry, is committed to broad-based research investigating basic neurobiological principles related to psychiatric disorders. While we invite applications from all areas of neuroscience, we are particularly interested in applicants using electrophysiological approaches in mammalian systems to investigate mechanisms underlying neuronal plasticity. The BNRI, situated in a state-of-the-art laboratory facility, is an integral part of the campus-wide Program in Neuroscience, which consists of over 55 basic neuroscientists. The successful candidate will establish and/or maintain an independent research program and play an integral role in new Program initiatives. The position is highly competitive with regard to salary, start-up funds and laboratory space.

Applicants should send a CV, statement of research interests, and names and addresses of three references by **June 1, 2009** to:

Dr. Paul D. Gardner, Search Committee Chair
Brudnick Neuropsychiatric Research Institute
University of Massachusetts Medical School
303 Belmont Street
Worcester, MA 01604
E-mail: bnri@umassmed.edu
www.umassmed.edu/bnri

An Equal Opportunity/Affirmative Action Employer.

UF UNIVERSITY of FLORIDA

Faculty Positions (Associate/Full Professor)
Department of Molecular Genetics and Microbiology

The Department of Molecular Genetics and Microbiology in the College of Medicine at the University of Florida, Gainesville (**http://www.mgm.ufl.edu**) seeks highly motivated and successful candidates who will contribute to our developing research portfolio in mouse disease models and viral pathogenesis. The department currently hosts 23 full-time faculty members with expertise in animal disease models, molecular virology, and bacteriology. The latter two areas have a strong emphasis on host/pathogen interactions with a focus on bioinformatics and genomics approaches. We are especially interested in candidates utilizing contemporary genetic approaches and animal models to further our understanding of inherited diseases and human viral pathogens, preferentially RNA viruses. However, highly qualified candidates working in related research areas are also encouraged to apply.

Successful candidate(s) will join a vibrant Department which plays a central role in several interdisciplinary research programs in the Health Science Center. Affiliated Centers include the UF Genetics Institute (**http://www.ufgi.ufl.edu**), the Powell Gene Therapy Center (**http://www.gtc.ufl.edu/**), the UF Brain Institute (**http://www.mbi.ufl.edu/**), the Emerging Pathogens Institute (**http://epi.ufl.edu/**), and the UF Shands Cancer Center (**http://www.ufscc.ufl.edu/**). The successful candidate will be expected to maintain and further develop a strong and innovative research program and contribute to medical and graduate student teaching. Highly competitive start-up packages and salaries are available and complemented by outstanding core facilities, new laboratory space, and the highly collegial and interactive atmosphere at the University of Florida.

For consideration PhD, MD/PhD, or MD degree candidates should have nationally recognized and extramurally funded research programs. Applicants should submit a cover letter, curriculum vitae, a brief summary of current and future research plans and contact information for three references as a pdf file attached to an e-mail to: **MGM-FacultySearch@mgm.ufl.edu**.

Review of applications will commence immediately, with the search committee determinations beginning circa **May 15, 2009**. The search may remain open until the position is filled.

UF is an Equal Opportunity Institution with a strong commitment to excellence through diversity.

RUPRECHT-KARLS-
UNIVERSITÄT
HEIDELBERG

The Medical Faculty Mannheim of the University of Heidelberg invites applications for a

Full Professorship (W 3) in Medical Microbiology and Hygiene

to be appointed as soon as possible.

The full professorship (W 3) in medical microbiology and hygiene is assigned to the Institute for Medical Microbiology and Hygiene of the Mannheim University Teaching Hospital. The incumbent will also take over the position of Director of the Institute.

The requirements to be fulfilled by the full professorship (W 3) in medical microbiology and hygiene necessitate the appointment of a dedicated physician and internationally recognised researcher who will be expected to be able to represent the full scope of the subjects of medical microbiology and hygiene in research and teaching. In research the future incumbent shall place a point of particular emphasis on bacteriology and infection biology, an additional interest in infection immunology would be especially desirable. Research into microbiological inflammation is to have been conducted on the highest scientific level. In teaching duties the future incumbent shall be prepared to contribute actively to the development and success of the integrative concept of the model curriculum MaReCuM (Mannheim Reformed Curriculum of Medicine). Extensive experience in the education of medical students is essential for this purpose. In the sector of patient care the incumbent shall in particular be responsible for ensuring cooperative interaction with partners from the diagnostic and clinical disciplines as well as for utilising his/her competence to represent the concerns of clinical infectiology and hospital hygiene.

The successful candidate shall hold the certification as a medical specialist in microbiology, virology and infection epidemiology, an additional certification as a medical specialist in hygiene and environmental medicine is desirable. Further requirements are proven competence and an internationally recognised qualification in the research of microbiological inflammation (inflammation and cancerogenesis or inflammation and vascular damage), a doctorate as well as the post-doctoral qualification as a university lecturer (or a comparable outstanding scientific record), excellent didactic skills and experience in the acquisition of third-party funding, a high capacity for in cooperation and leadership, integrative ability in the structural development of the model curriculum MaReCuM and commitment in the academic self-administration.

The incumbent shall perform tasks in patient care at the Mannheim University Teaching Hospital. In this regard a separate contract is to be concluded with the hospital authorities.

The University of Heidelberg is committed to increasing the number of women in professorships and therefore explicitly encourages qualified female candidates to apply. Applications from disabled persons of equal aptitude and qualification level will be favoured.

Applications including the usual pertinent documentation (curriculum vitae with passport photograph, academic / professional record, testimonials, certificates, statement of third-party funding acquired, list of publications) are to be submitted **within 3 weeks following the appearance of this announcement to the following address: Herrn Prof. Dr. Dr. h.c. Klaus van Ackern, Dekan der Medizinischen Fakultät Mannheim der Universität Heidelberg, Universitätsmedizin Mannheim, 68135 Mannheim, Germany.**

The Sahlgrenska Academy is the faculty of health sciences at the University of Gothenburg. Education and research are conducted within the fields of pharmacy, medicine, odontology and health care sciences. About 4000 undergraduate students and 1200 postgraduate students are enrolled at Sahlgrenska Academy. The staff is about 1400 persons. 850 of them are researchers and/or teachers. 2008 Sahlgrenska Academy had a turnover of 1900 million SEK.

Post Doc position E 36 861/09

In Biomedicine at Sahlgrenska Academy, University of Gothenburg

An opening for young scientists (less than 3-5 years since the PhD degree) with interest in adipocyte biology is available at the Institute of Biomedicine, The Sahlgrenska Academy, University of Gothenburg, Göteborg, Sweden. We welcome applicants with experience in all aspects of cell biology/molecular biology. The work will be centered around gene regulatory mechanisms and their relevance for metabolism. Broad ranges of techniques are applied, from studies of DNA-protein interactions to construction of tissue specific and conditional knock-out mice. Recently, we have been focusing on forkhead transcription factors in muscle, brown and white adipose tissue. The position is for 2 years with a possibility of a 2-year extension.

Applicants should submit a CV and bibliography, and names and addresses (including e-mail addresses) of three scientists that can provide references.

For further information, contact the research group leader Prof. Sven Enerbäck (sven.enerback@medgen.gu.se).

The application should be organized as follows: Curriculum vitae (max 2 pages). Scientific track record (max 2 pages) describing your early scientific contributions to your own research field.
Please indicate your most important findings.

Union representatives:
Gunnel Lindö, SACO phone + 46 (0) 31-786 1078
Astrid Igerud, OFRS-S, phone + 46 (0) 31-786 1167
Lennart Olsson, SEKO, phone +46 (0) 31-786 1173

Send the application, including refnr E 36 861/09, to following address: The Registry, Sahlgrenska Academy at the University of Gothenburg, Box 400, 405 30 Göteborg, Sweden. The finial date for the application to reach the Registry is 18 May 2009.

UNIVERSITAS GOTHOBURGENSIS 1891

GÖTEBORGS UNIVERSITET

www.gu.se

江苏大学

Job Opportunities at Jiangsu University

Jiangsu University is located at Zhenjiang, a historic city at the southern bank of the Yangtze River. It is a university with a history of more than one hundred years. It is now developing very fast together with China, and offers opportunities for scholars across the world in the following fields: biology, pharmacy, clinic medicine, pre-clinic medicine, chemistry, mathematics, mechanic engineering, power engineering and engineering thermophysics, electrical engineering, electrical science and technology, information and telecommunication engineering, control science and technology, safety technology and engineering, traffic and transportation engineering, agricultural engineering, environmental engineering, food science and engineering, material science and engineering, computer software and theory. We will provide good working conditions and good salary and welfare.

The applicants should be doctor degree holders and high academic achievers fluent in both Chinese and English. They should offer such information as education, work experience, academic achievements and proof, in the field they apply for. Those who apply for special professorship should fill out a form (http://www.ujs.edu.cn/jsdw/teping.htm), listing their research interest and plan, and offer at least two copies of their representative papers.

The opportunities are waiting for you. If you want to join us, please contact
Mr. Lu Yulin
Human Resource Department
Jiangsu University
No. 301, Xuefu Rd.
Zhenjiang 212013
P. R. of China.
Tel.:86-511-88780061 Fax:86-511-88780227
Email: **hr@ujs.edu.cn** Website: **www.ujs.edu.cn**

LMU LUDWIG-MAXIMILIANS-UNIVERSITÄT MÜNCHEN

MUNICH CENTER FOR NEUROSCIENCES – MCN^{LMU}

The **Division of Neurobiology** at the **LMU Biocenter** in Munich invites applications for several

Postdoc Positions (Auditory Processing)

in experimental neurobiology and computational neuroscience. Positions are associated with the research group of Professor Benedikt Grothe, Chair of Neurobiology (www.zi.biologie.uni-muenchen.de/institute/zi/abtlgn/neurobiologie/).

Scientists with a background in neuroscience or cell biology and a particular interest in the *in vivo* or *in vitro* physiology of mammalian auditory brainstem circuits are invited to apply.

Our campus facilitates collaborative research and teaching by hosting an exceptional number of excellent neuroscience groups and institutions, including Max-Planck and Helmholtz institutes. Apart from outstanding research conditions, Munich offers a rich variety of cultural and leisure activities, and is one of the most beautiful and exciting cities in Germany.

Please submit your application in one single PDF-document (include a short description of research interests, CV, list of publications, list of referees, and relevant certificates) by e-mail to **neurojobs.mcn@lmu.de**.

DALIAN INSTITUTE OF CHEMICAL PHYSICS
CHINESE ACADEMY OF SCIENCES

Lab Director and Division Directors, Dalian National Laboratory for Clean Energy

Dalian National Laboratory for Clean Energy (DNL), based mainly in Dalian Institute of Chemical Physics (DICP), Chinese Academy of Sciences (CAS), is looking for outstanding candidates for **DNL director and directors for its nine research divisions: optimized utilization of fossil energy, low carbon catalysis and engineering, energy saving & energy environment, fuel cell & energy storage, hydrogen energy, biomass energy, solar energy, maritime renewable energy, basic & strategic studies on energy, and service center for energy researches**. More details about DICP can be found at **http://www.dicp.ac.cn/.**

Successful candidates for these positions should have a Ph. D. degree and are expected to be an accomplished scientist in his or her academic field, who has demonstrated a strong record of scientific publications in leading scientific journals. Candidates for the DNL director should be under age of 55 and at the rank of full professor or equivalent position with a track record of management in universities or research institutions; while candidates, applying from abroad, for the DNL division directors should be at the rank of associate professor or above, and under age of 50.

Successful candidates will be provided with competitive salary and benefits. A generous start-up research fund for each successful candidate will also be provided.

Candidates, who are interested in these positions, should send a complete CV and publication list to Dr. Hua'an Zhang, Department of Personnel (86-411-84379556, **talents@dicp.ac.cn**), Mr. Zhiyuan Mao (**maozy@dicp.ac.cn**), Prof. Can Li (**canli@dicp.ac.cn**) and Prof. Tao Zhang (**taozhang@dicp.ac.cn**).

UNIVERSITY OF OXFORD

www.ox.ac.uk/jobs

Two Post-Doctoral Research Assistant posts: tropical forests and climate change

£30,594 - £32,458 pa

School of Geography and the Environment, University of Oxford

Applications are invited for two fixed-term three-year postdoctoral research assistant positions to start June 2009 or as soon as possible thereafter, based in the Ecosystems Group of the Environmental Change Institute, School of Geography and the Environment, University of Oxford, South Parks Road, Oxford, OX1 3QY.

i) The first post researches dynamics and carbon implications of fires in the Andes and will conduct a detailed evaluation of the spatial and temporal dynamics of fire at the Andean treeline, and a quantification of their carbon emissions. The successful candidate will have a PhD in a quantitative environmental science, remote sensing and GIS skills, availability and enthusiasm to spend 3-5 months each year in Peru and either proficiency in Spanish or a clear ability to rapidly become proficient, and excellent field leadership skills. **Closing date is noon on Friday 15 May 2009.**

ii) The second post will work on modelling the ecophysiology and dynamics of Amazonian forests. It will involve compiling existing field data on forest function and dynamics and then using these to parametrise and improve the UK community vegetation model, JULES. The ultimate goal of this modelling effort is to better simulate the response of Amazonian vegetation to climate change. The successful candidate will have a PhD or equivalent experience in a relevant field, experience in running one or more of vegetation-atmosphere models, biogeochemical models, and dynamic vegetation models and experience in programming or model development. There are likely to be opportunities to travel to the Amazon to participate in field data collection.
Closing date: Noon on Wednesday 20 May 2009.

For further information please see our website on **http://www.geog.ox.ac.uk/news/jobs/** or contact the HR Office on 01865 285082. Informal enquiries to Professor Yadvinder Malhi (yadvinder.malhi@ouce.ox.ac.uk).

Committed to equality and valuing diversity

VTC Virginia Tech Carilion RESEARCH INSTITUTE

FOUNDING DIRECTOR

The Virginia Tech Carilion Research Institute (VTCRI) invites applications for its founding Director. With the benefit of a robust research university collaborating with a transformational, integrated health system, the Director will have the rare opportunity to help lead, create, and transform health-related research. The VTC Research Institute is a result of the partnership of Carilion Clinic, the newly formed Virginia Tech Carilion School of Medicine, and the solid biomedical and life science research programs at Virginia Tech. VTCRI has the strong support of senior leadership across VT and Carilion, and their partnership is committed to excellence in all aspects of health sciences.

The mission of VTCRI is to be a premier institute of interdisciplinary and translational research within the health sciences. The Director will provide leadership for VTCRI, with responsibility for development of research strategy, the recruitment of up to 40 research teams, development of collaborative programs of translational research, and integration of VTCRI with the VTC School of Medicine, Carilion Clinic, and existing programs at Virginia Tech.

VTCRI will be part of an emerging biomedical complex that includes the Carilion Clinic and VTC School of Medicine. The VTC facility is currently under construction in Roanoke, Virginia, with an anticipated Fall 2010 completion date.

The successful candidate will be an MD or PhD scientist of national distinction having a track record of discovery and publication who will continue his or her research activities. Applicants should have exceptional communication and strategic planning skills, an established record of leading and fostering large research programs, a commitment to translational research, and the ability to work with VT, VTCSOM, and CC leaders, faculty, and clinicians to develop a common vision and purpose. Area of expertise and specialization are open.

Candidates should submit a cover letter, curriculum vitae, and contact information for three references to **www.jobs.vt.edu** posting **#090048**. After a preliminary review, references will be contacted and asked to submit letters of recommendation for selected candidates. The review of candidates will begin on June 1, 2009 and will continue until a candidate is selected. The anticipated start date for the successful candidate is on or before January 1, 2010.

Virginia Tech is the recipient of the National Science Foundation ADVANCE Institutional Transformation Award to increase the participation of women in academic science and engineering careers.

Southwestern Virginia is a wonderful location with strong communities, plentiful recreation and arts, and never-ending vistas across beautiful mountains. It provides a diversity of lifestyles with remarkably easy access to Washington DC, Richmond, North Carolina, mountains and beaches. A more complete description of VTCRI can be found at the VTCRI website **www.vtc.vt.edu.**

Virginia Tech does not discriminate against employees, students, or applicants on the basis of race, color, sex, sexual orientation, disability, age, veteran status, national origin, religion or political affiliation. Anyone having questions concerning discrimination should contact the Office for Equal Opportunity.

a partnership of CARILION CLINIC and VirginiaTech

PENNSTATE University Park

FACULTY Appointments in Infectious Disease The Evolution and Dynamics of Pathogens

The Eberly College of Science, The College of Agricultural Sciences, The College of Earth and Mineral Sciences, The Huck Institutes of Life Sciences, and The Penn State Institutes of Energy and the Environment are seeking to appoint a number of faculty positions in the fields of theoretical and empirical infectious disease biology. Specifically we are interested in exciting, interdisciplinary candidates who are **Mathematicians, Physicists, Climate Modelers or Biologists, to provide novel insights into parasite-host interactions that range from within-host interactions, between-host transmission events and population-level dynamics**.

We seek interactive people who can work across disciplines and identify novel insights and solutions to managing the disease burden. We encourage candidates interested in dynamical issues relating to **pathogen epidemiology and evolution**, such as the evolutionary impact of drugs, vaccines and insecticides and the role of ecological and evolutionary factors in the invasion and emergence of diseases. We also seek candidates with expertise in **theoretical modeling and the interaction of climate and disease** - specifically dynamical downscaling of global and regional climate to elucidate the biological processes of disease transmission. The candidates will become integral to one of our centers of excellence such as The Center for Infectious Disease Dynamics (**http://www.cidd.psu.edu/**), The Center for Molecular Immunology and Infectious Disease (**http://cmiid.psu.edu**) or The Earth Systems Science Center (**http://www.essc.psu.edu/**).

We are cluster hiring in this area and will consider appointment at any scale for Assistant, Associate or Full Professor. Penn State offers highly competitive salaries and startup package with institutional support for students. Please submit one electronic application consisting of a cover letter including future research plans, curriculum vitae and the contact information of three references to **Judie Burns** at **jeb2@psu.edu**. Review will start **June 15, 2009** and continue until a number of positions have been filled.

Penn State is committed to Affirmative Action, Equal Opportunity and the diversity of its workforce.

1867 THAYER SCHOOL OF ENGINEERING AT DARTMOUTH DARTMOUTH 1769

TENURE TRACK FACULTY POSITION
BIOENGINEERING / BIOTECHNOLOGY

Thayer School of Engineering at Dartmouth College invites applications for a faculty position in the Biotechnology/Bioengineering area. This position strengthens one of Thayer's core research thrusts, **Engineering in Medicine**. Successful applicants will have a Ph.D. in the life sciences and/or engineering and will be evaluated based on (i) the potential to establish an internationally recognized research program and (ii) the desire to excel as a teacher at both the undergraduate and graduate level. Priority will be given to candidates who can build a distinctive research program in the area of **engineered living systems** (e.g., cell and metabolic engineering, protein engineering, glyco-engineering etc.) or engineered systems that interact with **living systems** (e.g.,biomaterials, bioimaging, ex-vivo protein engineering etc.). The potential to collaborate with faculty at the Dartmouth Hitchcock Medical Center and life science departments at Dartmouth is a significant advantage. Candidates with industrial research experience are particularly encouraged to apply. The position is at the Assistant Professor level, although exceptional candidates at other ranks will be considered.

A cover letter and curriculum vitae should be sent to **Prof. Tillman Gerngross, Thayer School of Engineering, Dartmouth College, Hanover, NH 03755, USA** or e-mailed to **Bioengineering.Faculty.Search@dartmouth.edu**. Review of candidates will begin immediately and continue until the position is filled.

Dartmouth College is an equal opportunity/affirmative action employer.

http://engineering.dartmouth.edu

Seattle Children's
HOSPITAL · RESEARCH · FOUNDATION

Neurological Surgery
Associate Professor / Professor

The recently established Center for Neuroscience at the Seattle Children's Research Institute invites applications for a full-time faculty position, with the University of Washington School of Medicine Department of Neurological Surgery, at the rank of Associate Professor or full Professor, without tenure. Qualified applicants should be established investigators who are applying techniques of molecular, genetic or cellular biology to study mechanisms underlying hydrocephalus. The Center for Neuroscience at the Seattle Children's Research Institute's research vision is to restore children's health through a mechanistic understanding. The applicant's area of research interest should be complementary to the interests of current faculty working on various areas of neuroscience and bioengineering. Researchers interested in understanding CSF hydrodynamics, choroid plexus function, neuroendocrinology, brain metabolism, blood brain barrier function, brainstem neurobiology and proteomics research are particularly encouraged to apply. The successful candidate must have a M.D. and/or Ph.D. degree and have active nationally funded research grants. Level and salary will be based on applicant's qualifications and experience. Responsibilities of the position include development of an independent, extramurally funded research program, establishing a hydrocephalus section within the Center for Neuroscience and mentoring graduate and post-doctoral students and junior faculty investigators.

This position is open until filled. Address any inquiries to **Dr. Jan-Marino Ramirez, Center Director**, at **nino.ramirez@seattlechildrens.org**. Please send CV, a statement of current and future research interests and the names and contact information of three references to: **Wendy Kramer, Seattle Children's Research Institute, 1900 Ninth Avenue, M/S C9S-9, Seattle, WA 98101**.

For more information about Seattle Children's Research Institute, please visit:
http://research.seattlechildrens.org.

All University of Washington faculty engage in teaching, research, and service.
The University of Washington is an Equal Opportunity/Affirmative Action Employer.
Women and minorities are encouraged to apply.

UW Medicine
SCHOOL OF MEDICINE

WORKSHOPS

CBRN Medical Countermeasures Workshop 2009

sponsored by the:
U.S. Department of Health and Human Services (HHS)
Assistant Secretary for Preparedness and Response (ASPR)
Biomedical Advanced Research and Development Authority (BARDA)
Chemical, Biological, Radiological and Nuclear Medical Countermeasures (CBRN)
and Acquisitions Management Systems (AMS)

June 25–26, 2009

Hyatt Regency Bethesda
One Bethesda Metro Center
Bethesda, MD 20814

To register, visit
www.medicalcountermeasures.gov

For further information, e-mail
CBRN-Workshop@hhs.gov

Discover and Develop Drugs in China

Shanghai Hengrui Pharmaceuticals Co., Ltd. is now seeking highly motivated professionals in drug discovery and development to fill the following positions at Manager, Group Leader or Director levels:

Clinical Project Management (Oncology and Diabetic): Manage clinical product development and manufacturing. Develop and implement regulatory strategies. Review and approve protocols and clinical site monitoring for compliance. MS/PhD with 5-8 yrs pharm/biotech experience, knowledgeable and skillful in US clinical study design and implementation preferred.

QA/QC/Regulatory Affairs/Documentation: MS/PhD with 5-8 yrs strong experience in NDA and ANDA fillings for NCEs and generic drugs.

Biologics: Senior PhDs in Biochemistry or Protein chemistry with successful industrial experience in discovery and development of biologic drugs.

Molecular/Cellular Biology: PhDs in modern molecular and cellular biology with experience in target identifications and validations, assay and reagent development and mechanism studies etc.

Synthetic Organic Chemistry: PhDs in synthetic organic chemistry with strong synthetic problem solving skills and extensive and in-depth knowledge of modern organic synthesis.

Molecular Modeling: PhD in structural/computational chemistry with at least 5 yrs experience in computer aided drug design in pharmaceutical industry with successful track record.

Animal Modeling: PhD in pharmacology or related discipline with 3 yrs of postdoctoral experience in conducting in vivo efficacy studies in diabetic, cardiovascular or oncology.

Depending on the positions, proficient bilingual (English/Chinese) ability is required. We offer a competitive relocation and compensation package in an open, challenging and smoke-free environment. If interested, please forward your resume to Miss Wang (career@shhrp.com)

SHANGHAI HENGRUI PHARMACEUTICALS CO., LTD.
www.shhrp.com

SPECIAL CAREER FEATURE

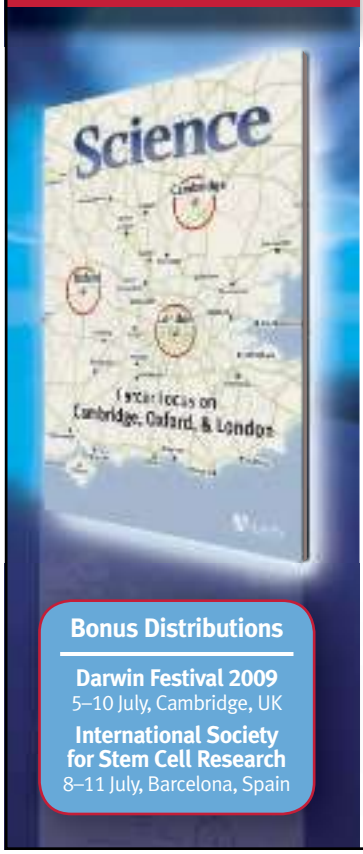

Bonus Distributions

Darwin Festival 2009
5–10 July, Cambridge, UK
International Society for Stem Cell Research
8–11 July, Barcelona, Spain

Career Focus on Cambridge, Oxford, and London

Issue date
26 June
Reserve ad space by 9 June

The power of *Science* is in the journal's 131,000 weekly subscribers and 700,000 weekly readers. In our 26 June issue we will use this power to highlight the state of the scientific job market in and around these renowned British seats of learning.

Contact: Alex Palmer
Telephone:
+44 (0) 1223 326 500
E-mail:
ads@science-int.co.uk

Science Careers
From the journal *Science* AAAS
ScienceCareers.org

PROFESSOR

In Experimental Surface Physics

The Department of Applied Physics now invites applications for a full professorship in Experimental Surface Physics. We offer excellent opportunities for intra- and interdepartmental interactions with other groups on issues of importance for a sustainable society, such as energy conversion, catalysis and novel functional materials. Interdisciplinary research is promoted by a stimulating infrastructure, including top class clean room facilities and deep involvement in synchrotron based activities at MAX-lab.

Application deadline is June 19, 2009. For further information and how to apply please visit Vacancies, Ref no 2009/36, at:

www.chalmers.se/en

Chalmers University of Technology conducts research and education in engineering sciences, architecture, technology-related mathematical sciences, natural and nautical sciences – in close collaboration with industry and society. The aim is to make an active contribution to a sustainable future. Chalmers has about 10,000 students and 2,200 employees. New knowledge and improved technology has characterised Chalmers since its foundation in 1829 in accordance with the testament of William Chalmers, and his motto: Avancez!

CHALMERS

COURSE

Okinawa Institute of Science and Technology

"DNA Topology Course"

Date: November 2 – 7, 2009
Location: Okinawa, Japan

DNA topology is one of the areas in which cutting-edge pure mathematics and biology meet very directly, in the study of topoisomers.

The point of the course is to give young and early-career biologists a chance to learn about this exciting and active research field from international experts. This will be achieved through a combination of introductory lectures with coursework, and also a short series of conference-level research talks, to give the participants an understanding of both the basic theory and current research directions.

The course will be targeted at PhD level biologists, with postdoctoral researchers also welcome.

Confirmed Speakers:

De Witt Sumners	Patrick Forterre
Jun O'Hara	Javier Arsuaga
Dorothy Buck	Isabel Darcy
Christian Laing	Koya Shimokawa
Andrzej Stasiak	Lynn Zechiedrich

More information can be obtained from
http://web.me.com/oist_mbu/DNA_Topology_Course/Home.html
or the course secretariat at **topo@oist.jp**

Okinawa Institute of Science and Technology http://www.oist.jp/

Imperial College London

EPSRC Centre for Synthetic Biology & Innovation

Lecturer in Synthetic Biology – Engineering Design x2

Department of Bioengineering, Faculty of Engineering

Lecturer in Experimental Synthetic Biology

Division of Molecular Biosciences, Faculty of Natural Sciences

Salary: £42,060 - £45,680 p.a.

Fixed Term for 57 months

Applications are invited for three posts at Lectureship level in the new EPSRC Centre for Synthetic Biology and Innovation (CSynBI) at Imperial College London. The Centre was established in partnership with the London School of Economics and Political Science through an EPSRC Science and Innovation award that aims to build new activity in areas of national strategic importance, with a particular focus on supporting new research leaders.

The Centre for Synthetic Biology and Innovation, (www.imperial.ac.uk/syntheticbiology), is part of Imperial's Institute for Systems and Synthetic Biology (www.imperial.ac.uk/systemsbiology) - a multidisciplinary, multi faculty institute focused on developing novel approaches to research in biology, medicine and engineering. A major strategic aim of the Centre is to establish a robust engineering framework for the design and optimisation of new synthetic biology parts, devices and systems and to integrate this research with emerging ethical legal and societal issues.

The Centre is seeking to appoint three new Lecturers with a focus on either the Engineering or Experimental Aspects of Synthetic Biology.

Two Lecturers will be appointed in Engineering in the areas of engineering design and process control/quality assurance in relation to Synthetic Biology and one Lecturer will be appointed in Experimental Synthetic Biology to work on either metabolic engineering or biocatalysis.

Applicants must have a PhD (or equivalent) and an outstanding research record as demonstrated by their publications. Teaching experience is also highly desirable.

An application form and further particulars can be obtained from: www.imperial.ac.uk/employment In addition you should enclose a full CV (including list of publications), a research plan and a brief statement of teaching interests.

For informal queries or discussion please contact: Professor Richard Kitney (r.kitney@imperial.ac.uk) for the Lecturer positions in Synthetic Biology – Engineering and Design. Professor Paul Freemont (p.freemont@imperial.ac.uk) for the Lecturer position in Experimental Synthetic Biology.

Closing date: 26 May 2009.

Committed to equality and valuing diversity. We are also an Athena Silver SWAN Award winner and a Stonewall Diversity Champion.

POSITIONS OPEN

Northern Virginia firm has multiple openings for:

SCIENTIFIC INFORMATION ANALYSTS (code #501)

Analyze technical medical/scientific text applying concepts from scientific thesaurus; perform scientific coding/indexing; analyze research activities; validate, classify, and index information; prepare reports. Requires B.S. or M.S. or equivalent in medical, biomedical, life science, computer engineering, or related plus three to five years of experience in job offered or as a scientific knowledge manager.

SENIOR BIOINFORMATICS SCIENTISTS/ FUNCTIONAL SPECIALISTS (code #502)

Perform research in the area of molecular biology database services and published guidance documents; prepare documentation; assist in business process analysis, quality assurance/quality control, ensuring project quality. Create materials, teach, and develop scientific outreach and bioeducational training programs. Requires Ph.D. in biochemistry or molecular biology or related plus three years of experience in job offered or as a research scientist.

Job location: Northern Virginia/D.C./Maryland metropolitan area. May require travel and/or relocation to other sites. Mail resume with code number to: **Information Management Consultants, 11480 Commerce Park Drive, Reston, VA 20191.** *Equal Opportunity Employer.*

POSTDOCTORAL RESEARCH FELLOWSHIP POSITION

The University of Massachusetts Medical School invites applications for research opportunities in the broad fields of diabetes and endocrinology. UMMS is a designated NIH Diabetes and Endocrinology Research Center (DERC), with over 70 active members, engaged in state-of-the-art research in an array of basic and clinical research programs (**website: http://www.umassmed.edu/derc**). We seek Postdoctoral Fellows with intellectual curiosity, eager to explore critical questions in biology, relevant to mechanisms in diabetes, metabolic, and endocrine disease, or fundamental clinical processes affecting the course of diabetes. Applicants should have Ph.D. or M.D. degrees, and should identify the DERC member laboratory they wish to join. Under the auspices of an NIH Training Grant, the Fellow is guaranteed three years of support. The first start date is July 1, 2009. Applications and inquiries should be directed to: **Michael Czech, Ph.D., DERC Director, e-mail: michael.czech@umassmed.edu; Roger Davis, Ph.D., Director, DERC Pilot Programs, e-mail: roger.davis@umassmed.edu; or Neil Aronin, M.D., Director, Endocrine Division and Search Committee Chair, e-mail: neil.aronin@umassmed.edu.**

MARKETPLACE

Eppendorf & Science Prize for

Neurobiology

$25,000 Prize

Get recognized!

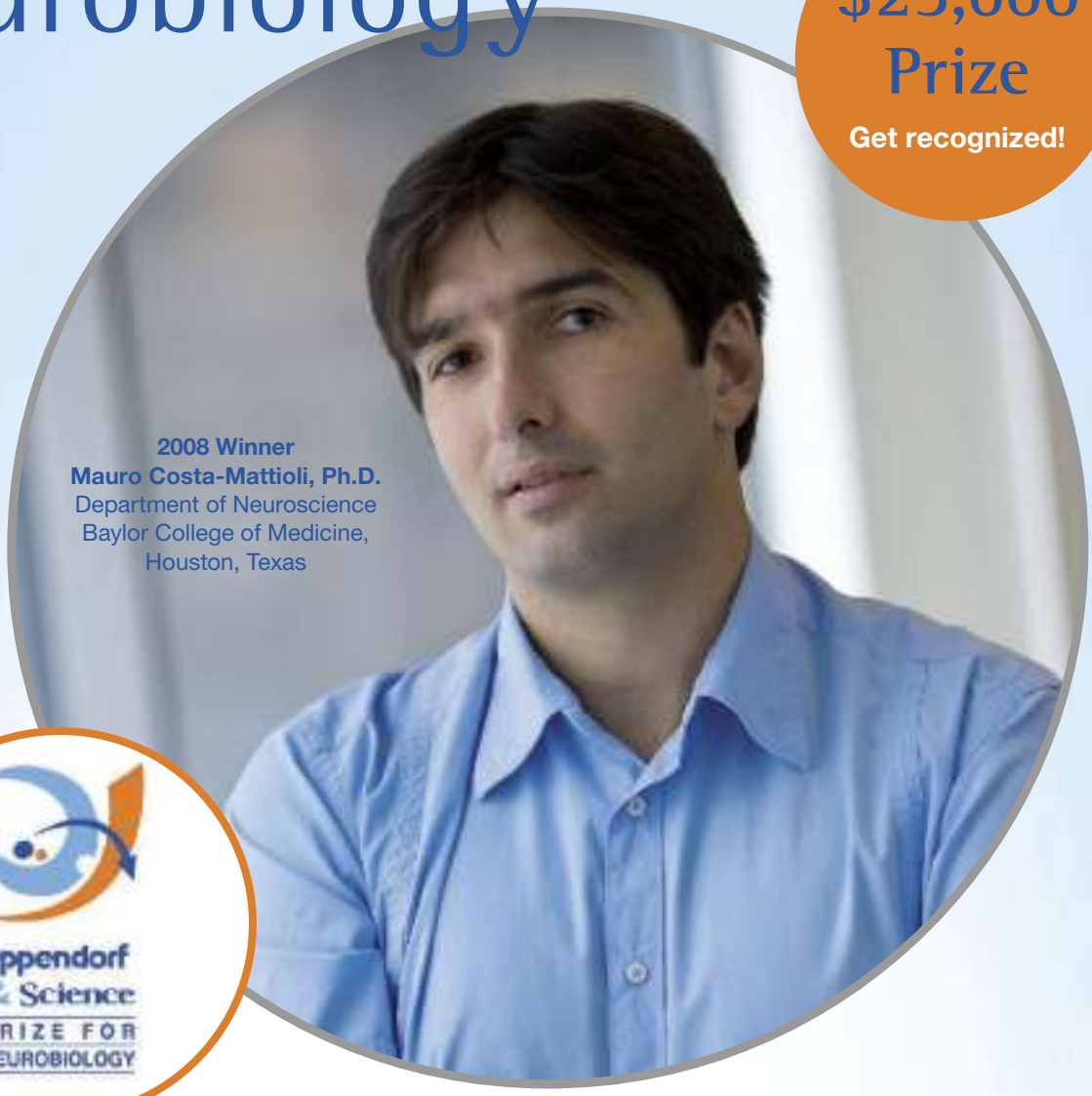

2008 Winner
Mauro Costa-Mattioli, Ph.D.
Department of Neuroscience
Baylor College of Medicine,
Houston, Texas

eppendorf & Science PRIZE FOR NEUROBIOLOGY

Deadline for entries
June 15, 2009

For more information
www.eppendorf.com/prize

This annual international research prize recognizes accomplishments in neurobiology research based on methods of molecular and cell biology. The winner and finalists are selected by a committee of independent scientists, chaired by the Editor-in-Chief of *Science*. Past winners include postdoctoral scholars and assistant professors.

To be eligible, you must be 35 years of age or younger. If you´re selected as this year´s winner, you will receive $25,000, have your work published in the prestigious journal *Science* and be invited to visit Eppendorf in Hamburg, Germany.

eppendorf
In touch with life

Science AAAS

Kurstin Roe Photography

PCR ARRAYS

Focus on Your Pathway™

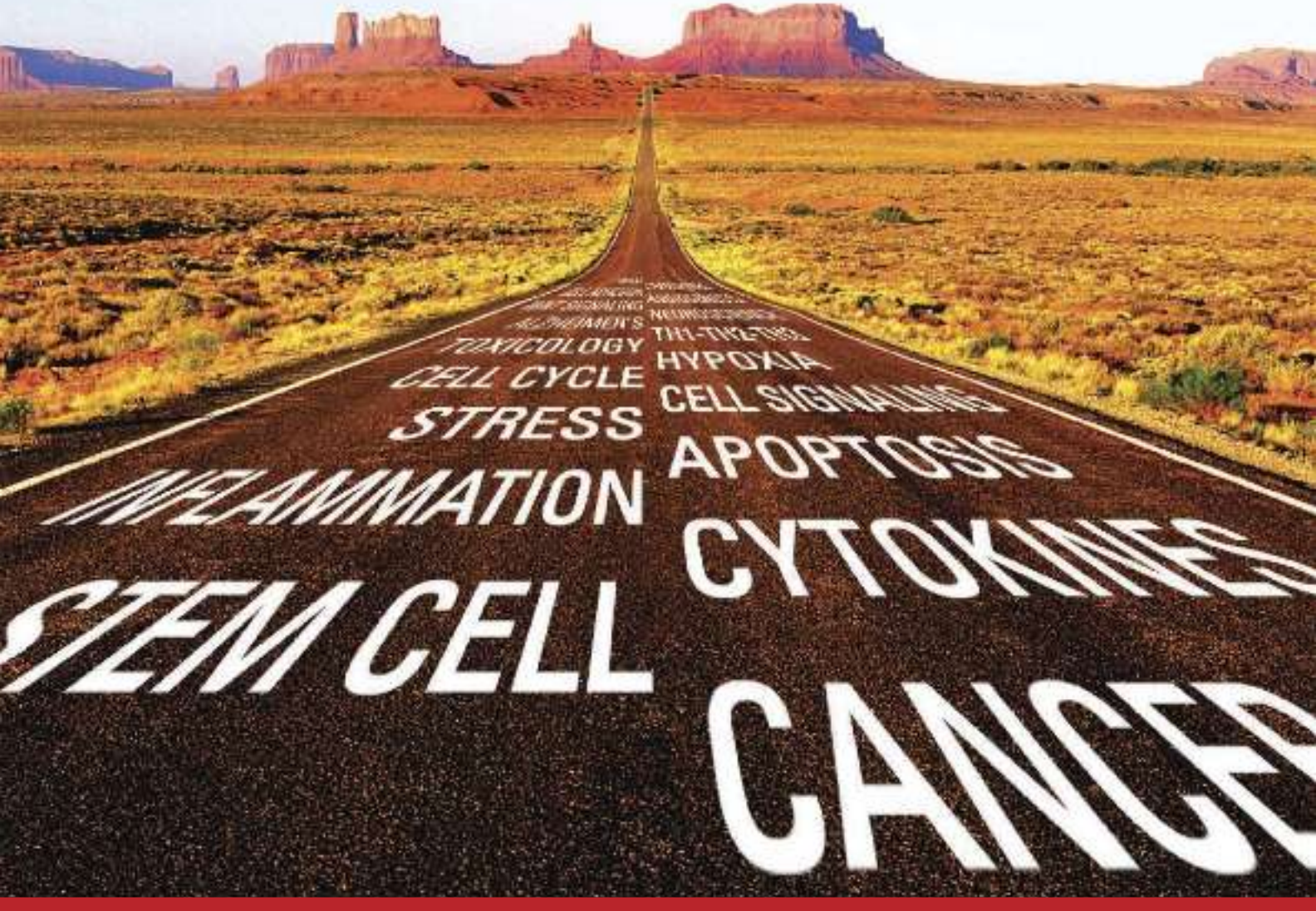

Over 100 Pathways Available **The PCR Array Experts**

SABiosciences™

www.SABiosciences.com

FREE PCR ARRAY T-Shirt* and PCR ARRAY Handbook!

Please Register Online: *www.SABiosciences.com/Science3.php*

ACT NOW! Offer Ends 22nd of May 2009

* While supplies last